

**Deanship of Graduate Studies
Al-Quds University**



**Formation, Characterization and Antimicrobial Activity of
Mixed Non-ionic Surfactant Micellar system**

Lubna Abd Almughni Kazem Abu Khalaf

M.Sc Thesis

Jerusalem-Palestine

1438/2017

**Formation, Characterization and Antimicrobial Activity of
Mixed Non-ionic Surfactant Micellar system**

Prepared By :

Lubna Abd Almughni Kazem Abu Khalaf

**B.Sc. Food Science and Technology/ Al-Quds University.
Palestine**

Supervisor: Dr. Monzer Fanun

**A thesis submitted in partial fulfillment of requirements for
the degree of Master of Food Processing Technology in
Applied and Industrial Technology
Al-Quds University/ Palestine**

1438/2017

Al-Quds University
Deanship of Graduate Studies
Applied and Industrial Technology Program



Thesis Approval

Formation, Characterization and Antimicrobial Activity of Mixed Non-ionic Surfactant Micellar system

Prepared By: Lubna A.K. Abu Khalaf

Registration No:21120171

Supervisor: Dr. Monzer Fanun

Master thesis submitted and accepted, Date 17/5/2017

The names and signatures of the committee members are as follows:

1. Head of Committee/Dr. Monzer Fanun
2. Internal Examiner/ Dr. Ibrahim Kayali
3. External Examiner/ Dr. Ahmed Ayyad

Signature

Signature:.....

Signature:.....

Jerusalem-Palestine

1438/2017

Dedication

I would like to dedicate this work to Mutaz my be loveing husband ,my lovely children; beautiful Yasmeen ,Ahmad my buddy & precious Hamza , who gave me confidence from the beginning and gave me the power and enthusiasm to continue studying and working efficiently. My parents ,all my family and friends .

Finally, to Dr. Monzer Fanun who was a great supervisor and to all of the wonderful members of the Food and Technology Department whom truly I consider as friends .

Lubna Abu Khalaf

Declaration

I Certify that this thesis submitted for the degree of master is the result of my own research, except where otherwise acknowledged, and that this thesis (or any part of the same) has not been submitted for a higher degree to any other university or institution.

Signed:

Lubna Abd Almughni Kazem Abu Khalaf

Date: 17/5/2017

Acknowledgements:

I would like first of all to express my deep gratitude to my supervisor Dr. Monzer Fanun for his special tremendous efforts on my experiments that I respect and admire the most.

I would also like to thank the Department of Food Science and Technology at Al-Quds University for their help through this work.

Finally, but by no means least, I wish to thank all of my friends and colleagues for the support and encouragement they generously provided through my study period.

Lastly, I offer my regards and blessings to all of those who supported me in any respect during the completion of the project.

Lubna Abu Khalaf

Abstract

Sucrose myristate based sugar microemulsions were formulated, characterized and applied as antimicrobial agents.

The systems studied were (water/ propylene glycol)/(sucrose myristate (M1695)/polyethoxylated sorbitan esters (Tween 80))/(oil / ethanol).The oil phase consists of cyclic oils including R(+)-limonene oil (LIM),linear oil including isopropylmyristate oil (IPM) and triglyceride oils including caprylic-capric triglyceride (CCT).

The effect of different types and percentages of the surfactants ; the weight ratio of the polyethoxylated ester in the mixed surfactants that were varied from 0 to 100 wt% by steps of 25 wt% with equal unity of each oil with ethanol ,and water/ propylene glycol in the (2/1) weight ratio were investigated . The phase behavior of the systems were studied at three different temperatures 25, 37and 45°C .

We studied the phase behavior, water solubilization capacity and the area of the total one phase microemulsion region A_T (%)for each system were calculated . The area of the one phase microemulsion region increased as the weight ratio of the polyethoxylated ester in the mixed surfactants increased from 25 to 75 wt% . It was found that mixing the surfactants in equal unity showed the maximum water solubility in all the systems,(A_T (%)=85,80,74 for LIM, IPM, and CCT respectively). Structure and type of oil has great influence on the water solubility ;maximum water solubility was detected in the system consisting cyclic Limonene oil (LIM) due to the cyclic structure that enhance penetration on the surfactant surface and due to its low molecular volume, caprylic-capric triglyceride and linear oil isopropylmyristate have low total one phase microemulsion region because of their high molecular volume and so the ability to penetrate the interfacial film is very low and does not assist to obtain the optimum curvature of surfactants. Temperature insensitive microemulsion formation was confirmed for the systems .

The systems (water/propylene glycol) / (polyethoxylated sorbitan esters (Tween 80) / Sucrose myristate (M1695)) /(oil/ ethanol) with the three different oils were characterized using electrical conductivity, ultrasonic velocity and density. It was found that the increase in the water volume fraction induces exponential increase in electrical conductivity in all systems. Electrical conductivity increases slightly for water contents smaller than 20 wt% followed by an increase

observed for water contents between 20 and 70 wt%. A slight decrease in the electrical conductivity is also observed for water contents between 70 and 75 wt.%, then a sharp decrease is observed. Measurements confirm that a progressive transformation of the water in oil to bicontinuous and inversion to oil in water microemulsions occurs upon dilution with the aqueous medium. Results showed that systems with caprylic-capric triglyceride (CCT) oil had the highest electrical conductivity at constant temperature due to the longest chain length and the bulky fork shape that makes it hard to penetrate the palisade layer and thus more space and more interactions between the droplet results in higher electrical conductivity.

Microemulsion densities usually decreases with the increases in the aqueous volume content at constant temperatures, and decreases with the increase of temperatures. Most of the systems studied with the three different oils showed decrease in density up to about 15% aqueous content forming the water in oil microemulsion, passes through the bicontinuous stage between 20-65% aqueous content ending in the form of oil in water microemulsions above 70% aqueous content.

Microemulsions ultrasonic velocities increase with the increases in the aqueous volume content at constant temperatures. Most of the systems studied with the three different oils used showed an increase in ultrasonic velocity up to about 15% aqueous content forming the water in oil microemulsion passing through the bicontinuous stage between 20-65% aqueous content ending in the form of oil in water microemulsions above 70% aqueous content.

Inhibition effect was detected against *Staphylococcus aureus* and *Escherichia coli*. Inhibition effect was detected against Gram positive bacteria *Staphylococcus aureus* more than Gram negative *Escherichia coli*; in *Staphylococcus aureus* diameters of inhibition zone were larger than in *Escherichia coli* indicating better destruction; diameters of inhibition zone were less and there were reduction in population not total destruction. Most of the inhibition effect is shown in the bicontinuous phase. Rate of inhibition decreases with increase of ethoxylated surfactant ratio (decrease in sucrose myristate)

Highest inhibition were detected against *Staphylococcus aureus* in systems containing high content of sucrose myristate M(1695) and limonene oil due to the synergistic effect.

Inhibition decreases with the increase of the polyethoxylated surfactant concentration. Limonene oil systems showed maximum inhibition effect.

Content

1	Introduction	1
2	Literature review	9
3	Objective	16
4	Material and Method	17
4.1	Materials	17
4.1.1	Surfactants	17
4.1.2	oils	19
4.1.3	Co surfactants	21
4.1.4	Aqueous Phase	21
4.1.5	Materials for microbial test	22
4.2	Methods	23
4.2.1	Construction of ternary and pseudoternary phase diagrams	23
4.2.4	Determination of water solubilization capacity	24
4.2.3	Physiochemical characterization	25
4.2.3.1	Electrical conductivity measurements	25
4.2.3.2	Density	25
4.2.3.3	Ultrasonic velocity	25
4.2.4	Antimicrobial susceptibility test	26
5	Result and Discussion	28
5.1	Formulation of microemulsion	28
5.1.1	Phase behavior of mixed surfactants with LIM oil	28
5.1.2	Phase behavior of mixed surfactants with IPM oil	43
5.1.3	Phase behavior of mixed surfactants with CCT oil	58
5.2	Determination of the water solubilization capacity	73
5.3	Characterization	83
5.3.1	Electrical conductivity	83
5.3.1.1	Electrical conductivity of the systems using LIM oil	83
5.3.1.2	Electrical conductivity of the systems using IPM oil	91

5.3.1.3	Electrical conductivity of the systems using CCT oil	98
5.3.2	Density and ultrasonic velocity	109
5.3.2.1	Density measurements	110
5.3.2.1.1	Determining the density for the systems using IPM oil	110
5.3.2.1.2	Determining the density for the systems using IPM oil	118
5.3.2.1.3	Determining the density for the systems using CCT oil	128
5.3.2.2	Ultrasonic velocity measurements	138
5.3.2.2.1	Determining the ultrasonic velocity for the systems using LIM oil	138
5.3.2.2.2	Determining the ultrasonic velocity for the systems using IPM oil	147
5.3.2.2.3	Determining the ultrasonic velocity for the systems using CCT oil	157
5.4	Antimicrobial activity	167
5.4.1	Gram positive bacteria <i>Staphylococcus aureus</i>	169
5.4.1.1	Investigating the effect of LIM oil systems on the Gram positive bacteria	169
5.4.1.2	Investigating the effect of IPM oil systems on the Gram positive bacteria	178
5.4.1.3	Investigating the effect of CCT oil systems on the Gram positive bacteria	186
5.4.2	Gram negative bacteria <i>Escherichia coli</i>	192
5.4.2.1	Investigating the effect of LIM oil systems on the Gram negative bacteria	192
5.4.2.2	Investigating the effect of IPM oil systems on the Gram negative bacteria	200
5.4.2.3	Investigating the effect of CCT oil systems on the Gram negative bacteria	209
6	Conclusion	231
7	References	232

List of tables numbers and descriptions:

No.	Table #	Table name and description	Page #
1.	4:1	Systems that explains the different ratios in this work	24
2.	4:2	All materials used in this research	27
3.	5:1	Weight percent of Sm and Wm in systems with LIM oil at (25,37,and 45°C)	74
4.	5:2	Total monophasic area A_T (%) for LIM oil	74
5.	5:3	Weight percent of Sm and Wm in systems with IPM oil at (25,37,and 45°C)	75
6.	5:4	Total monophasic area A_T (%) for IPM oil	76
7.	5:5	Weight percent of Sm and Wm in systems with CCT oil at (25,37,and 45°C)	77
8.	5:6	Total monophasic area A_T (%) for CCT oil	77
9.	5:7	Total monophasic area A_T (%) at the optimum surfactant mixing ratio as a function of oil type.	78
10.	5:8	Total monophasic area A_T (%) at the optimum surfactant mixing ratio as a function of temperature.	79
11.	5:9	The electrical conductivity (σ) for system # 1 W+PG/ Sucrose myristate (M1695) /LIM+ ethanol at (25,37,and 45°C)	84
12.	5:10	The electrical conductivity (σ) for system # 2 W+PG/ TMAZ80 +Sucrose myristate (M1695) /LIM+ ethanol at (25,37,and 45°C)	85
13.	5:11	The electrical conductivity (σ) for system # 3 W+PG/ TMAZ80 +Sucrose myristate (M1695) /LIM+ ethanol at (25,37,and 45°C)	87
14.	5:12	The electrical conductivity (σ) for system # 4 W+PG/ TMAZ80 +Sucrose myristate (M1695) /LIM+ ethanol at (25,37,and 45°C)	88
15.	5:13	The electrical conductivity (σ) for system # 5 W+PG/ TMAZ80 /LIM+ ethanol at (25,37,and 45°C)	90
16.	5:14	The electrical conductivity (σ) for system # 6 W+PG/ Sucrose myristate (M1695) /IPM+ ethanol at (25,37,and 45°C)	91
17.	5:15	The electrical conductivity (σ) for system # 7W+PG/TMAZ80+	93

		Sucrose myristate (M1695) /IPM+ ethanol at (25,37,and 45 ⁰ C)	
18.	5:16	The electrical conductivity (σ) for system # 8 W+PG/TMAZ80+ Sucrose myristate (M1695) /IPM+ ethanol at (25,37,and 45 ⁰ C)	94
19.	5:17	The electrical conductivity (σ) for system # 9 W+PG/TMAZ80+ Sucrose myristate (M1695) /IPM+ ethanol at (25,37,and 45 ⁰ C)	96
20.	5:18	The electrical conductivity (σ) for system # 10 W+PG /TMAZ80 /IPM+ ethanol at (25,37,and 45 ⁰ C)	97
21.	5:19	The electrical conductivity (σ) for system # 11 W+PG/ Sucrose myristate (M1695) /CCT+ ethanol at (25,37,and 45 ⁰ C)	99
22.	5:20	The electrical conductivity (σ) for system # 12 W+PG/TMAZ80+ Sucrose myristate (M1695) /CCT+ ethanol at (25,37,and 45 ⁰ C)	100
23.	5:21	The electrical conductivity (σ) for system # 13 W+PG/TMAZ80+ Sucrose myristate (M1695) /CCT+ ethanol at (25,37,and 45 ⁰ C)	102
24.	5:22	The electrical conductivity (σ) for system # 14 W+PG/TMAZ80+ Sucrose myristate (M1695) /CCT+ ethanol at(25,37,and 45 ⁰ C)	103
25.	5:23	The electrical conductivity (σ) for system # 15 W+PG /TMAZ80 /CCT+ ethanol at (25,37,and 45 ⁰ C).	105
26.	5:24	The electrical conductivity at the optimum surfactant mixing ratio as a function of different oil type at constant temperature 25°C.	108
27.	5:25	The density (ρ) for the system #1 W+PG/ Sucrose myristate (M1695) /LIM +Ethanol at different aqueous contents and different temperatures	110
28.	5:26	The density (ρ) for the system #2 W+PG/ TMAZ80+Sucrose myristate (M1695) /LIM +Ethanol at different aqueous contents and different temperatures.	112
29.	5:27	The density (ρ) for the system #3 W+PG/ TMAZ80+Sucrose myristate (M1695) /LIM +Ethanol at different aqueous contents and different temperatures.	113
30.	5:28	The density (ρ) for the system #4 W+PG/ TMAZ80+Sucrose myristate (M1695) /LIM +Ethanol at different aqueous contents	115

		and different temperatures.	
31.	5:29	The density (ρ) for the system #5 W+PG/ TMAZ80/LIM +Ethanol at different aqueous contents and different temperatures	117
32.	5:30	The density (ρ) for the system #6 W+PG/ Sucrose myristate (M1695) /IPM +Ethanol at different aqueous contents and different temperatures.	119
33.	5:31	The density (ρ) for the system #7 W+PG/ TMAZ80+Sucrose myristate (M1695) /IPM+Ethanol at different aqueous contents and different temperatures	120
34.	5:32	The density (ρ) for the system #8 W+PG/ TMAZ80+Sucrose myristate (M1695) /IPM+Ethanol at different aqueous contents and different temperatures	122
35.	5:33	The density (ρ) for the system #9 W+PG/ TMAZ80+Sucrose myristate (M1695) /IPM+Ethanol at different aqueous contents and different temperatures	124
36.	5:34	The density (ρ) for the system #10 W+PG/ Tmaz8 /IPM+Ethanol at different aqueous contents and different temperatures.	126
37.	5:35	The density (ρ) for the system #11 W+PG/ Sucrose myristate (M1695) /CCT +Ethanol at different aqueous contents and different temperatures	128
38.	5:36	The density (ρ) for the system #12 W+PG/ TMAZ80+Sucrose myristate (M1695) /CCT +Ethanol at different aqueous contents and different temperatures	130
39.	5:37	The density (ρ) for the system #13 W+PG/ TMAZ80+Sucrose myristate (M1695) /CCT +Ethanol at different aqueous contents and different temperatures.	132
40.	5:38	The density (ρ) for the system #14 W+PG/ TMAZ80+Sucrose myristate (M1695) /CCT +Ethanol at different aqueous contents and different temperatures	134
41.	5:39	The density (ρ) for the system #15 W+PG/ TMAZ80/CCT +	136

		Ethanol at different aqueous contents and different temperatures.	
42.	5:40	The ultrasonic velocity (V) for the system #1 W+PG/ Sucrose myristate (M1695) /LIM +Ethanol at different aqueous contents and different temperatures.	138
43.	5:41	The ultrasonic velocity (V) for the system #2 W+PG/ TMAZ80 +Sucrose myristate (M1695) /LIM +Ethanol at different aqueous contents and different temperatures.	140
44.	5:42	The ultrasonic velocity (V) for the system #3 W+PG/ TMAZ80+Sucrose myristate (M1695) /LIM +Ethanol at different aqueous contents and different temperatures.	141
45.	5:43	The ultrasonic velocity (V) for the system #4 W+PG/ TMAZ80 +Sucrose myristate (M1695) /LIM +Ethanol at different aqueous contents and different temperatures	143
46.	5:44	The ultrasonic velocity (V) for the system #5 W+PG/ TMAZ80 /LIM +Ethanol at different aqueous contents and different temperatures.	145
47.	5:45	The ultrasonic velocity (V) for the system #6 W+PG/ Sucrose myristate (M1695) /IPM +Ethanol at different aqueous contents and different temperatures	147
48.	5:46	The ultrasonic velocity (V) for the system #7 W+PG/ TMAZ80 +Sucrose myristate (M1695) /IPM +Ethanol at different aqueous contents and different temperatures.	149
49.	5:47	The ultrasonic velocity (V) for the system #8 W+PG/ TMAZ80 +Sucrose myristate (M1695) /IPM +Ethanol at different aqueous contents and different temperatures.	151
50.	5:48	The ultrasonic velocity (V) for the system #9 W+PG/ TMAZ80 +Sucrose myristate (M1695) /IPM +Ethanol at different aqueous contents and different temperatures	153
51.	5:49	The ultrasonic velocity (V) for the system #10 W+PG/ TMAZ80 /IPM +Ethanol at different aqueous contents and different temperatures.	155

52.	5:50	The ultrasonic velocity (V) for the system #11 W+PG/ Sucrose myristate (M1695) /CCT +Ethanol at different aqueous contents and different temperatures	157
53.	5:51	The ultrasonic velocity (V) for the system #12 W+PG/ TMAZ80 +Sucrose myristate (M1695) /CCT +Ethanol at different aqueous contents and different temperatures	159
54.	5:52	The ultrasonic velocity (V) for the system #13 W+PG/ TMAZ80 +Sucrose myristate (M1695) /CCT +Ethanol at different aqueous contents and different temperatures.	161
55.	5:53	The ultrasonic velocity (V) for the system #14 W+PG/ TMAZ80 +Sucrose myristate (M1695) /CCT +Ethanol at different aqueous contents and different temperatures.	163
56.	5:54	The ultrasonic velocity (V) for the system #15 W+PG/ TMAZ80 /CCT +Ethanol at different aqueous contents and different temperatures.	165
57.	5:55	Effect of each component of the formed systems against <i>Staphylococcus aureus</i> and <i>Escherichia coli</i> .	167
58.	5:56	Inhibition of the microbial activity of the <i>Staphylococcus aureus</i> caused by system #1 W+PG/ Sucrose myristate (M1695) /LIM +Ethanol	169
59.	5:57	Inhibition of the microbial activity of the <i>Staphylococcus aureus</i> caused by system #2 W+PG/ TMAZ80+Sucrose myristate (M1695) /LIM +Ethanol	171
60.	5:58	Inhibition of the microbial activity of the <i>Staphylococcus aureus</i> caused by system #3 W+PG/ TMAZ80+Sucrose myristate (M1695) /LIM +Ethanol	173
61.	5:59	Diameter of inhibition zone (mm) as a function of surfactant concentration in LIM oil on <i>Staphylococcus aureus</i>	176
62.	5:60	Inhibition of the microbial activity of the <i>Staphylococcus aureus</i>	178

		caused by system #6 W+PG/ Sucrose myristate (M1695) /IPM +Ethanol	
63.	5:61	Inhibition of the microbial activity of the <i>Staphylocoous aureus</i> caused by system #7 W+PG/ TMAZ80+Sucrose myristate (M1695) /IPM +Ethanol	180
64.	5:62	Inhibition of the microbial activity of the <i>Staphylocoous aureus</i> caused by system #8 W+PG/ TMAZ80+Sucrose myristate (M1695) /IPM +Ethanol	182
65.	5:63	Diameter of inhibition zone (mm) as a function of surfactant concentration in IPM oil on <i>Staphylocoous aureus</i>	184
66.	5:64	Inhibition of the microbial activity of the <i>Staphylocoous aureus</i> caused by system #11 W+PG/ Sucrose myristate (M1695) /CCT +Ethanol	186
67.	5:65	Inhibition of the microbial activity of the <i>Staphylocoous aureus</i> caused by system #12 W+PG/ TMAZ80+Sucrose myristate (M1695) /CCT +Ethanol	188
68.	5:66	Diameter of inhibition zone (mm) as a function of surfactant concentration in CCT oil on <i>Staphylocoous aureus</i>	190
69.	5:67	Inhibition of the microbial activity of the <i>Escherichia coli</i> caused by system #1 W+PG/ Sucrose myristate (M1695) /LIM +Ethanol	192
70.	5:68	Inhibition of the microbial activity of the <i>Escherichia coli</i> caused by system #2 W+PG/ TMAZ80+Sucrose myristate (M1695) /LIM +Ethanol	194
71.	5:69	Inhibition of the microbial activity of the <i>Escherichia coli</i> caused by system #3 W+PG/ TMAZ80+Sucrose myristate (M1695) /LIM +Ethanol	196
72.	5:70	Diameter of inhibition zone (mm) as a function of surfactant concentration in LIM oil on <i>Escherichia coli</i>	198
73.	5:71	Inhibition of the microbial activity of the <i>Escherichia coli</i> caused by system #6 W+PG/ Sucrose myristate (M1695) /IPM +Ethanol	200

74.	5:72	Inhibition of the microbial activity of the <i>Escherichia coli</i> caused by system #7 W+PG/TMAZ80+ Sucrose myristate (M1695) /IPM +Ethanol	203
75.	5:73	Inhibition of the microbial activity of the <i>Escherichia coli</i> caused by system #8 W+PG/TMAZ80+ Sucrose myristate (M1695) /IPM +Ethanol	205
76.	5:74	Diameter of inhibition zone (mm) as a function of surfactant concentration in IPM oil on <i>Escherichia coli</i>	207
77.	5:75	Inhibition of the microbial activity of the <i>Escherichia coli</i> caused by system #11 W+PG/ Sucrose myristate (M1695) /CCT +Ethanol	209
78.	5:76	Inhibition of the microbial activity of the <i>Escherichia coli</i> caused by system #13 W+PG/TMAZ80+ Sucrose myristate (M1695) /CCT +Ethanol	211
79.	5:77	Inhibition of the microbial activity of the <i>Escherichia coli</i> caused by system #15 W+PG/TMAZ80/CCT +Ethanol	214
80.	5:78	Diameter of inhibition zone (mm) as a function of surfactant concentration in CCT oil on <i>Escherichia coli</i>	216
81.	5:79	Comparison in diameter of inhibition zone against <i>Staphylococcus aureus</i> and <i>Escherichia coli</i> using W+PG/ TMAZ80+Sucrose myristate (M1695) /oil +Ethanol with equal unity of surfactants	218

List of figure numbers and descriptions

No.	# of Figure	Figure name and description	Page #
1.	Fig 1:1	Schematic illustration of surfactant molecule	1
2.	Fig 1:2	Effect of molecular geometry and system conditions on the packing parameter and HLB number	3
3.	Fig 1:3	Illustrate of the stages of micelle formation in phase diagram microemulsion	4
4.	Fig 1:4	Winsor classification of microemulsion	5
5.	Fig 4:1	The chemical structure of sucrose myristate M1695	17
6.	Fig 4:2	The chemical structure of sucrose polysorbate 80	18
7.	Fig 4:3	The chemical structure of R (+)-LIMonene oil	19
8.	Fig 4:4	The chemical structure of Isopropylmyristate oil	19
9.	Fig 4:5	The chemical structure of Caprylic/Capric Triglyceride oil	20
10.	Fig 4:6	The chemical structure of 1, 2-Propandiol (propylene glycol, PG).	21
11.	Fig 4:7	The chemical structure of Ethanol	21
12.	Fig 5:1	Phase diagram of the system#1 water+ propylene glycol/ Sucrose myristate(M1695) /LIM oil+ ethanol at 25°C.	28
13.	Fig 5:2	Phase diagram of the system#2 water+ propylene glycol/ TMAZ80+Sucrose myristate(M1695) /LIM oil+ ethanol at 25°C.	29
14.	Fig 5:3	Phase diagram of the system#3 water+ propylene glycol/ TMAZ80+Sucrose myristate(M1695) /LIM oil+ ethanol at 25°C.	30
15.	Fig 5:4	Phase diagram of the system #4 water+ propylene glycol/ TMAZ80 + Sucrose myristate(M1695) /LIM	31

		oil+ ethanol at 25°C.	
16.	Fig 5:5	Phase diagram of the system #5 water+ propylene glycol/ TMAZ80 /LIM oil+ ethanol at 25°C	32
17.	Fig 5:6	Phase diagram of the system #1 water+ propylene glycol/ Sucrose myristate(M1695) /LIM oil+ ethanol at 37°C.	33
18.	Fig 5:7	Phase diagram of the system #2 water+ propylene glycol/ TMAZ80+ Sucrose myristate(M1695) /LIM oil+ ethanol at 37°C.	34
19.	Fig 5:8	Phase diagram of the system #3 water+ propylene glycol/ TMAZ80+ Sucrose myristate(M1695) /LIM oil+ ethanol at 37°C.	35
20.	Fig 5:9	Phase diagram of the system #4 water+ propylene glycol/ TMAZ80 + Sucrose myristate(M1695) /LIM oil+ ethanol at 37°C.	36
21.	Fig 5:10	Phase diagram of the system #5 water+ propylene glycol/ TMAZ80/LIM oil+ ethanol at 37°C.	37
22.	Fig 5:11	Phase diagram of the system#1 water+ propylene glycol/ Sucrose myristate(M1695) /LIM oil+ ethanol at 45°C.	38
23.	Fig 5:12	Phase diagram of the system #2 water+ propylene glycol/ TMAZ80+ Sucrose myristate(M1695) /LIM oil+ ethanol at 45°C.	39
24.	Fig 5:13	Phase diagram of the system #3 water+ propylene glycol/ TMAZ80+ Sucrose myristate(M1695) /LIM oil+ ethanol at 45°C	40
25.	Fig 5:14	Phase diagram of the system #4 water+ propylene glycol/ TMAZ80+ Sucrose myristate(M1695) /LIM oil+ ethanol at 45°C.	41
26.	Fig 5:15	Phase diagram of the system #5 water+ propylene	42

		glycol/ TMAZ80 /LIM oil+ ethanol at 45°C.	
27.	Fig 5:16	Phase diagram of the system #6 water+ propylene glycol/ Sucrose myristate(M1695) /IPM oil+ ethanol at 25°C.	43
28.	Fig 5:17	Phase diagram of the system #7 water+ propylene glycol/ TMAZ80+ Sucrose myristate(M1695) /IPM oil+ ethanol at 25°C.	44
29.	Fig 5:18	Phase diagram of the system#8 water+ propylene glycol/ TMAZ80 + Sucrose myristate(M1695) /IPM oil+ ethanol at 25°C.	45
30.	Fig 5:19	Phase diagram of the system #9 water+ propylene glycol/ TMAZ80 + Sucrose myristate(M1695) /IPM oil+ ethanol at 25°C	46
31.	Fig 5:20	Phase diagram of the system #10 water+ propylene glycol/ TMAZ80 /IPM oil+ ethanol at 25°C.	47
32.	Fig 5:21	Phase diagram of the system #6 water+ propylene glycol/ Sucrose myristate(M1695) /IPM oil+ ethanol at 37°C.	48
33.	Fig 5:22	Phase diagram of the system #7 water+ propylene glycol/ TMAZ80+ Sucrose myristate(M1695) /IPM oil+ ethanol at 37°C.	49
34.	Fig 5:23	Phase diagram of the system #8 water+ propylene glycol/ TMAZ80+ Sucrose myristate(M1695) /IPM oil+ ethanol at 37°C.	50
35.	Fig 5:24	Phase diagram of the system #9 water+ propylene glycol/ TMAZ80 + Sucrose myristate(M1695) /IPM oil+ ethanol at 37°C.	51
36.	Fig 5:25	Phase diagram of the system #10 water+ propylene glycol/ TMAZ80/IPM oil+ ethanol at 37°C.	52
37.	Fig 5:26	Phase diagram of the system#6 water+ propylene	53

		glycol/ Sucrose myristate(M1695) /IPM oil+ ethanol at 45°C.	
38.	Fig 5:27	Phase diagram of the system #7 water+ propylene glycol/ TMAZ80+ Sucrose myristate(M1695) /IPM oil+ ethanol at 45°C.	54
39.	Fig 5:28	Phase diagram of the system#8 water+ propylene glycol/ TMAZ80+ Sucrose myristate(M1695) /IPM oil+ ethanol at 45°C.	55
40.	Fig 5:29	Phase diagram of the system#9 water+ propylene glycol/ TMAZ80 + Sucrose myristate(M1695) /IPM oil+ ethanol at 45°C.	56
41.	Fig 5:30	Phase diagram of the system#10 water+ propylene glycol/ TMAZ80/IPM oil+ ethanol at 45°C.	57
42.	Fig 5:31	Phase diagram of the system #11 water+ propylene glycol/ Sucrose myristate(M1695) /CCT oil+ ethanol at 25°C.	58
43.	Fig 5:32	Phase diagram of the system #12 water+ propylene glycol/ TMAZ80+ Sucrose myristate(M1695) /CCT oil+ ethanol at 25°C.	59
44.	Fig 5:33	Phase diagram of the system#13 water+ propylene glycol/ TMAZ80+ Sucrose myristate(M1695) /CCT oil+ ethanol at 25°C	60
45.	Fig 5:34	Phase diagram of the system #14 water+ propylene glycol/ TMAZ80+ Sucrose myristate(M1695) /CCT oil+ ethanol at 25°C.	61
46.	Fig 5:35	Phase diagram of the system#15 water+ propylene glycol/ TMAZ80 /CCT oil+ ethanol at 25°C.	62
47.	Fig 5:36	Phase diagram of the system#11 water+ propylene glycol/ Sucrose myristate(M1695) /CCT oil+ ethanol at 37°C.	63

48.	Fig 5:37	Phase diagram of the system#12 water+ propylene glycol/ TMAZ80+ Sucrose myristate(M1695) /CCT oil+ ethanol at 37°C.	64
49.	Fig 5:38	Phase diagram of the system #13 water+ propylene glycol/ TMAZ80+ Sucrose myristate(M1695) /CCT oil+ ethanol at 37°C.	65
50.	Fig 5:39	Phase diagram of the system #14 water+ propylene glycol/ TMAZ80+ Sucrose myristate(M1695) /CCT oil+ ethanol at 37°C.	66
51.	Fig 5:40	Phase diagram of the system#15 water+ propylene glycol/ TMAZ80 /CCT oil+ ethanol at 37°C.	67
52.	Fig 5:41	Phase diagram of the system #11 water+ propylene glycol/ Sucrose myristate(M1695) /CCT oil+ ethanol at 45°C.	68
53.	Fig 5:42	Phase diagram of the system #12 water+ propylene glycol/ TMAZ80+ Sucrose myristate(M1695) /CCT oil+ ethanol at 45°C.	69
54.	Fig 5:43	Phase diagram of the system #13 water+ propylene glycol/ TMAZ80+ Sucrose myristate(M1695) /CCT oil+ ethanol at 45°C.	70
55.	Fig 5:44	Phase diagram of the system #14 water+ propylene glycol/ TMAZ80+ Sucrose myristate(M1695) /CCT oil+ ethanol at 45°C.	71
56.	Fig 5:45	Phase diagram of the system#15 water+ propylene glycol/ TMAZ80/CCT oil+ ethanol at 45°C.	72
57.	Fig 5:46	Solubilization parameters for a schematic phase diagram.	73
58.	Fig 5:47	Variation of the total monophasic region area A_T (%) as function of surfactants ratio TMAZ80/sucrose myristate M1695 with LIM oil at different	75

		temperatures(25,37,and 45 °C).	
59.	Fig 5:48	Variation of the total monophasic region area A_T (%) as function of surfactants ratio TMAZ80/sucrose myristate M1695 with IPM oil at different temperatures(25,37, and 45 °C).	76
60.	Fig 5:49	Variation of the total monophasic region area A_T (%) as function of surfactants ratio TMAZ80/sucrose myristate M1695 with CCT oil at different temperatures(25,37, and 45 °C).	78
61.	Fig 5:50	Variation of the total monophasic region area A_T (%) as function of type of oil at different temperatures(25,37, and 45 °C).	79
62.	Fig 5:51	Variation of the total monophasic region area A_T (%) as function of different temperatures (25,37, and 45 °C) for the used oils.	80
63.	Fig 5:52	Variation of the electrical conductivity (σ) of the system# 1 MT0LE W+PG/ Sucrose myristate (M1695) /LIM+ Ethanol as function of aqueous content along the dilution line N65. The phase diagrams is presented in Figures (5:1),(5:6),(5:11) at different temperatures (25, 37 and 45°C)respectively .	84
64.	Fig 5:53	Variation of the electrical conductivity (σ) of the system# 2 MT25LE W+PG/TMAZ80+ Sucrose myristate (M1695) /LIM+ Ethanol as function of aqueous content along the dilution line N65. The phase diagrams is presented in Figures (5:2),(5:7),(5:12) at different temperatures (25, 37 and 45°C)respectively .	86
65.	Fig 5:54	Variation of the electrical conductivity (σ) of the system# 3 MT50LE W+PG/TMAZ80+ Sucrose myristate (M1695) /LIM+ Ethanol as function of aqueous content along the dilution line N65. The phase	87

		diagrams is presented in Figures (5:3),(5:8),(5:13) at different temperatures (25, 37 and 45°C)respectively .	
66.	Fig 5:55	Variation of the electrical conductivity (σ) of the system # 4 MT75LE W+PG/TMAZ80+ Sucrose myristate (M1695) /LIM+ Ethanol as function of aqueous content along the dilution line N65. The phase diagrams is presented in Figures (5:4),(5:9),(5:14) at different temperatures (25, 37 and 45°C)respectively .	89
67.	Fig 5:56	Variation of the electrical conductivity (σ) of the system # 5 MT100LE W+PG/TMAZ80/LIM+ Ethanol as function of aqueous content along the dilution line N65. The phase diagrams is presented in Figures (5:5),(5:10),(5:15) at different temperatures (25, 37 and 45°C)respectively .	90
68.	Fig 5:57	Variation of the electrical conductivity (σ) of the system # 6 MT11E W+PG/ Sucrose myristate (M1695) /IPM+ Ethanol as function of aqueous content along the dilution line N65. The phase diagrams is presented in Figures (5:16),(5:21),(5:26) at different temperatures (25, 37 and 45°C)respectively .	92
69.	Fig 5:58	Variation of the electrical conductivity (σ) of the system # 7 MT25IE W+PG/ TMAZ80+Sucrose myristate (M1695) /IPM+ Ethanol as function of aqueous content along the dilution line N65. The phase diagrams is presented in Figures (5:17),(5:22),(5:27) at different temperatures (25, 37 and 45°C)respectively .	93
70.	Fig 5:59	Variation of the electrical conductivity (σ) of the system # 8 MT50IE W+PG/ TMAZ80+Sucrose myristate (M1695) /IPM+ Ethanol as function of aqueous content along the dilution line N65. The phase diagrams is presented in Figures (5:18),(5:23),(5:28) at	95

		different temperatures (25,37 and 45°C)respectively .	
71.	Fig 5:60	Variation of the electrical conductivity (σ) of the system # 9 MT75IE W+PG/ TMAZ80+Sucrose myristate (M1695) /IPM+ Ethanol as function of aqueous content along the dilution line N65. The phase diagrams is presented in Figures (5:19),(5:24),(5:29) at different temperatures (25, 37 and 45°C)respectively .	96
72.	Fig 5:61	Variation of the electrical conductivity (σ) of the system # 10 MT100IE W+PG/ TMAZ80+Sucrose myristate (M1695) /IPM+ Ethanol as function of aqueous content along the dilution line N65. The phase diagrams is presented in Figures (5:20),(5:25),(5:30) at different temperatures (25, 37 and 45°C)respectively .	98
73.	Fig 5:62	Variation of the electrical conductivity (σ) of the system # 11 MT0CE W+PG/ Sucrose myristate (M1695) /CCT+ Ethanol as function of aqueous content along the dilution line N65. The phase diagrams is presented in Figures (5:31),(5:36),(5:41) at different temperatures (25, 37 and 45°C)respectively .	99
74.	Fig 5:63	Variation of the electrical conductivity (σ) of the system # 12 MT25CE W+PG/TMAZ80+ Sucrose myristate (M1695) /CCT+ Ethanol as function of aqueous content along the dilution line N65. The phase diagrams is presented in Figures (5:32),(5:37),(5:42) at different temperatures (25, 37 and 45°C)respectively .	101
75.	Fig 5:64	Variation of the electrical conductivity (σ) of the system # 13 MT50CE W+PG/TMAZ80+ Sucrose myristate (M1695) /CCT+ Ethanol as function of aqueous content along the dilution line N65. The phase diagrams is presented in Figures (5:33),(5:38),(5:43) at different temperatures (25, 37 and 45°C)respectively .	102

76.	Fig 5:65	Variation of the electrical conductivity (σ) of the system # 14 MT75CE W+PG/TMAZ80+ Sucrose myristate (M1695) /CCT+ Ethanol as function of aqueous content along the dilution line N65. The phase diagrams is presented in Figures (5:34),(5:39),(5:44) at different temperatures (25, 37 and 45°C)respectively .	104
77.	Fig 5:66	Variation of the electrical conductivity (σ) of the system # 15 MT100CE W+PG/TMAZ80/CCT+ Ethanol as function of aqueous content along the dilution line N65. The phase diagrams is presented in Figures (5:35),(5:40),(5:45) at different temperatures (25, 37 and 45°C)respectively .	105
78.	Fig 5:67	Variation of the electrical conductivity (σ) for the system W+PG/TMAZ80+ Sucrose myristate (M1695) /oil+ Ethanol as function of water content along the dilution line N65 for different oils (LIM,IPM,CCT) ,mixing surfactant ratio equal unity at 25°C. The phase diagrams are presented in figures (5:54), (5:59), (5:64) respectively.	109
79.	Fig 5:68	Variation of the density (ρ) of the system # 1 W+PG/ Sucrose myristate (M1695) /LIM +Ethanol as function of aqueous content along the dilution line N65 at different temperatures. The phase diagrams is presented in Figures (5:1),(5:6),(5:11) at different temperatures (25, 37 and 45°C)respectively .	111
80.	Fig 5:69	Variation of the density (ρ) of the system # 2 W+PG/ TMAZ80+Sucrose myristate (M1695) /LIM +Ethanol as function of aqueous content along the dilution line N65 at different temperatures. The phase diagrams is presented in Figures (5:2),(5:7),(5:12) at different temperatures (25, 37 and 45°C)respectively .	112

81.	Fig 5:70	Variation of the density (ρ) of the system # 3 W+PG/TMAZ80+Sucrose myristate (M1695) /LIM +Ethanol as function of aqueous content along the dilution line N65 at different temperatures. The phase diagrams is presented in Figures (5:3),(5:8),(5:13) at different temperatures (25, 37 and 45°C)respectively .	114
82.	Fig 5:71	Variation of the density (ρ) of the system # 4 W+PG/TMAZ80+Sucrose myristate (M1695) /LIM +Ethanol as function of aqueous content along the dilution line N65 at different temperatures. The phase diagrams is presented in Figures (5:4),(5:9),(5:14) at different temperatures (25, 37 and 45°C)respectively .	116
83.	Fig 5:72	Variation of the density (ρ) of the system # 5 W+PG/TMAZ80 /LIM +Ethanol as function of aqueous content along the dilution line N65 at different temperatures. The phase diagrams is presented in Figures (5:5),(5:10),(5:15) at different temperatures (25, 37 and 45°C)respectively .	118
84.	Fig 5: 73	Variation of the density (ρ) of the system # 6 W+PG/Sucrose myristate (M1695) /IPM +Ethanol as function of aqueous content along the dilution line N65 at different temperatures. The phase diagrams is presented in Figures (5:16),(5:21),(5:26) at different temperatures (25, 37 and 45°C)respectively .	119
85.	Fig 5:74	Variation of the density (ρ) of the system # 7 W+PG/TMAZ80+ Sucrose myristate (M1695) /IPM +Ethanol as function of aqueous content along the dilution line N65 at different temperatures. The phase diagrams is presented in Figures (5:17),(5:22),(5:27) at different temperatures (25, 37 and 45°C)respectively	121
86.	Fig 5:75	Variation of the density (ρ) of the system # 8	123

		W+PG/TMAZ80+ Sucrose myristate (M1695) /IPM +Ethanol as function of aqueous content along the dilution line N65 at different temperatures. The phase diagrams is presented in Figures (5:18),(5:23),(5:28) at different temperatures (25, 37 and 45°C)respectively .	
87.	Fig 5:76	Variation of the density (ρ) of the system # 9 W+PG/TMAZ80+ Sucrose myristate (M1695) /IPM +Ethanol as function of aqueous content along the dilution line N65 at different temperatures. The phase diagrams is presented in Figures (5:19),(5:24),(5:29) at different temperatures (25, 37 and 45°C)respectively .	125
88.	Fig 5:77	Variation of the density (ρ) of the system # 10 W+PG/TMAZ80/IPM +Ethanol as function of aqueous content along the dilution line N65 at different temperatures. The phase diagrams is presented in Figures (5:20),(5:25),(5:30) at different temperatures (25, 37, and 45°C)respectively .	127
89.	Fig 5:78	Variation of the density (ρ) of the system # 11 W+PG/ Sucrose myristate (M1695) /CCT +Ethanol as function of aqueous content along the dilution line N65 at different temperatures. The phase diagrams is presented in Figures (5:31),(5:36),(5:41) at different temperatures (25, 37, and 45°C)respectively .	129
90.	Fig 5:79	Variation of the density (ρ) of the system # 12 W+PG/TMAZ80+Sucrose myristate (M1695) /CCT +Ethanol as function of aqueous content along the dilution line N65 at different temperatures. The phase diagrams is presented in Figures (5:32),(5:37),(5:42) at different temperatures (25, 37, and 45°C)respectively .	131
91.	Fig 5:80	Variation of the density (ρ) of the system # 13 W+PG/TMAZ80+Sucrose myristate (M1695) /CCT	133

		+Ethanol as function of aqueous content along the dilution line N65 at different temperatures. The phase diagrams is presented in Figures (5:33),(5:38),(5:43) at different temperatures (25, 37, and 45°C)respectively .	
92.	Fig 5:81	Variation of the density (ρ) of the system # 14 W+PG/TMAZ80+Sucrose myristate (M1695) /CCT +Ethanol as function of aqueous content along the dilution line N65 at different temperatures. The phase diagrams is presented in Figures (5:34),(5:39),(5:44) at different temperatures (25, 37, and 45°C)respectively	135
93.	Fig 5:82	Variation of the density (ρ) of the system # 15 W+PG/TMAZ80 /CCT +Ethanol as function of aqueous content along the dilution line N65 at different temperatures. The phase diagrams is presented in Figures (5:35),(5:40),(5:45) at different temperatures (25, 37, and 45°C)respectively .	137
94.	Fig 5:83	Variation of the ultrasonic velocity of the system # 1 W+PG/ Sucrose myristate (M1695) /LIM +Ethanol as function of aqueous content along the dilution line N65 at different temperatures. The phase diagrams is presented in Figures (5:1),(5:6),(5:11) at different temperatures (25, 37, and 45°C)respectively .	139
95.	Fig 5:84	Variation of the ultrasonic velocity of the system # 2 W+PG/ TMAZ80+Sucrose myristate (M1695) /LIM +Ethanol as function of aqueous content along the dilution line N65 at different temperatures. The phase diagrams are presented in figures (5:2),(5:7),(5:12) at different temperatures (25,37,and 45°C)respectively.	140
96.	Fig 5:85	Variation of the ultrasonic velocity of the system # 3 W+PG/ TMAZ80+Sucrose myristate (M1695) /LIM +Ethanol as function of aqueous content along the	142

		dilution line N65 at different temperatures. The phase diagrams are presented in figures (5:3),(5:8),(5:13) at different temperatures (25,37,and 45°C)respectively.	
97.	Fig 5:86	Variation of the ultrasonic velocity of the system # 4 W+PG/ TMAZ80+Sucrose myristate (M1695) /LIM +Ethanol as function of aqueous content along the dilution line N65 at different temperatures. The phase diagrams are presented in figures (5:4),(5:9),(5:14) at different temperatures (25,37,and 45°C)respectively.	144
98.	Fig 5:87	Variation of the ultrasonic velocity of the system # 5 W+PG/ TMAZ80+Sucrose myristate (M1695) /LIM +Ethanol as function of aqueous content along the dilution line N65 at different temperatures. The phase diagrams are presented in figures (5:5),(5:10),(5:15) at different temperatures (25,37,and 45°C)respectively.	146
99.	Fig 5:88	Variation of the ultrasonic velocity of the system # 6 W+PG/ Sucrose myristate (M1695) /IPM +Ethanol as function of aqueous content along the dilution line N65 at different temperatures. The phase diagrams are presented in figures (5:16),(5:21),(5:26) at different temperatures (25,37,and 45°C)respectively.	148
100.	Fig 5:89	Variation of the ultrasonic velocity of the system # 7 W+PG/ TMAZ80+Sucrose myristate (M1695) /IPM +Ethanol as function of aqueous content along the dilution line N65 at different temperatures. The phase diagrams are presented in figures (5:17),(5:22),(5:27) at different temperatures (25,37,and 45°C)respectively.	150
101.	Fig :90	Variation of the ultrasonic velocity of the system # 8 W+PG/ TMAZ80+Sucrose myristate (M1695) /IPM +Ethanol as function of aqueous content along the dilution line N65 at different temperatures. The phase	152

		diagrams are presented in figures (5:18),(5:23),(5:28) at different temperatures (25,37,and 45°C)respectively.	
102.	Fig 5:91	Variation of the ultrasonic velocity of the system # 9 W+PG/ TMAZ80+Sucrose myristate (M1695) /IPM +Ethanol as function of aqueous content along the dilution line N65 at different temperatures. The phase diagrams are presented in figures (5:19),(5:24),(5:29) at different temperatures (25,37,and 45°C)respectively.	154
103.	Fig 5:92	Variation of the ultrasonic velocity of the system # 10 W+PG/ TMAZ80/IPM +Ethanol as function of aqueous content along the dilution line N65 at different temperatures. The phase diagrams are presented in figures (5:20),(5:25),(5:30) at different temperatures (25,37,and 45°C)respectively.	156
104.	Fig 5:93	Variation of the ultrasonic velocity of the system # 11 W+PG/ Sucrose myristate (M1695) /CCT +Ethanol as function of aqueous content along the dilution line N65 at different temperatures. The phase diagrams are presented in figures (5:31),(5:36),(5:41) at different temperatures (25,37,and 45°C)respectively.	158
105.	Fig 5:94	Variation of the ultrasonic velocity of the system # 12 W+PG/TMAZ80+ Sucrose myristate (M1695) /CCT +Ethanol as function of aqueous content along the dilution line N65 at different temperatures. The phase diagrams are presented in figures (5:32),(5:37),(5:42) at different temperatures (25,37,and 45°C)respectively.	160
106.	Fig 5:95	Variation of the ultrasonic velocity of the system # 13 W+PG/TMAZ80+ Sucrose myristate (M1695) /CCT +Ethanol as function of aqueous content along the dilution line N65 at different temperatures. The phase diagrams are presented in figures (5:33),(5:38),(5:43)	162

		at different temperatures (25,37,and 45°C)respectively	
107.	Fig 5:96	Variation of the ultrasonic velocity of the system # 14 W+PG/TMAZ80+ Sucrose myristate (M1695) /CCT +Ethanol as function of aqueous content along the dilution line N65 at different temperatures. The phase diagrams are presented in figures (5:34),(5:39),(5:44) at different temperatures (25,37,and45°C)respectively.	164
108.	Fig 5:97	Variation of the ultrasonic velocity of the system # 15 W+PG/TMAZ80/CCT +Ethanol as function of aqueous content along the dilution line N65 at different temperatures. The phase diagrams are presented in figures (5:35),(5:40),(5:45) at different temperatures (25,37,and 45°C)respectively.	166
109.	Fig 5:98	Diameter of inhibition zone (mm) for individual contents on <i>Staphylococcus aureus</i>	168
110.	Fig 5:99	Diameter of inhibition zone (mm) for individual contents on <i>Escherichia coli</i> .	168
111.	Fig 5:100	Inhibition of the microbial growth of the <i>Staphylococcus aureus</i> caused by system #1 W+PG/ Sucrose myristate (M1695) /LIM +Ethanol as function of aqueous content along the dilution line N65. The phase diagrams are presented in figures (5:1),(5:6),(5:11) at different temperatures (25,37,and 45°C)respectively .	170
112.	Fig 5:101	Diameter of inhibition zone (mm) for system #1 W+PG/Sucrose myristate M(1695)/LIM+EOH on <i>Staphylococcus aureus</i>	170
113.	Fig 5:102	Inhibition of the microbial growth of the <i>Staphylococcus aureus</i> caused by system #2 W+PG/ TMAZ80+Sucrose myristate (M1695) /LIM +Ethanol as function of aqueous content along the dilution line	172

		N65. The phase diagrams are presented in figures (5:2),(5:7),(5:12) at different temperatures (25,37,and 45°C)respectively .	
114.	Fig 5:103	Diameter of inhibition zone (mm) for system #2 W+PG/TMAZ+ Sucrose myristate M(1695)/LIM+EOH on <i>Staphylococcus aureus</i>	172
115.	Fig 5:104	Inhibition of the microbial growth of the <i>Staphylococcus aureus</i> caused by system #3 W+PG/TMAZ80+Sucrose myristate (M1695) /LIM +Ethanol as function of aqueous content along the dilution line N65. The phase diagrams are presented in figures (5:3),(5:8),(5:13) at different temperatures (25,37,and 45°C)respectively	174
116.	Fig 5:105	Diameter of inhibition zone (mm) for system #3 W+PG/TMAZ+Sucrose myristate M(1695)/LIM+EOH on <i>Staphylococcus aureus</i>	175
117.	Fig 5:106	Comparison of the microbial inhibition of the <i>Staphylococcus aureus</i> growth as a function of surfactant concentration using LIM oil .W+PG/TMAZ80+Sucrose myristate (M1695) /LIM +Ethanol	177
118.	Fig 5:107	Inhibition of the microbial growth of the <i>Staphylococcus aureus</i> caused by system #6 W+PG/Sucrose myristate (M1695) /IPM +Ethanol as function of aqueous content along the dilution line N65. The phase diagrams are presented in figures (5:16),(5:21),(5:26) at different temperatures (25,37,and 45°C)respectively .	179
119.	Fig 5:108	Diameter of inhibition zone (mm) for system #6 W+PG/Sucrose myristate M(1695)/IPM+EOH on <i>Staphylococcus aureus</i>	179

120.	Fig 5:109	Inhibition of the microbial growth of the <i>Staphylococcus aureus</i> caused by system #7 W+PG/ TMAZ80+Sucrose myristate (M1695) /IPM +Ethanol as function of aqueous content along the dilution line N65. The phase diagrams are presented in figures (5:17),(5:22),(5:27) at different temperatures (25,37,and 45°C)respectively .	181
121.	Fig 5:110	Inhibition of the microbial growth of the <i>Staphylococcus aureus</i> caused by system #8 W+PG/ TMAZ80+Sucrose myristate (M1695) /IPM +Ethanol as function of aqueous content along the dilution line N65. The phase diagrams are presented in figures (5:18),(5:23),(5:28) at different temperatures (25,37,and 45°C)respectively .	183
122.	Fig 5:111	Diameter of inhibition zone (mm) for system #8 W+PG/ TMAZ80+ Sucrose myristate M (1695)/ IPM+EOH on <i>Staphylococcus aureus</i>	183
123.	Fig 5:112	Comparison of the microbial inhibition of the <i>Staphylococcus aureus</i> growth as a function of surfactant concentration using IPM oil .W+PG/ TMAZ80+Sucrose myristate (M1695) /IPM +Ethanol	185
124.	Fig 5:113	Inhibition of the microbial growth of the <i>Staphylococcus aureus</i> caused by system #11 W+PG/ Sucrose myristate (M1695) /CCT +Ethanol as function of aqueous content along the dilution line N65. The phase diagrams are presented in figures (5:31),(5:36),(5:41) at different temperatures (25,37,and 45°C)respectively .	187
125.	Fig 5:114	Diameter of inhibition zone (mm) for system #11 W+PG/Sucrose myristate M(1695)/CCT+EOH on <i>Staphylococcus aureus</i>	187

126.	Fig 5:115	Inhibition of the microbial growth of the <i>Staphylococcus aureus</i> caused by system #12 W+PG/TMAZ80+Sucrose myristate (M1695) /CCT +Ethanol as function of aqueous content along the dilution line N65. The phase diagrams are presented in figures (5:32),(5:37),(5:42) at different temperatures (25,37,and 45°C) respectively .	189
127.	Fig 5:116	Diameter of inhibition zone (mm) for system #12 W+PG/TMAZ80+Sucrose myristate M(1695)/CCT+EOH on <i>Staphylococcus aureus</i>	189
128.	Fig 5:117	Comparison of the microbial inhibition of the <i>Staphylococcus aureus</i> growth as a function of surfactant concentration using CCT oil .W+PG/TMAZ80+Sucrose myristate (M1695) /CCT +Ethanol.	191
129.	Fig 5:118	Inhibition of the microbial growth of the <i>Escherichia coli</i> caused by system #1 W+PG/ Sucrose myristate (M1695) /LIM +Ethanol as function of aqueous content along the dilution line N65. The phase diagrams are presented in figures (5:1),(5:6),(5:11) at different temperatures (25,37,and 45°C)respectively .	193
130.	Fig 5:119	Diameter of inhibition zone (mm) for system #1 W+PG/ Sucrose myristate M (1695) / LIM + EOH on <i>Escherichia coli</i>	193
131.	Fig 5:120	Inhibition of the microbial growth of the <i>Escherichia coli</i> caused by system #2 W+PG/TMAZ80+ Sucrose myristate (M1695) /LIM +Ethanol as function of aqueous content along the dilution line N65. The phase diagrams are presented in figures (5:2),(5:7),(5:12) at different temperatures (25,37,and 45°C)respectively .	195
132.	Fig 5:121	Diameter of inhibition zone (mm) for system #2 W+PG/ TMAZ80+Sucrose myristate M (1695) / LIM + EOH on <i>Escherichia coli</i>	195

133.	Fig 5:122	Inhibition of the microbial growth of the <i>Escherichia coli</i> caused by system #3 W+PG/TMAZ80+ Sucrose myristate (M1695) /LIM +Ethanol as function of aqueous content along the dilution line N65. The phase diagrams are presented in figures (5:3),(5:8),(5:13) at different temperatures (25,37,and 45°C)respectively .	197
134.	Fig 5:123	Diameter of inhibition zone (mm) for system #3 W+PG/TMAZ80+Sucrose myristate M(1695) /LIM+EOH on <i>Escherichia coli</i>	197
135.	Fig 5:124	Comparison of the microbial inhibition of the <i>Escherichia coli</i> growth as a function of surfactant concentration using LIM oil .W+PG/ TMAZ80+Sucrose myristate (M1695) /LIM +Ethanol.	199
136.	Fig 5:125	Inhibition of the microbial growth of the <i>Escherichia coli</i> caused by system #6 W+PG/ Sucrose myristate (M1695) /IPM +Ethanol as function of aqueous content along the dilution line N65. The phase diagrams are presented in figures (5:16),(5:21),(5:26) at different temperatures (25,37,and 45°C)respectively	201
137.	Fig 5:126	Diameter of inhibition zone (mm) for system #6 W+PG/ Sucrose myristate M (1695) / IPM +EOH on <i>Escherichia coli</i>	202
138.	Fig 5:127	Inhibition of the microbial growth of the <i>Escherichia coli</i> caused by system #7 W+PG/TMAZ80+ Sucrose myristate (M1695) /IPM +Ethanol as function of aqueous content along the dilution line N65. The phase diagrams are presented in figures (5:17),(5:22),(5:27) at different temperatures (25,37,and 45°C)respectively	204
139.	Fig 5:128	Diameter of inhibition zone (mm) for system #7 W+PG/TMAZ80+Sucrose myristate M(1695)/IPM+EOH on <i>Escherichia coli</i>	204

140.	Fig 5:129	Inhibition of the microbial growth of the <i>Escherichia coli</i> caused by system #8 W+PG/TMAZ80+ Sucrose myristate (M1695) /IPM +Ethanol as function of aqueous content along the dilution line N65. The phase diagrams are presented in figures (5:18),(5:23),(5:28) at different temperatures (25,37,and 45°C)respectively	206
141.	Fig 5:130	Diameter of inhibition zone (mm) for system #8 W+PG/TMAZ80+Sucrose myristate M(1695)/IPM+EOH on <i>Escherichia coli</i>	206
142.	Fig 5:131	Comparison of the microbial inhibition of the <i>Escherichia coli</i> growth as a function of surfactant concentration using IPM oil .W+PG/ TMAZ80+Sucrose myristate (M1695) /IPM +Ethanol.	208
143.	Fig 5:132	Inhibition of the microbial growth of the <i>Escherichia coli</i> caused by system #11 W+PG/ Sucrose myristate (M1695) /CCT +Ethanol as function of aqueous content along the dilution line N65. The phase diagrams are presented in figures (5:31),(5:36),(5:41) at different temperatures (25,37,and 45°C)respectively	210
144.	Fig 5:133	Diameter of inhibition zone (mm) for system #11 W+PG/ Sucrose myristate M (1695) /CCT+EOH on <i>Escherichia coli</i>	210
145.	Fig 5:134	Inhibition of the microbial growth of the <i>Escherichia coli</i> caused by system #13 W+PG/TMAZ80+ Sucrose myristate (M1695) /CCT +Ethanol as function of aqueous content along the dilution line N65. The phase diagrams are presented in figures (5:33),(5:38),(5:43) at different temperatures (25,37,and 45°C)respectively	212
146.	Fig 5:135	Diameter of inhibition zone (mm) for system #13 W+PG/ TMAZ 80+ Sucrose myristate M (1695) /CCT+EOH on <i>Escherichia coli</i>	213

147.	Fig 5:136	Inhibition of the microbial growth of the <i>Escherichia coli</i> caused by system #15 W+PG/TMAZ80/CCT +Ethanol as function of aqueous content along the dilution line N65. The phase diagrams are presented in figures (5:35),(5:40),(5:45) at different temperatures (25,37,and 45°C)respectively .	215
148.	Fig 5:137	Comparison of the microbial inhibition of the <i>Escherichia coli</i> growth as a function of surfactant concentration using CCT oil .W+PG/ TMAZ80+Sucrose myristate (M1695) /CCT +Ethanol.	217
149.	Fig 5:138	Comparison of the microbial inhibition of the <i>Staphylococcus aureus</i> and <i>Escherichia coli</i> growth using W+PG/ TMAZ80+Sucrose myristate (M1695) /LIM +Ethanol with equal unity of surfactant	219
150.	Fig 5:139	Comparison of the microbial inhibition of the <i>Staphylococcus aureus</i> and <i>Escherichia coli</i> growth using W+PG/ TMAZ80+Sucrose myristate (M1695) /IPM +Ethanol with equal unity of surfactants.	219
151.	Fig 5:140	Viewing all the results for system #1 W+PG/ Sucrose myristate M (1695) /LIM+EOH	221
152.	Fig 5:141	Viewing all the results for system #2 W+PG/ TMAZ80 + Sucrose myristate M (1695) /LIM+EOH	222
153.	Fig 5:142	Viewing all the results for system #3 W+PG/ TMAZ80 +Sucrose myristate M (1695) /LIM+EOH	223
154.	Fig 5:143	Viewing all the results for system #6W+PG/ Sucrose myristate M (1695) /IPM+EOH	224
155.	Fig 5:144	Viewing all the results for system #7 W+PG/ TMAZ80 + Sucrose myristate M (1695) /IPM+EOH	225
156.	Fig 5:145	Viewing all the results for system #8 W+PG/ TMAZ80 + Sucrose myristate M (1695) /IPM+EOH	226
157.	Fig 5:146	Viewing all the results for system #11 W+PG/ Sucrose	227

		myristate M (1695) /CCT+EOH	
158.	Fig 5:147	Viewing all the results for system #12W+PG/TMAZ80 + Sucrose myristate M (1695) /CCT+EOH	228
159.	Fig 5:148	Viewing all the results for system #13W+PG/TMAZ80 + Sucrose myristate M (1695) /CCT+EOH	229
160.	Fig 5:149	Viewing all the results for system #15W+PG/TMAZ80 + Sucrose myristate M (1695) /CCT+EOH	230

Abbreviations, Symbols & Terminology:

CCT: Caprylic-capric triglyceride oil

LIM: R (+)-limonene oil

IPM: Isopropylmyristate oil

M1695: Sucrose myristate

SE: Sucrose ester

TMAZ80: Sucrose polysorbate 80

A_T (%): Total one-phase microemulsion area (total monophasic area)

Co-S: Cosurfactant

EOH: Ethanol

HLB: Hydrophilic-lipophilic balance

IFT: Interfacial tension

ME: Microemulsion

O/W: Oil in water

W/O: Water in oil

O: Oil

W: Water

PG: Propylene glycol

PIT: Phase inversion temperature

S: Surfactant

S_m : The amount of surfactant needed to obtain maximum water solubilization

W_m : The maximum amount of solubilized water

Winsor I: Oil-in-water microemulsion coexists with excess oil

Winsor II: Water-in-oil microemulsion coexists with excess water

Winsor III: Bicontinuous middle phase microemulsion

Winsor IV: Microemulsion which is not in equilibrium with oil or water

μS : Microsiemens

ρ : Density

σ : Electrical conductivity

USV: Ultrasonic velocity

1Φ: One phase

ATCC: American Tube Culture Collection

Chapter one

Introduction

It is a well-known that oil and water do not mix, this is because hydrocarbon molecules are non-polar and cannot interact strongly with the polar water molecules, which have to be forced apart to incorporate the hydrocarbon solute molecules. When oil and water are vigorously shaken together a droplet emulsion can be formed. This mixture will destabilize fairly quickly and phase-separate into oil and water, typically within less than an hour, because of the high interfacial energy of the oil–water droplets. The stability of these emulsions can be enhanced by the addition of surfactants which will reduce the interfacial energy of the droplets. (Richard) ₁

Surface active agent or simply "surfactant", is a general term used to describe molecules that interact with an interface. amphiphilic compounds consist of two parts, one of which is highly soluble in one of the phases while the other is not (Goodwin)₂. They are classified according to their chemical structure into four categories, all consist of a hydrophobic tail (water hating) which is usually a hydrocarbon, and differ in the polar hydrophilic head (water loving) which may be ; anionic surfactants which are dissociated in water in an amphiphilic anion, and a cation, nonionic surfactant (the type that will be used in this study as sugar base surfactant) they do not ionize in aqueous solution, because their hydrophilic group is of a non-dissociable type, such as alcohol, phenol, ether, ester, or amide. Cationic surfactants are dissociated in water into an amphiphilic cation and an anion and amphoteric or zwitterionic have two functional group, one anionic and one cationic, they are quite biocompatible, and are used in pharmaceuticals and cosmetics like amino acids (Eastoe)₃. as shown in the fig (1:1)

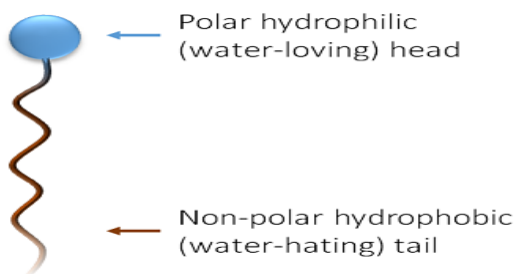


Fig 1:1 Schematic illustration of surfactant molecule .

Being amphiphilic compounds, when added they adsorb so effectively at the water–air interface and, they substantially reduce its surface energy, also have remarkable ability to self-assemble in aqueous solution leading to formation of self-assembled structures called ‘micelles’. micelle formed at specific concentration due to hydrophobic driving force at which the surfactant molecule reline and the polar head will react with the water molecules by hydrogen bonding and to each other by electrostatic force (if charged) forming and the nonpolar tail to each other by London force, and this formed micelle dispersed in water phase with surfactant–oil (A_{co}) and surfactant–water cohesive force (A_{cw}). Using non ionic surfactants forms W/O microemulsion which formation and stability are controlled by different parameters. Winsor expressed qualitative relation to describe the tendency formation and roles the packing parameter in microemulsion formation ;

$$R = A_{co} / A_{cw}$$

R-ratio of cohesive energies, stemming from interaction of the interfacial layer with oil, divided by energies resulting from interactions with water, determines the preferred interfacial curvature. $R > 1$; the interface tends to increase its area of contact with oil while decreasing its area of contact with water. Thus oil tends to become the continuous phase and the corresponding characteristic system is (Winsor II) related surfactant molecular structure to interfacial film curvature topology ; the curvature is governed by relative areas of the head group, a_o , and the tail group, v/l_c . Relation between these two parameters predicts the microemulsion formed as follows:

if $a_o > v/l_c$, then an oil-in-water microemulsion forms

if $a_o < v/l_c$, then a water-in-oil microemulsion forms

if $a_o \approx v/l_c$, then a middle-phase microemulsion is the preferred structure. (Microemulsion)₄

The spontaneous film curvature (H_0); the curvature that the amphiphilic film would like to attain, describes the microstructure of the microemulsion and the elasticity (κ) of the amphiphilic film describes the elastic properties of the surfactant film affect the phase behavior and the microstructure of microemulsions. These two parameters describes how difficult it is to deform the amphiphilic film. For $H_0 > 0$, the surfactant film is convex toward water (O/W droplet microemulsion). For H_0 close to 0, bicontinuous microemulsions or lamellar liquid crystalline phases are formed. If $H_0 < 0$ the surfactant film is convex toward oil (W/O droplet microemulsion).

H_0 can be affected by the nature of the surfactant and the composition of the polar and apolar phases. (Fanun)₅

Griffin introduced relation between molecular structure to interfacial packing and film curvature is HLB, the hydrophilic–lipophilic balance which is expressed as an empirical equation based on the relative proportions of hydrophobic and hydrophilic groups within the molecule. measures to which degree a surfactant is hydrophilic or lipophilic, enable the correct type of surfactant to be chosen. It a scale (0-20). Low HLB value surfactants such as sorbitan monoesters are preferred for water in oil (w/o) emulsion, while high HLB surfactants such as polysorbate 80 are preferred for oil in water (o/w) emulsions.

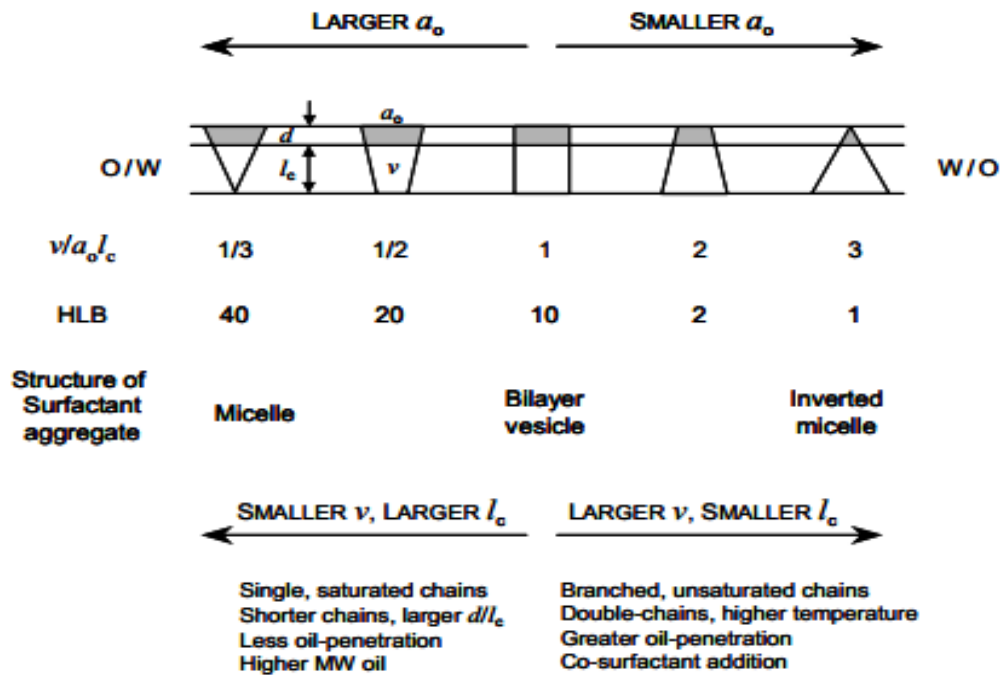
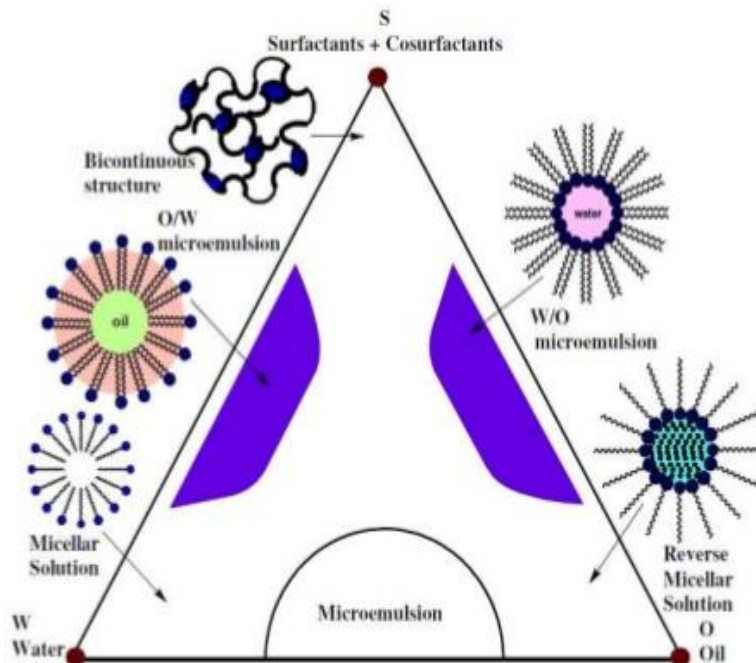


Fig 1:2 Effect of molecular geometry and system conditions on the packing parameter and HLB number

Critical micelle concentration', or CMC is the concentration at which micelles are formed is a characteristic of the particular surfactant . Spherical normal micelles (L1) are formed at high water content (oil/water), while revered micelle (L2) are formed at high oil content (water/oil), between these two phases exists an intermediate situation forming different stages (liquid crystals ,bilayer) . Microemulsions are usually characterized by ternary phase diagram, which three edges are the components of a microemulsion; namely oil, water and surfactant. Any co-surfactant used are usually

grouped together with the surfactant at a fixed ratio and treated as a pseudo-component (Griffin)⁶ as illustrated in Fig(1.3)



Malik M.A. *et al*, Arabian Journal of Chemistry (2012) 5, 397–417

Fig 1:3 Schematic illustrate of the stages of micelle formation in phase diagram microemulsion

Surfactants do not bring the inter facial tension (IFT) down to the required very low value so another substances need to be added to obtain the required (IFT) for the formation of a stable microemulsion such as short chain alcohols. This surfactant and a short chain substance called a cosurfactant. (Prince)⁷. Lowering the(IFT) enables the formation of high surface-area emulsions .

Microemulsions are classified according to Winsor depending on the phase equilibria to:
 Winsor I : the surfactant is soluble in water , (o/w) microemulsions forms with excess oil phase.
 Winsor II: the surfactant is soluble in the oil phase and (w/o) microemulsions forms with excess water phase.
 Winsor III: three-phase system where a surfactant-rich middle-phase coexists with both excess water and oil surfactant-poor phases.
 Winsor IV: a single-phase (isotropic) micellar solution, that forms upon addition of a sufficient quantity of amphiphile (surfactant plus

alcohol).as illustrated in Fig (1.4). Upon increasing temperature the phase behavior sequence will depend on the total amphiphile concentration.

At low amphiphile concentration the sequence will be: Winsor I- Winsor III- Winsor II, while at high amphiphile concentration the sequence will be: Winsor I- Winsor IV- Winsor II.

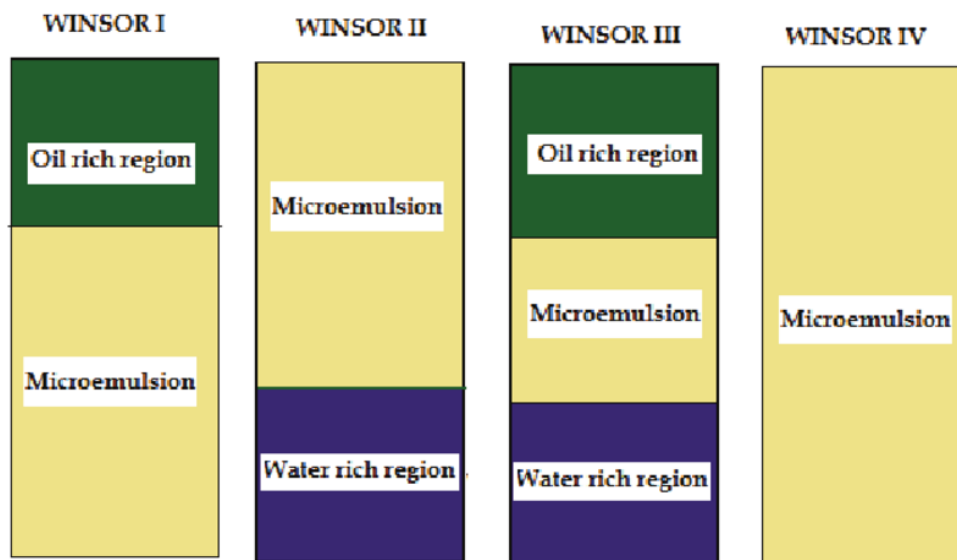


Fig 1:4 Winsor classification of microemulsion

In some respects, microemulsions can be considered as small-scale versions of emulsions , droplets range (5-50 nm) range. The term “microemulsion” was first used in 1959 by Schulman and his group . Different, terms like transparent emulsion, swollen micelle, micellar solution, and solubilized oil were used for such systems. It is a single optically isotropic and thermodynamically stable liquid solution with droplet A microemulsion is defined as Microemulsions are generally defined as isotropic, transparent, thermodynamically stable mixtures of at least three components: a water, oil and a surfactant; usually in combination with a cosurfactant, typically a short chain alcohol (Aboofazeli and Lawrence)₈. The character of a microemulsion to be formed is determined by variables such as the type and concentration of the surfactant and co- surfactant employed, temperature, the nature and concentration of the oil phase, aqueous electrolytes and the relative ratios of the components. Depending on the

composition of the system of oil, water, and surface-active agent, the microstructure of a microemulsion may exist as (w/o) droplets, (o/w) droplets, or a bicontinuous structure (Kumar)⁹. The unique properties of microemulsions that include ultralow interfacial tension, large interfacial area, low viscosity, and high solubilization capacity attracted researchers. (Fanun)¹⁰.

Sugar-based surfactants are the final result of a product concept, which is based on the greatest possible use of renewable resources, are characterized by having the hydrophilic sugar head group and the hydrophobic alkyl chain. The most important sugar-based surfactants are alkyl polyglycosides, sorbitan esters, and sucrose esters. Sucrose ester (SE), nonionic surfactants, contain sucrose as the hydrophilic group and a fatty acid as the hydrophobic (Fanun)¹¹. They are tasteless, odorless, nontoxic and non irritant to eyes and skin, biodegradable and approved as food, pharmaceutical and cosmetics emulsifiers. An advantageous property of sucrose ester surfactants is their weak temperature dependence of the head group hydration, also temperature insensitive microemulsions were formulated using this surfactant (Fanun)¹². SE are obtained by etherifying sucrose with methyl fatty acids, by varying the degree of esterification of the sucrose molecule it is possible to obtain emulsifiers with HLB values ranging from 1 (high degree of etherification; low monoester content) up to 16 (partially esterified products; high monoester contents). Sucrose contains in its structure eight-hydroxyl groups that can be esterified. If the esterification degree increases on the hydroxyl groups by fatty acids, the hydrophobicity will increase. Partial esterification will produce sucrose ester with amphiphilic properties. Mono, di and tri ester of sucrose usually used as emulsifier in foods, cosmetic, detergent. The surfactants to be used in this study are Sucrose myristate (sucrose ester) and sorbitan monooleate (sorbitan esters).

The primary aim of microemulsion research is to find the conditions under which the surfactant solubilises the maximum amounts of water and oil, which means to study the phase behavior of the emulsion; Phase behavior of nonionic amphiphiles is characterized by the change in the distribution of the amphiphile between the water-rich and oil-rich phase with the change in temperature (Fanun)¹¹.

Characterizing the formulated emulsion to investigate the physiochemical properties using electrical conductivity, ultrasonic velocity and density measuring , since conductivity measurements provide a means of determining whether a microemulsion is oil continuous or water-continuous as well as providing a means of monitoring percolation or phase inversion phenomena. As well as the density and ultrasonic velocity which provides information about the micellar interactions.

It has been suggested that microemulsions are self-preserving antimicrobials in their own right (Friberg)¹³. This suggestion is made on the basis that bacteria cannot survive in pure fat or oil and that water is necessary for their growth and reproduction (Al adham)¹⁴ .In microemulsions, the water (majority component, v/v) present is effectively bound by the structure of the microemulsion and therefore, access to the water by micro-organisms is Limited. Hence, these systems are potentially antimicrobial(Friberg)¹³ .The morphology of the microbes using transmission electron microscopy (TEM) showed action against the bacterial cytoplasmic membrane. Gross disturbance and disfunction of membrane structure. (Al adham)¹⁴

The impact of the microemulsion on the microbial activity of the bacteria will be investigated . The classification of bacteria are different according to different points of intrests (scientist, clinician, epidemiologist), clinically depends on bacterial morphology and staining properties of the organism, as well as O₂ growth requirements of the species combined with a variety of biochemical tests. Gram stain and bacterial morphology is the most common classification which classify bacteria into Gram positive bacteria as *Staphylococcus aureus* and Gram negative bacteria as *Escherichia coli*. The main difference between the two groups is believed to be due to a much larger peptidoglycan (cell wall) in Gram positives. Table: 1.1 shows some of the differences between the two groups .

Table:1.1 Differences between Gram positive and Gram negative bacteria

Character	Gram positive	Gram negative
Thickness	Thicker	Thinner
Periplasmic space	Absent	Present
Lipids	Absent or small	Present
Teichoic acid	Present	Absent
Peptidoglycan	16-80 nm	2 nm

Microbial activity of Gram positive and a Gram negative bacteria was investigated using The Kirby-Bauer antimicrobial disk diffusion procedure with Mueller Hinton Agar plates. It is based on the use of an antimicrobial impregnated filter paper disk. The impregnated disk is placed on an agar surface, resulting in diffusion of the antimicrobial into the surrounding medium. Effectiveness of the antimicrobial can be shown by measuring the zone of inhibition for a pure culture of an organism. Müeller-Hinton agar is a protein free medium for isolating pathogenic considered to be the best for routine susceptibility testing of nonfastidious bacteria . Contains beef infusion, casamino acids, and starch. Starch acts as a colloid that protects against toxic material in the medium. Beef infusion and casamino acids provide energy and nutrients. Agar is added as solidifying agent.

Microemulsions have found extensive use and applications in important fields of science and technology among them biotechnology, pharmacy and oil recovery, have been intensively studied during the last decade by many scientists and technologists because of their great potential in many applications . In most industrial applications the use of mixed surfactants is preferred over the use of pure surfactant based system .

Chapter Two

Literature review

Mixed non ionic surfactants

In most industrial applications, the use of mixed surfactants system is preferred over the use of pure surfactant-based systems. A number of authors reported on the effect of polar oils such as triglycerides, middle- or long-chain alcohols or fatty acids, fatty acid ester on the water solubilization, and properties of microemulsions for different technological applications. It was found that the total surfactant concentration needed to solubilize an equal amount of water and oil increases with the increase in the lipophilicity (molecular weight) of the oil.

Due to the fact that sucrose esters do not lose solubility with change in temperatures, attempts have been made to prepare temperature insensitive microemulsions based on sucrose monoalkanoate and cosurfactants. (N.Garti)¹⁵

Investigating and understanding the phase behavior of the microemulsion and studying the water solubility is complex process which has many involving factors; chain length compatibility of the surfactant oil, and co- surfactant; the chain length of surfactant must be equal to the sum of the co- surfactant chain length and the hydrocarbon chain length in order to minimize disruption in the interfacial region by either maximum cohesive interaction between hydrocarbon chains or minimum disruption in the interfacial region. Molecular volume of the oil and its tendency to penetrate inside the system and increase the water solubilization, the carbon effective number of the oil, surfactant and the co- surfactant, and the three dimensional arrangement of the surfactant according to the head group area, and others.

(Thevenin)¹⁶ Studied microemulsion systems containing different kinds and amounts of surfactant; sucrose esters. Sucrose esters are not able to form microemulsions without a co-surfactant since the solubility of sucrose esters in the oil and water phases at room temperature was poor the use of a co- surfactant was necessary. Microemulsion areas were investigated for numerous systems including sucrose esters/cetearyl octanoate/alcohols/water at different surfactant/co- surfactant mass ratios, and different HLB values. It was found that mixing two

surfactants which have the same alkyl chain length but a quite opposite solubilizing ability towards oil and water may enhance the mutual solubilization of oil and water. Shorter alcohols are favourable to a disordered interfacial film and the inversion phase between L_2 and L_1 occurs without any discontinuity in the macroscopic properties of the system.

(Fanun)¹⁷&(Garti)¹⁸ Studied different sucrose ester surfactants, investigated the effect of the surfactant chain length. The interfacial area per surfactant head group and the monophasic area (A_T %) decreases with the increase in the surfactant chain length, and increase in the lipophilic tail of the surfactant, which increases the molar volume of the lipophilic tail of the surfactant with a short cosurfactant, results in an increase in oil penetration into the alkyl chains of the surfactant. This increases the attractive interaction potential, thereby suppressing the elasticity leading to smaller water droplets and lowering water solubilization. For a sucrose ester with a given chain length the interfacial area per surfactant head group decreases with the increase in the surfactant monoester content. The interfacial area per surfactant head group increases with the increase in the surfactant concentration and the water core volume in the formulated microemulsion. The role of the surfactant tail in determining the interfacial area is explicit in the sense that the surfactant chain length directly influences the molecules packing in the droplets. This role is implicit in the sense that the tail interactions are affected by the aqueous core volume.

(Fanun)⁵ Studied the effect of addition of ethoxylated surfactants to sucrose ester surfactants in different ratios, the systems studied were water/sucrose laurate/ethoxylated mono-di-glyceride/(isopropylmyristate + ethanol) at a weight ratio equal to unity. The weight ratio of ethoxylated mono-di-glyceride in the mixed surfactants was varied from 0 to 100 wt.% by steps of 25 wt.%. It was found that the mixing increases the mutual solubility of oil and water and temperature insensitive microemulsions are formed. It seems that the mixture (blend) of surfactants enhances the surfactants partitioning at the water-oil interface, by increasing the solubility of mixed surfactants in both oil and water thus increasing the stability of the amphiphilic film. The total area of the one phase microemulsion region (A_T) increases as the weight ratio of ethoxylated surfactant in the mixed surfactants increases from 25 to 75 wt.%, by changing the polarity of the polar and apolar phases. Investigated the effect of addition of short

chain alcohol(ethanol) in an equal unity with the oil was also significant to increase the total monophasic area (A_T). This significant change in phase behavior happened due to the destabilization of the liquid crystal phase and more flexibility in the surfactant film which allows more connections between the aqueous with the oil phase.

(Fanun)¹¹ The phase behavior of the systems water/sucrose laurate/ethoxylated mono-di-glyceride/oil was investigated as function of temperature and the weight ratio of EMDG in the mixed surfactants. The oils were R (1)-LIMonene, isopropylmyristate, and caprylic-capric triglyceride. This study demonstrates that the phase inversion temperature (PIT) decreases and the efficiency of the mixed surfactants (minimum amount of surfactant needed to solubilize equal amount of oil and water) increase as the weight ratio of the EMDG in the mixed surfactants increases. R (1)-LIMonene gave lower phase inversion temperatures and higher efficiencies compared to isopropylmyristate, and caprylic-capric triglyceride. The solubilization capacity of the system water/sucrose laurate/oil increased upon the addition of ethoxylated mono-di-glyceride which stabilize the surfactant layer and increase the interfacial area. Synergistic effect of the mixed surfactant enhances the surfactants partitioning at the interface, increases the stability of the amphiphilic film better curvature and improved flexibility, and enhances the mutual solubilization of water and oil. This also will decrease the phase inversion temperature and increases the efficiency of the mixed surfactants.

(Fanun)⁵ The presence of alcohol influences the extent of the microemulsions regions and their internal structure. The roles of alcohol in microemulsions are to delay the occurrence of liquid crystalline phases, to increase the fluidity of the interfacial layer separating oil and water, to decrease the interfacial tension between the microemulsion phase and excess oil and water, and to increase the disorder in these interfacial layers as well as their dynamic character.

Adding ethanol which is completely soluble in water increases the mutual solubility between water and mixed surfactant by decreasing their hydrophobicity, decreases the interfacial tension between the water and the oil phases and reduces the spontaneous curvature leading to increased water solubilization.

(Bansa)¹⁹ The solubilization capacity of water/oil microemulsions formed with fatty acid soaps and alcohols was studied as a function of alkyl chain length of oil (C_8 to C_{16}), soap (C_{14} and C_{18}), and alcohol (C_4 to C_7). It was concluded that when the oil chain length is increased, the

solubilization capacity of microemulsions can increase, decrease, or show a maximum, depending upon the structure of the alcohol used

Type of oil influence the surfactant layer curvature in aggregates or self-organized structures when solubilized. The placement of the solubilized oil in the surfactant aggregates highly affects the change in surfactant layer curvature. If oil tends to penetrate in the surfactant palisade layer and locates near the interface of the water–lipophilic surfactant moiety, the curvature would be less positive or negative. If oil is solubilized deep inside the aggregates and tends to form an oil pool (swelling).

(Fanun)₂, In principle, the substitution of a dilute aqueous solution of NaCl for water may induce variation in the size and shape of the different regions of the phase diagram and, at the microscopic level, in the mode of aggregation of the surfactant molecules, but lately independence of phase behavior in the presence of a small amount of electrolyte is reported by different literatures.

At water contents below 20 wt.% the dynamic viscosity for samples increases. For water contents between 20 wt.% and 60 wt.% the viscosity of the microemulsion samples decreases slightly. Above 60 wt.% of water content a small increase, then a sharp decrease in the viscosity is observed. The increase in the dynamic viscosity for water contents below 20 wt.% indicates shape changes of microemulsion droplets since a growth of spherical droplets into larger non-spherical shapes is followed by a significant increase in the solution viscosity. The reduction in the viscosity with the increase in water content above 20 wt.% to about 60 wt.% seems to be attributed to the fact that the mixed surfactants move from the bulk to the interface to cover the water and oil in a bicontinuous structure. The small increase in the dynamic viscosity for water contents above 60 wt.% suggests a structural transformation from a bicontinuous structure to oil in water structure. This phenomenon can also be explained in terms of a decrease in the hydrophobic interaction of the surfactant tails. High water contents cause a reduction in the inter-droplet interactions and reduction in the viscosity. The relatively low viscosity values indicate that the microemulsions formulated are composed of individual spherical droplets or bicontinuous structures and no anisometric aggregates are present.

(Aladham)¹⁴ used 15% Tween 80, 6% pentanol, 3% ethyl oleate and 76% water against cultures of *Pseudomonas aeruginosa* and *Staph. aureus* started with a viable count of approximately 10^6 cfu. Results showed that a five log reduction in bacterial was obtained in approximately 45 s. The LT90% value (time at which 90% of the original population has been killed by the antimicrobial) for this experiment was approximately 15 s for both micro-organisms. LT90% values of this order suggest that the antimicrobial compound involved is highly and effectively biocide.

(Al adham)²¹ Used the same formula (Tween 80, pentanol, ethyl oleate and water) did a comparison using the cetramide which is an antiseptic substance, and destroys certain types of bacteria that can infect the skin and Sodium pyrithione which inhibits growth of fungi, yeast, mold and bacteria. upon established biofilm cultures of *Ps. aeruginosa* for a period of 4h, which gave a three log cycle reduction while the two substances gave one log reduction .

(Hui)²² Used Glycerol Monolaurate GML, glycerol monoester of lauric acid GML/Tween 20/Tween 80/1 pentanol/water , the microbial affectivity of the formed emulsion against *Staphylococcus aureus* and as individual component was tested and measured as inhibition zone; showed significantly high antimicrobial activity (95.56%) and as individual component GML (63.52%). Mixing some antimicrobial substances contributes to homogeneous and dynamically stable system with enhanced antimicrobial activities .

(Anjali)²³ used surfactants with refined sunflower oil/ Tween 20 / water. made three different concentrations keeping the oil/surfactant in all (1/2). Individual components were tested against *E. coli*, *S. aureus*, *P. aeruginosa*, of the three microorganisms; it was observed that microemulsion with concentration 15 % of oil and 30 % of surfactant showed maximum antibacterial effect. Oil and Surfactant alone showed no zone of inhibition .

(Aladham)²⁴ Studied whether the position of the microemulsion within the stability zone of the pseudo-ternary phase structure predicts the efficiency of the antimicrobial action of the microemulsion The results observed for the rate of killing significant antibacterial activity of the microemulsions systems at all points within the microemulsion existence area and that the most effective one is that point representing the center of the microemulsion stability zone; water bound to the microemulsion structure is higher in the center of the microemulsion existence area

than the perimeter areas, which may contain more free water molecules. Six log reductions in bacterial number was achieved in less than 15 s.

(Bardhan)²⁵ Used mixed surfactants; cationic & nonionic. water/CTAB/Brij-35/Pn/ IPM (w/o) microemulsion .The effect of individual constituents of the microemulsion systems, as well as the formulated on antimicrobial activity has been examined against the bacterial strains, gram positive *B. subtilis* and gram-negative *E. coli*, results showed higher antimicrobial activity against both bacterial strains was at concentration (XBrij-35 = 0.2–0.8), CTAB exhibits considerable antimicrobial activity at different concentrations.

Pn and Brij-35 showed insignificant antimicrobial activity against both strains, IPM did not show antimicrobial activity at all.

(Xin)²⁶ Did research article about antimicrobial structure-efficacy relationship of sugar fatty acid esters; Polyglycerol esters of fatty acids (PGEs) have been reported to have antibacterial activity, particularly against gram-positive bacteria. The first fatty acid esters of sugars reported to display antimicrobial activity were sucrose dicaprylate and sucrose monolaurate, which were shown to be active against some gram-negative and gram-positive bacteria, as well as fungi. sucrose esters were reported as effective inhibitors of *Bacillus stearothermophilus*, *Bacillus coagulans*, *Desulfotomaculum nigrificans*, and some typical anaerobic spore forming bacteria including *Clostridi* . The experiments showed that as little as 200 µg/ml of sucrose palmitate could prevent the spoilage of canned milk coffee. Commercial sucrose fatty acid esters can decrease acid production from sugar by oral bacteria; use of fatty acids and their sugar esters potentially represents a non-toxic and non-allergenic means of controlling the acidogenic organisms associated with dental caries.

Synergism effect was observed when sucrose palmitate(P1570) and sucrose stearate(P1670) were added into nisin, a synergist enhancement of the bacteriostatic activity of nisin against some gram-positive bacteria as strains of *L. monocytogenes*, *Bacillus cereus*, *Lactobacillus Plantarum* and *Staphylococcus aureus* was noticed, however, the combination of nisin with sucrose fatty acid esters showed no inhibition against gram-negative bacteria.

Galactose and fructose laurates showed the greatest growth-inhibitory effect against *Streptococcus mutans*, while hexose laurates showed no antibacterial activity, indicating that

configuration of the hydroxyl group in the carbohydrate moiety of carbohydrate esters markedly affects the antibacterial activity.

Fatty acid esters of sucrose, maltose and maltriose for use as inhibitors of *Streptococcus sobrinus*, showed that lauroyl esters completely inhibit the growth of *Streptococcus sobrinus*, indicating that the chain length of fatty acid markedly affect the antibacterial activity. The investigation of the relationships between surfactant structure and antibacterial activity showed that both the length and orientation of alkyl chain affect antibacterial activity. Dodecyl α -L-2,6-dideoxy-L-arabino-hexopyranoside (C12) had a higher activity against *Bacillus cereus* and *Bacillus subtili* than against *Enterococcus faecalis* and *Listeria monocytogenes*. In regard to the octyl α -L-glycoside (C8), some inhibition of the growth of *Bacillus cereus*, *Bacillus subtilis*, *Enterococcus faecalis*, *Listeria monocytogenes* and *Staphyloco ccus aureus* was observed as well.

Effects of sugar fatty acid esters on biofilm formation by food-borne pathogenic bacteria were investigated, sugar fatty acid esters with long chain fatty acid residues (C14-16) inhibited biofilm formation by *Streptococcus mutans* and *Listeria monocytogenes* at 0.01% (w/w), but bacterial growth was not affected at this low concentration.

Chapter Three

Objectives

- 1- Formulation of microemulsion systems using different components of non ionic surfactant composed of sucrose mirystate and sorbitan monoolieat(food and pharmaceutical grade) in a different percentage ,biologically compatible oil phase (cyclic oils such as (R)-Limonene, linear oil such as isopropyl myristate and triglyceride oils such as caprylic capric triglyceride), aqueous phase of water and propylene glycol . Co-surfactant was added.
- 2- Evaluation of the water solubilization capacity of the formed microemulsion systems by calculating the area of the one-phase microemulsion region (A_T) that is area limited by the micro- emulsification failure boundaries.
- 3- Exploring the microstructures of the formed microemulsion by density and ultrasonic velocity (USV), electrical conductivity .These techniques will be used to study how changes in the relative amounts of the surfactant and in the chain length of the surfactants or oil, the presence of co-surfactant and the addition of water influence the microemulsion microstructure within the one-phase region.
- 4- The main objective is to investigate the antimicrobial affectivity of the formed microemulsion on some of the bacteria using disk diffusion and soaking methods.

Chapter Four

Material and methods

4.1 Materials

4.1.1 Surfactants (surface active agents)

4.1.1 .1 Sucrose myristate(M1695)

Sucrose esters are food grade emulsifiers, they are sucrose fatty acid ester (sugar ester), and nonionic, ultra-mild and highly pure, strong water binders. .Sucrose Myristate (M1695) is nonionic strongly hydrophilic sugar ester surfactant possess a high monoester of myristic acid content (80%,polyesters 20%), have a great affinity towards water ,HLB 16. Sucrose myristate M1695 has unique properties (biodegradable, nontoxic and capable of forming temperature-insensitive microemulsions), which make them suitable for a variety of food-based and pharmaceutical application. Sucrose myristate M1695 was obtained from Mitsubishi-Kasei Food Corp. (Mie, Japan).

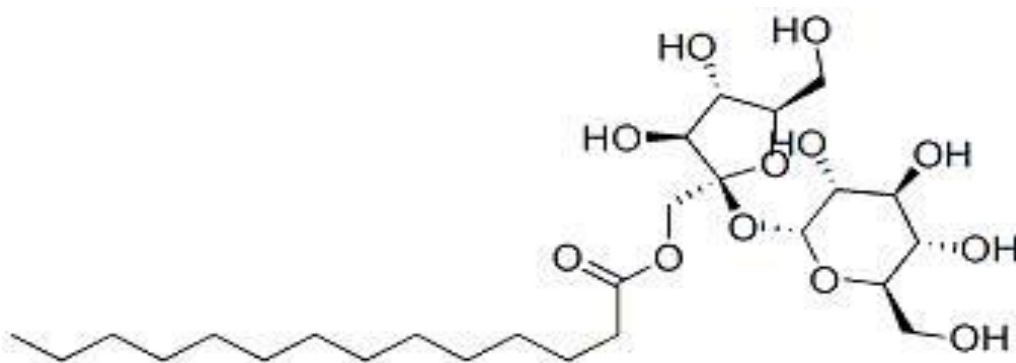


Fig 4:1 The chemical structure of sucrose myristate M1695

4.1.1.2 TMAZ80

TMAZ 80K is a sorbitan monooleate that has been ethoxylated with approximately 20 moles of ethylene oxide to give a water soluble, oil and water emulsifier. This surfactant is a mixture of partial esters of sorbitol and its anhydrides made from fatty acids, primarily oleic, which is then reacted with ethylene oxide to make it hydrophilic in nature. This product is designated with a "K" which means it has Kosher U Certification.

TMAZ 80K can be used as a solubilizer and emulsifier of oils and fragrances, wetting agent, viscosity modifier, stabilizer or dispersing agent, can also be used in the food, textile, and metalworking industries. Food applications include ice cream, shortening and edible oils, yeast defoamers, pickle products, vitamins and mineral preparations, whipped vegetable toppings, gelatin dessert mixes, defoamers in cottage cheese, and artificial colors in barbecue sauce.

TMAZ 80 surfactants are generally soluble or dispersible in water, and, soluble in varying degrees in organic liquids. They are used for oil-in-water emulsions, dispersions, and solubilizing oils and to make anhydrous ointments water soluble or washable. It has 15 HLB

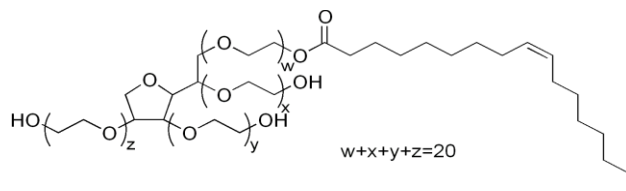


Fig 4:2 The chemical structure of sucrose polysorbate 80

4.1.2 Oils

4.1.2.1 The cyclic R (+)-Limonene.

R(+)-limonene:(LIM),(R)-4-Isopropenyl-1-methyl-1cyclohexene (98%) was purchased from Sigma Chemicals Co. (St. Louis, USA

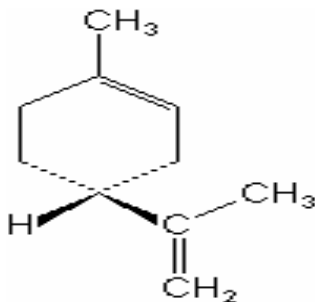


Fig 4:3 The chemical structure of R (+)-LIMonene oil

4.1.2.2 The linear Isopropylmyristate (IPM), Tetradecanoic acid, 1-methylethyl ester (99%), polar oil manufactured by condensing myristic acid with isopropyl alcohol, HLB=11.5, purchased from Sigma Chemicals Co. (St. Louis, USA).

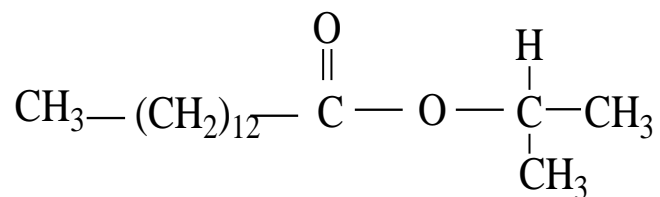


Fig 4:4 The chemical structure of Isopropylmyristate oil

4.1.2.3 The triglyceride caprylic/capric triglyceride (CCT)

Produced by the esterification of glycerol (plant sugars) with mixtures of caprylic (C:8) and capric (C:10) fatty acids from coconut or palm kernel oils. The special combination, and esterification, are responsible for the silky oil feel .HLB =5

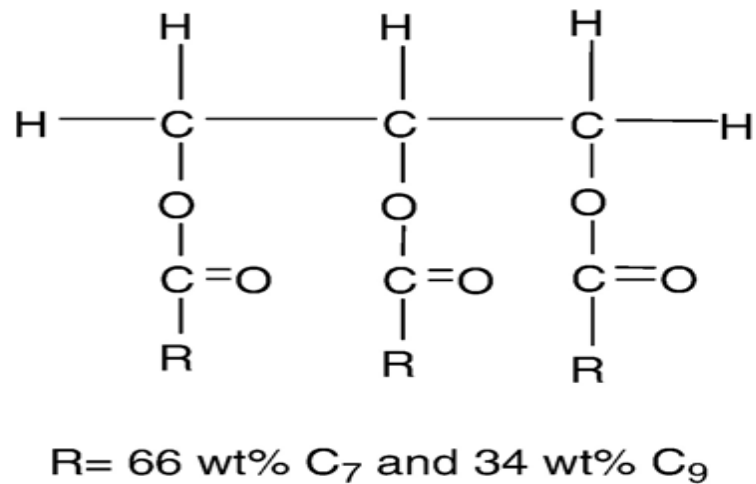


Fig: 4:5 chemical structure of Caprylic/Capric Triglyceride oil

4.1.3 Co-surfactant

4.1.3.1 Propylene glycol, PG

The co-surfactant used is 1,2-Propandiol (Propylene glycol, PG) (99.5%) was purchased from BDH (poole, UK).

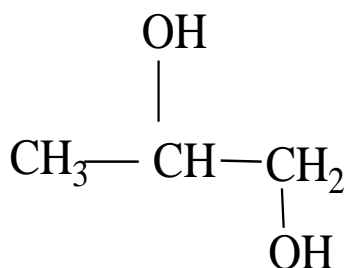


Fig 4:6 The chemical structure of 1, 2-Propandiol (propylene glycol, PG).

4.1.3.2 Ethanol

Ethanol is a straight-chain alcohol, and its molecular formula is C₂H₅OH

Absolute Ethanol (minimum 99.8%) which has the molecular formula (CH₃CH₂OH) was obtained from Frutarom (Haifa, Israel)

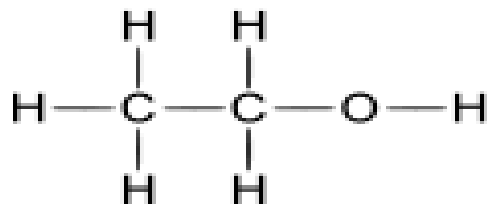


Fig 4:7 The chemical structure of Ethanol.

4.1.4 Aqueous phase

Which was done as water /propylene glycol as 2/1 ratio Milli Q Water was used.

4.1.5 Materials for microbial test

4.1.5.1 Muller Hinton agar

Commonly used for antibiotic susceptibility test, contains: casein acid hydrolysate, beef heart infusion, starch, and agar. It has a few properties that make it excellent for antibiotic use. First of all, it is a non-selective, non-differential medium. This means that almost all organisms plated on here will grow. Additionally, it contains starch. Starch is known to absorb toxins released from bacteria, so that they cannot interfere with the antibiotics. Second, it is a loose agar. This allows for better diffusion of the antibiotics than most other plates. A better diffusion leads to a clear zone of inhibition. Was purchased from Centrum Microbiology Emapol, Poland.

4.1.5.2 Nutrient agar

Nutrient Agar is a general purpose, nutrient medium used for the cultivation of microbes supporting growth of a wide range of non-fastidious organisms.

4.1.5.3 Nutrient broth

Is a liquid medium that contains peptone and beef extract. Nutrients necessary for the replication and growth of a large number of nonfastidious microorganisms

4.1.5.4 saline

Solution of sodium chloride which contains 9gm of salt per litre

4.1.5.5 McFarland Standard

Turbidity of the McFarland tube no. 0.5 is considered as reference for the growth cultures to be considered as (10^8 cfu/ml), prepared as follows; (0.5 ml aliquot of 0.048 mol/L BaCl_2 (1.175% w/v

BaCl₂·H₂O) is added to 99.5 ml of 0.18 ml/L H₂SO₄ (1%v/v) with constant stirring to maintain a suspension).

4.1.5.6 Bacteria

Bacteria are unicellular microorganisms, which lack chlorophyll pigments. The cell structure is simpler than that of other organisms as there is no nucleus. Due to the presence of a rigid cell wall, bacteria maintain a definite shape, though they vary as shape, size and structure. May be classified into Gram positive and Gram negative.

4.1.5.6.1 *Staphylococcus aureus*

S.aureus is a genus of the *Staphylococcaceae* grape-cluster berry, is a facultative anaerobic, gram-positive coccal bacterium also known as "golden staph", non-motile and does not form spores. The average diameter of spherical bacteria is 0.5-2.0 μm.

4.1.5.6.2 *Escherichia coli*

Escherichia is a genus of the family **Enterobacteriaceae**, gram-negative, facultative anaerobic, rod-shaped. Cells are typically rod-shaped, and are about 2.0 μm long and 0.25–1.0 μm in diameter.

4.2 Methods

4.2.1 Construction of ternary and pseudoternary phase diagrams

The phase behaviour of the systems consisting of water (with co-surfactant), oil, mixed surfactants are to be described on a phase tetrahedron whose apexes respectively represent the pure components. 1g of a mixture consisting of single oil (LIM, IPM, CCT), mixed surfactants (sucrose myristate, sorbitan monooleate) at different five weight ratios were prepared (0, 25, 50, 75, 100) in culture tubes

sealed and stirred at high temperature (45°C) by vortex until clear solution was obtained. Titration for these samples using mQ water and co- surfactant (propylene glycol),4% increment were added drop wise until its solubilisation limit was reached. Vigorous stirring followed all of the aqueous phase additions on a vortex mixer. The time for equilibration between each addition was typically, from a few minutes up to 24 h. Phase transitions were detected visually by the appearance of cloudiness .All phase diagrams were investigated at three temperatures (25,37,and 45°C).Table 4.1 explains the constructed phase diagram

Table 4.1 Systems that explains the different ratios in this work

System #	System Name	Ratios	Symbol	(TMAZ80/ M(1695) +TMAZ80) %
1	W+PG/ M1695/ LIM /EOH	(2/1)/(1)(1/1)	MT 0 LE	0
2	W+PG/TMAZ80/M1695/ LIM /EOH	(2/1)/(1/4)(1/1)	MT 25 LE	25
3	W+PG/TMAZ80/M1695/ LIM /EOH	(2/1)/(1/1)(1/1)	MT 50 LE	50
4	W+PG/TMAZ80/M1695/ LIM /EOH	(2/1)/(3/4)(1/1)	MT 75 LE	75
5	W+PG/TMAZ80 /LIM/EOH	(2/1)/(1)(1/1)	MT100LE	100
6	W+PG/ M1695/ IPM /EOH	(2/1)/(1)(1/1)	MT 0 IE	0
7	W+PG/TMAZ80/M1695/ IPM /EOH	(2/1)/(1/4)(1/1)	MT 25 IE	25
8	W+PG/TMAZ80/M1695/ IPM /EOH	(2/1)/(1/1)(1/1)	MT 50 IE	50
9	W+PG/TMAZ80/M1695/ IPM /EOH	(2/1)/(3/4)(1/1)	MT 75 IE	75
10	W+PG/TMAZ80 /IPM/EOH	(2/1)/(1)(1/1)	MT 100IE	100
11	W+PG/ M1695/ CCT /EOH	(2/1)/(1)(1/1)	MT 0 CE	0
12	W+PG/TMAZ80/M1695/ CCT /EOH	(2/1)/(1/4)(1/1)	MT 25 CE	25
13	W+PG/TMAZ80/M1695/ CCT /EOH	(2/1)/(1/1)(1/1)	MT 50 CE	50
14	W+PG/TMAZ80/M1695/ CCT /EOH	(2/1)/(3/4)(1/1)	MT 75 CE	75
15	W+PG/TMAZ80 /CCT/EOH	(2/1)/(1)(1/1)	MT100CE	100

4.2.2 Determination of water solubilization capacity

The water solubilization capacity of different amphiphilic systems should be compared at optimal conditions (Garti, N., Clement, V., Fanun, M. et al, 2000). Li et al, 1989 have employed as a solubilization parameter the area of the one-phase microemulsion region (A_T) % that is area limited by the microemulsification failure boundaries. In this research we used the one phase microemulsion region to compare the water solubilization capacity in the studied systems.

A_T (%) was calculated as $\pm 2\%$.

4.2.3 physiochemical characterization

4.2.3.1 Electrical conductivity measurements

Electrical Conductivity measurements were performed to the same fifteen microemulsion sets as in table # 1 ;(three different oil type with five different ratios), constructions were made according to dilution line N65, measurements were taken at ten different temperatures 10 to 50°C in increasing steps of 5°C each time with the 2% titration aqueous increment until 10% ,then 10% increment until 90% . The conductivity cell used is Tetra Con® 325, the electrode material is graphite and the cell constant is 0.475 cm⁻¹ ±1.5%.the temperature range is from 14 to 50 °C. The device was Lutron , YK-2014CD conductivity meter.

The electrode was dipped in the microemulsion sample until equilibrium was reached and reading becomes stable at 1 min. Reproducibility was checked for certain samples and no significant differences were observed. The constant of the conductivity cell was calibrated using standard KCl solutions at the first of every month during the characterization or when the conductivity meter needs that .Electrical conductivity measurements are performed to determine the type of microemulsion droplets formed (i.e. water-in-oil (W/O), bicontinues, or oil-in-water (O/W)).

4.2.3.2 Density

The aqueous phase density is determined using an oscillating U-tube density meter , calculated from the quotient of the period of oscillations of the U-tube and the reference oscillator at different temperatures

4.2.3.2.1 sample preparation

Samples were also made according to dilution line N65 , fifteen microemulsion sets as in table # 1; (three different oil type with five different ratios),with 5% aqueous increment (0%,5%,10%,15%...90%) sealed in a culture tubes, which then went through the density and ultrasonic velocity test measurements at four different temperatures;(25,30,37,and45°C).

4.2.3.3 Ultrasonic velocity

The aqueous phase velocity is determined using an oscillating U-tube velocity meter, the sound velocity v is calculated from the period of oscillation of the sound velocity measuring cell. Same samples in 4.2.3.2.1 were used.

Density and ultrasonic velocity measurements were made using DSA 5000M device.

4.2.4 Antimicrobial Susceptibility test

4.2.4.1 Sample preparation

Same samples which were prepared in section 4.2.3.1 were also used for the microbial test which was made for two pure strains; *Escherichia coli* as Gram negative and *Staphylococcus aureus* as Gram positive bacteria.

4.2.4.2 Inocula preparation

Isolated bacterial colony of each of the two bacterial types were inoculated into five ml nutrient broth media tube and incubated for 4-8 h at 37°C. The growth turbidity in nutrient broth was inoculated into sterile saline tube and adjusted by further inoculation or dilution after comparison with that of a MacFarland nephelometer tube no. 0.5 (10^8 cfu/ml) using spectrophotometer at 625nm giving an optical density range (0.08-0.1).

4.2.4.3 Antimicrobial activity investigating

It is done using the Kirby-Bauer antimicrobial disk diffusion procedure with Mueller Hinton Agar plates as follows: a sterile cotton applicator was dipped into the bacterial suspension (10^8 cfu/ml), rotated several times and pressed against the inside of the tube wall to remove excess inoculum. The Muller Hinton agar plates were streaked in three different directions (rotating the plate approximately 60° each time) and around the agar margin to ensure even distribution of the

inoculum. Plates were left to dry .Sterile Whatman filter paper no. 1 (6mm diameter)were soaked in the samples prepared in section (4.2.3.1) using sterile forceps and put onto the streaked Muller Hinton agar plates after being pressed against the inside wall of the tubes .The plates were incubated upside down at 37°C for 24hrs.The inhibition growth zone was measured with transparent ruler including the disk diameter. Each test was done in triplicate ,also representative sample of each batch of the Muller Hinton agar media was tested for sterility by incubating at 37°C for 24hrs.

4.2.4.3 Viable count

After adjusting the microbial growth of each microbe according to the spectrophotometer ,it was tested as viable count .

Table 4.2 All materials used in this research:

Oil Phase	Surfactant	Cosurfactant	Aqueous phase	Bacterial Strains & media
R(+)-Limonene oil.(LIM) Isopropyl myristate oil .(IPM) Caprylic/capric triglyceride oil.(CCT)	M1695 TMAZ80	Propylene glycol Ethanol	MQ water	<i>Staphylococcus aureus</i> ATCC 25923 <i>Escherichia coli</i> ATCC 25922 Muller Hinton agar Plate count agar Nutrient broth

Chapter Five

Result and Discussion

5.1 Formulation of microemulsion

5.1.1 Phase behaviour of mixed surfactants TMAZ80 + Sucrose myristate (M1695) with LIM oil at (25,37 ,and 45°C)

Figure 5.1 Presents the phase diagram of the system water+ propylene glycol/Sucrose myristate(M1695) / LIM oil + Ethanol at 25°C,with aqueous solution made of (2/1)ratio ,100% Sucrose myristate (M1695) and equal unity of LIM oil with ethanol.The one phase microemulsion region appears from the first addition of water and extend to up to the water apex (100%) .27% is the maximum water solubilization was reached using 23% of the surfactant along the dilution line N65.For surfactant below 23 wt% the multiple phase regions extends.

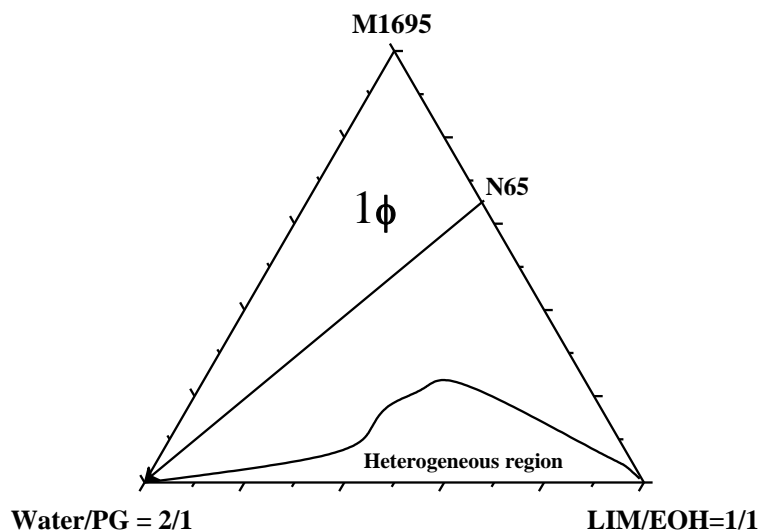


Fig: 5.1 Phase diagram of the system #1 water+ propylene glycol/ Sucrose myristate(M1695) /LIM oil+ ethanol at 25°C. In the figure the one phase region is designated by 1Φ, and the multiple phase regions are designated by heterogeneous region . N65 is the dilution line where the weight ratio of surfactant / single oil is 65/35.

Figure 5.2 Presents the phase diagram of the system water+ propylene glycol/ TMAZ80 + Sucrose myristate(M1695) / LIM oil+ ethanol at 25°C, with aqueous solution made of (2/1)ratio , mixed surfactants TMAZ80+ Sucrose myristate(M1695) with (1/4) ratio and equal unity of LIM oil with ethanol .The one phase microemulsion region appears from the first addition of water and extend to up to the water apex (100%). 38% is the maximum water solubilization was reached using 16 % of the surfactant along the dilution line N65. For surfactant below 16 wt% the multiple phase regions extends.

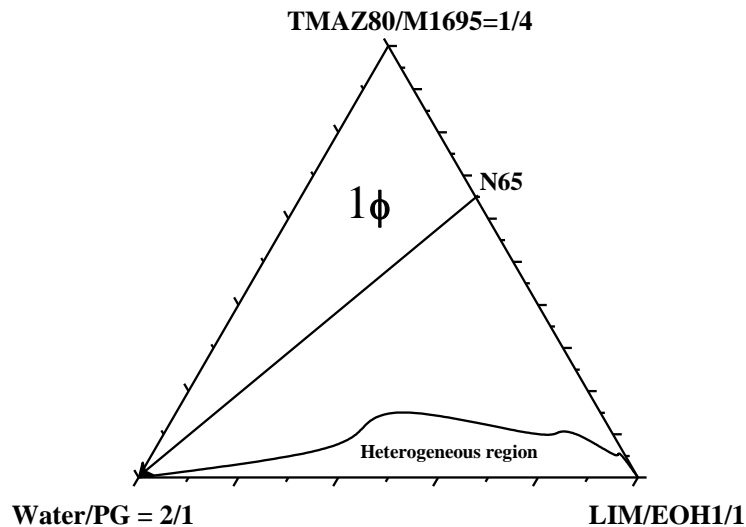


Fig:5.2 Phase diagram of the system #2 water+ propylene glycol/ TMAZ80+Sucrose myristate(M1695) /LIM oil+ ethanol at 25°C. In the figure the one phase region is designated by 1Φ , and the multiple phase regions are designated by heterogeneous region . N65 is the dilution line where the weight ratio of surfactant / single oil is 65/35.

Figure 5.3 Presents the phase diagram of the system water+ propylene glycol/ TMAZ80+ Sucrose myristate(M1695) / LIM oil+ ethanol at 25°C, with aqueous solution made of (2/1)ratio , mixed surfactants TMAZ80+ Sucrose myristate(M1695) with (1/1) ratio and equal unity of LIM oil with ethanol .The one phase microemulsion region appears from the first addition of water and extend to up to the water apex (100%) . 45 % is the maximum water solubilization was reached using 17 % of the surfactant along the dilution line N65. For surfactant below 17 wt% the multiple phase regions extends.

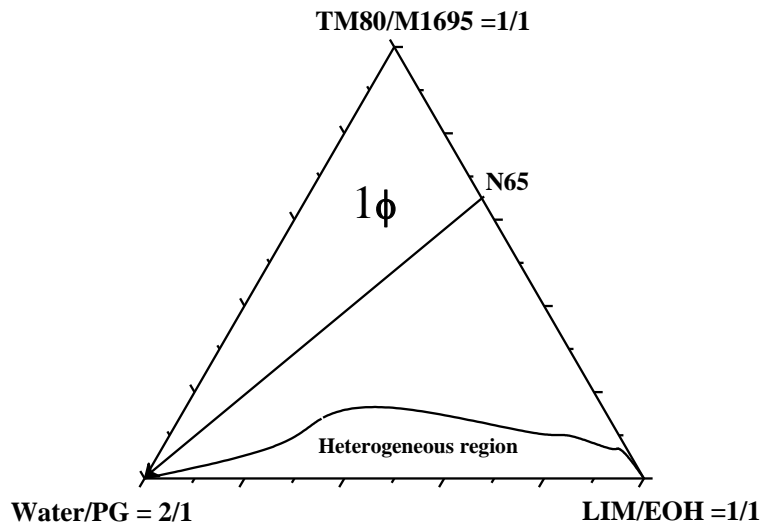


Fig:5.3 Phase diagram of the system #3 water+ propylene glycol/ TMAZ80+Sucrose myristate(M1695) /LIM oil+ ethanol at 25°C. In the figure the one phase region is designated by 1Φ , and the multiple phase regions are designated by heterogeneous region . N65 is the dilution line where the weight ratio of surfactant / single oil is 65/35.

Figure 5.4 Presents the phase diagram of the system water+ propylene glycol/ TMAZ80 + Sucrose myristate(M1695) / LIM oil+ ethanol at 25°C, with aqueous solution made of (2/1)ratio , mixed surfactants TMAZ80+ Sucrose myristate(M1695) with (3/4) ratio and equal unity of LIM oil with ethanol .The one phase microemulsion region appears from the first addition of water and extend to up to the water apex (100%). 75 % is the maximum water solubilization was reached using 8 % of the surfactant along the dilution line N65. For surfactant below 8 % the multiple phase regions extends.

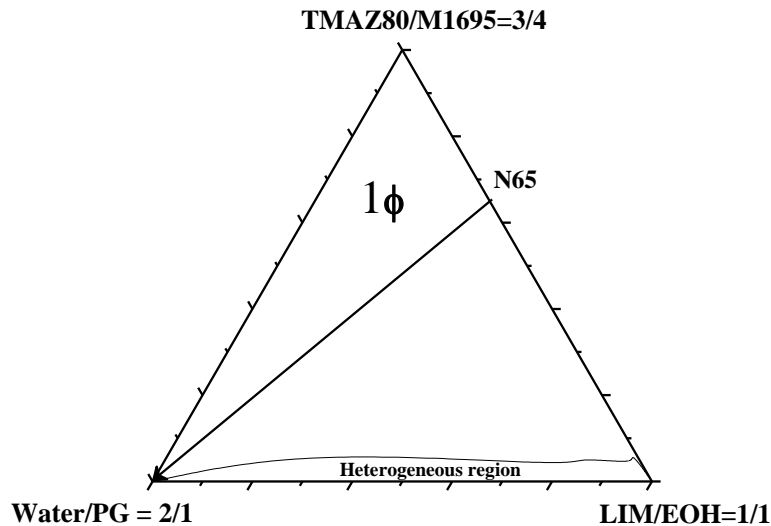


Fig: 5.4 Phase diagram of the system #4 water+ propylene glycol/ TMAZ80 + Sucrose myristate(M1695) /LIM oil+ ethanol at 25°C. In the figure the one phase region is designated by 1Φ , and the multiple phase regions are designated by heterogeneous region . N65 is the dilution line where the weight ratio of surfactant / single oil is 65/35.

Figure 5.5 Presents the phase diagram of the system water+ propylene glycol/ TMAZ80/ LIM oil+ ethanol at 25°C, with aqueous solution made of (2/1)ratio , surfactant TMAZ80 (100%) and equal unity of LIM oil with ethanol .The one phase microemulsion region appears from the first addition of water and extend to up to the water apex (100%). 45 % is the maximum water solubilization was reached using 17 % of the surfactant along the dilution line N65. For surfactant below 17 wt% the multiple phase regions extends.

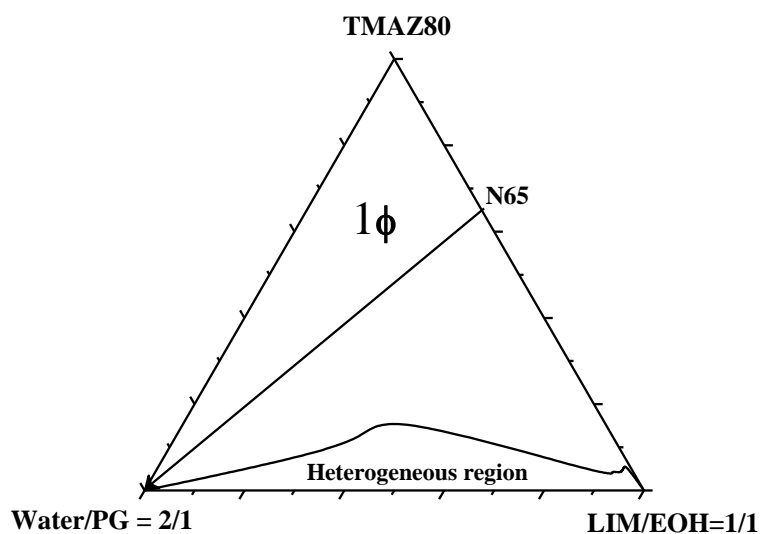


Fig:5.5 Phase diagram of the system #5 water+ propylene glycol/ TMAZ80 /LIM oil+ ethanol at 25°C. In the figure the one phase region is designated by 1Φ , and the multiple phase regions are designated by heterogeneous region . N65 is the dilution line where the weight ratio of surfactant / single oil is 65/35.

Figure 5.6 Presents the phase diagram of the system water+ propylene glycol/ Sucrose myristate(M1695) / LIM oil+ ethanol at 37°C, with aqueous solution made of (2/1)ratio , surfactant Sucrose myristate(M1695) (100%) and equal unity of LIM oil with ethanol .The one phase microemulsion region appears from the first addition of water and extend to up to the water apex (100%). 30 % is the maximum water solubilization was reached using 24 % of the surfactant along the dilution line N65. For surfactant below 24 % the multiple phase regions extends.

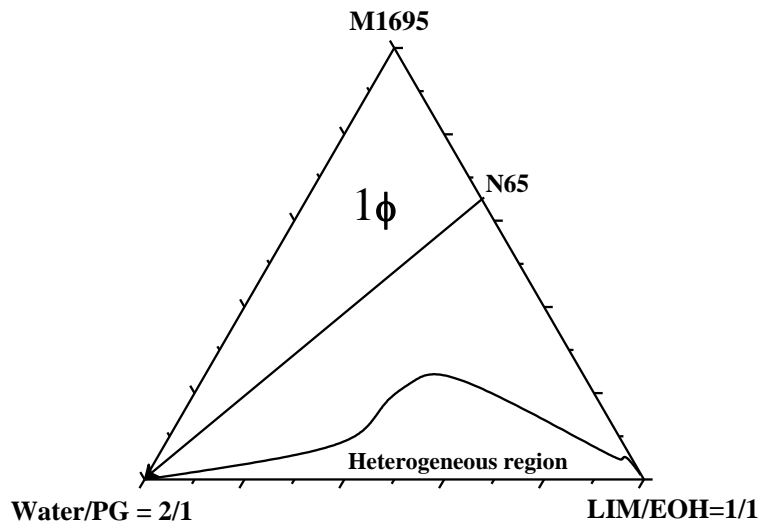


Fig: 5.6 Phase diagram of the system #1 water+ propylene glycol/ Sucrose myristate(M1695) /LIM oil+ ethanol at 37°C. In the figure the one phase region is designated by 1Φ , and the multiple phase regions are designated by heterogeneous region . N65 is the dilution line where the weight ratio of surfactant / single oil is 65/35.

Figure 5.7 Presents the phase diagram of the system water+ propylene glycol/ TMAZ80+ Sucrose myristate(M1695) / LIM oil+ ethanol at 37°C, with aqueous solution made of (2/1)ratio , mixed surfactants TMAZ80+ Sucrose myristate(M1695) with (1/4) ratio and equal unity of LIM oil with ethanol .The one phase microemulsion region appears from the first addition of water and extend to up to the water apex (100%) . 42 % is the maximum water solubilization was reached using 18 % of the surfactant along the dilution line N65. For surfactant below 18 wt% the multiple phase regions extends.

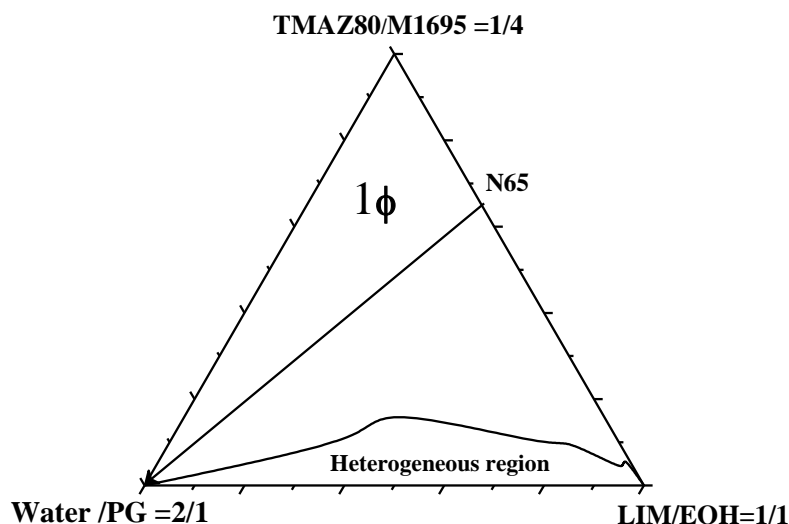


Fig: 5.7 Phase diagram of the system #2 water+ propylene glycol/ TMAZ80+ Sucrose myristate(M1695) /LIM oil+ ethanol at 37°C. In the figure the one phase region is designated by 1Φ , and the multiple phase regions are designated by heterogeneous region . N65 is the dilution line where the weight ratio of surfactant / single oil is 65/35.

Figure 5.8 Presents the phase diagram of the system water+ propylene glycol/ TMAZ80 + Sucrose myristate(M1695) / LIM oil+ ethanol at 37°C, with aqueous solution made of (2/1)ratio , mixed surfactants TMAZ80+ Sucrose myristate(M1695) with (1/1) ratio and equal unity of LIM oil with ethanol .The one phase microemulsion region appears from the first addition of water and extend to up to the water apex (100%) . 45 % is the maximum water solubilization was reached using 16 % of the surfactant along the dilution line N65. For surfactant below 16 wt% the multiple phase regions extends.

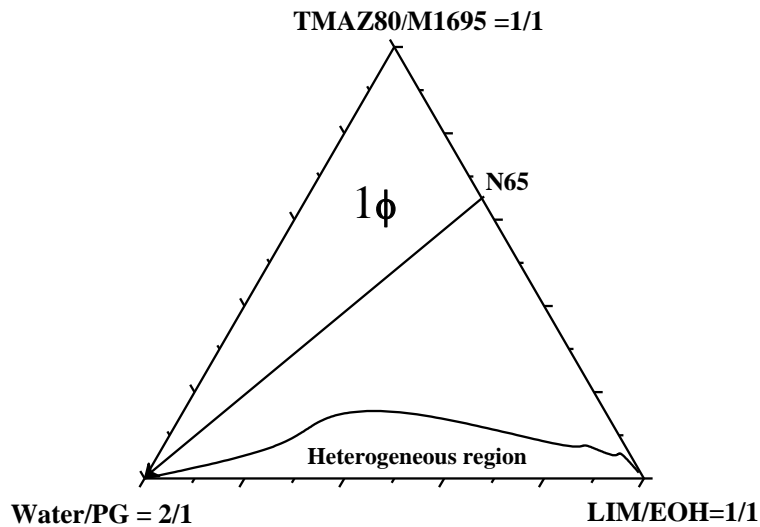


Fig: 5.8 Phase diagram of the system #3 water+ propylene glycol/ TMAZ80+ Sucrose myristate(M1695) /LIM oil+ ethanol at 37°C. In the figure the one phase region is designated by 1Φ , and the multiple phase regions are designated by heterogeneous region . N65 is the dilution line where the weight ratio of surfactant / single oil is 65/35.

Figure 5.9 Presents the phase diagram of the system water+ propylene glycol/ TMAZ80+ Sucrose myristate(M1695) / LIM oil+ ethanol at 37°C, with aqueous solution made of (2/1)ratio , mixed surfactants TMAZ80+ Sucrose myristate(M1695) with (3/4) ratio and equal unity of LIM oil with ethanol .The one phase microemulsion region appears from the first addition of water and extend to up to the water apex (100%) . 45 % is the maximum water solubilization was reached using 17 % of the surfactant along the dilution line N65. For surfactant below 17 wt% the multiple phase regions extends.

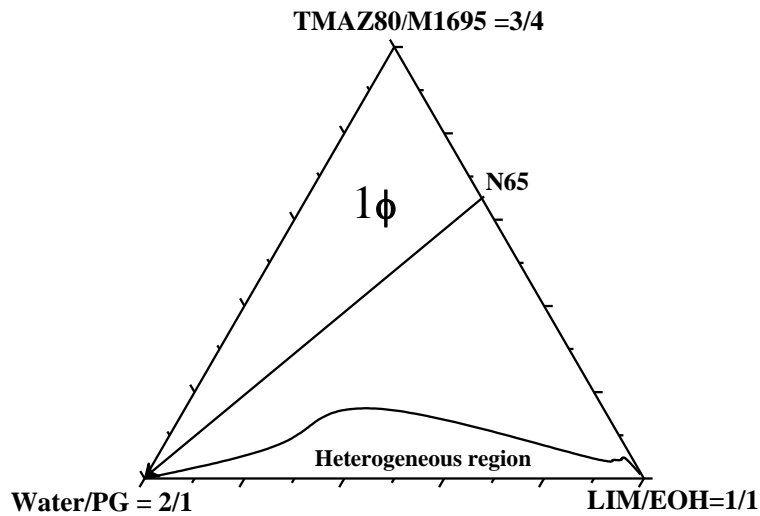


Fig: 5.9 Phase diagram of the system #4 water+ propylene glycol/ TMAZ80 + Sucrose myristate(M1695) /LIM oil+ ethanol at 37°C. In the figure the one phase region is designated by 1Φ, and the multiple phase regions are designated by heterogeneous region . N65 is the dilution line where the weight ratio of surfactant / single oil is 65/35.

Figure 5.10 Presents the phase diagram of the system water+ propylene glycol/ TMAZ80 / LIM oil+ ethanol at 37°C, with aqueous solution made of (2/1)ratio , surfactant TMAZ80 (100%) and equal unity of LIM oil with ethanol .The one phase microemulsion region appears from the first addition of water and extend to up to the water apex (100%) . 45 % is the maximum water solubilization was reached using 17 % of the surfactant along the dilution line N65. For surfactant below 17 wt% the multiple phase regions extends.

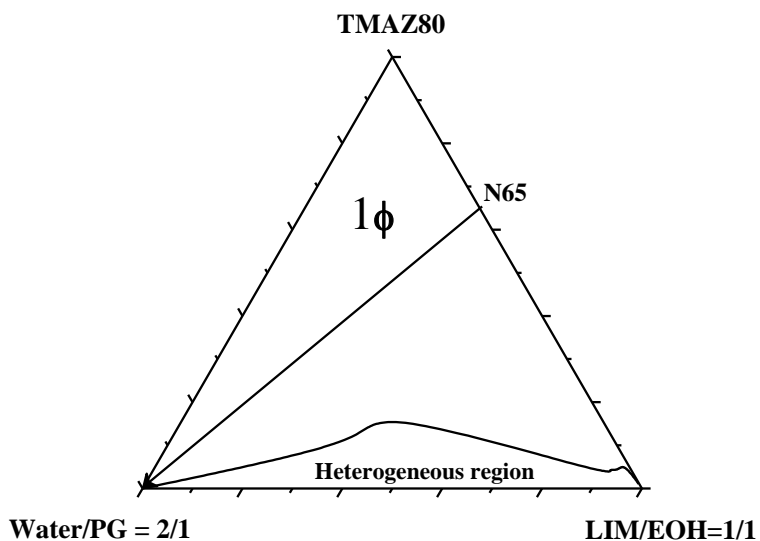


Fig: 5.10 Phase diagram of the system #5 water+ propylene glycol/ TMAZ80/LIM oil+ ethanol at 37°C. In the figure the one phase region is designated by 1Φ , and the multiple phase regions are designated by heterogeneous region . N65 is the dilution line where the weight ratio of surfactant / single oil is 65/35.

Figure 5.11 Presents the phase diagram of the system water+ propylene glycol/ Sucrose myristate(M1695) / LIM oil+ ethanol at 45°C, with aqueous solution made of (2/1)ratio , surfactant myristate(M1695) (100%) and equal unity of LIM oil with ethanol .The one phase microemulsion region appears from the first addition of water and extend to up to the water apex (100%).32 % is the maximum water solubilization was reached using 25 % of the surfactant along the dilution line N65. For surfactant below 25 wt% the multiple phase regions extends.

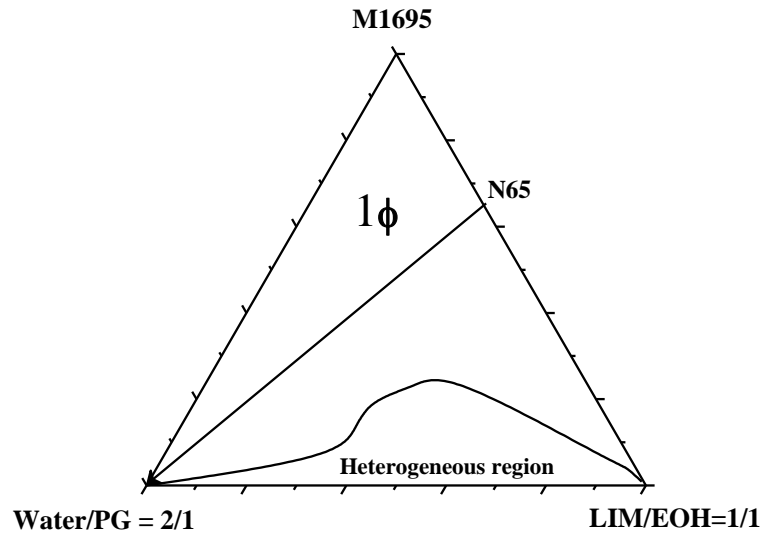


Fig: 5.11 Phase diagram of the system #1 water+ propylene glycol/ Sucrose myristate(M1695) /LIM oil+ ethanol at 45°C. In the figure the one phase region is designated by 1Φ , and the multiple phase regions are designated by heterogeneous region . N65 is the dilution line where the weight ratio of surfactant / single oil is 65/35.

Figure 5.12 Presents the phase diagram of the system water+ propylene glycol/ TMAZ80+Sucrose myristate(M1695) / LIM oil+ ethanol at 45°C, with aqueous solution made of (2/1)ratio , mixed surfactants TMAZ80+ Sucrose myristate(M1695) in the ratio (1/4) and equal unity of LIM oil with ethanol .The one phase microemulsion region appears from the first addition of water and extend to up to the water apex (100%) . 42 % is the maximum water solubilization was reached using 18 % of the surfactant along the dilution line N65. For surfactant below 18 % the multiple phase regions extends.

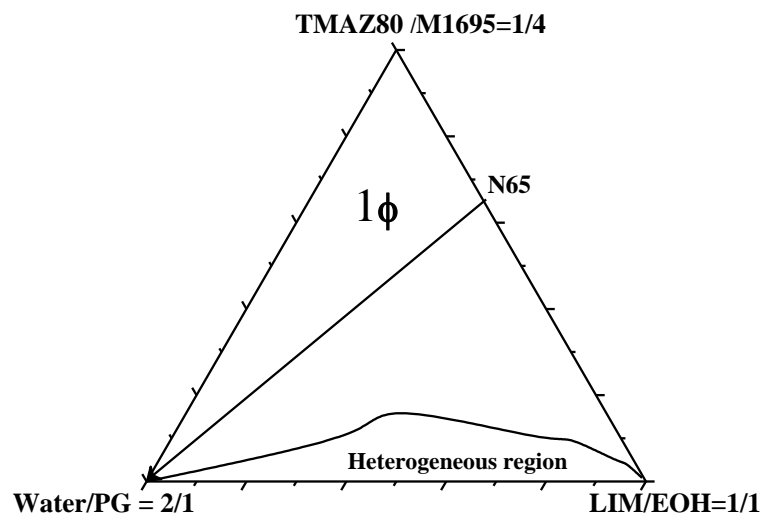


Fig: 5.12 Phase diagram of the system #2 water+ propylene glycol/ TMAZ80+ Sucrose myristate(M1695) /LIM oil+ ethanol at 45°C. In the figure the one phase region is designated by 1Φ , and the multiple phase regions are designated by heterogeneous region . N65 is the dilution line where the weight ratio of surfactant / single oil is 65/35.

Figure 5.13 Presents the phase diagram of the system water+ propylene glycol/ TMAZ80+Sucrose myristate(M1695) / LIM oil+ ethanol at 45°C, with aqueous solution made of (2/1)ratio , mixed surfactants TMAZ80 + myristate(M1695) in the ratio (1/1) and equal unity of LIM oil with ethanol .The one phase microemulsion region appears from the first addition of water and extend to up to the water apex (100%) . 45 % is the maximum water solubilization was reached using 17 % of the surfactant along the dilution line N65. For surfactant below 17 wt% the multiple phase regions extends.

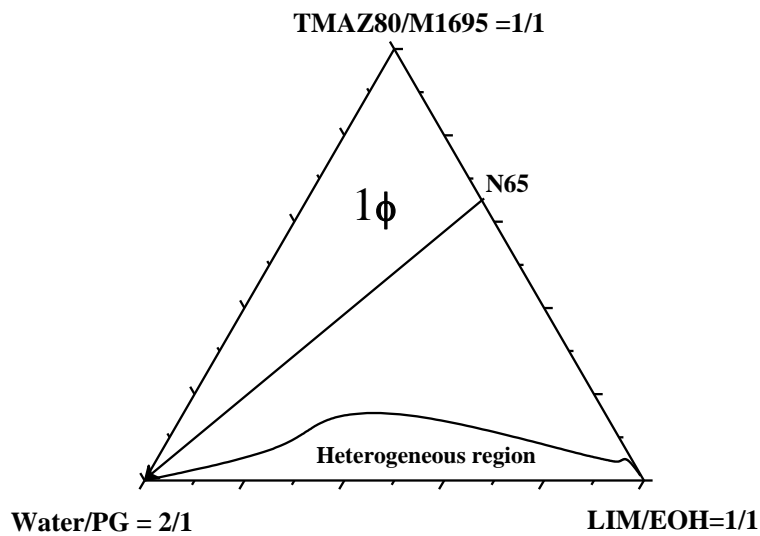


Fig: 5.13 Phase diagram of the system #3 water+ propylene glycol/ TMAZ80+ Sucrose myristate(M1695) /LIM oil+ ethanol at 45°C. In the figure the one phase region is designated by 1Φ , and the multiple phase regions are designated by heterogeneous region . N65 is the dilution line where the weight ratio of surfactant / single oil is 65/35.

Figure 5.14 Presents the phase diagram of the system water+ propylene glycol/ TMAZ80+Sucrose myristate(M1695) / LIM oil+ ethanol at 45°C, with aqueous solution made of (2/1)ratio , mixed surfactants TMAZ80+ Sucrose myristate(M1695) in the ratio (3/4) and equal unity of LIM oil with ethanol .The one phase microemulsion region appears from the first addition of water and extend to up to the water apex (100%).45 % is the maximum water solubilization was reached using 16 % of the surfactant along the dilution line N65. For surfactant below 16 % the multiple phase regions extends.

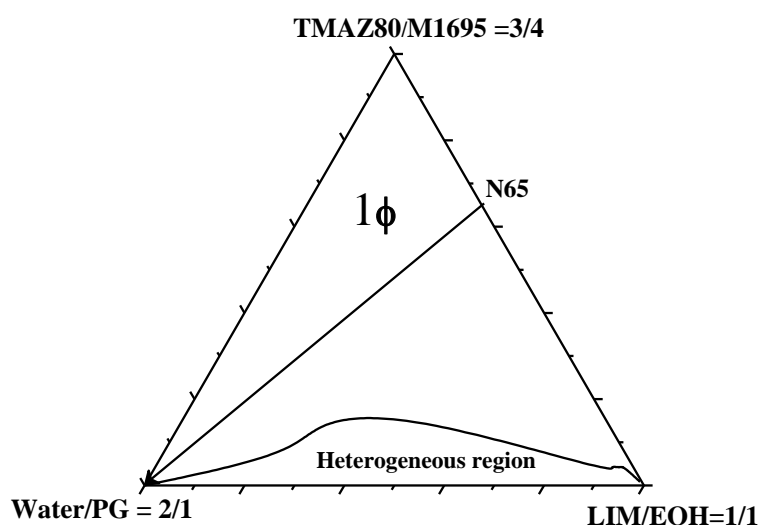


Fig: 5.14 Phase diagram of the system #4 water+ propylene glycol/ TMAZ80+ Sucrose myristate(M1695) /LIM oil+ ethanol at 45°C. In the figure the one phase region is designated by 1Φ , and the multiple phase regions are designated by heterogeneous region . N65 is the dilution line where the weight ratio of surfactant / single oil is 65/35.

Figure 5.15 Presents the phase diagram of the system water+ propylene glycol/ TMAZ80 / LIM oil+ ethanol at 45°C, with aqueous solution made of (2/1)ratio,surfactant TMAZ80 with 100% ratio and equal unity of LIM oil with ethanol .The one phase microemulsion region appears from the first addition of water and extend to up to the water apex (100%) .45 % is the maximum water solubilization was reached using 17 % of the surfactant along the dilution line N65. For surfactant below 17 wt% the multiple phase regions extends.

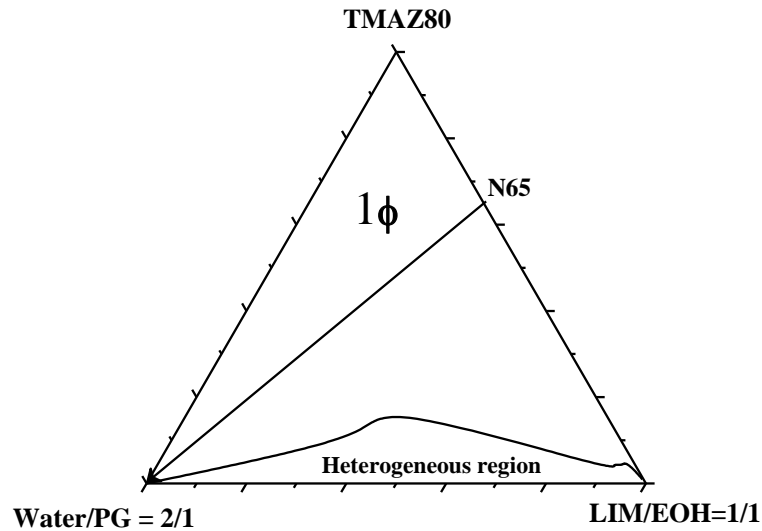


Fig:5.15 Phase diagram of the system #5 water+ propylene glycol/ TMAZ80 /LIM oil+ ethanol at 45°C. In the figure the one phase region is designated by 1Φ , and the multiple phase regions are designated by heterogeneous region . N65 is the dilution line where the weight ratio of surfactant / single oil equals 65/35

Studying the phase behavior of the systems to determine the boundary of one phase region at different temperature (25,37,and 45°C), the results from phase diagrams will determine the total area of the one phase microemulsion region A_T (%) (The total monophasic area A_T

(%). Calculations of the area are made with $\pm 2\%$, comparisons are made for each oil at different concentrations of the surfactants .

5.1.2 Phase behaviour of mixed surfactants TMAZ80+ Sucrose myristate (M1695) with IPM oil at (25,37 ,and 45°C).

Figure 5.16 Presents the phase diagram of the system water+ propylene glycol/ Sucrose myristate(M1695) / IPM oil+ ethanol at 25°C, with aqueous solution made of (2/1)ratio , surfactant myristate(M1695) (100%) and equal unity of IPM oil with ethanol .The one phase microemulsion region appears from the first addition of water and extend to up to the water apex (100%) .20 % is the maximum water solubilization was reached using 38 % of the surfactant along the dilution line N65. For surfactant below 17 wt% the multiple phase regions extends.

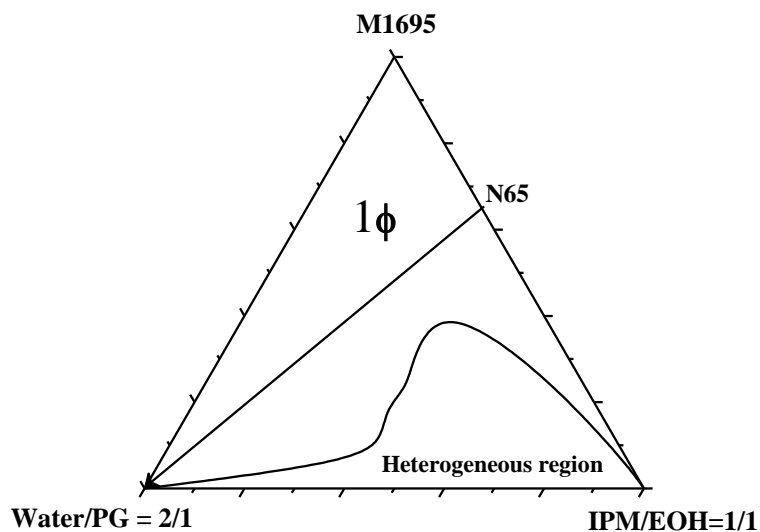


Fig:5.16 Phase diagram of the system #6 water+ propylene glycol/ Sucrose myristate(M1695) /IPM oil+ ethanol at 25°C. In the figure the one phase region is designated by 1Φ , and the multiple phase regions are designated by heterogeneous region .N65 is the dilution line where the weight ratio of surfactant / single oil is 65/35.

Figure 5.17 Presents the phase diagram of the system water+ propylene glycol/ TMAZ80+Sucrose myristate(M1695) / IPM oil+ ethanol at 25°C, with aqueous solution made of (2/1)ratio , mixed surfactants TMAZ80+ Sucrose myristate(M1695) in the ratio (1/4) and equal unity of IPM oil with ethanol .The one phase microemulsion region appears from the first addition of water and extend to up to the water apex (100%) .32 % is the maximum water solubilization was reached using 27 % of the surfactant along the dilution line N65. For surfactant below 27 wt% the multiple phase regions extends.

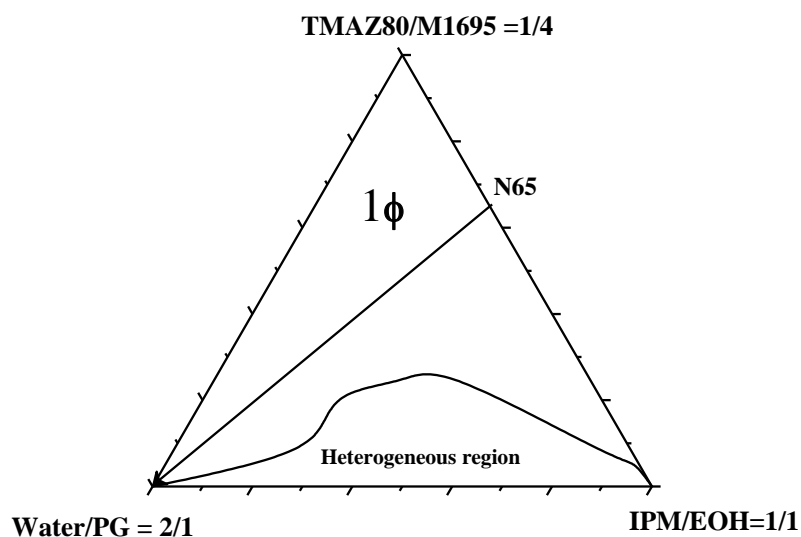


Fig: 5.17 Phase diagram of the system #7 water+ propylene glycol/ TMAZ80+ Sucrose myristate(M1695) /IPM oil+ ethanol at 25°C. In the figure the one phase region is designated by 1Φ , and the multiple phase regions are designated by heterogeneous region . N65 is the dilution line where the weight ratio of surfactant / single oil is 65/35.

Figure 5.18 Presents the phase diagram of the system water+ propylene glycol/ TMAZ80 +Sucrose myristate(M1695) / IPM oil+ ethanol at 25°C, with aqueous solution made of (2/1)ratio , mixed surfactants TMAZ80+ Sucrose myristate(M1695) in the ratio (1/1) and equal unity of IPM oil with ethanol .The one phase microemulsion region appears from the first addition of water and extend to up to the water apex (100%) .38 % is the maximum water solubilization was reached using 21 % of the surfactant along the dilution line N65. For surfactant below 21 % the multiple phase regions extends.

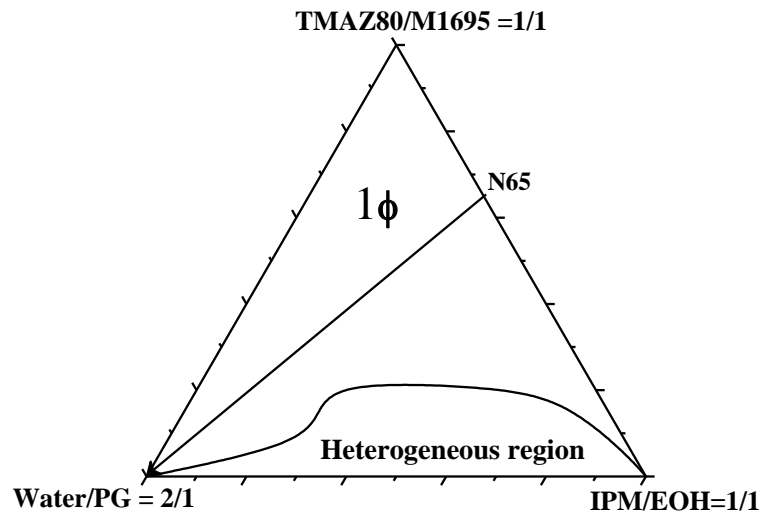


Fig: 5.18 Phase diagram of the system #8 water+ propylene glycol/ TMAZ80 + Sucrose myristate(M1695) /IPM oil+ ethanol at 25°C. In the figure the one phase region is designated by 1Φ , and the multiple phase regions are designated by heterogeneous region . N65 is the dilution line where the weight ratio of surfactant / single oil is 65/35.

Figure 5.19 Presents the phase diagram of the system water+ propylene glycol/ TMAZ80+Sucrose myristate(M1695) / IPM oil+ ethanol at 25°C, with aqueous solution made of (2/1)ratio , mixed surfactants TMAZ80 + myristate(M1695) in the ratio (3/4) and equal unity of IPM oil with ethanol .The one phase microemulsion region appears from the first addition of water and extend to up to the water apex (100%) .35 % is the maximum water solubilization was reached using 28 % of the surfactant along the dilution line N65. For surfactant below 28 % the multiple phase regions extends.

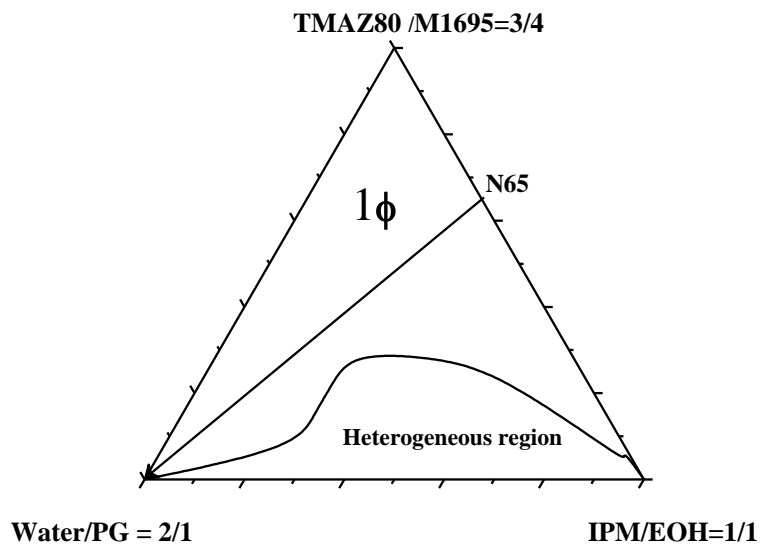


Fig: 5.19 Phase diagram of the system #9 water+ propylene glycol/ TMAZ80 + Sucrose myristate(M1695) /IPM oil+ ethanol at 25°C. In the figure the one phase region is designated by 1Φ , and the multiple phase regions are designated by heterogeneous region . N65 is the dilution line where the weight ratio of surfactant / single oil is 65/35.

Figure 5.20 Presents the phase diagram of the system water+ propylene glycol/ TMAZ80/ IPM oil+ ethanol at 25°C, with aqueous solution made of (2/1)ratio , surfactant TMAZ80 (100%) and equal unity of IPM oil with ethanol .The one phase microemulsion region appears from the first addition of water and extend to up to the water apex (100%) .20 % is the maximum water solubilization was reached using 33 % of the surfactant along the dilution line N65. For surfactant below 33 wt% the multiple phase regions extends.

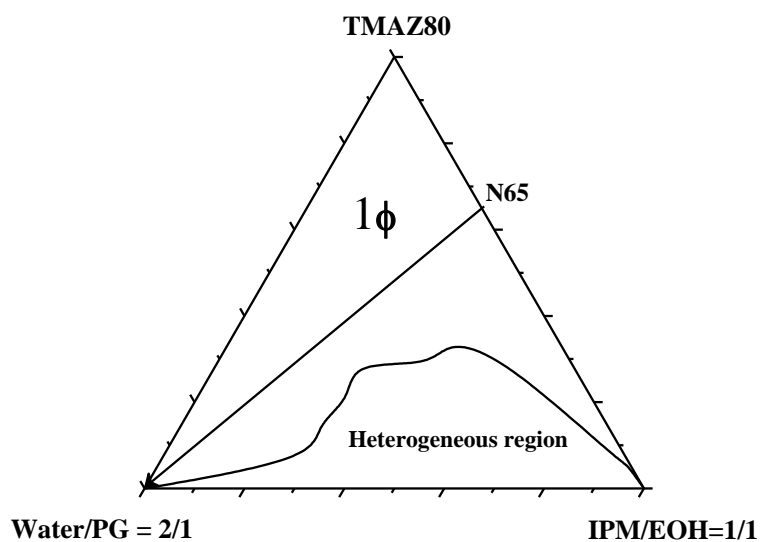


Fig: 5.20 Phase diagram of the system #10 water+ propylene glycol/ TMAZ80 /IPM oil+ ethanol at 25°C. In the figure the one phase region is designated by 1Φ , and the multiple phase regions are designated by heterogeneous region . N65 is the dilution line where the weight ratio of surfactant / single oil is 65/35.

Figure 5.21 Presents the phase diagram of the system water+ propylene glycol/ Sucrose myristate(M1695) / IPM oil+ ethanol at 37°C, with aqueous solution made of (2/1)ratio , surfactant myristate(M1695) (100%) and equal unity of IPM oil with ethanol .The one phase microemulsion region appears from the first addition of water and extend to up to the water apex (100%),42 % is the maximum water solubilization was reached using 41 % of the surfactant along the dilution line N65. For surfactant below 41 % the multiple phase regions extends.

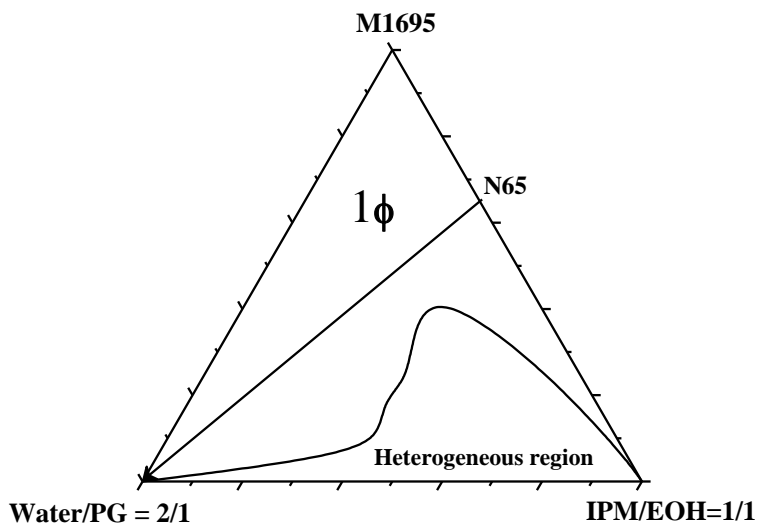


Fig: 5.21 Phase diagram of the system#6 water+ propylene glycol/ Sucrose myristate(M1695) /IPM oil+ ethanol at 37°C. In the figure the one phase region is designated by 1Φ , and the multiple phase regions are designated by heterogeneous region . N65 is the dilution line where the weight ratio of surfactant / single oil is 65/35.

Figure 5.22 Presents the phase diagram of the system water+ propylene glycol/ TMAZ80+Sucrose myristate(M1695) / IPM oil+ ethanol at 37°C, with aqueous solution made of (2/1)ratio , mixed surfactants TMAZ80 + myristate(M1695) in the ratio (1/4) and equal unity of IPM oil with ethanol .The one phase microemulsion region appears from the first addition of water and extend to up to the water apex (100%). 33 % is the maximum water solubilization was reached using 28 % of the surfactant along the dilution line N65. For surfactant below 28 wt% the multiple phase regions extends.

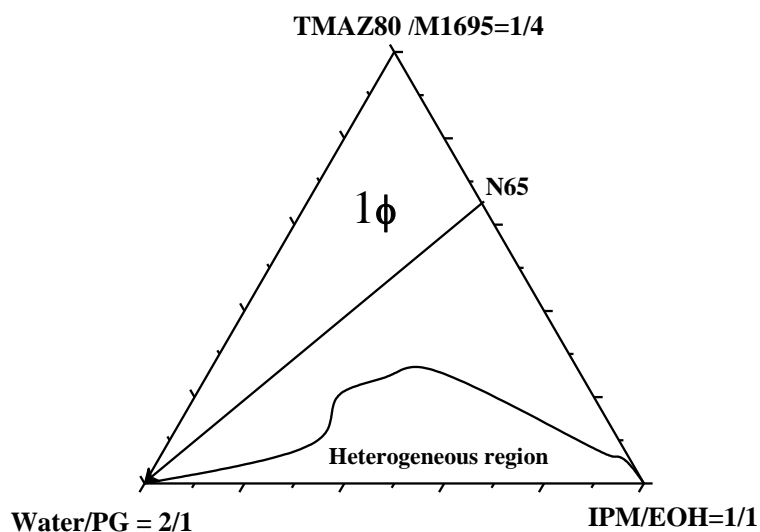


Fig: 5.22 Phase diagram of the system#7 water+ propylene glycol/ TMAZ80+ Sucrose myristate(M1695) /IPM oil+ ethanol at 37°C. In the figure the one phase region is designated by 1Φ , and the multiple phase regions are designated by heterogeneous region . N65 is the dilution line where the weight ratio of surfactant / single oil is 65/35.

Figure 5.23 Presents the phase diagram of the system water+ propylene glycol/ TMAZ80+Sucrose myristate(M1695) / IPM oil+ ethanol at 37°C, with aqueous solution made of (2/1)ratio , mixed surfactants TMAZ80+ Sucrose myristate(M1695) in the ratio (1/1) and equal unity of IPM oil with ethanol .The one phase microemulsion region appears from the first addition of water and extend to up to the water apex (100%). 45 % is the maximum water solubilization was reached using 18 % of the surfactant along the dilution line N65. For surfactant below 18 wt% the multiple phase regions extends.

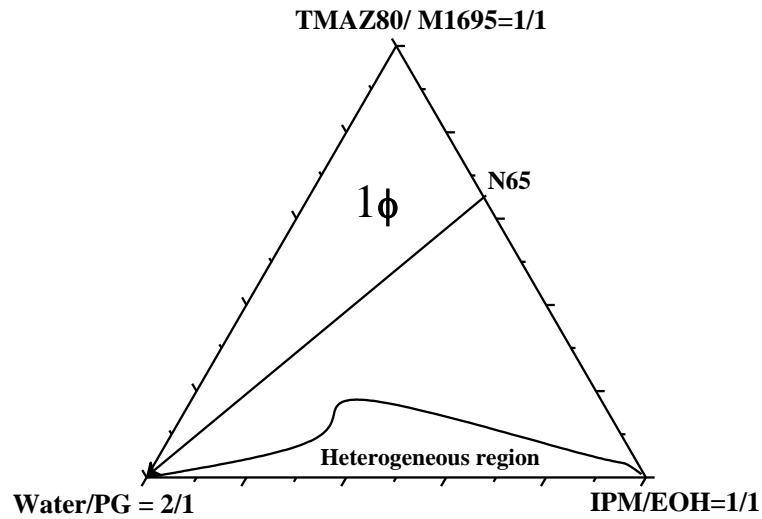


Fig: 5.23 Phase diagram of the system#8 water+ propylene glycol/ TMAZ80+ Sucrose myristate(M1695) /IPM oil+ ethanol at 37°C. In the figure the one phase region is designated by 1Φ , and the multiple phase regions are designated by heterogeneous region . N65 is the dilution line where the weight ratio of surfactant / single oil is 65/35.

Figure 5.24 Presents the phase diagram of the system water+ propylene glycol/ TMAZ80 +Sucrose myristate(M1695) / IPM oil+ ethanol at 37°C, with aqueous solution made of (2/1)ratio , mixed surfactants TMAZ80+ Sucrose myristate(M1695) in the ratio (3/4) and equal unity of IPM oil with ethanol .The one phase microemulsion region appears from the first addition of water and extend to up to the water apex (100%). 35 % is the maximum water solubilization was reached using 28 % of the surfactant along the dilution line N65. For surfactant below 28 % the multiple phase regions extends.

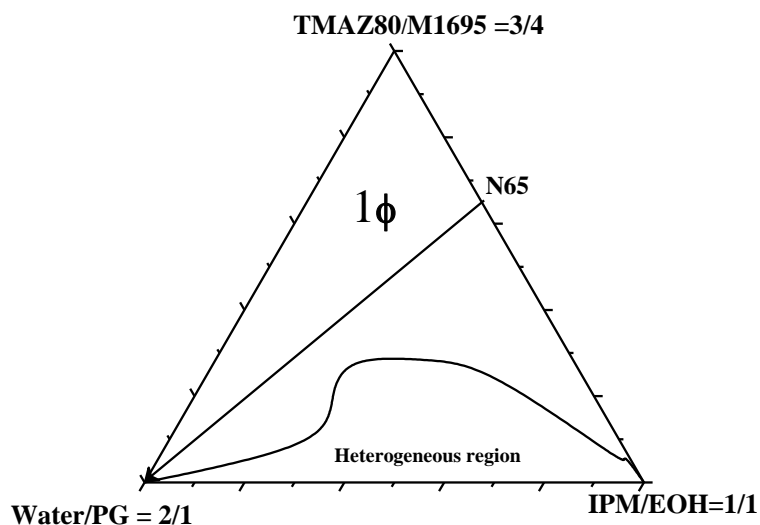


Fig: 5.24 Phase diagram of the system #9 water+ propylene glycol/ TMAZ80 + Sucrose myristate(M1695) /IPM oil+ ethanol at 37°C. In the figure the one phase region is designated by 1Φ , and the multiple phase regions are designated by heterogeneous region . N65 is the dilution line where the weight ratio of surfactant / single oil is 65/35.

Figure 5.25 Presents the phase diagram of the system water+ propylene glycol/ TMAZ80 / IPM oil+ ethanol at 37°C, with aqueous solution made of (2/1)ratio , surfactant TMAZ80 (100%) and equal unity of IPM oil with ethanol .The one phase microemulsion region appears from the first addition of water and extend to up to the water apex (100%) . 20 % is the maximum water solubilization was reached using 33 % of the surfactant along the dilution line N65. For surfactant below 33 % the multiple phase regions extends.

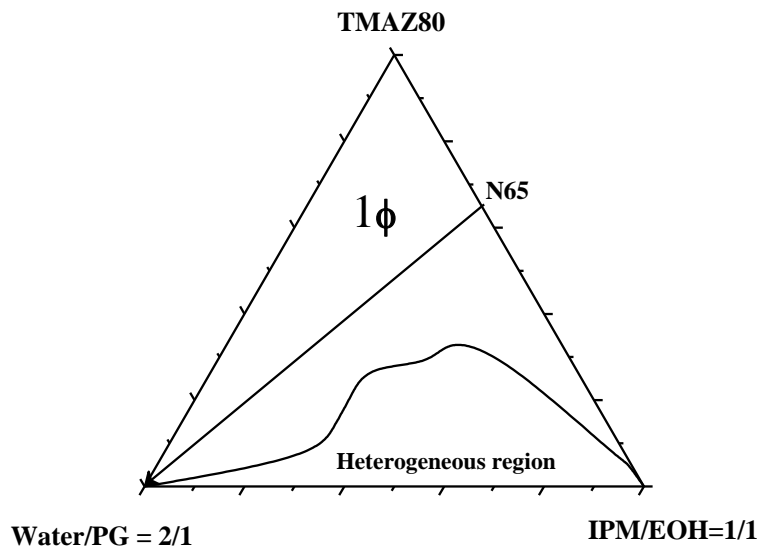


Fig: 5.25 Phase diagram of the system#10 water+ propylene glycol/ TMAZ80/IPM oil+ ethanol at 37°C. In the figure the one phase region is designated by 1Φ , and the multiple phase regions are designated by heterogeneous region . N65 is the dilution line where the weight ratio of surfactant / single oil is 65/35.

Figure 5.26 Presents the phase diagram of the system water+ propylene glycol/ Sucrose myristate(M1695) / IPM oil+ ethanol at 45°C, with aqueous solution made of (2/1)ratio , surfactant myristate(M1695) (100%) and equal unity of IPM oil with ethanol .The one phase microemulsion region appears from the first addition of water and extend to up to the water apex (100%). 20 % is the maximum water solubilization was reached using 38 % of the surfactant along the dilution line N65. For surfactant below 38 wt% the multiple phase regions extends.

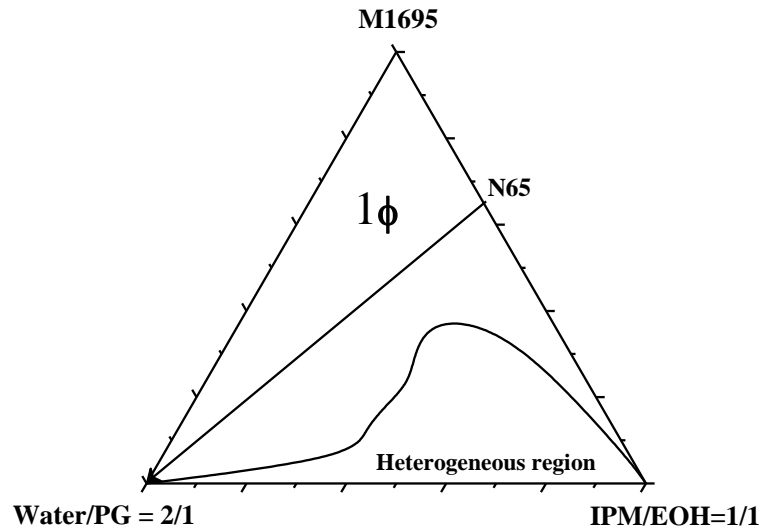


Fig: 5.26 Phase diagram of the system#6 water+ propylene glycol/ Sucrose myristate(M1695) /IPM oil+ ethanol at 45°C. In the figure the one phase region is designated by 1Φ , and the multiple phase regions are designated by heterogeneous region . N65 is the dilution line where the weight ratio of surfactant / single oil is 65/35.

Figure 5.27 Presents the phase diagram of the system water+ propylene glycol/ TMAZ80+Sucrose myristate(M1695) / IPM oil+ ethanol at 45°C, with aqueous solution made of (2/1)ratio , mixed surfactants TMAZ80+ Sucrose myristate(M1695) in the ratio (1/4) and equal unity of IPM oil with ethanol .The one phase microemulsion region appears from the first addition of water and extend to up to the water apex (100%) . 40 % is the maximum water solubilization was reached using 31 % of the surfactant along the dilution line N65. For surfactant below 31 wt% the multiple phase regions extends.

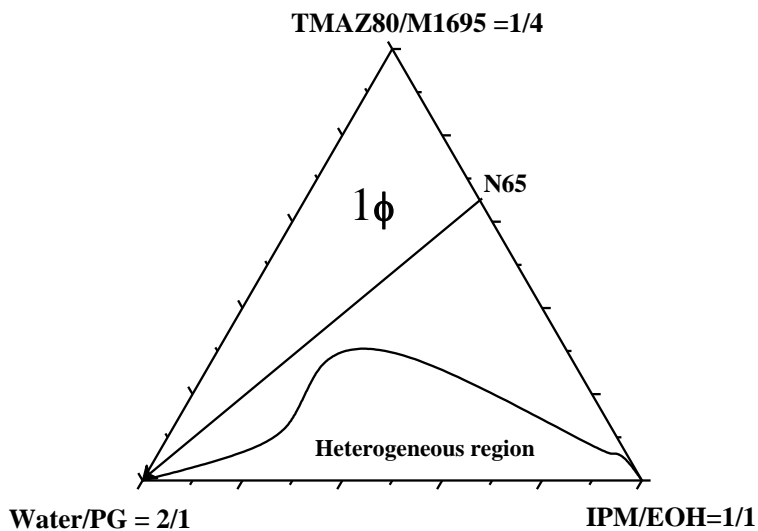


Fig: 5.27 Phase diagram of the system #7 water+ propylene glycol/ TMAZ80+ Sucrose myristate(M1695) /IPM oil+ ethanol at 45°C. In the figure the one phase region is designated by 1ϕ , and the multiple phase regions are designated by heterogeneous region . N65 is the dilution line where the weight ratio of surfactant / single oil is 65/35.

Figure 5.28 Presents the phase diagram of the system water+ propylene glycol/ TMAZ80+Sucrose myristate(M1695) / IPM oil+ ethanol at 45°C, with aqueous solution made of (2/1)ratio , mixed surfactants TMAZ80+ Sucrose myristate(M1695) in the ratio (1/1) and equal unity of IPM oil with ethanol .The one phase microemulsion region appears from the first addition of water and extend to up to the water apex (100%). 55 % is the maximum water solubilization was reached using 19 % of the surfactant along the dilution line N65. For surfactant below 19 % the multiple phase regions extends.

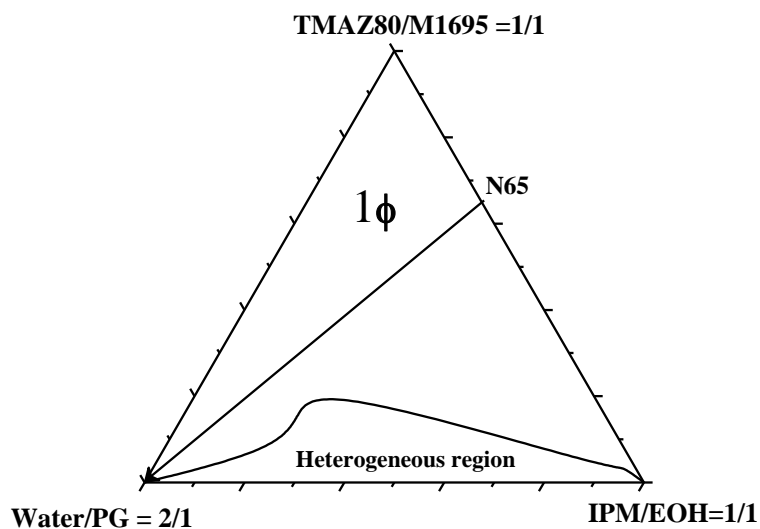


Fig: 5.28 Phase diagram of the system#8 water+ propylene glycol/ TMAZ80+ Sucrose myristate(M1695) /IPM oil+ ethanol at 45°C. In the figure the one phase region is designated by 1Φ , and the multiple phase regions are designated by heterogeneous region . N65 is the dilution line where the weight ratio of surfactant / single oil is 65/35.

Figure 5.29 Presents the phase diagram of the system water+ propylene glycol/ TMAZ80+Sucrose myristate(M1695) / IPM oil+ ethanol at 45°C, with aqueous solution made of (2/1)ratio , mixed surfactants TMAZ80+ Sucrose myristate(M1695) in the ratio (3/4) and equal unity of IPM oil with ethanol .The one phase microemulsion region appears from the first addition of water and extend to up to the water apex (100%) .40 % is the maximum water solubilization was reached using 30 % of the surfactant along the dilution line N65. For surfactant below 30 % the multiple phase regions extends.

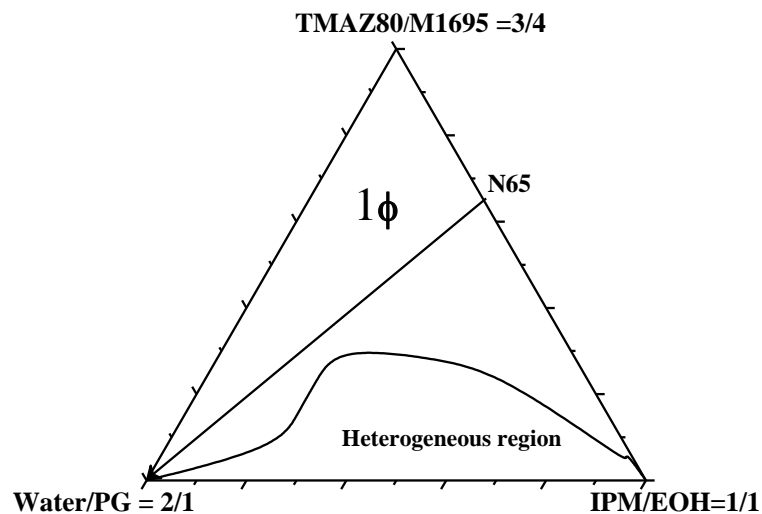


Fig: 5.29 Phase diagram of the system#9 water+ propylene glycol/ TMAZ80 + Sucrose myristate(M1695) /IPM oil+ ethanol at 45°C. In the figure the one phase region is designated by 1Φ , and the multiple phase regions are designated by heterogeneous region . N65 is the dilution line where the weight ratio of surfactant / single oil is 65/35.

Figure 5.30 Presents the phase diagram of the system water+ propylene glycol/ TMAZ80/ IPM oil+ ethanol at 45°C, with aqueous solution made of (2/1)ratio , surfactant TMAZ80 (100%) and equal unity of IPM oil with ethanol .The one phase microemulsion region appears from the first addition of water and extend to up to the water apex (100%) . 28 % is the maximum water solubilization was reached using 34 % of the surfactant along the dilution line N65. For surfactant below 34 wt% the multiple phase regions extends.

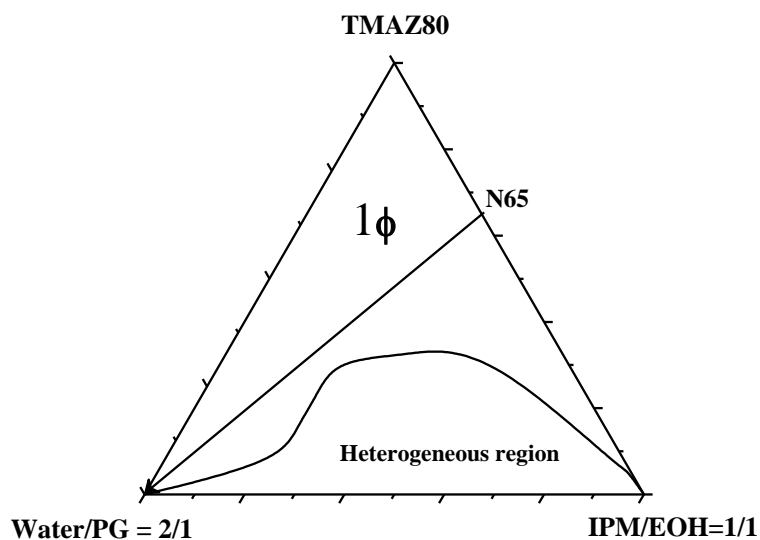


Fig: 5.30 Phase diagram of the system#10 water+ propylene glycol/ TMAZ80/IPM oil+ ethanol at 45°C. In the figure the one phase region is designated by 1Φ , and the multiple phase regions are designated by heterogeneous region . N65 is the dilution line where the weight ratio of surfactant / single oil is 65/35.

5.1.3 Phase behaviour of mixed surfactants TMAZ80+ Sucrose myristate (M1695) with CCT oil at (25,37 ,and 45°C).

Figure 5.31 Presents the phase diagram of the system water+ propylene glycol/ Sucrose myristate(M1695) / CCT oil+ ethanol at 25°C, with aqueous solution made of (2/1)ratio , surfactant myristate(M1695) (100%) and equal unity of CCT oil with ethanol .The one phase microemulsion region appears from the first addition of water and extend to up to the water apex (100%) . 15 % is the maximum water solubilization was reached using 40 % of the surfactant along the dilution line N65. For surfactant below 40 % the multiple phase regions extends.

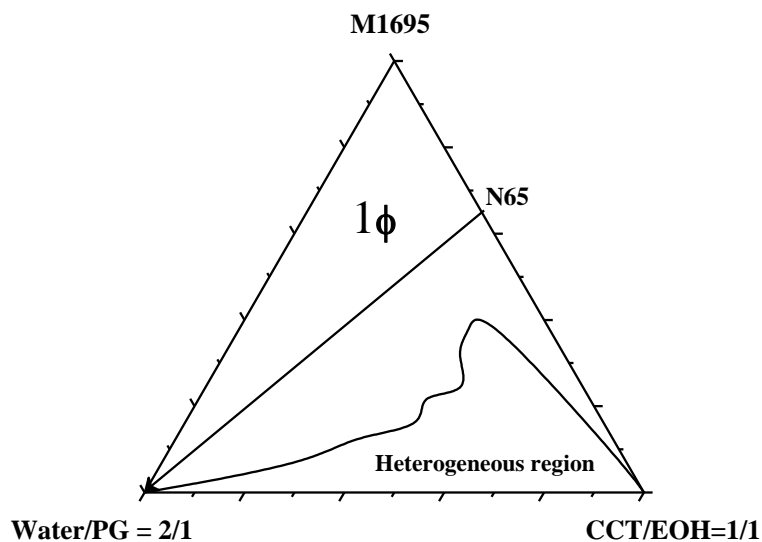


Fig: 5.31 Phase diagram of the system #11 water+ propylene glycol/ Sucrose myristate(M1695) /CCT oil+ ethanol at 25°C. In the figure the one phase region is designated by 1Φ , and the multiple phase regions are designated by heterogeneous region . N65 is the dilution line where the weight ratio of surfactant / single oil is 65/35.

Figure 5.32 Presents the phase diagram of the system water+ propylene glycol/ TMAZ80 +Sucrose myristate(M1695) /CCT oil+ ethanol at 25°C, with aqueous solution made of (2/1)ratio , mixed surfactants TMAZ80+ Sucrose myristate(M1695) in the ratio (1/4) and equal unity of CCT oil with ethanol .The one phase microemulsion region appears from the first addition of water and extend to up to the water apex (100%). 40 % is the maximum water solubilization was reached using 28 % of the surfactant along the dilution line N65. For surfactant below 28 wt% the multiple phase regions extends.

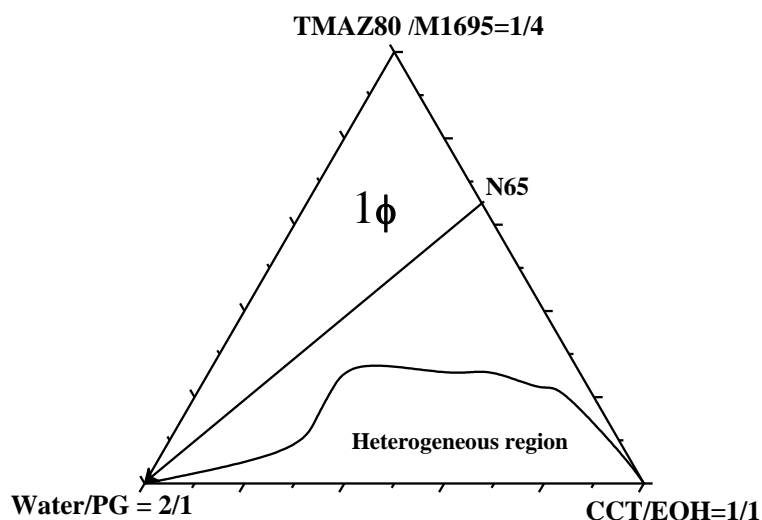


Fig: 5.32 Phase diagram of the system #12 water+ propylene glycol/ TMAZ80+ Sucrose myristate(M1695) /CCT oil+ ethanol at 25°C. In the figure the one phase region is designated by 1Φ , and the multiple phase regions are designated by heterogeneous region . N65 is the dilution line where the weight ratio of surfactant / single oil is 65/35.

Figure 5.33 Presents the phase diagram of the system water+ propylene glycol/ TMAZ80+Sucrose myristate(M1695) /CCT oil+ ethanol at 25°C, with aqueous solution made of (2/1)ratio , mixed surfactants TMAZ80 + myristate(M1695) in the ratio (1/1) and equal unity of CCT oil with ethanol .The one phase microemulsion region appears from the first addition of water and extend to up to the water apex (100%) . 35 % is the maximum water solubilization was reached using 24 % of the surfactant along the dilution line N65. For surfactant below 24 wt% the multiple phase regions extends.

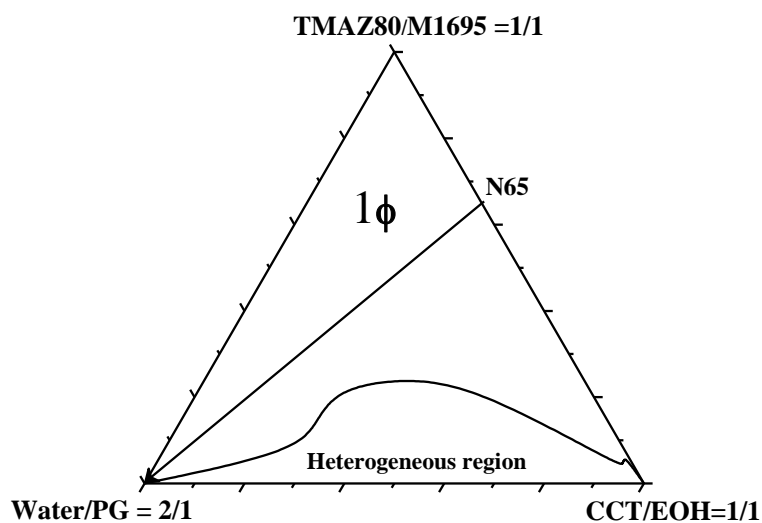


Fig: 5.33 Phase diagram of the system#13 water+ propylene glycol/ TMAZ80+ Sucrose myristate(M1695) /CCT oil+ ethanol at 25°C. In the figure the one phase region is designated by 1Φ , and the multiple phase regions are designated by heterogeneous region . N65 is the dilution line where the weight ratio of surfactant / single oil is 65/35.

Figure 5.34 Presents the phase diagram of the system water+ propylene glycol/ TMAZ80 +Sucrose myristate(M1695) /CCT oil+ ethanol at 25°C, with aqueous solution made of (2/1)ratio , mixed surfactants TMAZ80+ Sucrose myristate(M1695) in the ratio (3/4) and equal unity of CCT oil with ethanol .The one phase microemulsion region appears from the first addition of water and extend to up to the water apex (100%). 25 % is the maximum water solubilization was reached using 32 % of the surfactant along the dilution line N65. For surfactant below 32 wt% the multiple phase regions extends.

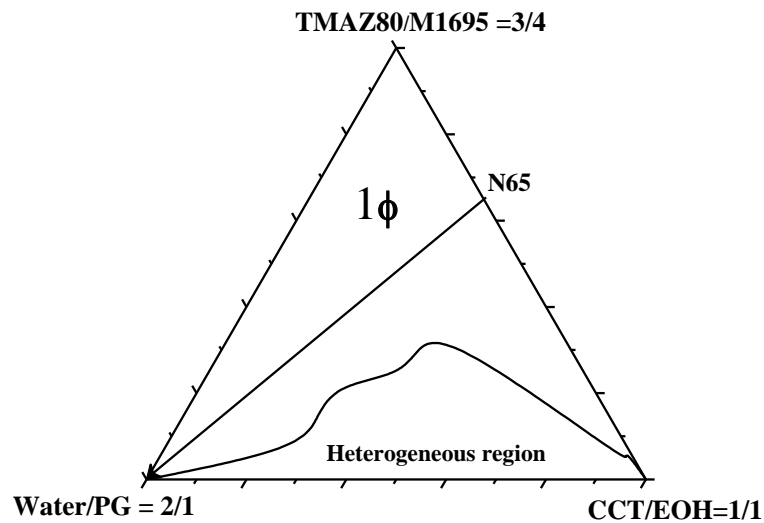


Fig: 5.34 Phase diagram of the system #14 water+ propylene glycol/ TMAZ80+ Sucrose myristate(M1695) /CCT oil+ ethanol at 25°C. In the figure the one phase region is designated by 1Φ , and the multiple phase regions are designated by heterogeneous region . N65 is the dilution line where the weight ratio of surfactant / single oil is 65/35.

Figure 5.35 Presents the phase diagram of the system water+ propylene glycol/ TMAZ80/ CCT oil+ ethanol at 25°C, with aqueous solution made of (2/1)ratio , surfactant TMAZ80 (100%) and equal unity of CCT oil with ethanol .The one phase microemulsion region appears from the first addition of water and extend to up to the water apex (100%). 30 % is the maximum water solubilization was reached using 25 % of the surfactant along the dilution line N65. For surfactant below 25 wt% the multiple phase regions extends.

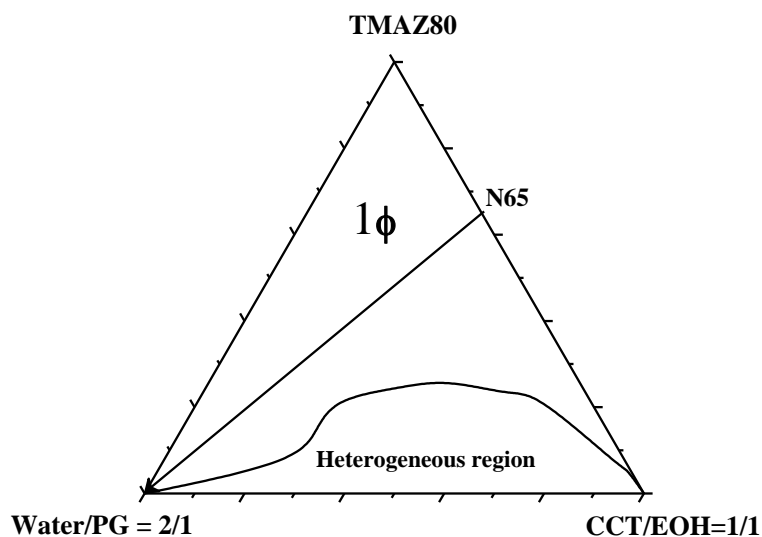


Fig: 5.35 Phase diagram of the system#15 water+ propylene glycol/ TMAZ80 /CCT oil+ ethanol at 25°C. In the figure the one phase region is designated by 1Φ , and the multiple phase regions are designated by heterogeneous region . N65 is the dilution line where the weight ratio of surfactant / single oil is 65/35.

Figure 5.36 Presents the phase diagram of the system water+ propylene glycol/ Sucrose myristate(M1695) / CCT oil+ ethanol at 37°C, with aqueous solution made of (2/1)ratio , surfactant myristate(M1695) (100%) and equal unity of CCT oil with ethanol .The one phase microemulsion region appears from the first addition of water and extend to up to the water apex (100%). 13 % is the maximum water solubilization was reached using 37 % of the surfactant along the dilution line N65. For surfactant below 37 wt% the multiple phase regions extends.

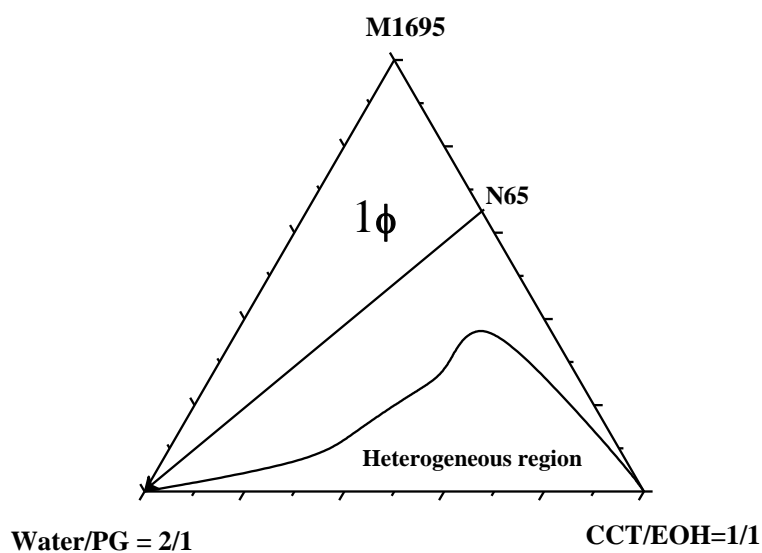


Fig: 5.36 Phase diagram of the system#11 water+ propylene glycol/ Sucrose myristate(M1695) /CCT oil+ ethanol at 37°C. In the figure the one phase region is designated by 1Φ , and the multiple phase regions are designated by heterogeneous region . N65 is the dilution line where the weight ratio of surfactant / single oil is 65/35.

Figure 5.37 Presents the phase diagram of the system water+ propylene glycol/ TMAZ80 +Sucrose myristate(M1695) /CCT oil+ ethanol at 37°C, with aqueous solution made of (2/1)ratio , mixed surfactants TMAZ80+ Sucrose myristate(M1695) in the ratio (1/4) and equal unity of CCT oil with ethanol .The one phase microemulsion region appears from the first addition of water and extend to up to the water apex (100%). 40 % is the maximum water solubilization was reached using 28 % of the surfactant along the dilution line N65. For surfactant below 28 % the multiple phase regions extends.

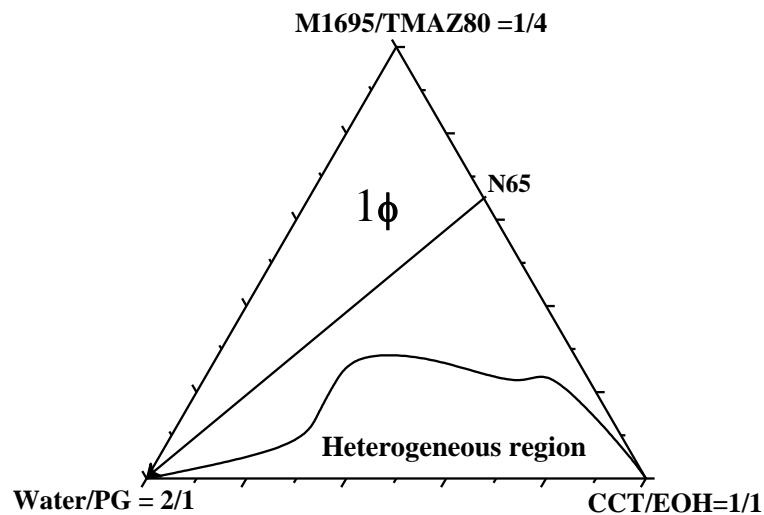


Fig: 5.37 Phase diagram of the system#12 water+ propylene glycol/ TMAZ80+ Sucrose myristate(M1695) /CCT oil+ ethanol at 37°C. In the figure the one phase region is designated by 1Φ , and the multiple phase regions are designated by heterogeneous region . N65 is the dilution line where the weight ratio of surfactant / single oil is 65/35.

Figure 5.38 Presents the phase diagram of the system water+ propylene glycol/ TMAZ80+Sucrose myristate(M1695) /CCT oil+ ethanol at 37°C, with aqueous solution made of (2/1)ratio , mixed surfactants TMAZ80+ Sucrose myristate(M1695) in the ratio (1/1) and equal unity of CCT oil with ethanol .The one phase microemulsion region appears from the first addition of water and extend to up to the water apex (100%) . 35 % is the maximum water solubilization was reached using 24 % of the surfactant along the dilution line N65. For surfactant below 24 % the multiple phase regions extends.

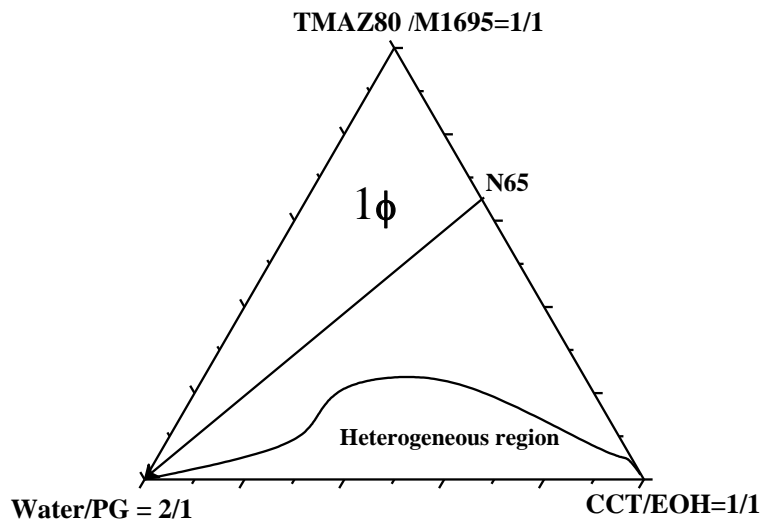


Fig: 5.38 Phase diagram of the system #13 water+ propylene glycol/ TMAZ80+ Sucrose myristate(M1695) /CCT oil+ ethanol at 37°C. In the figure the one phase region is designated by 1Φ , and the multiple phase regions are designated by heterogeneous region . N65 is the dilution line where the weight ratio of surfactant / single oil is 65/35.

Figure 5.39 Presents the phase diagram of the system water+ propylene glycol/ TMAZ80+Sucrose myristate(M1695) /CCT oil+ ethanol at 37°C, with aqueous solution made of (2/1)ratio , mixed surfactants TMAZ80+ Sucrose myristate(M1695) in the ratio (3/4) and equal unity of CCT oil with ethanol .The one phase microemulsion region appears from the first addition of water and extend to up to the water apex (100%) . 28 % is the maximum water solubilization was reached using 31 % of the surfactant along the dilution line N65. For surfactant below 31 % the multiple phase regions extends.

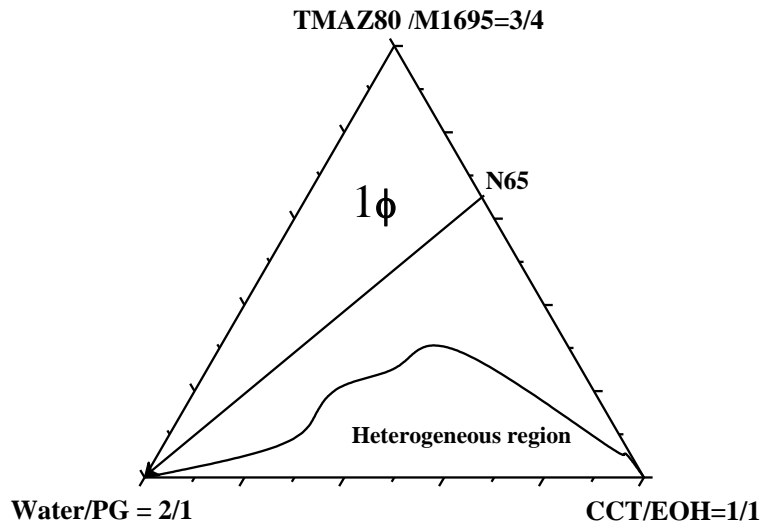


Fig: 5.39 Phase diagram of the system #14 water+ propylene glycol/ TMAZ80+ Sucrose myristate(M1695) /CCT oil+ ethanol at 37°C. In the figure the one phase region is designated by 1Φ , and the multiple phase regions are designated by heterogeneous region . N65 is the dilution line where the weight ratio of surfactant / single oil is 65/35.

Figure 5.40 Presents the phase diagram of the system water+ propylene glycol/ TMAZ80/ CCT oil+ ethanol at 37°C, with aqueous solution made of (2/1)ratio , surfactant TMAZ80 (100%) and equal unity of CCT oil with ethanol .The one phase microemulsion region appears from the first addition of water and extend to up to the water apex (100%). 27 % is the maximum water solubilization was reached using 26 % of the surfactant along the dilution line N65. For surfactant below 26 % the multiple phase regions extends.

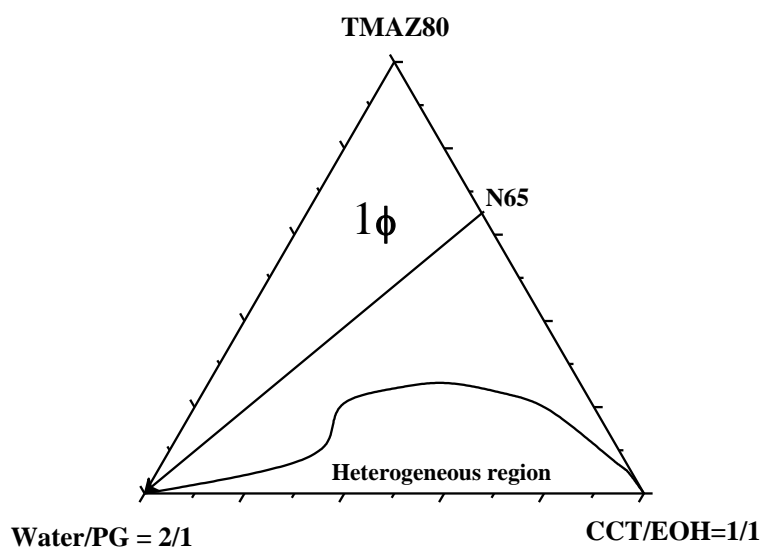


Fig: 5.40 Phase diagram of the system#15 water+ propylene glycol/ TMAZ80 /CCT oil+ ethanol at 37°C. In the figure the one phase region is designated by 1Φ , and the multiple phase regions are designated by heterogeneous region . N65 is the dilution line where the weight ratio of surfactant / single oil is 65/35.

Figure 5.41 Presents the phase diagram of the system water+ propylene glycol/ Sucrose myristate(M1695) / CCT oil+ ethanol at 45°C, with aqueous solution made of (2/1)ratio , surfactant myristate(M1695) (100%) and equal unity of CCT oil with ethanol .The one phase microemulsion region appears from the first addition of water and extend to up to the water apex (100%). 17% is the maximum water solubilization was reached using 39 % of the surfactant along the dilution line N65. For surfactant below 39 % the multiple phase regions extends.

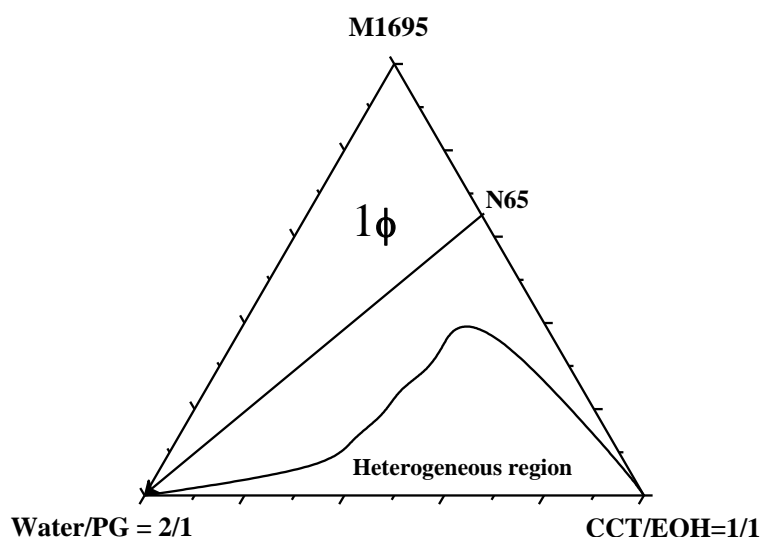


Fig: 5.41 Phase diagram of the system #11 water+ propylene glycol/ Sucrose myristate(M1695) /CCT oil+ ethanol at 45°C. In the figure the one phase region is designated by 1Φ , and the multiple phase regions are designated by heterogeneous region . N65 is the dilution line where the weight ratio of surfactant / single oil is 65/35.

Figure 5.42 Presents the phase diagram of the system water+ propylene glycol/ TMAZ80+Sucrose myristate(M1695) /CCT oil+ ethanol at 45°C, with aqueous solution made of (2/1)ratio , mixed surfactants TMAZ80+ Sucrose myristate(M1695) in the ratio (1/4) and equal unity of CCT oil with ethanol .The one phase microemulsion region appears from the first addition of water and extend to up to the water apex (100%). 35 % is the maximum water solubilization was reached using 32% of the surfactant along the dilution line N65. For surfactant below 32 % the multiple phase regions extends.

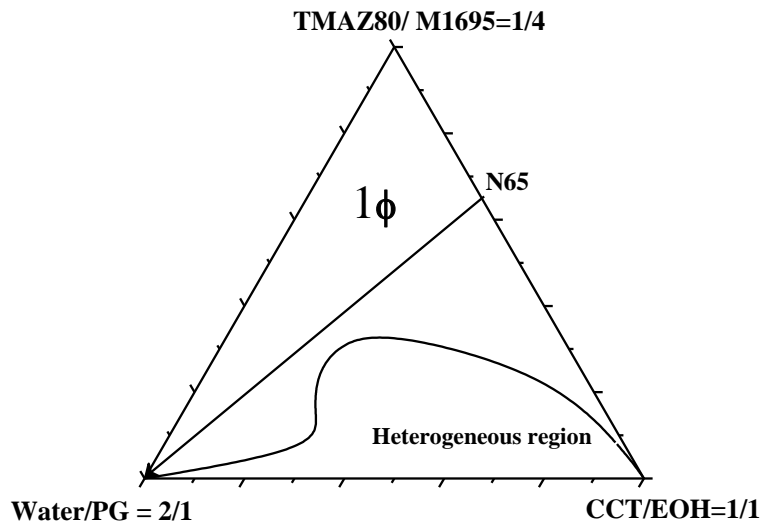


Fig: 5.42 Phase diagram of the system #12 water+ propylene glycol/ TMAZ80+ Sucrose myristate(M1695) /CCT oil+ ethanol at 45°C. In the figure the one phase region is designated by 1Φ , and the multiple phase regions are designated by heterogeneous region . N65 is the dilution line where the weight ratio of surfactant / single oil is 65/35.

Figure 5.43 Presents the phase diagram of the system water+ propylene glycol/ TMAZ80 +Sucrose myristate(M1695) /CCT oil+ ethanol at 45°C, with aqueous solution made of (2/1)ratio , mixed surfactants TMAZ80 + myristate(M1695) in the ratio (1/1) and equal unity of CCT oil with ethanol .The one phase microemulsion region appears from the first addition of water and extend to up to the water apex (100%) . 35 % is the maximum water solubilization was reached using 25 % of the surfactant along the dilution line N65. For surfactant below 25 % the multiple phase regions extends.

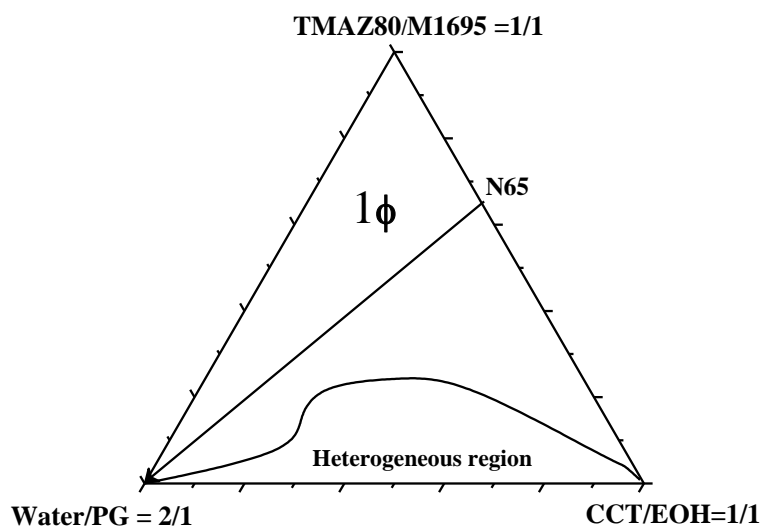


Fig: 5.43 Phase diagram of the system #13 water+ propylene glycol/ TMAZ80+ Sucrose myristate(M1695) /CCT oil+ ethanol at 45°C. In the figure the one phase region is designated by 1Φ , and the multiple phase regions are designated by heterogeneous region . N65 is the dilution line where the weight ratio of surfactant / single oil is 65/35.

Figure 5.44 Presents the phase diagram of the system water+ propylene glycol/ TMAZ80+Sucrose myristate(M1695) /CCT oil+ ethanol at 45°C, with aqueous solution made of (2/1)ratio , mixed surfactants TMAZ80+ Sucrose myristate(M1695) in the ratio (3/4) and equal unity of CCT oil with ethanol .The one phase microemulsion region appears from the first addition of water and extend to up to the water apex (100%).25 % is the maximum water solubilization was reached using 31 % of the surfactant along the dilution line N65. For surfactant below 31 wt% the multiple phase regions extends.

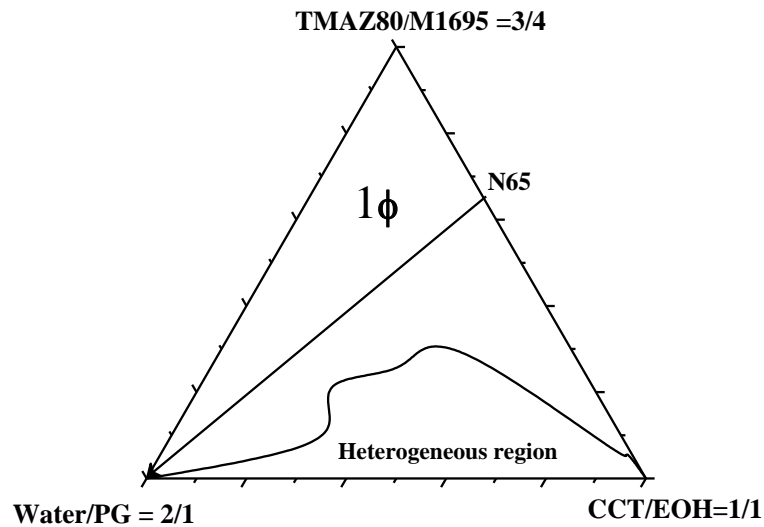


Fig: 5.44 Phase diagram of the system #14 water+ propylene glycol/ TMAZ80+ Sucrose myristate(M1695) /CCT oil+ ethanol at 45°C. In the figure the one phase region is designated by 1Φ , and the multiple phase regions are designated by heterogeneous region . N65 is the dilution line where the weight ratio of surfactant / single oil is 65/35.

Figure 5.45 Presents the phase diagram of the system water+ propylene glycol/ TMAZ80 / CCT oil+ ethanol at 45°C, with aqueous solution made of (2/1)ratio , surfactant TMAZ80 (100%) and equal unity of CCT oil with ethanol .The one phase microemulsion region appears from the first addition of water and extend to up to the water apex (100%) . 30 % is the maximum water solubilization was reached using 25 % of the surfactant along the dilution line N65. For surfactant below 25 % the multiple phase regions extends.

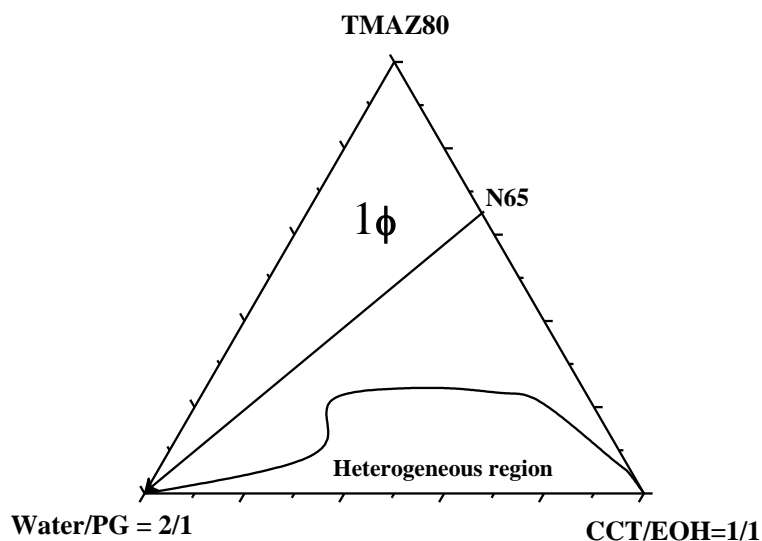


Fig: 5.45 Phase diagram of the system#15 water+ propylene glycol/ TMAZ80/CCT oil+ ethanol at 45°C. In the figure the one phase region is designated by 1Φ , and the multiple phase regions are designated by heterogeneous region . N65 is the dilution line where the weight ratio of surfactant / single oil is 65/35.

5.2 Determination of water solubilization capacity

The study of the phase behavior of mixed nonionic surfactants in water and oil demonstrated that the amount of surfactants present at the water–oil interface determines the extent of water and oil mutual solubilization. This amount of surfactants depends on factors like surfactant's chemical structure and hydrophilicity, the monomeric solubility of surfactants in oil and water, and the presence of additives.

Water solubilization capacity of different amphiphilic systems should be compared at optimal solubilization capacity (Fanun)²⁷. Because the maximum solubilization of water appears on different water dilution lines (a line in the phase diagram beginning with a mixture of oil, and surfactants at a fixed ratio, which is diluted with water). In our work it was N65 which means Surfactant/Oil (65 /35). have employed as a solubilization parameter, the total monophasic area (A_T). It is the sum of the five crosssectional areas in the tetrahedral phase diagram, each with a different surfactant /oil ratio as shown in fig 5:46

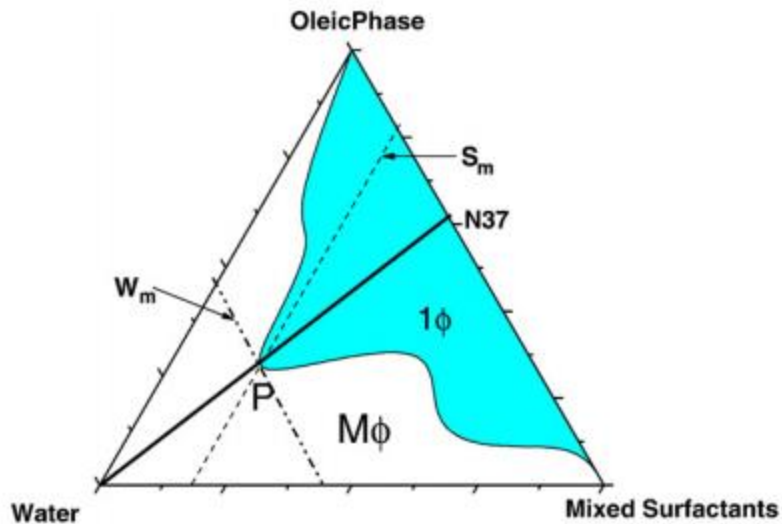


Fig 5:46 Solubilization parameters for a schematic phase diagram.

1ϕ is the area of the W/ O, bicontinuous, and O/W microemulsion (one phase region), $M\phi$ is the area of the multiple phase region. W_m is the maximum amount of solubilized water, S_m is the amount of surfactant needed to obtain maximum water solubilization, and P is a point on the boundary of the monophasic area at which the water content reaches maximum. $N37$ is a dilution line where the initial surfactant concentration is 37 wt.%.

According to the figures above, determining the S_m ; amount of surfactant needed to obtain maximum water solubilization and the W_m ; maximum water solubilization detected for all the systems as well as the total monophasic area A_T (%) along the N65 dilution line would be as follows .

Table 5:1 Weight percent of S_m and W_m in systems with LIM oil at (25,37, and 45°C)

T(°C) System	25°C		37°C		45°C	
	W_m	S_m	W_m	S_m	W_m	S_m
MT0 LE	27	23	30	24	32	25
MT25LE	38	16	42	18	42	18
MT50LE	45	17	45	16	45	17
MT75LE	75	8	45	17	45	16
MT100 LE	45	17	45	17	45	17

The table shows that there is no significant difference with the change in temperature which proves the temperatures insensitive systems built with the sucrose esters surfactants. It is noticed that the maximum water solubility increases up to an equal unity of the two mixed surfactants, when combining the lowest surfactant used. It reaches up to 45% water solubility with 17% surfactant solubility . The calculated total monophasic area A_T (%) for the system W+PG/TMAZ80 + Sucrose myristate (M1695)/LIM+EOH with the five different ratios at (25,37 ,and 45°C) are shown as follows in table 5:2

Table 5:2: Total monophasic region area A_T (%) for LIM oil

System	Total monophasic region area A_T (%)		
	25°C	37°C	45°C
MT0 LE	80	80	78
MT25LE	85	83	83
MT50LE	80	82	82
MT75LE	91	82	83
MT100 LE	84	84	84

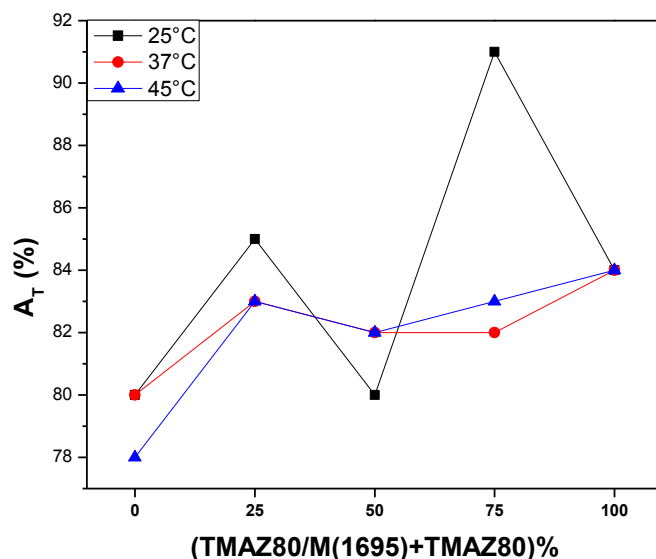


Fig.5:47 Variation of the total monophasic region area A_T (%) as function of surfactants ratio TMAZ80/sucrose myristate M1695 with LIM oil at different temperatures(25,37,45 °C).

Table 5:3 Weight percent of S_m and W_m in systems with IPM oil at (25,37,and 45°C)

T(°C) System	25°C		37°C		45°C	
	W _m	S _m	W _m	S _m	W _m	S _m
MT0 IE	20	38	20	41	20	38
MT25IE	32	27	33	28	40	31
MT50IE	38	21	45	18	55	19
MT75IE	35	28	35	28	40	30
MT100 IE	20	33	20	33	28	34

The table shows that there is no significant difference with the change in temperature which proves the temperatures insensitive systems built with the sucrose esters surfactants. It is noticed that the maximum water solubility increases up to an equal unity of the two mixed surfactants, when combining the lowest surfactant used. It reaches up to 45% water solubility with 19% surfactant solubility

The calculated total monophasic region area A_T (%) for the system W+PG/ TMAZ80 + Sucrose myristate (M1695)/IPM+EOH with the five different ratios at (25,37 ,and 45⁰C) is as follows in table 5:4

Table 5:4 Total monophasic region area A_T (%) for IPM oil

System	Total monophasic region area A_T (%)		
	25°C	37°C	45°C
MT0IE	72	72	71
MT25IE	73	74	69
MT50IE	80	81	78
MT75IE	70	70	67
MT100 IE	67	69	64

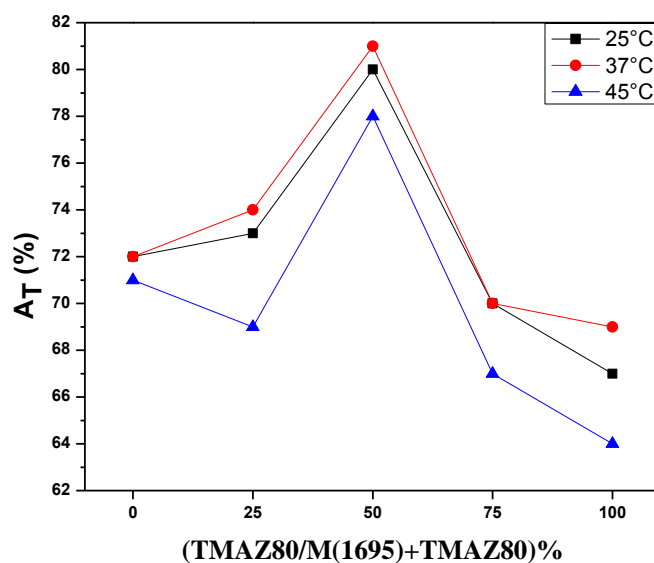


Fig 5:48 Variation of the total monophasic region A_T (%) as function of surfactants ratio TMAZ80/sucrose myristate M1695 with IPM oil at different temperatures(25,37,45 °C).

Table 5:5 Weight percent of Sm and Wm in systems with CCT oil at (25,37,and 45°C)

T(°C) System	25°C		37°C		45°C	
	Wm	Sm	Wm	Sm	Wm	Sm
MT0 CE	15	40	13	37	17	39
MT25CE	40	28	40	28	35	32
MT50CE	35	24	35	24	35	25
MT75CE	25	32	28	31	25	31
MT100 CE	30	25	27	26	30	25

The table shows that there is no significant difference with the change in temperature which proves the temperatures insensitive systems built with the sucrose esters surfactants. It is noticed that the maximum water solubility increases up to an equal unity of the two mixed surfactants, when combining the lowest surfactant used. It reaches up to 3% water solubility with 24 % surfactant solubility .The calculated total monophasic area A_T (%) for the system W+PG/TMAZ80 + Sucrose myristate (M1695)/CCT+EOH with the five different ratios at (25,37 ,and 45°C) is as follows in table 5:6

Table 5:6 Total monophasic region area A_T (%) for CCT oil

System	Total monophasic region area A_T (%)		
	25°C	37°C	45°C
MT0CE	71	69	67
MT25CE	69	69	66
MT50CE	74	75	72
MT75CE	70	71	71
MT100CE	71	72	72

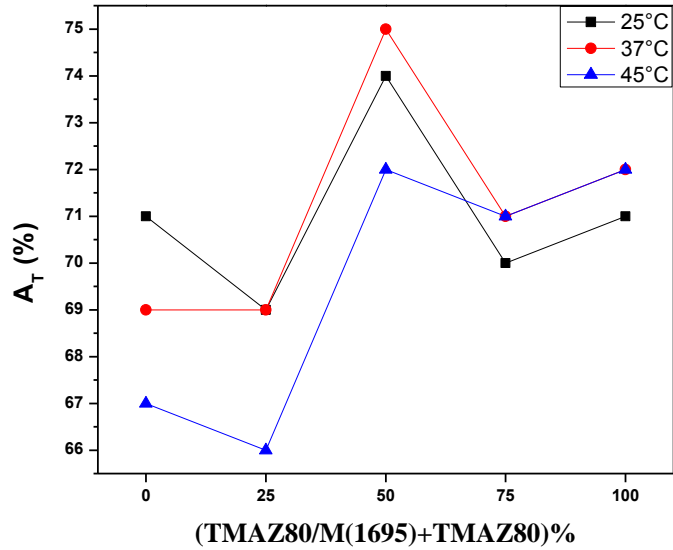


Fig 5:49 Variation of the total monophasic region A_T (%) as function of surfactants ratio TMAZ80/sucrose myristate M1695 with CCT oil at different temperatures(25,37,45 °C).

When comparing the optimum surfactant ratio(50%) as a function of different oil as in table 5:7 results will be as follows .

Table 5:7 Total monophasic region area A_T (%) at the optimum surfactant mixing ratio as a function of oil type.

Type of oil	Total monophasic region area A_T (%)		
	25°C	37°C	45°C
LIM	80	82	82
IPM	80	81	78
CCT	74	75	72

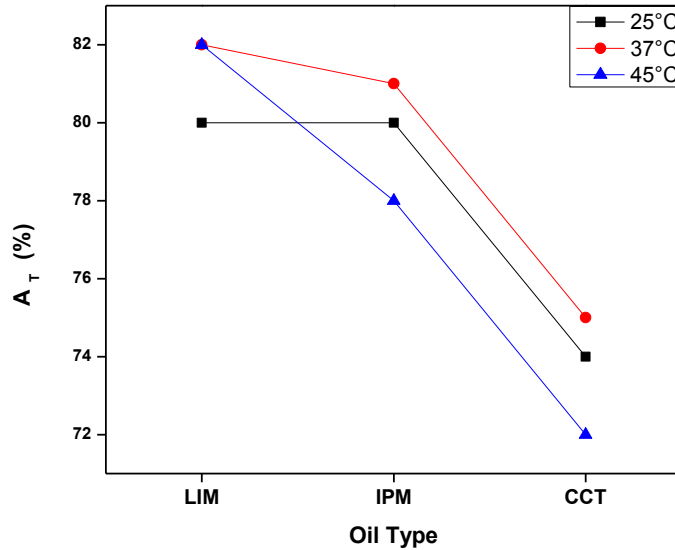


Fig 5:50 Variation of the total monophasic region area A_T (%) as function of type of oil at different temperatures(25,37,45 °C).

As it is well noticed ;the triglyceride oil has the least monophasic area among all.

Triglyceride oil caprylic/capric triglyceride oil and linear oil isopropylmyristate has lower total monophasic area because of its high molecular volume and so the ability to penetrate the interfacial film is very low and does not assist to obtain the optimum curvature of surfactants.

when comparing the optimum surfactant ratio as a function of different temperatures as in table 5:8 results will be as follows .

Table 5:8 Total monophasic region area A_T (%) at the optimum surfactant mixing ratio as a function of temperature.

Temperature (°C)	Total monophasic region area A_T (%)		
	LIM	IPM	CCT
25	80	80	74
37	82	81	75
45	82	78	72

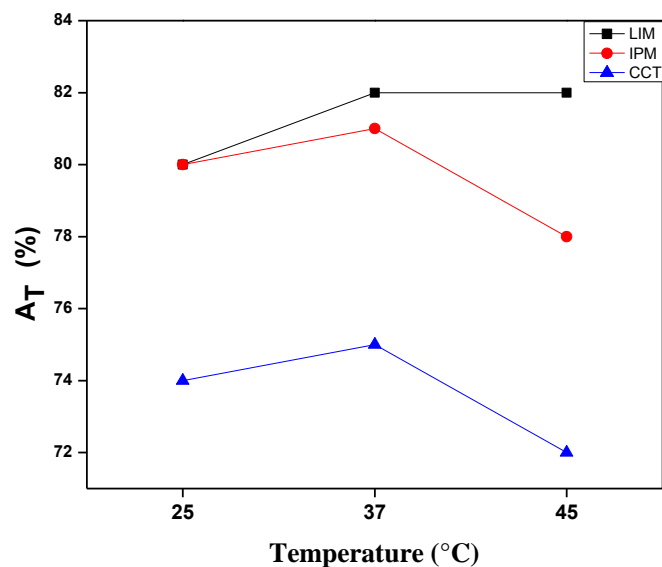


Fig 5:51 Variation of the total monophasic region A_T (%) as function of different temperatures (25,37,45 °C) for the used oils.

Sucrose myristate molecules are present only at the surfactant layers inside the microemulsion phase. While the TMAZ80 molecules are distributed between the microwater domains and the interface inside the microemulsion phase in a one-phase microemulsions. Mixing these two surfactants increase the solubilization capacity of the oil and water by enhancing the surfactants partitioning at the interface, thus increasing the stability of the amphiphilic film .

Non ionic surfactants with polyoxyethylene-type as in the case of TMAZ80 become relatively lipophilic as temperature increased a cause of the dehydration that takes place as a result of the conformational change in hydrophilic polyoxyethylene chains. Sucrose ester (SE) nonionic surfactants whose hydrophilic groups are not polyoxyethylene chains are less affected, a nonionic surfactant, contains sucrose as the hydrophilic group and a fatty acid as the hydrophobic are not affected ; the microemulsions formed using sucrose ester can be temperature insensitive .Increasing temperature from 25°C to 37 °C and to 45°C induces small change in the monophasic area indicating temperature insensitive microemulsions formation.

Addition of alcohol in microemulsions delays the occurrence of liquid crystalline phases, increases the fluidity of the interfacial layer separating oil and water, decreases the interfacial

tension between the microemulsion phase and excess oil and water, increases the disorder in these interfacial layers as well as their dynamic character as a result presence of alcohol influences the extent of the microemulsions regions and their internal structure.

Up to a certain extent, the alcohol from the oil phase can partition into the interface to stabilize the additional interfacial area. However, as the alcohol in the oil phase is depleted, further growth of water droplets would increase the interfacial tension at the oil/water interface due to an increase in the area per molecule and thus destabilize the microemulsion, and hence prevent further solubilization of water.

The highest monophasic area A_T (%) was for the system (W+PG/TMAZ80+M1695/oil+ ethanol) using the cyclic LIM oil and this refers to the cyclic structure of R (+)-limonene oil that tends to penetrate in the surfactant layer and widen the effective cross-sectional area per surfactant leading to more water solubilization.

There is a rapid decrease in the solubilization; total monophasic area A_T (%); with the increase in the molecular volume of the linear hydrocarbons.

Solubilization and placement of polar oils in aggregates or self-organized structures influences the surfactant layer curvature and the structure of the self-assembled systems. If the oils have a tendency to penetrate in the surfactant palisade layer and locate near the interface of the water - lipophilic surfactant moiety, the curvature would be less positive or negative as in the case of IPM oil, which is a polar oil, has large penetration tendency in the surfactant palisade layer and this layer will be less positive or less convex toward water which leads to lower in water solubilization .

As for caprylic capric triglyceride oil CCT having the highest molecular volume ($530 \text{ cm}^3/\text{mol}$) among all, ($181,317 \text{ cm}^3/\text{mol}$, for LIM and IPM respectively) and with bulky fork shape due to the glyceride body structure ,it was noticed to have the least monophasic area A_T (%) due to the low ability to penetrate the interfacial film and does not assist to obtain the optimum curvature of surfactants.

Solubilization of water in reverse micellar systems has been found to be dependent on various factors such as the rigidity of the interfacial film, which in turn depends upon the size of the polar head group and hydrocarbon moiety of the surfactant, the composition, the type of oils. The growth of microemulsion droplets during the solubilization process and consequently the phase separation in such systems is limited by two opposing factors, namely the radius of

spontaneous curvature(R_0) of the water -oil interface as the result of curvature effect and the critical radius of droplets (R_c); critical radius which limits the increase of droplet size due to interdroplet attractive interactions. The curvature effect is related to the cohesive force between the hydrocarbon chains at the interface as well as to the rigidity of the interface. R ratio which is the cohesive energy stemming from the interaction of the interfacial layer surfactant polar and hydrophobic group with oil divided by the cohesive interaction with water.

In the case of small molecular oil volume, starting from a short chain alkane, increasing the oil interface and decrease the interfacial rigidity due to decreasing oil penetration. The solubilization for such systems thus increases due to the decrease in packing parameter (P) and consequent increase in natural radius. On the other hand, for systems with greater chain length alkanes, the interdroplet interaction governs the solubilization process. Consequently one would expect a decrease in solubilization in microemulsion with further increase in oil chain length. At the point of oil chain length compatibility, both of these interactions are minimized; hence a maximum solubilization results.

Oil can influence the property of an interface through a surfactant chain-oil interaction. Strong interaction leads to a large penetration of oil molecules into the surfactant chain layer (solvation), thus increasing the rigidity and curvature (or packing ratio) of the interface. Oil molecules with a small molecular volume as LIM oil or high polarity often produce strong solvation effects on the interface.

Decreasing the alcohol chain length can increase the interfacial fluidity and hence the attractive interdroplet interaction. On the other hand, increasing the alcohol chain length often increases the rigidity and curvature of the interface. For alcohols which promote interfacial fluidity, increasing alcohol partitioning at the interface can increase the natural radius and fluidity of the interface.

5.3 Characterization

5.3.1 Electrical conductivity

Electrical conductivity has been measured as function of water volume fraction as a method of characterization of microemulsions interdroplet interactions, which explains the properties and types of microemulsion droplets formed (i.e. water-in-oil (W/O), bicontinuous, or oil-in-water (O/W)).

Electrical conductivity was measured for the fifteen different systems in table 4:1 emulsion formed from mixed and single surfactants TMAZ80 + Sucrose myristate (M1695) in different ratios (0,25,50,75,100), and the three different oils mixed with ethanol (99,9%) in (1/1) ratio, titrated with an aqueous solution made of water and propylene glycol in (2/1) ratio. Titrations were made as 2% addition until 10% and then made with 10% addition each time until 90%. Data of electrical conductivity were collected at 10 different temperatures 10 to 50°C in increasing steps of 5°C for each system as shown in the appendix tables, representative temperature samples (25,37, and 45°C) were taken.

5.3.1.1 Electrical conductivity of the systems using LIM oil

System #1 MT0LE W+PG/ Sucrose myristate (M1695) /LIM+Ethanol

Aqueous solution made of (2/1)ratio, 100% Sucrose myristate(M1695) and equal unity of LIM oil with ethanol.

The first additions from the beginning (0%) up to (20%) couldn't be measured because it was too viscous. Representative data at the three different temperatures are shown in table 5:9. For the whole data collected see appendix A1

Table 5:9 The electrical conductivity (σ) for system # 1 W+PG/ Sucrose myristate (M1695) /LIM+ Ethanol at three different temperatures.

# of additions	W+PG (2/1) wt%	σ ($\mu\text{S}/\text{cm}$)		
		25°C	37°C	45°C
1	30	45.2	54.3	102.3
2	40	74.8	95.7	167.4
3	50	94.6	113.3	226
4	60	99	122.3	242
5	70	94	111	227
6	80	73.7	81	168.5
7	90	40.2	45.5	92.3

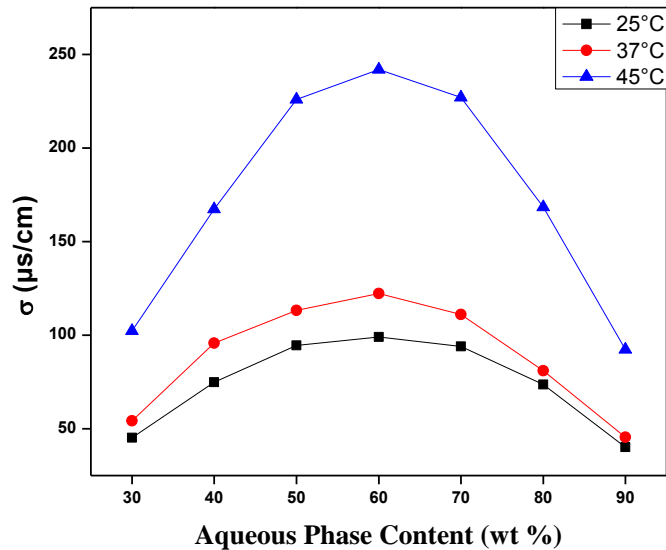


Fig 5:52 Variation of the electrical conductivity (σ) of the system# 1 MT0LE W+PG/ Sucrose myristate (M1695) /LIM+ Ethanol as function of aqueous content along the dilution line N65. The phase diagrams are presented in figures (5:1),(5:6),(5:11) at different temperatures (25, 37 and 45°C) respectively .

It is noticed that electrical conductivity for the system #1 W+PG/ Sucrose myristate (M1695) /LIM+ Ethanol increases with the increase in the aqueous content, samples with aqueous content less than 30 % couldn't be measured . High electrical conductivity above 30 % water content along the N65 line, suggests that the system undergoes a structural inversion to bicontinues microemulsion. Decrease the electrical conductivity above 55% suggests that the system undergoes a structural inversion to O/W. Electrical Conductivity increased as temperature increased in steadily fashion at aqueous content higher than 30 wt % .

System #2 MT25LE W+PG/ TMAZ 80+Sucrose myristate (M1695) /LIM+ Ethanol

Aqueous solution made of (2/1)ratio , mixed surfactants TMAZ80+ Sucrose myristate (M1695) in the ratio (1/4) and equal unity of LIM oil with ethanol. Representative data at the three different temperatures are shown in table 5:10 . For the whole data collected see appendix A2

Table 5:10 The electrical conductivity (σ) for system # 2 W+PG/ TMAZ80+Sucrose myristate (M1695) /LIM+ Ethanol at three different temperatures.

# of additions	W+PG (2/1) wt%	σ ($\mu\text{S}/\text{cm}$)		
		25°C	37°C	45°C
1	2	0.7	1.4	2.4
2	4	0.3	0.3	0.6
3	6	0.3	0.5	2.5
4	10	1.2	0.7	5.4
5	20	7.5	15	25.5
6	30	31.8	50.3	89.2
7	40	65.9	89.6	173
8	50	94.4	126.2	255
9	60	93.85	110	231.5
10	70	80.6	93	199
11	80	58.8	67.7	124
12	90	29.4	36	73.6

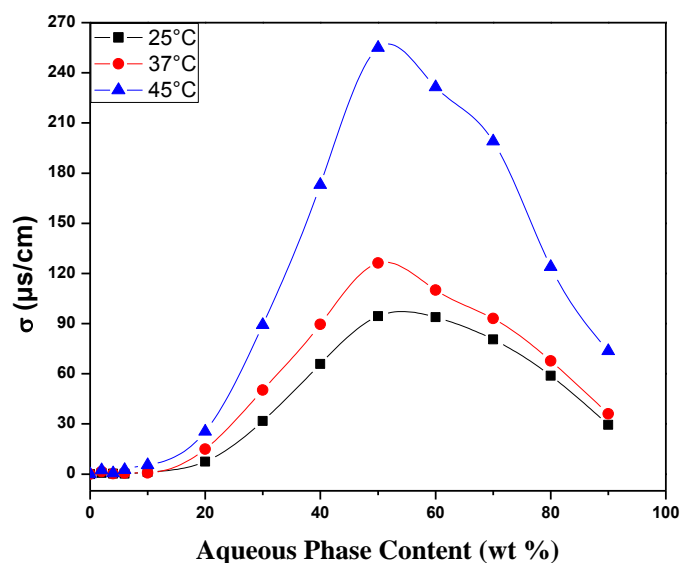


Fig 5:53 Variation of the electrical conductivity (σ) of the system # 2 MT25LE W+PG/TMAZ80+ Sucrose myristate (M1695) /LIM+ Ethanol as function of aqueous content along the dilution line N65. The phase diagrams are presented in figures (5:2),(5:7),(5:12) at different temperatures (25,37,and 45°C)respectively .

It is noticed that electrical conductivity for the system #2 W+PG/TMAZ80+ Sucrose myristate (M1695) /LIM+ Ethanol increases with the increase in the aqueous content, samples with aqueous content less than 20 % have low values of electrical conductivity, this indicates restricted water mobility in this region. High electrical conductivity above 20 % water content along the N65 line, suggests that the system undergoes a structural inversion to bicontinues microemulsion. Decrease the electrical conductivity above 55% suggests that the system undergoes a structural inversion to O/W. Electrical Conductivity increased as temperature increased in steadily fashion at aqueous content higher than 20 wt %.

System #3 MT50LE W+PG/ TMAZ 80+Sucrose myristate (M1695) /LIM+ Ethanol

Aqueous solution made of (2/1)ratio , mixed surfactants TMAZ80+ Sucrose myristate(M1695) in the ratio (1/1) and equal unity of LIM oil with ethanol. Representative data at the three different temperatures are shown in table 5:11 . For the whole data collected see appendix A3.

Table 5:11 The electrical conductivity (σ) for system # 3 W+PG/ TMAZ80+Sucrose myristate (M1695) /LIM+ Ethanol at three different temperatures.

# of additions	W+PG (2/1) wt%	σ ($\mu\text{S}/\text{cm}$)		
		25°C	37°C	45°C
1	0	1	1.7	3.3
2	2	0.8	1.7	3.3
3	4	0.8	1.5	3.3
4	6	0.8	1.7	2.4
5	10	1	2.1	3.6
6	20	3.6	6.6	13.3
7	30	15.6	22.7	53.2
8	40	32.1	50.2	76.3
9	50	50.5	66.4	139.8
10	60	53.6	64.5	148
11	70	49	57.5	122
12	80	37.4	41.1	86.5
13	90	20	22.6	46.2

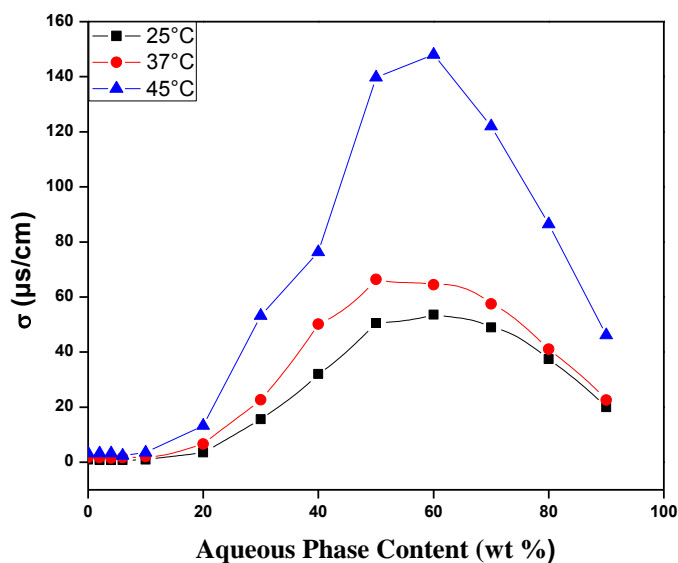


Fig 5:54 Variation of the electrical conductivity (σ) of the system # 3 MT50LE W+PG/TMAZ80+ Sucrose myristate (M1695) /LIM+ Ethanol as function of aqueous content

along the dilution line N65. The phase diagrams are presented in figures (5:3),(5:8),(5:13) at different temperatures (25,37,and 45°C)respectively .

It is noticed that electrical conductivity for the system #3 W+PG/TMAZ80+ Sucrose myristate (M1695) /LIM+ Ethanol increases with the increase in the aqueous content, samples with aqueous content less than 20 % have low values of electrical conductivity, this indicates restricted water mobility in this region. High electrical conductivity above 20 % water content along the N65 line, suggests that the system undergoes a structural inversion to bicontinues microemulsion. Decrease the electrical conductivity above 55% suggests that the system undergoes a structural inversion to O/W. Electrical Conductivity increased as temperature increased in steadily fashion at aqueous content higher than 20 wt %.

System #4 MT75LE W+PG/ TMAZ 80+Sucrose myristate (M1695) /LIM+ Ethanol with aqueous solution made of (2/1)ratio , mixed surfactants TMAZ80+ Sucrose myristate(M1695) in the ratio (3/4) and equal unity of LIM oil with ethanol. Representative data at the three different temperatures are shown in table 5:12 . For the whole data collected see appendix A4

Table 5:12 The electrical conductivity (σ) for system # 4 W+PG/ TMAZ80+Sucrose myristate (M1695) /LIM+ Ethanol at three different temperatures.

# of additions	W+PG (2/1) wt%	σ ($\mu\text{S}/\text{cm}$)		
		25°C	37°C	45°C
1	2	2	3.7	5
2	4	1.4	0.4	0.4
3	6	0.3	0.6	0.7
4	10	0.7	2	1.5
5	20	1.5	5.7	1.4
6	30	5.9	10.4	52
7	40	15.5	31.2	101.8
8	50	33.3	82.2	207
9	60	41.4	64.35	177
10	70	27.9	46.6	151
11	80	23.7	29.3	79.4
12	90	19	21.1	47.2

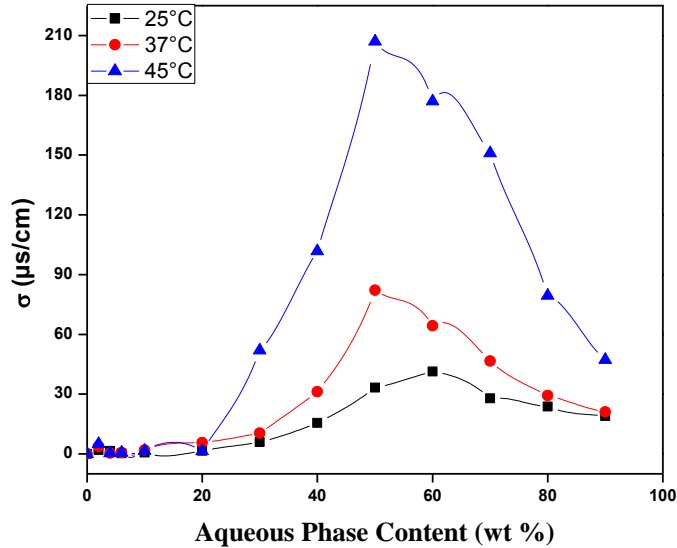


Fig 5:55 Variation of the electrical conductivity (σ) of the system # 4 MT75LE

W+PG/TMAZ80+ Sucrose myristate (M1695) /LIM+ Ethanol as function of aqueous content along the dilution line N65. The phase diagrams are presented in figures (5:4),(5:9),(5:14) at different temperatures (25,37,and 45°C)respectively .

It is noticed that electrical conductivity for the system #4 W+PG/TMAZ80+ Sucrose myristate (M1695) /LIM+ Ethanol increases with the increase in the aqueous content, samples with aqueous content less than 20 % have low values of electrical conductivity, this indicates restricted water mobility in this region. High electrical conductivity above 20 % water content along the N65 line, suggests that the system undergoes a structural inversion to bicontinuous microemulsion. Decrease the electrical conductivity above 50% suggests that the system undergoes a structural inversion to O/W. Electrical Conductivity increased as temperature increased in steadily fashion at aqueous content higher than 20 wt %.

System #5 MT100LE W+PG/ TMAZ80 /LIM+ Ethanol

Aqueous solution made of (2/1)ratio , TMAZ 80 (100%) and equal unity of LIM oil with ethanol Representative data at the three different temperatures are shown in table 5:13 For the whole data collected see appendix A5.

Table 5:13 The electrical conductivity (σ) for system # 5 W+PG/ TMAZ80 /LIM+ Ethanol at three different temperatures.

# of additions	W+PG (2/1) wt%	σ ($\mu\text{S}/\text{cm}$)		
		25°C	37°C	45°C
1	2	3.5	4.3	5.6
2	4	1.1	1.5	2.2
3	6	0.7	0.7	2.2
4	10	1	1.1	2.2
5	20	2	4.5	8.8
6	30	8.8	14.2	20.1
7	40	5.1	12.2	64.8
8	50	6.2	14.8	117.6
9	60	10.3	13.1	120.6
10	70	12.7	13.6	27
11	80	10.1	12.3	18.4
12	90	13	14.8	24.3

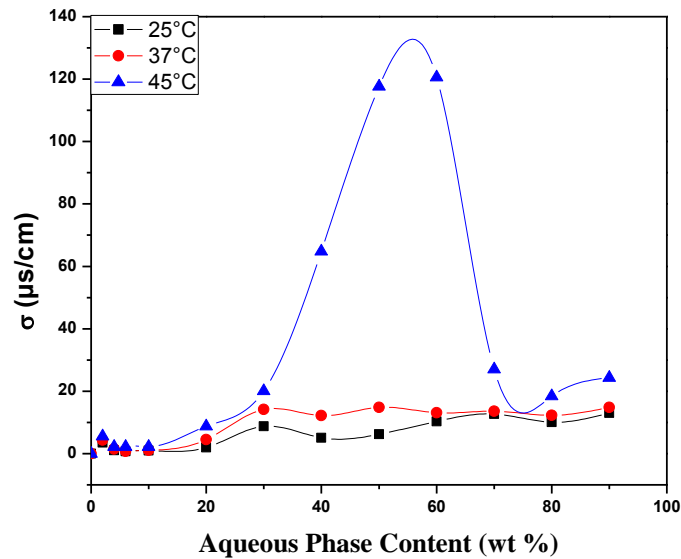


Fig 5:56 Variation of the electrical conductivity (σ) of the system # 5 MT100LE W+PG/TMAZ80/LIM+ Ethanol as function of aqueous content along the dilution line N65. The phase diagrams are presented in figures (5:5),(5:10),(5:15) at different temperatures (25,37,and 45°C)respectively .

It is noticed that electrical conductivity for the system #5 W+PG/TMAZ80/LIM+ Ethanol increases with the increase in the aqueous content, samples with aqueous content less than 20 % have low values of electrical conductivity, this indicates restricted water mobility in this region. High electrical conductivity above 20 % water content along the N65 line, suggests that the system undergoes a structural inversion to bicontinues microemulsion. Decrease the electrical conductivity above 55% suggests that the system undergoes a structural inversion to O/W. Electrical Conductivity increased as temperature increased in steadily fashion at aqueous content higher than 20 wt %.

5.3.1.2 Electrical conductivity of the systems using IPM oil

System #6 MTOIE W+PG/ Sucrose myristate (M1695) /IPM+ Ethanol .

Aqueous solution made of (2/1)ratio ,100% Sucrose myristate(M1695) and equal unity of IPM oil with ethanol.

The first additions from the beginning (0%) up to (10%) couldn't be measured because it was too viscous .Representative data at the three different temperatures are shown in table 5:14. For the whole data collected see appendix B1

Table 5:14 The electrical conductivity (σ) for system # 6 W+PG/ Sucrose myristate (M1695) /IPM+ Ethanol at three different temperatures.

# of additions	W+PG (2/1) wt%	σ ($\mu\text{S}/\text{cm}$)		
		25°C	37°C	45°C
1	20	-	26.5	28.6
2	30	35.7	55.4	89.3
3	40	69.5	92.8	182.8
4	50	88.5	106.5	223
5	60	88.1	103.5	231
6	70	78.15	89.8	187
7	80	57	63.2	128.5
8	90	30.3	34.1	70

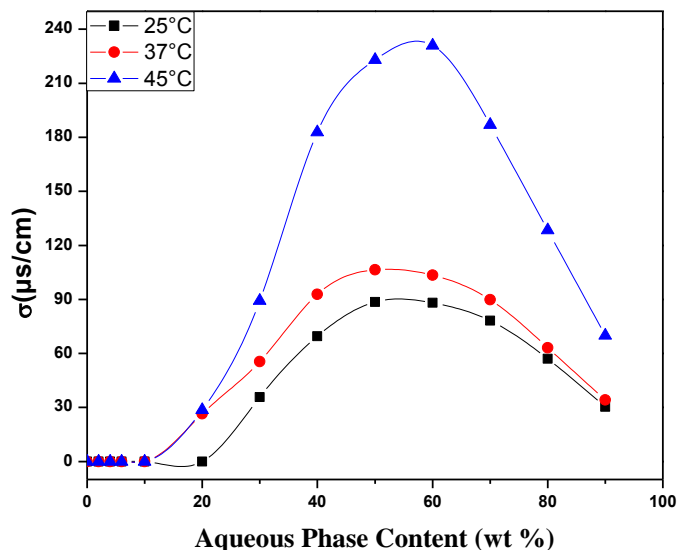


Fig 5:57 Variation of the electrical conductivity (σ) of the system # 6 MT1IE W+PG/ Sucrose myristate (M1695) /IPM+ Ethanol as function of aqueous content along the dilution line N65. The phase diagrams are presented in figures (5:16),(5:21),(5:26) at different temperatures (25, 37, and 45°C) respectively .

It is noticed that electrical conductivity for the system #6 W+PG/ Sucrose myristate (M1695) /IPM+ Ethanol increases with the increase in the aqueous content, samples with aqueous content less than 20 % couldn't be measured . High electrical conductivity above 20 % water content along the N65 line, suggests that the system undergoes a structural inversion to bicontinuous microemulsion. Decrease the electrical conductivity above 55% suggests that the system undergoes a structural inversion to O/W. Electrical Conductivity increased as temperature increased in steadily fashion at aqueous content higher than 20 wt %.

System #7 MT25IE W+PG/ TMAZ80+Sucrose myristate (M1695) /IPM+ Ethanol

Aqueous solution made of (2/1)ratio , mixed surfactants TMAZ80+ Sucrose myristate (M1695) in the ratio (1/4) and equal unity of IPM oil with ethanol

Representative data at the three different temperatures are shown in table 5:15. For the whole data collected see appendix B2.

Table 5:15 The electrical conductivity (σ) for system # 7 W+PG/TMAZ80+ Sucrose myristate (M1695) /IPM+ Ethanol at three different temperatures.

# of additions	W+PG (2/1) wt%	σ ($\mu\text{S}/\text{cm}$)		
		25°C	37°C	45°C
1	2	1.5	1.5	2.3
2	4	0.7	1	2.2
3	6	0.3	1.3	2.1
4	10	1.3	2.2	3.2
5	20	5.5	11.6	24.3
6	30	20.6	34.4	74.4
7	40	48.5	64.1	142.6
8	50	67.7	81.7	171.3
9	60	68.3	83.2	175
10	70	61.1	71.2	150
11	80	45.6	51.3	101
12	90	24.6	28	58

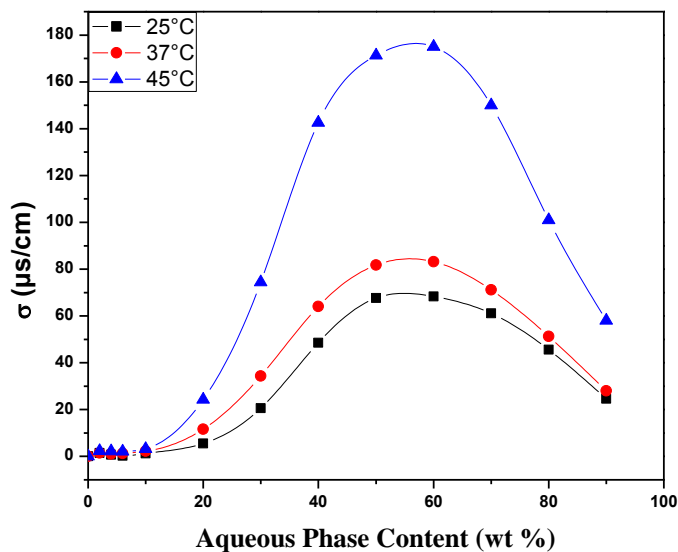


Fig 5:58 Variation of the electrical conductivity (σ) of the system # 7 MT25IE W+PG/TMAZ80+Sucrose myristate (M1695) /IPM+ Ethanol as function of aqueous content along the

dilution line N65. The phase diagrams are presented in figures (5:17),(5:22),(5:27) at different temperatures (25,37,and 45°C)respectively .

It is noticed that electrical conductivity for the system #7 W+PG/TMAZ80+ Sucrose myristate (M1695) /IPM+ Ethanol increases with the increase in the aqueous content, samples with aqueous content less than 20 % have low values of electrical conductivity, this indicates restricted water mobility in this region. High electrical conductivity above 20 % water content along the N65 line, suggests that the system undergoes a structural inversion to bicontinues microemulsion. Decrease the electrical conductivity above 55% suggests that the system undergoes a structural inversion to O/W. Electrical Conductivity increased as temperature increased in steadily fashion at aqueous content higher than 20 wt %.

System #8 MT50IE W+PG/ TMAZ80+Sucrose myristate (M1695) /IPM+ Ethanol

Aqueous solution made of (2/1)ratio , mixed surfactants TMAZ80+ Sucrose myristate(M1695) in the ratio (1/1) and equal unity of IPM oil with ethanol

Representative data at the three different temperatures are shown in table 5:16. For the whole data collected see appendix B3

Table 5:16 The electrical conductivity (σ) for system # 8 W+PG/TMAZ80+ Sucrose myristate (M1695) /IPM+ Ethanol at three different temperatures.

# of additions	W+PG (2/1) wt%	σ ($\mu\text{S}/\text{cm}$)		
		25°C	37°C	45°C
1	0	0.7	0.9	2.1
2	2	0.6	1.2	2.1
3	4	0.5	1	0.8
4	6	0.4	0.8	1.2
5	10	0.8	1.9	1.5
6	20	0.7	2.6	15.4
7	30	9.8	28.5	49.7
8	40	23	52.1	143.4
9	50	42.4	50.1	131.5
10	60	37.7	51.8	133.9
11	70	7.55	18.5	92
12	80	7.2	9.9	21
13	90	9.1	12.5	21.8

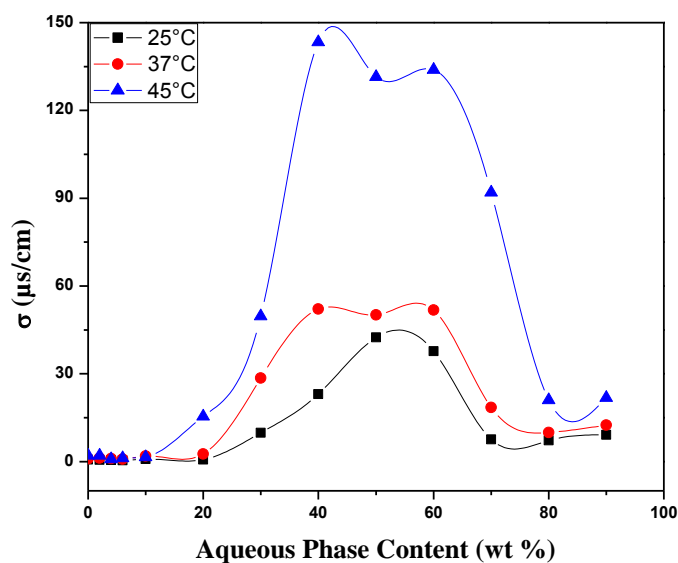


Fig 5:59 Variation of the electrical conductivity (σ) of the system # 8 MT50IE W+PG/TMAZ80+Sucrose myristate (M1695) /IPM+ Ethanol as function of aqueous content along the dilution line N65. The phase diagrams are presented in figures (5:18),(5:23),(5:28) at different temperatures (25,37,and 45°C)respectively .

It is noticed that electrical conductivity for the system #8 W+PG/TMAZ80+ Sucrose myristate (M1695) /IPM+ Ethanol increases with the increase in the aqueous content, samples with aqueous content less than 20 % have low values of electrical conductivity, this indicates restricted water mobility in this region. High electrical conductivity above 20 % water content along the N65 line, suggests that the system undergoes a structural inversion to bicontinuous microemulsion. Decrease the electrical conductivity above 55% suggests that the system undergoes a structural inversion to O/W. Electrical Conductivity increased as temperature increased in steadily fashion at aqueous content higher than 20 wt %.

System #9 MT75 IE W+PG/ TMAZ80+Sucrose myristate (M1695) /IPM+ Ethanol

Aqueous solution made of (2/1)ratio , mixed surfactants TMAZ80+ Sucrose myristate(M1695) in the ratio (3/4) and equal unity of IPM oil with ethanol.

Representative data at the three different temperatures are shown in table 5:17. For the whole data collected see appendix B4

Table 5:17 The electrical conductivity (σ) for system # 9 W+PG/TMAZ80+ Sucrose myristate (M1695) /IPM+ Ethanol at three different temperatures.

# of additions	W+PG (2/1) wt%	σ ($\mu\text{S}/\text{cm}$)		
		25°C	37°C	45°C
1	2	2	2.2	4.3
2	4	0.5	1	1.1
3	6	0.3	0.3	1.2
4	10	0.4	1.1	0.8
5	20	1.5	2.7	2.4
6	30	4.2	8	18.3
7	40	15.2	25	55.6
8	50	36.1	45.5	95.2
9	60	43.3	52.7	104.6
10	70	44.9	52.7	107.6
11	80	38.3	42.2	82.6
12	90	25.2	27.6	56.6

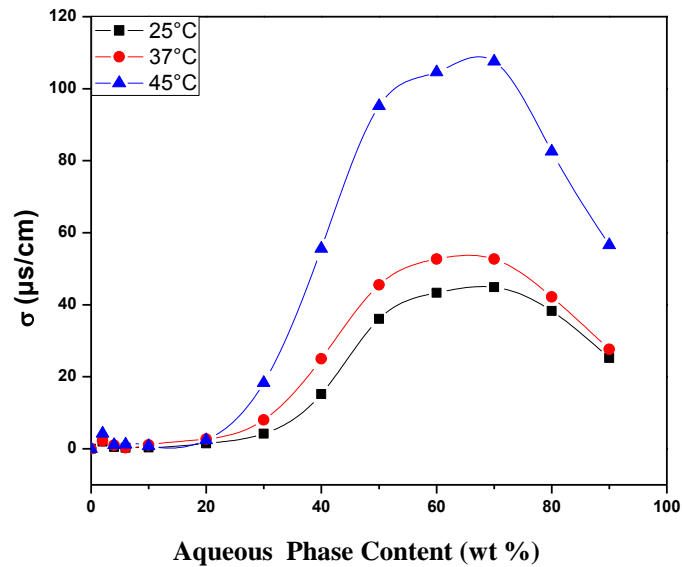


Fig 5:60 Variation of the electrical conductivity (σ) of the system # 9 MT75IE W+PG/TMAZ80+Sucrose myristate (M1695) /IPM+ Ethanol as function of aqueous content along the dilution line N65. The phase diagrams are presented in figures (5:19),(5:24),(5:29) at different temperatures (25,37,and 45°C)respectively .

It is noticed that electrical conductivity for the system #9 W+PG/TMAZ80+ Sucrose myristate (M1695) /IPM+ Ethanol increases with the increase in the aqueous content, samples with aqueous content less than 20 % have low values of electrical conductivity, this indicates restricted water mobility in this region. High electrical conductivity above 20 % water content along the N65 line, suggests that the system undergoes a structural inversion to bicontinuous microemulsion. Decrease the electrical conductivity above 65% suggests that the system undergoes a structural inversion to O/W. Electrical Conductivity increased as temperature increased in steadily fashion at aqueous content higher than 20 wt %.

System #10 MT100 IE W+PG/ TMAZ80 /IPM+ Ethanol

Aqueous solution made of (2/1)ratio , surfactant TMAZ80(100%) and equal unity of IPM oil with ethanol.

Representative data at the three different temperatures are shown in table 5:18. For the whole data collected see appendix B5

Table 5:18 The electrical conductivity (σ) for system # 10 W+PG/TMAZ80/IPM+ Ethanol at three different temperatures.

# of additions	W+PG (2/1) wt%	σ ($\mu\text{S}/\text{cm}$)		
		25°C	37°C	45°C
1	2	2	2.3	0.4
2	4	0.3	0.3	0.3
3	6	0.3	0.5	0.6
4	10	0.5	1.2	0.5
5	20	1.1	1.4	4
6	30	6	8.7	13.2
7	40	15.1	23.1	49.5
8	50	27.3	33.3	68.5
9	60	33.5	40.4	79.5
10	70	36.7	42.7	89
11	80	37.7	39.7	94
12	90	30.8	32.5	66.2

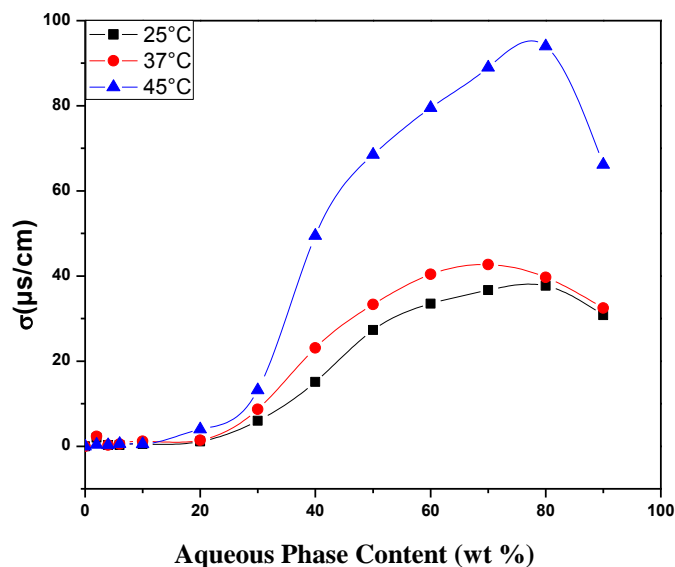


Fig 5:61 Variation of the electrical conductivity (σ) of the system # 10 MT100IE W+PG/TMAZ80+Sucrose myristate (M1695) /IPM+ Ethanol as function of aqueous content along the dilution line N65. The phase diagrams are presented in figures (5:20),(5:25),(5:30) at different temperatures (25,37,and 45°C)respectively .

It is noticed that electrical conductivity for the system #10 W+PG/TMAZ80/IPM+ Ethanol increases with the increase in the aqueous content, samples with aqueous content less than 20 % have low values of electrical conductivity, this indicates restricted water mobility in this region. High electrical conductivity above 20 % water content along the N65 line, suggests that the system undergoes a structural inversion to bicontinues microemulsion. Decrease the electrical conductivity above 80% suggests that the system undergoes a structural inversion to O/W. Electrical Conductivity increased as temperature increased in steadily fashion at aqueous content higher than 20 wt %.

5.3.1.3 Electrical conductivity of the systems using CCT oil

System #11 MT0CE W+PG/ Sucrose myristate (M1695) /CCT+ Ethanol

Aqueous solution made of (2/1)ratio , surfactant Sucrose myristate (100%) and equal unity of CCT oil with ethanol .

Representative data at the three different temperatures are shown in table 5:19. For the whole data collected see appendix C1

Table 5:19 The electrical conductivity (σ) for system # 11 W+PG/ Sucrose myristate (M1695) /CCT+ Ethanol at three different temperatures.

# of additions	W+PG (2/1) wt%	σ ($\mu\text{S}/\text{cm}$)		
		25°C	37°C	45°C
1	0	-	0.2	0.5
2	2	-	0.3	0.7
3	4	-	0.3	0.8
4	20	13.8	24.8	46.1
5	30	40.6	57.2	113
6	40	70.7	86.1	176
7	50	90.6	103.8	213
8	60	89.7	121	258
9	70	82.7	95.2	191
10	80	62.3	68.5	130.5
11	90	34.4	38.7	77.6

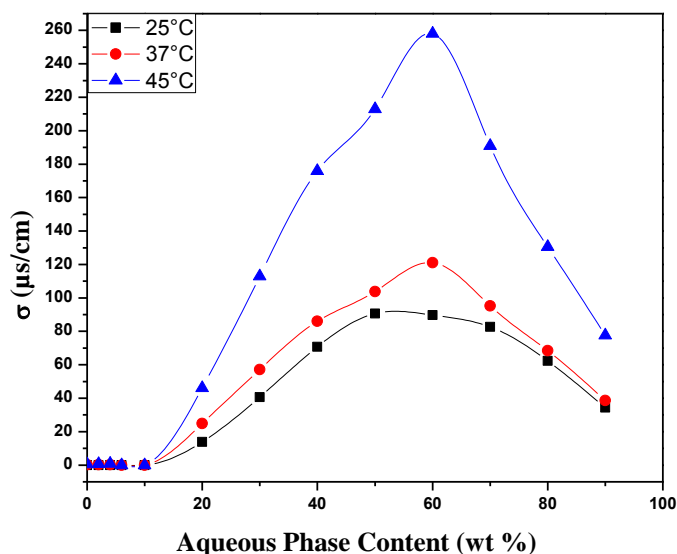


Fig 5:62 Variation of the electrical conductivity (σ) of the system # 11 MT0CE W+PG/ Sucrose myristate (M1695) /CCT+ Ethanol as function of aqueous content along the dilution line N65. The phase diagrams are presented in figures (5:31),(5:36),(5:41) at different temperatures (25,37,and 45°C)respectively .

It is noticed that electrical conductivity for the system #11 W+PG/ Sucrose myristate (M1695) /CCT+ Ethanol increases with the increase in the aqueous content, samples with aqueous content less than 20 % couldn't be measured . High electrical conductivity above 20 % water content along the N65 line, suggests that the system undergoes a structural inversion to bicontinues microemulsion. Decrease the electrical conductivity above 60% suggests that the system undergoes a structural inversion to O/W. Electrical Conductivity increased as temperature increased in steadily fashion at aqueous content higher than 20 wt %.

System #12 MT25 CE W+PG/ TMAZ80+Sucrose myristate (M1695) /CCT+ Ethanol

Aqueous solution made of (2/1)ratio , mixed surfactants TMAZ80+ Sucrose myristate(M1695) in the ratio (1/4) and equal unity of CCT oil with ethanol.

Representative data at the three different temperatures are shown in table 5:20

For the whole data collected see appendix C2

Table 5:20 The electrical conductivity (σ) for system # 12 W+PG/TMAZ80+ Sucrose myristate (M1695) /CCT+ Ethanol at three different temperatures.

# of additions	W+PG (2/1) wt%	σ ($\mu\text{S}/\text{cm}$)		
		25°C	37°C	45°C
1	2	0.5	1.2	1.6
2	4	-	-	0.3
3	6	-	-	0.3
4	20	0.2	0.4	1.5
5	30	5.4	8.5	11.3
6	40	24.8	31.3	73.3
7	50	51.7	71.7	141.7
8	60	66.5	80.3	182
9	70	68.3	83.3	165
10	80	54.5	60.8	122
11	90	30.9	35.2	50

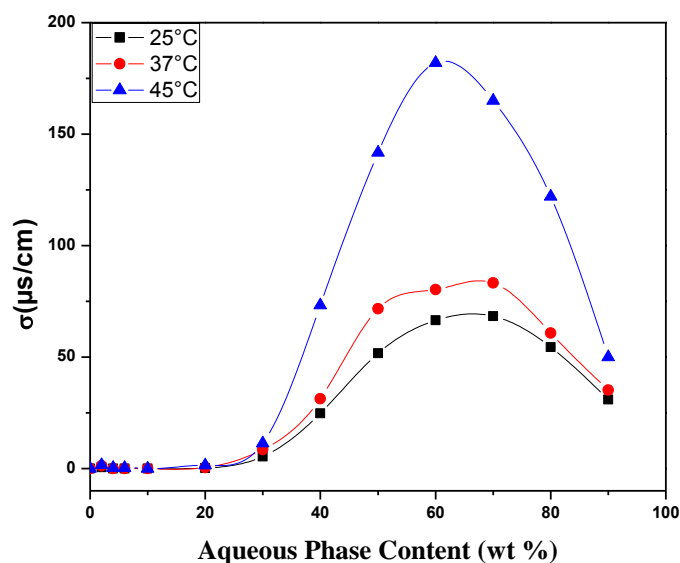


Fig 5:63 Variation of the electrical conductivity (σ) of the system # 12 MT25CE W+PG/TMAZ80+ Sucrose myristate (M1695) /CCT+ Ethanol as function of aqueous content along the dilution line N65. The phase diagrams are presented in figures (5:32),(5:37),(5:42) at different temperatures (25,37,and 45°C)respectively .

It is noticed that electrical conductivity for the system #12 W+PG/TMAZ80+ Sucrose myristate (M1695) /CCT+ Ethanol increases with the increase in the aqueous content, samples with aqueous content less than 20 % have low values of electrical conductivity, this indicates restricted water mobility in this region. High electrical conductivity above 20 % water content along the N65 line, suggests that the system undergoes a structural inversion to bicontinues microemulsion. Decrease the electrical conductivity above 60% suggests that the system undergoes a structural inversion to O/W. Electrical Conductivity increased as temperature increased in steadily fashion at aqueous content higher than 20 wt %.

System #13 MT50CE W+PG/ TMAZ80+Sucrose myristate (M1695) /CCT+ Ethanol

Aqueous solution made of (2/1)ratio , mixed surfactants TMAZ80+ Sucrose myristate(M1695) in the ratio (1/1) and equal unity of CCT oil with ethanol.

Representative data at the three different temperatures are shown in table 5:21. For the whole data collected see appendix C3

Table 5:21 The electrical conductivity (σ) for system # 13 W+PG/TMAZ80+ Sucrose myristate (M1695) /CCT+ Ethanol at three different temperatures.

# of additions	W+PG (2/1) wt%	σ ($\mu\text{S}/\text{cm}$)		
		25°C	37°C	45°C
1	0	0.3	0.3	0.3
2	2	0.7	2	2.1
3	4	0.3	0.4	1.5
4	6	0.3	0.5	0.8
5	10	0.2	0.7	0.5
6	20	0.3	0.4	0.6
7	30	2.1	4.6	11.3
8	40	19.1	24.7	27.8
9	50	37.9	54	114.3
10	60	54.4	67.4	147.6
11	70	59.6	72.2	140.6
12	80	51.3	57.2	107.5
13	90	35.5	38.1	78

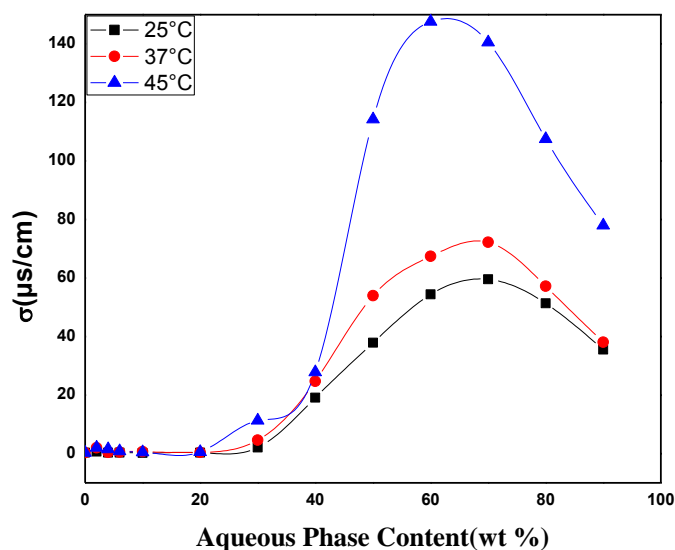


Fig 5:64 Variation of the electrical conductivity (σ) of the system # 13 MT50CE W+PG/TMAZ80+ Sucrose myristate (M1695) /CCT+ Ethanol as function of aqueous content along the dilution line N65. The phase diagrams are presented in figures (5:33),(5:38),(5:43) at different temperatures (25,37,and 45°C)respectively .

It is noticed that electrical conductivity for the system #13 W+PG/TMAZ80+ Sucrose myristate (M1695) /CCT+ Ethanol increases with the increase in the aqueous content, samples with aqueous content less than 30 % have low values of electrical conductivity, this indicates

restricted water mobility in this region. High electrical conductivity above 30 % water content along the N65 line, suggests that the system undergoes a structural inversion to bicontinuous microemulsion. Decrease the electrical conductivity above 65% suggests that the system undergoes a structural inversion to O/W. Electrical Conductivity increased as temperature increased in steadily fashion at aqueous content higher than 30 wt %.

System #14 MT75CE W+PG/ TMAZ80+Sucrose myristate (M1695) /CCT+ Ethanol

Aqueous solution made of (2/1)ratio , mixed surfactants TMAZ80+ Sucrose myristate(M1695) in the ratio (3/4) and equal unity of CCT oil with ethanol.

Representative data at the three different temperatures are shown in table 5:22. For the whole data collected see appendix C4

Table 5:22 The electrical conductivity (σ) for system # 14 W+PG/TMAZ80+ Sucrose myristate (M1695) /CCT+ Ethanol at three different temperatures.

# of additions	W+PG (2/1) wt%	σ ($\mu\text{S}/\text{cm}$)		
		25°C	37°C	45°C
1	0	1.2	1.4	2.8
2	2	0.8	1.4	2.8
3	4	0.8	1.7	2.9
4	6	0.8	1.1	2.2
5	10	0.8	1.3	2.4
6	20	2.4	2.6	11.5
7	30	13.6	22.5	50.4
8	40	35.8	51.5	90.7
9	50	72.2	83.8	164.4
10	60	78.9	89	181
11	70	73.5	93.5	192
12	80	58.8	72.2	135.2
13	90	34.9	51.7	106

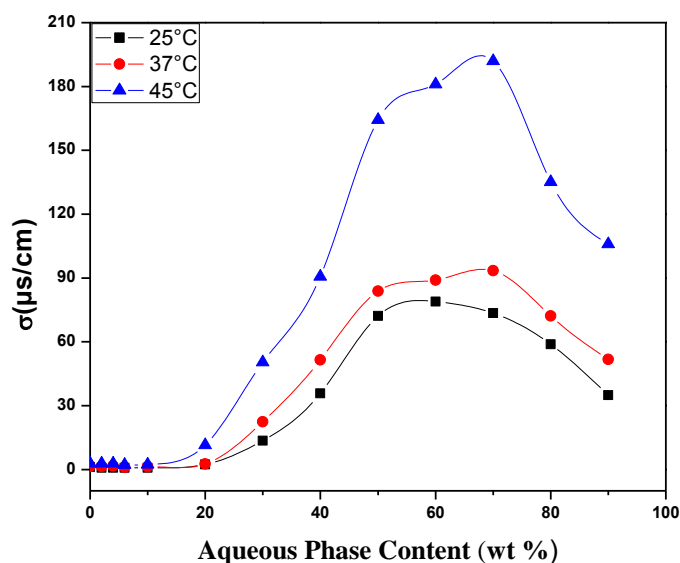


Fig 5:65 Variation of the electrical conductivity (σ) of the system # 14 MT75CE W+PG/TMAZ80+ Sucrose myristate (M1695) /CCT+ Ethanol as function of aqueous content along the dilution line N65. The phase diagrams are presented in figures (5:34),(5:39),(5:44) at different temperatures (25,37,and 45°C)respectively.

It is noticed that electrical conductivity for the system #14 W+PG/TMAZ80+ Sucrose myristate (M1695) /CCT+ Ethanol increases with the increase in the aqueous content, samples with aqueous content less than 20 % have low values of electrical conductivity, this indicates restricted water mobility in this region. High electrical conductivity above 20 % water content along the N65 line, suggests that the system undergoes a structural inversion to bicontinues microemulsion. Decrease the electrical conductivity above 65% suggests that the system undergoes a structural inversion to O/W. Electrical Conductivity increased as temperature increased in steadily fashion at aqueous content higher than 20 wt %.

System #15 MT100CE W+PG/ TMAZ80/CCT+ Ethanol

Aqueous solution made of (2/1)ratio , surfactant TMAZ80 (100 %) and equal unity of CCT oil with ethanol.

Representative data at the three different temperatures are shown in table 5:23. For the whole data collected see appendix C5

Table 5:23 The electrical conductivity (σ) for system # 15 W+PG/TMAZ80/CCT+ Ethanol at three different temperatures.

# of additions	W+PG (2/1) wt%	σ ($\mu\text{S}/\text{cm}$)		
		25°C	37°C	45°C
1	0	0.8	1	1.6
2	2	0.5	0.8	0.6
3	4	0.3	0.3	0.3
4	6	0.3	0.4	0.6
5	10	0.4	0.8	1.6
6	20	1.1	2.2	1.9
7	30	2.9	3.7	6.6
8	40	9.8	12.2	27.3
9	50	18.3	24.5	47.8
10	60	20	25	52.4
11	70	20.9	26.2	63.9
12	80	17.2	19.5	38.3
13	90	10.5	12.3	25.2

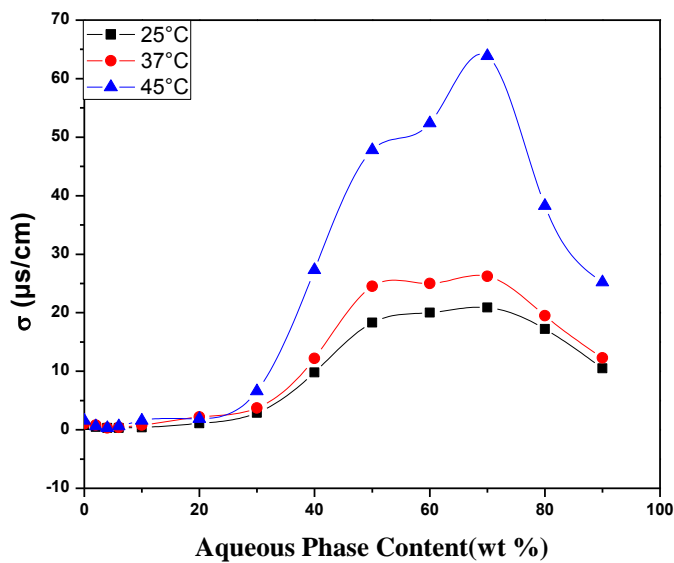


Fig 5:66 Variation of the electrical conductivity (σ) of the system # 15 MT100CE W+PG/TMAZ80/CCT+ Ethanol as function of aqueous content along the dilution line N65. The

phase diagrams are presented in figures (5:35),(5:40),(5:45) at different temperatures (25,37,and 45°C)respectively .

It is noticed that electrical conductivity for the system #15 W+PG/TMAZ80/CCT+ Ethanol increases with the increase in the aqueous content, samples with aqueous content less than 20 % have low values of electrical conductivity, this indicates restricted water mobility in this region. High electrical conductivity above 20 % water content along the N65 line, suggests that the system undergoes a structural inversion to bicontinues microemulsion. Decrease the electrical conductivity above 70% suggests that the system undergoes a structural inversion to O/W. Electrical Conductivity increased as temperature increased in steadily fashion at aqueous content higher than 20 wt %.

The influence of water volume fraction change on the electrical conductivity (σ) with respect to volume fraction of water was measured. The increase in the water volume fraction induces the increase in electrical conductivity exponentially in all systems. These change have been attributed to the occurrence of a percolation transition at which the conductivity remains low up to a certain volume fraction(ϕ_c)of water at constant temperature ,which can be seen in almost all of the systems tested ,which differs according to the type of oil used . These conducting w/o droplets below ϕ_c are isolated from each other embedded in non conducting continuum oil phase and hence contribute very little to the conductance. However, as the volume fraction of water reaches the percolation threshold ϕ_c , some of these conductive droplets begin to contact each other and form clusters which are sufficiently close to each other. The number of such clusters increases very rapidly above the percolation threshold ϕ_c , giving rise to the observed changes of properties, in particular to the increase of electrical conductivity. The electrical conductivity above ϕ_c has been attributed to the transfer of counter ions from one droplet to another through water channels opening between droplets during sticky collisions through transient merging of droplets

Along aqueous titration electrical conductivity increases since more space will exist between molecules giving rise in the attractive interactions to a point where there will be minimum space for particles to interact results in lowering the electrical conductivity .Under investigating electrical conductivity might have static percolation where the appearance of bicontinuous

microemulsions can be detected or dynamic percolation which is rapid processes of fusion–fission among the droplets(no bicontinuous detection).

Electrical conductivity increased with increase in temperature ,this is due to the decrease in viscosity which in turn causes increase the collision between droplet and increase of movement of ions. Steadily fashion in conductance indicates to no structural transformation. By raising the temperature, the collision probability between the droplets increases and the opening and reforming of droplets will increase the mobility of water and the electrical conductivity will again rises with temperature.

Type of oil studied in this work differ in it water volume threshold which is relatively low for the nonionic surfactants, attributed to the surfactants mixing effect and to the presence of alcohol in the system which proves the synergetic effect of mixing surfactants

Comparing the electrical conductivity for the three different oils at its maximum water solubilization (equal surfactant unity) at 25° C as representative temperature , table 5:24and Fig 5:67 reveals that CCT and LIM oils have higher electrical conductivity than IPM oil. Shape, structure ,molecular volume of the oil and effective carbon number of the oil (6,17,10 for LIM,IPM,CCT oil respectively)play important role in determining the interactions responsible for the determination of the electrical conductivities of these microemulsions. Since each has its own attitude in penetrating and participating in microemulsiom formation and stability

LIM tends to be solubilized inside the palisade layer of the mixed surfactants aggregates at an initial stage of solubilization and the mixed surfactants layer curvature changes to be less positive.

LIM has low electrical conductivity values, since LIM tends to form gel microemulsion, so the viscous microemulsion have low electrical conductivity because the structure more network form between water and surfactant the movement of water between the droplets is low .

IPM is mainly solubilized deep inside of the mixed surfactants aggregate and makes an oil pool, curvature layer tends to be more positive, forming smaller water droplet size oil . For isopropyl myristate oil have ketones group that is soluble in water, carbonyl compounds they can hydrogen-bond to water through the carbonyl oxygen, but ketones decrease solubility in water when the increase in molecular volume, isopropyl myristate make in microemulsion as penetration enhancer its causes to increase electrical conductivity of system isopropyl myristate.

CCT oil having the higher carbon effective number of all and the largest molecular volume ,longest chain length and the bulky fork shape makes it the hardest to penetrate so it is partially solubilized inside the palisade layer, thus more space and more interactions between the droplets resulting in higher electrical conductivity.

Table 5:24 The electrical conductivity at the optimum surfactant mixing ratio as a function of different oil type at constant temperature 25°C.

# of additions	W+PG (2/1) wt%	σ ($\mu\text{S}/\text{cm}$)		
		LIM	IPM	CCT
1	0	1	0.7	0.3
2	2	0.8	0.6	0.7
3	4	0.8	0.5	0.3
4	6	0.8	0.4	0.3
5	10	1	0.8	0.2
6	20	3.6	0.7	0.3
7	30	15.6	9.8	2.1
8	40	32.1	23	19.1
9	50	50.5	42.4	37.9
10	60	53.6	37.7	54.4
11	70	49	7.55	59.6
12	80	37.4	7.2	51.3
13	90	20	9.1	35.5

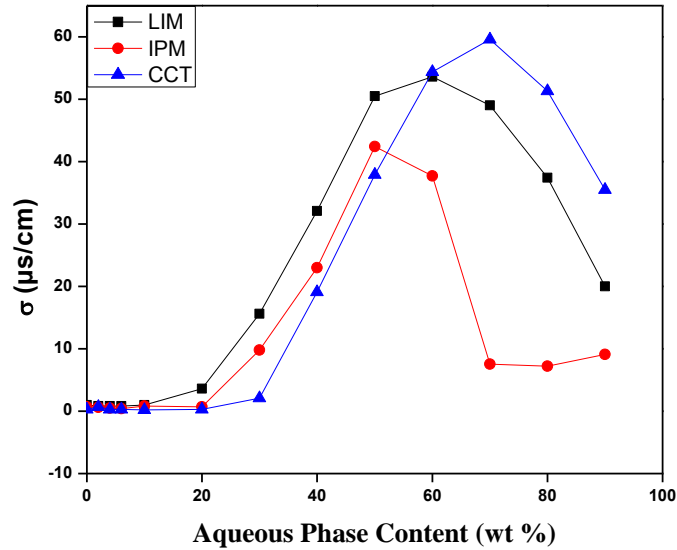


Fig 5:67 Variation of the electrical conductivity (σ) for the system W+PG/TMAZ80+ Sucrose myristate (M1695) /oil+ Ethanol as function of water content along the dilution line N65 for different oils (LIM,IPM,CCT) ,mixing surfactant ratio equal unity at 25°C. The phase diagrams are presented in figures (5:54), (5:59), (5:64) respectively.

5.3.2 Density and ultrasonic velocity

Density and ultrasonic velocity were measured for the fifteen different systems in table 4:1 emulsion formed from mixed and single surfactants TMAZ80 + Sucrose myristate (M1695) in different ratios (0,25,50,75,100), and the three different oils mixed with ethanol (99,9%) in (1/1) ratio, titrated with an aqueous solution made of water and propylene glycol in (2/1) ratio. Titration with the aqueous solution was made with 5% increment as mentioned in sample preparation in 4.2.4.1. Measurements were taken at four different temperatures (25,30,37,and45°C). Data of density were taken as (kg/m³) and the ultrasonic velocity as (m/s). These methods used in characterization of microemulsion by obtaining information about micellar interactions.

Density and ultrasonic velocity were also measured for all the components (oils surfactants and co surfactants)except for the Sucrose myristate (M1695) surfactant , see appendix D for the density data and appendix E for the ultrasonic velocity data.

5.3.2.1 Density Measurements

5.3.2.1.1 Determining the density for the systems using LIM oil

System # 1 MT0LE W+PG/ Sucrose myristate (M1695) /LIM +Ethanol

The density was measured for the system W+PG/ M1695/LIM+ Ethanol where with aqueous solution made of (2/1)ratio , surfactant Sucrose myristate (M1695) (100%) and equal unity of LIM oil with ethanol along the dilution line N65. Figures (5:68) and Table (5.25) displays the influence of aqueous content and temperature on the density (ρ). Some of the samples couldn't be measured because they were too viscous in the system data were as follows.

Table 5:25 The density (ρ) for the system #1 W+PG/ Sucrose myristate (M1695) /LIM +Ethanol at different aqueous contents and different temperatures.

W+PG (2/1) wt%	Density(kg/m ³)				
	T(°C) →	25	30	37	45
70		1049.89	1045.418	1038.783	1030.644
75		1046.333	1043.593	1037.682	1030.87
80		1041.699	1037.659	1032.056	1025.236
85		1044.822	1040.961	1035.461	1029.094
90		1040.026	1036.303	1030.958	1024.758

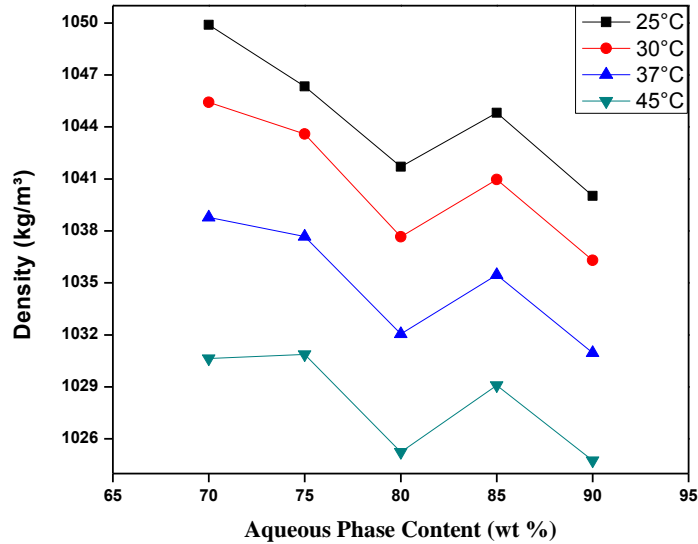


Fig 5:68 Variation of the density (ρ) of the system # 1 W+PG/ Sucrose myristate (M1695) /LIM +Ethanol as function of aqueous content along the dilution line N65 at different temperatures. The phase diagrams are presented in figures (5:1),(5:6),(5:11) at different temperatures (25,37,and 45°C)respectively .

Density results in static percolation model of data; since it is well noticed that density of the system decreases as the temperature increases. Density decreases with aqueous addition up to 75% aqueous content system maintained it w/o structure ,between 75 to 85 % it passes through bicontinuous structure going from oil rich to water rich medium ending in the o/w reverse micelles after 85% aqueous content . Results showed steady fashion between density and temperature.

System # 2 MT25LE W+PG/ TMAZ80+Sucrose myristate (M1695) /LIM +Ethanol

The density was measured for the system W+PG/ TMAZ80+M1695/LIM+Ethanol where with aqueous solution made of (2/1)ratio , surfactant TMAZ80/Sucrose myristate (M1695) in the ratio(1/4) and equal unity of LIM oil with ethanol along the dilution line N65. Figures (5:69) and Table (5:26) displays the influence of aqueous content and temperature on the density (ρ).

Table 5.26 The density (ρ) for the system #2 W+PG/ TMAZ80+Sucrose myristate (M1695) /LIM +Ethanol at different aqueous contents and different temperatures.

W+PG (2/1) wt%	Density(kg/m ³)				
	T(°C) →	25	30	37	45
65		1099.598	1094.559	1087.699	1078.884
70		1103.543	1099.708	1094.188	1087.581
75		1109.456	1105.873	1100.689	1094.719
80		1108.978	1105.223	1099.859	1093.538
85		1101.559	1097.033	1090.754	1083.485
90		1100.873	1097.249	1091.453	1084.685

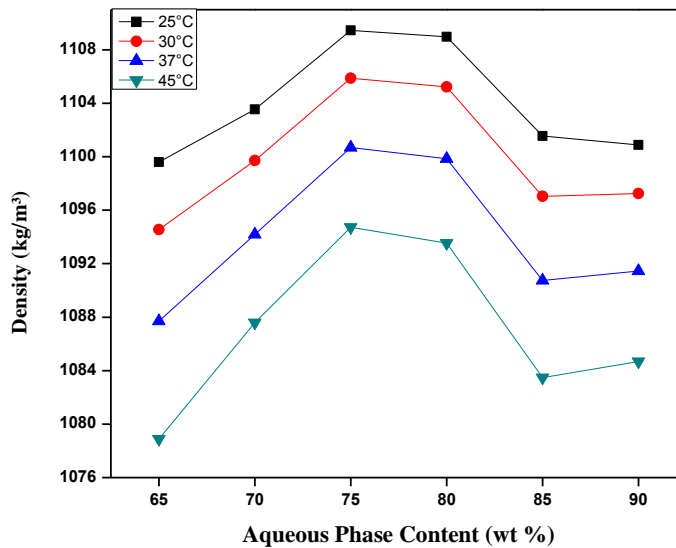


Fig 5:69 Variation of the density (ρ) of the system # 2 W+PG/ TMAZ80+Sucrose myristate (M1695) /LIM +Ethanol as function of aqueous content along the dilution line N65 at different temperatures. The phase diagrams are presented in figures (5:2),(5:7),(5:12) at different temperatures (25,37,and 45°C)respectively .

Density results in static percolation model of data; since it is well noticed that density of the system decreases as the temperature increases. From 65% aqueous content up to 75% density increases indicating w/o structure ,between 75 to 80 % it passes through bicontinuous structure

ending in the o/w reverse micelles after 85% aqueous content Results showed steady fashion between density and temperature.

System # 3 MT50LE W+PG/ TMAZ80+Sucrose myristate (M1695) /LIM +Ethanol

The density was measured for the system W+PG/ TMAZ80+M1695/LIM+Ethanol where with aqueous solution made of (2/1)ratio , surfactant TMAZ80/Sucrose myristate (M1695) in the ratio(1/1) and equal unity of LIM oil with ethanol along the dilution line N65. Figures (5:70) and Table (5:27)displays the influence of aqueous content and temperature on the density (ρ).some of the samples couldn't be measured because they were too viscous.

Table 5.27 The density (ρ) for the system #3 W+PG/ TMAZ80+Sucrose myristate (M1695) /LIM +Ethanol at different aqueous contents and different temperatures.

W+PG (2/1) wt%	Density(kg/m ³)				
	T(°C) →	25	30	37	45
15		1086.161	1082.393	1077.192	1071.763
30		1093.759	1089.931	1084.561	1078.075
35		1089.835	1085.952	1080.51	1074.259
40		1093.908	1090.137	1084.791	1078.644
45		1096.352	1093.205	1088.426	1082.758
50		1092.324	1088.445	1082.974	1075.774
55		1093.217	1089.439	1084.056	1077.659
65		1093.894	1090.044	1084.587	1078.128
70		1091.633	1087.855	1082.473	1075.862
75		1091.775	1087.898	1082.43	1075.912
80		1081.549	1077.363	1072.013	1065.795
85		1090.788	1086.916	1081.376	1075.057
90		1088.366	1084.515	1079.007	1072.733

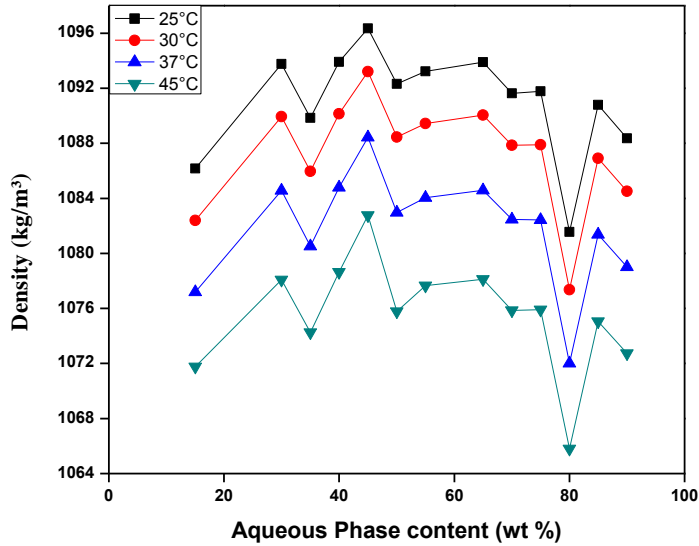


Fig 5:70 Variation of the density (ρ) of the system # 3 W+PG/ TMAZ80+Sucrose myristate (M1695) /LIM +Ethanol as function of aqueous content along the dilution line N65 at different temperatures. The phase diagrams are presented in figures (5:3),(5:8),(5:13) at different temperatures (25,37,and 45°C)respectively .

Density results in static percolation model of data; since it is well noticed that density of the system decreases as the temperature increases. Up to 30% aqueous content system maintained it w/o structure ,between 35 to 45 % it passes through water rich bicontinuous structure, continues going through the conversion process until 75% ,going from 75% up to85% system under goes the next stage of bicontinuous exiting in oil rich medium ending in the o/w reverse micelles indicated by the decrease in density between 85% and 90% aqueous content .Results showed steady fashion between density and temperature.

System # 4 MT75LE W+PG/ TMAZ80+Sucrose myristate (M1695) /LIM +Ethanol

The density was measured for the system W+PG/ TMAZ80+M1695/LIM+Ethanol where with aqueous solution made of (2/1)ratio , surfactant TMAZ80/Sucrose myristate (M1695) in the ratio(3/4) and equal unity of LIM oil with ethanol along the dilution line N65. Figures (5:71) and Table (5:28) displays the influence of aqueous content and temperature on the density (ρ).

Table 5.28 The density (ρ) for the system #4 W+PG/ TMAZ80+Sucrose myristate (M1695) /LIM +Ethanol at different aqueous contents and different temperatures.

W+PG (2/1) wt%	Density(kg/m ³)				
	T(°C) →	25	30	37	45
0		1073.45	1069.482	1063.998	1057.68
5		1065.165	1061.436	1055.973	1049.665
10		1071.932	1067.916	1062.354	1055.822
15		1064.173	1061.693	1056.254	1049.093
20		1067.151	1063.1	1057.714	1051.534
25		1071.583	1067.57	1062.015	1055.533
30		1071.344	1067.66	1062.338	1056.106
35		1072.804	1069.281	1063.878	1057.648
40		1074.999	1071.023	1066.543	1060.207
45		1073.695	1069.516	1064.061	1057.725
50		1073.866	1069.916	1064.428	1058.098
55		1073.932	1070.208	1064.748	1058.46
60		1074.885	1070.932	1065.426	1057.741
65		1075.549	1071.767	1066.311	1060.013
70		1074.88	1071.064	1065.595	1059.276
75		1073.378	1069.431	1063.837	1057.434
80		1076.177	1072.262	1066.763	1060.433
85		1075.427	1071.463	1065.937	1059.496
90		1073.331	1069.458	1063.809	1057.438

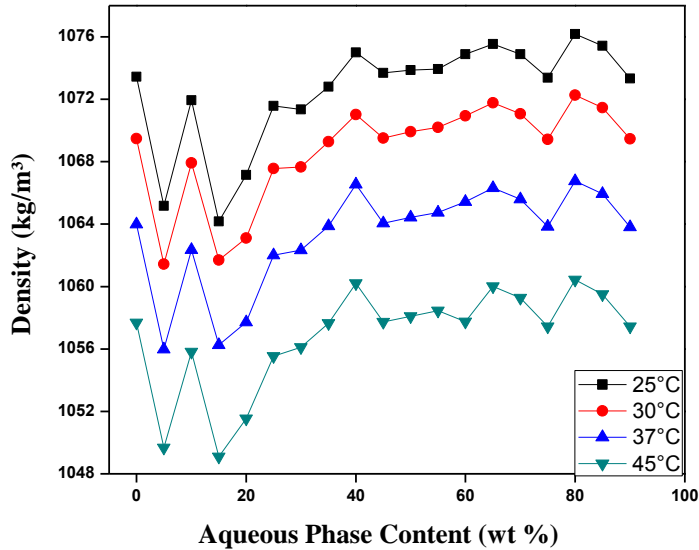


Fig 5:71 Variation of the density (ρ) of the system # 4 W+PG/ TMAZ80+Sucrose myristate (M1695) /LIM +Ethanol as function of aqueous content along the dilution line N65 at different temperatures. The phase diagrams are presented in figures (5:4),(5:9),(5:14) at different temperatures (25,37,and 45°C)respectively .

Density results in static percolation model of data; since it is well noticed that density of the system decreases as the temperature increases. Density decreases with aqueous addition up to 5% aqueous content system maintained it w/o structure ,between 5 to 15 % it passes through water rich bicontinuous structure, continues going through the conversion process until 80% after 80% aqueous content o/w is formed .Results showed steady fashion between density and temperature.

System # 5 MT100LE W+PG/ TMAZ80/LIM +Ethanol

The density was measured for the system W+PG/ TMAZ80/LIM+ Ethanol where with aqueous solution made of (2/1)ratio , surfactant TMAZ80 (100%) and equal unity of LIM oil with ethanol along the dilution line N65. Figures (5:72) and Table (5:29) displays the influence of aqueous content and temperature on the density (ρ).

Table 5.29 The density (ρ) for the system #5 W+PG/ TMAZ80/LIM +Ethanol at different aqueous contents and different temperatures.

W+PG (2/1) wt%	Density(kg/m ³)				
	T(°C) →	25	30	37	45
0		951.673	947.755	942.214	935.807
5		955.288	951.369	945.865	939.542
10		956.778	952.882	947.41	941.085
15		958.734	954.801	949.262	942.758
20		980.871	976.995	971.538	965.276
25		961.088	957.166	951.655	945.325
30		967.888	964.028	958.555	952.246
35		965.015	961.101	955.602	949.281
40		972.674	968.789	963.325	957.046
45		968.864	964.952	959.455	953.06
50		960.925	957.07	951.608	945.281
55		971.831	967.924	962.384	956.118
60		984.213	980.337	974.857	968.554
65		973.607	969.696	964.199	957.856
70		990.255	986.386	980.917	974.618
75		987.603	983.706	978.226	971.914
80		973.225	969.382	963.878	957.527
85		993.578	989.485	983.684	976.904
90		976.445	972.531	967.021	960.662

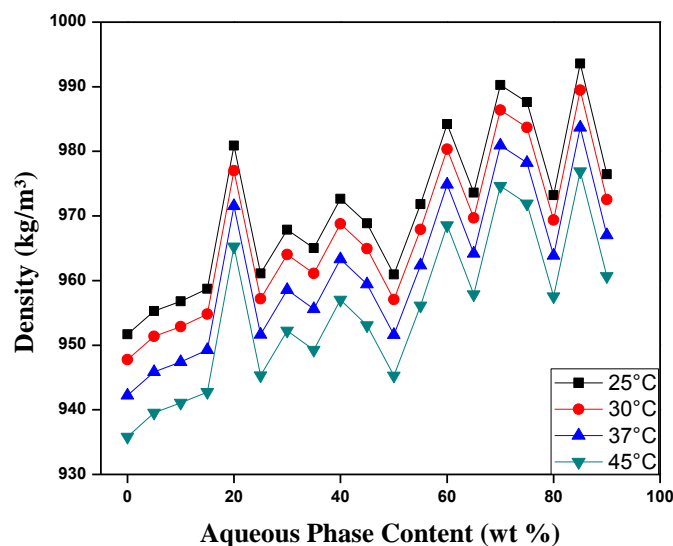


Fig 5:72 Variation of the density (ρ) of the system # 5 W+PG/ TMAZ80 /LIM +Ethanol as function of aqueous content along the dilution line N65 at different temperatures. The phase diagrams are presented in figures (5:5),(5:10),(5:15) at different temperatures (25,37, and 45°C)respectively .

Density results in static percolation model of data; since it is well noticed that density of the system decreases as the temperature increases. Density increases in low degree up to 15% forming w/o after which between 15%and 25% undergoes bicontinuous water rich system fluctuating between water rich medium to oil rich medium until 85% aqueous content after which o/w system is formed. Results showed steady fashion between density and temperature.

5.3.2.1.2 Determining the density for the systems using IPM oil

System # 6 MT0IE W+PG/ Sucrose myristate (M1695) /IPM +Ethanol

The density was measured for the system W+PG/ M1695/IPM+ Ethanol where with aqueous solution made of (2/1)ratio , surfactant Sucrose myristate (M1695) (100%) and equal unity of IPM oil with ethanol along the dilution line N65. Figures (5:73) and Table (5:30) displays the influence of aqueous content and temperature on the density (ρ). Some of the samples couldn't be measured because they were too viscous in the system data were as follows.

Table 5:30 The density (ρ) for the system #6 W+PG/ Sucrose myristate (M1695) /IPM +Ethanol at different aqueous contents and different temperatures.

W+PG (2/1) wt%	Density(kg/m ³)				
	T(°C) →	25	30	37	45
0		1039.806	1035.906	1030.061	1023.361
5		1044.88	1040.928	1035.027	1027.2
10		1044.081	1039.247	1033.751	1026.816
15		1037.489	1033.525	1027.799	1021.072
20		1041.566	1037.786	1032.35	1025.71
25		1041.425	1037.533	1031.921	1024.754
30		1036.149	1032.476	1027.156	1020.712
35		1051.579	1047.851	1042.573	1036.294
40		1039.575	1035.912	1030.645	1024.54

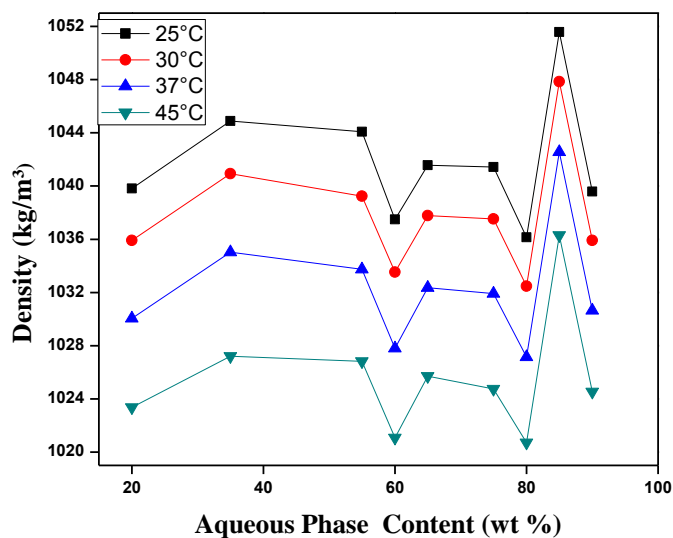


Fig 5:73 Variation of the density (ρ) of the system # 6 W+PG/ Sucrose myristate (M1695) /IPM +Ethanol as function of aqueous content along the dilution line N65 at different temperatures.

The phase diagrams are presented in figures (5:16),(5:21),(5:26) at different temperatures (25,37,and 45°C)respectively .

Density results in static percolation model of data; since it is well noticed that density of the system decreases as the temperature increases. Density increases in low degree up to 35% forming w/o after which between 35% and 85% undergoes bicontinuous water rich system fluctuating between water rich medium to oil rich medium until 85% aqueous content after which o/w system is formed. Results showed steady fashion between density and temperature

System # 7 MT25IE W+PG/ TMAZ80+Sucrose myristate (M1695) /IPM +Ethanol

The density was measured for the system W+PG/ TMAZ80+M1695/IPM+Ethanol where with aqueous solution made of (2/1)ratio , surfactant TMAZ80/Sucrose myristate (M1695) in the ratio(1/4) and equal unity of IPM oil with ethanol along the dilution line N65. Figures (5:74) and Table (5:31) displays the influence of aqueous content and temperature on the density (ρ).

Table 5:31 The density (ρ) for the system #7 W+PG/ TMAZ80+Sucrose myristate (M1695) /IPM+Ethanol at different aqueous contents and different temperatures.

W+PG (2/1) wt%	Density(kg/m ³)				
	T(°C) →	25	30	37	45
0		1017.77	1013.89	1008.405	1001.622
5		1051.561	1047.678	1041.836	1034.937
10		1021.071	1017.15	1011.6	1005.381
15		1016.425	1012.536	1007.04	1000.532
20		1024.06	1020.145	1014.526	1008.287
25		1025.7	1021.738	1016.07	1008.382
30		1017.122	1013.147	1007.544	1001.471
35		1027.177	1023.442	1018.084	1011.714
40		1017.055	1013.361	1007.953	1001.657
45		1027.585	1023.8	1018.455	1012.231
50		1023.105	1019.27	1013.78	1007.332
55		1030.137	1026.281	1020.799	1014.475
60		1025.845	1022.078	1016.73	1010.517
65		1022.36	1018.75	1013.368	1007.13
70		1026.419	1022.322	1016.564	1010.035
75		1023.775	1019.425	1013.756	1006.422
80		1023.55	1019.649	1014.13	1007.809
85		1027.927	1024.197	1018.768	1012.368
90		1017.77	1013.89	1008.405	1001.622

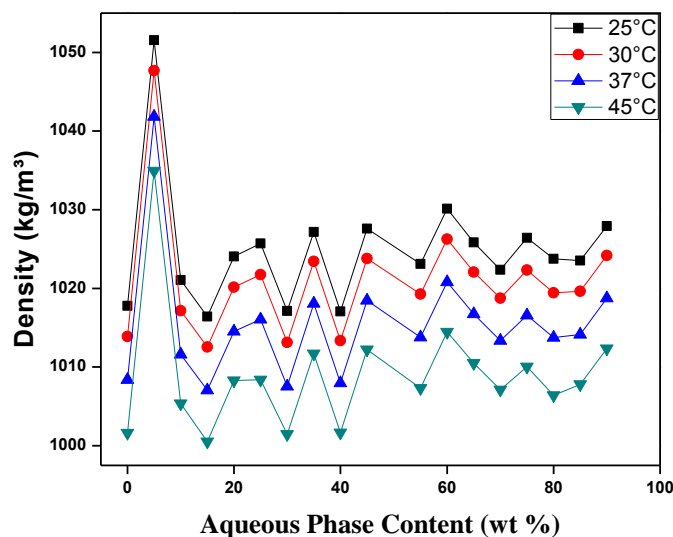


Fig 5:74 Variation of the density (ρ) of the system # 7 W+PG/TMAZ80+ Sucrose myristate (M1695) /IPM +Ethanol as function of aqueous content along the dilution line N65 at different temperatures. The phase diagrams are presented in figures (5:17),(5:22),(5:27) at different temperatures (25,37,and 45°C)respectively .

Density results in static percolation model of data; since it is well noticed that density of the system decreases as the temperature increases. Density increases in low degree up to 5% forming w/o after which between 15%and 85% undergoes bicontinuous water rich system fluctuating between water rich medium to oil rich medium until 85% aqueous content after which o/w system is formed. Results showed steady fashion between density and temperature.

System # 8 MT50IE W+PG/ TMAZ80+Sucrose myristate (M1695) /IPM +Ethanol

The density was measured for the system W+PG/ TMAZ80+M1695/IPM+Ethanol where with aqueous solution made of (2/1)ratio , surfactant TMAZ80/Sucrose myristate (M1695) in the ratio(1/1) and equal unity of IPM oil with ethanol along the dilution line N65. Figures (5:75) and Table (5:32) displays the influence of aqueous content and temperature on the density (ρ).

Table 5:32 The density (ρ) for the system #8 W+PG/ TMAZ80+Sucrose myristate (M1695) /IPM+Ethanol at different aqueous contents and different temperatures.

W+PG (2/1) wt%	Density(kg/m ³)				
	T(°C) →	25	30	37	45
0		1000.051	996.076	990.351	984.196
5		997.466	993.712	988.286	982.049
10		1001.856	998.044	992.632	986.381
15		1016.488	1012.672	1007.34	999.133
20		1005.91	1002.101	996.72	990.523
25		1021.662	1017.873	1012.607	1006.562
30		1031.221	1009.425	1004.08	997.911
35		1001.866	998.041	992.614	986.367
40		1001.515	997.703	992.258	986.009
45		1001.069	997.201	991.741	985.493
50		1026.871	1023.057	1017.644	1010.701
55		1005.689	1001.957	996.55	990.321
60		1006.926	1003.077	997.657	990.908
65		1002.258	998.422	992.994	986.741
70		1019.644	1015.947	1010.635	1004.485
75		1009.293	1005.321	999.66	992.946
80		1006.826	1003.014	997.605	991.37
85		1006.465	1002.608	997.152	990.623
90		1011.258	1007.453	1002.077	995.886

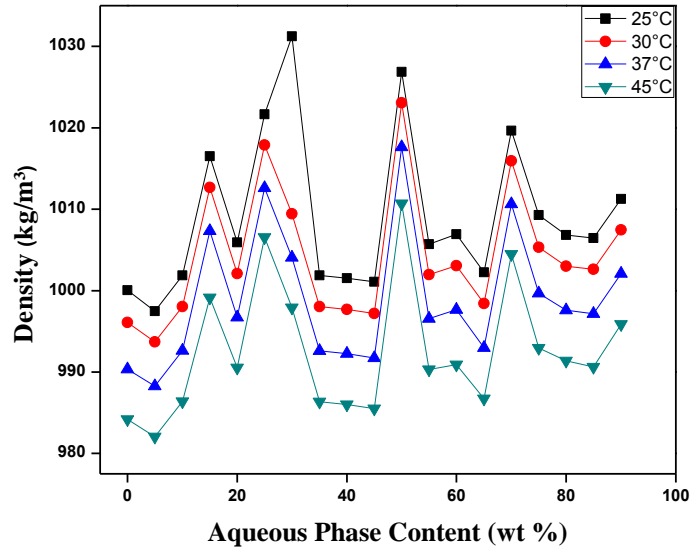


Fig 5:75 Variation of the density (ρ) of the system # 8 W+PG/TMAZ80+ Sucrose myristate (M1695) /IPM +Ethanol as function of aqueous content along the dilution line N65 at different temperatures. The phase diagrams are presented in figures (5:18),(5:23),(5:28) at different temperatures (25,37,and 45°C)respectively .

Density results in static percolation model of data; since it is well noticed that density of the system decreases as the temperature increases. Density increases in low degree up to 15% forming w/o after which between 15%and 70% undergoes bicontinuous water rich system fluctuating between water rich medium to oil rich medium until 75% aqueous content after which o/w system is formed. Results showed steady fashion between density and temperature.

System # 9 MT75IE W+PG/ TMAZ80+Sucrose myristate (M1695) /IPM +Ethanol

The density was measured for the system W+PG/ TMAZ80+M1695/IPM+Ethanol where with aqueous solution made of (2/1)ratio , surfactant TMAZ80/Sucrose myristate (M1695) in the ratio(3/4) and equal unity of IPM oil with ethanol along the dilution line N65. Figure (5:76) and Table (5:33) displays the influence of aqueous content and temperature on the density (ρ).

Table 5:33 The density (ρ) for the system #9 W+PG/ TMAZ80+Sucrose myristate (M1695) /IPM+ Ethanol at different aqueous contents and different temperatures.

W+PG (2/1) wt%	Density(kg/m ³)				
	T(°C) →	25	30	37	45
0		981.22	977.39	971.983	965.781
5		990.338	986.49	981.095	974.922
10		980.746	976.864	971.414	965.164
15		997.78	993.977	988.622	982.482
20		990.53	986.694	981.291	975.104
25		980.638	976.853	971.413	965.139
30		981.297	977.398	971.928	965.619
35		983.282	979.449	973.973	967.673
40		989.792	985.92	980.474	974.083
45		988.219	984.388	978.935	972.66
50		987.906	984.016	978.545	972.227
55		985.99	982.16	976.685	970.384
60		990.582	986.701	981.255	974.998
65		983.722	979.867	974.428	968.149
70		997.732	993.895	988.496	982.265
75		990.848	986.981	981.525	975.241
80		996.477	992.651	987.228	980.987
85		991.977	988.102	982.602	975.803
90		991.8	987.95	982.496	976.211

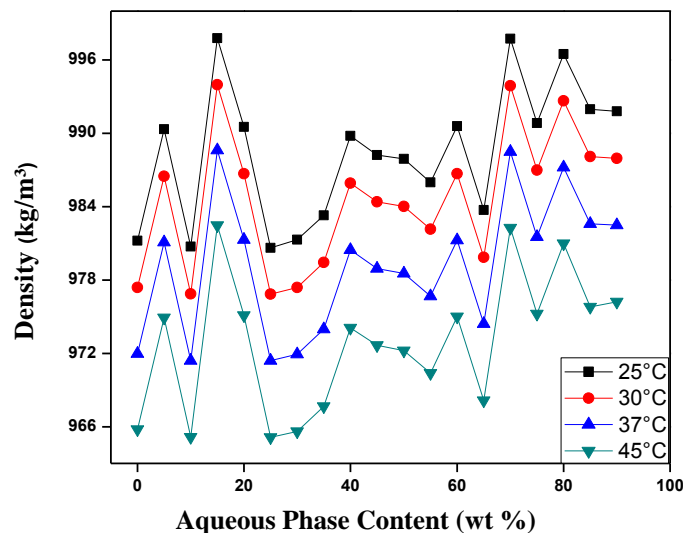


Fig 5:76 Variation of the density (ρ) of the system # 9 W+PG/TMAZ80+ Sucrose myristate (M1695) /IPM +Ethanol as function of aqueous content along the dilution line N65 at different temperatures. The phase diagrams are presented in figures (5:19),(5:24),(5:29) at different temperatures (25,37,and 45 °C)respectively .

Density results in static percolation model of data; since it is well noticed that density of the system decreases as the temperature increases. Density increases in low degree up to 5% forming w/o after which between 10 %and 25 % undergoes bicontinuous water rich system then fluctuating between water rich medium to oil rich medium until 75% aqueous content after which o/w system is formed. Results showed steady fashion between density and temperature.

System # 10 MT100IE W+PG/ TMAZ80/IPM +Ethanol

The density was measured for the system W+PG/ TMAZ80 /IPM+Ethanol where with aqueous solution made of (2/1)ratio , surfactant TMAZ80 in the ratio(100%) and equal unity of IPM oil with ethanol along the dilution line N65. Figures (5:77) and Table (5:34) displays the influence of aqueous content and temperature on the density (ρ).

Table 5:34 The density (ρ) for the system #10 W+PG/ TMAZ80/IPM+ Ethanol at different aqueous contents and different temperatures.

W+PG (2/1) wt%	Density(kg/m ³)				
	T(°C) →	25	30	37	45
0		987.34	983.563	978.256	972.128
5		991.338	987.398	982.514	976.64
10		958.142	954.238	948.756	942.304
15		993.964	990.253	984.991	978.949
20		971.603	967.72	962.266	955.997
25		964.25	960.341	954.835	948.5
30		992.195	988.455	983.193	977.181
35		964.576	960.683	955.183	948.859
40		966.619	962.707	957.207	950.888
45		968.417	964.513	959.014	952.689
50		970.971	967.001	961.609	955.034
55		967.689	963.805	958.292	951.95
60		967.311	963.39	957.831	951.328
65		970.129	966.243	960.769	954.471
70		988.238	984.469	979.175	973.129
75		971.016	967.108	961.624	955.311
80		967.708	963.275	957.913	957.273
85		973.03	969.169	963.711	957.402
90		993.114	989.339	984.001	977.805

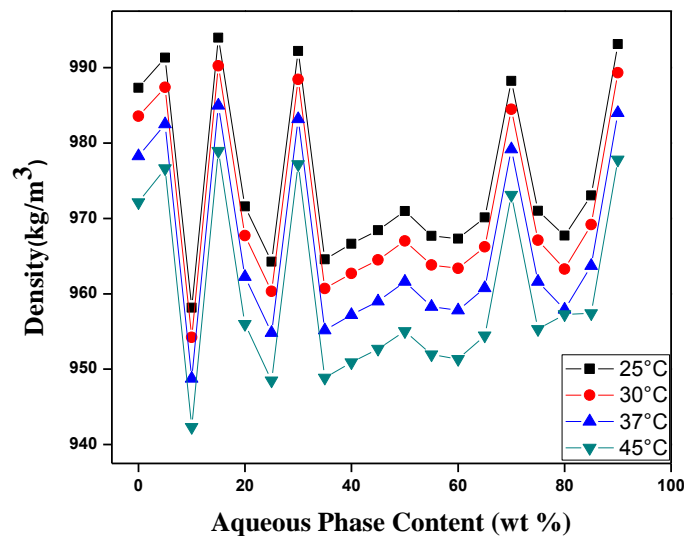


Fig 5:77 Variation of the density (ρ) of the system # 10 W+PG/TMAZ80/IPM +Ethanol as function of aqueous content along the dilution line N65 at different temperatures. The phase diagrams are presented in figures (5:20),(5:25),(5:30) at different temperatures (25,37,and 45°C)respectively .

Density results in static percolation model of data; since it is well noticed that density of the system decreases as the temperature increases. Density increases in low degree up to 5% forming w/o after which between 10 %and 80 % undergoes bicontinuous water rich system ,fluctuating between water rich medium to oil rich medium until 85% aqueous content after which o/w system is formed. Results showed steady fashion between density and temperature.

5.3.2.1.3 Determining the density for the systems using CCT oil

System # 11 MT0CE W+PG/ Sucrose myristate (M1695) /CCT +Ethanol

The density was measured for the system W+PG/ M1695/CCT+ Ethanol where with aqueous solution made of (2/1)ratio , surfactant Sucrose myristate (M1695) (100%) and equal unity of CCT oil with ethanol along the dilution line N65. Figures (5:78) and Table (5:35) displays the influence of aqueous content and temperature on the density (ρ). Some of the samples couldn't be measured because they were too viscous in the system data were as follows.

Table 5:35 The density (ρ) for the system #11 W+PG/ Sucrose myristate (M1695) /CCT +Ethanol at different aqueous contents and different temperatures.

W+PG (2/1) wt%	Density(kg/m ³)				
	T(°C) →	25	30	37	45
0		1046.063	1042.245	1036.77	1030.502
5		1045.988	1042.095	1036.519	1030.3
20		1046.345	1042.465	1037.011	1030.713
30		1044.973	1041.084	1035.5	1028.938
35		1044.395	1040.36	1035.036	1029.753
45		1044.875	1041.123	1035.717	1029.404
55		1045.711	1041.843	1036.298	1029.826
60		1044.298	1040.473	1034.933	1028.473
65		1046.318	1042.289	1036.542	1029.951
70		1044.98	1041.203	1035.765	1029.498
75		1046.562	1042.585	1036.672	1029.789
80		1045.924	1042.07	1036.545	1030.172
85		1046.842	1043.114	1037.744	1031.538
90		1050.701	1047.375	1042.057	1035.717

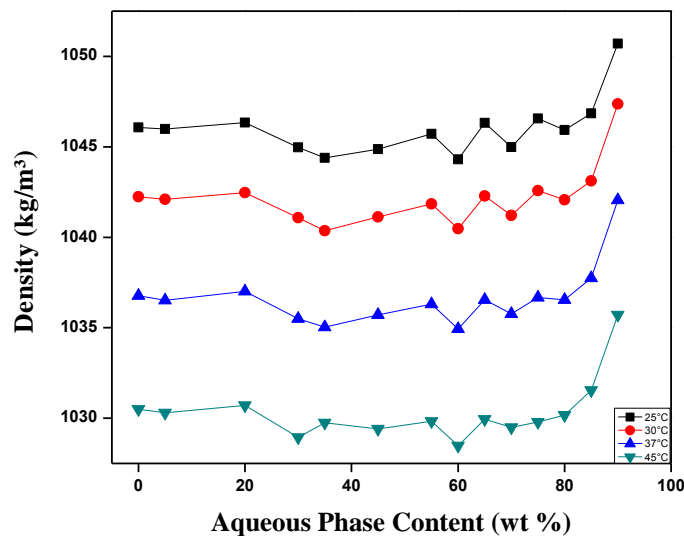


Fig 5:78 Variation of the density (ρ) of the system # 11 W+PG/ Sucrose myristate (M1695) /CCT +Ethanol as function of aqueous content along the dilution line N65 at different temperatures. The phase diagrams are presented in figures (5:31),(5:36),(5:41) at different temperatures (25,37,and 45°C)respectively .

Density results in static percolation model of data; since it is well noticed that density of the system decreases as the temperature increases. System has no change in density until 20% forming w/o after which undergoes fluctuation through bicontinuous water rich medium to oil rich medium until 65% aqueous content after which o/w system is formed. Results showed steady fashion between density and temperature.

System # 12 MT25CE W+PG/TMAZ80+Sucrose myristate (M1695) /CCT +Ethanol

The density was measured for the system W+PG/TMAZ80+ M1695/CCT+ Ethanol where with aqueous solution made of (2/1)ratio , surfactants TMAZ80/ Sucrose myristate (M1695) in the ratio of (1/4) and equal unity of CCT oil with ethanol along the dilution line N65. Figures (5:79) and Table (5:36) displays the influence of aqueous content and temperature on the density (ρ).

Table 5:36 The density (ρ) for the system #12 W+PG/ TMAZ80+Sucrose myristate (M1695) /CCT +Ethanol at different aqueous contents and different temperatures.

W+PG (2/1) wt%	Density(kg/m ³)				
	T(°C) →	25	30	37	45
0		1046.681	1042.669	1037.011	1030.522
5		1035.653	1031.774	1026.32	1020.002
10		1033.461	1029.604	1024.121	1017.797
15		1032.141	1028.259	1022.67	1016.098
20		1032.613	1028.757	1023.236	1016.817
30		1034.215	1030.27	1024.705	1018.153
35		1084.237	1080.399	1075.072	1070.207
40		1035.029	1031.147	1025.629	1019.231
45		1083.734	1080.267	1075.194	1069.041
50		1036.221	1032.299	1026.738	1020.097
55		1036.352	1032.531	1027.01	1020.652
60		1036.183	1032.685	1027.215	1020.865
65		1036.5	1032.575	1027.034	1020.39
70		1035.819	1031.98	1026.397	1019.916
75		1041.262	1037.413	1031.954	1025.667
80		1038.623	1034.725	1029.22	1022.876
85		1087.639	1083.804	1078.405	1072.06
90		1086.849	1082.924	1077.361	1071.04

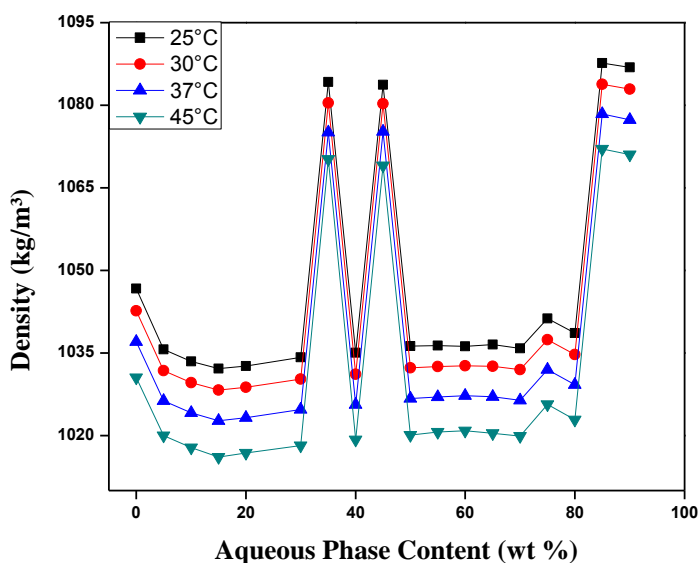


Fig 5:79 Variation of the density (ρ) of the system # 12 W+PG/TMAZ80+Sucrose myristate (M1695) /CCT +Ethanol as function of aqueous content along the dilution line N65 at different temperatures. The phase diagrams are presented in figures (5:32),(5:37),(5:42) at different temperatures (25,37,and 45°C)respectively .

Density results in static percolation model of data; since it is well noticed that density of the system decreases as the temperature increases. Density almost has no change until 35% w/o is formed , between 35% up to 80% undergoes fluctuation through bicontinuous water rich medium to oil rich medium until 80 % aqueous content after which o/w system is formed. Results showed steady fashion between density and temperature.

System # 13 MT50CE W+PG/TMAZ80+Sucrose myristate (M1695) /CCT +Ethanol

The density was measured for the system W+PG/TMAZ80+ M1695/CCT+Ethanol where with aqueous solution made of (2/1)ratio , surfactants TMAZ80/ Sucrose myristate (M1695) in the ratio of (1/1) and equal unity of CCT oil with ethanol along the dilution line N65. Figures (5:80) and Table (5:37) displays the influence of aqueous content and temperature on the density (ρ).

Table 5:37 The density (ρ) for the system #13 W+PG/ TMAZ80+Sucrose myristate (M1695) /CCT +Ethanol at different aqueous contents and different temperatures.

W+PG (2/1) wt%	Density(kg/m ³)				
	T(°C) →	25	30	37	45
0		1028.309	1024.581	1019.05	1012.288
5		1023.027	1019.008	1013.386	1006.922
10		1020.735	1016.789	1011.199	1004.791
15		1021.09	1016.859	1010.684	1004.201
20		1074.424	1070.687	1065.358	1059.185
25		1021.559	1017.555	1011.925	1005.342
30		1023.785	1019.846	1014.263	1007.829
35		1074.387	1070.555	1065.187	1059.024
40		1023.483	1019.478	1013.843	1007.368
45		1026.919	1022.917	1017.289	1010.825
50		1075.069	1071.223	1065.813	1059.685
55		1025.254	1021.247	1015.614	1009.131
60		1024.722	1020.753	1015.147	1008.692
65		1026.805	1022.838	1017.22	1010.755
70		1026.213	1022.253	1016.643	1010.18
75		1026.325	1022.326	1016.697	1010.197
80		1073.477	1069.629	1064.195	1058.056
85		1025.122	1021.346	1015.803	1009.26
90		1027.547	1023.569	1017.963	1011.501

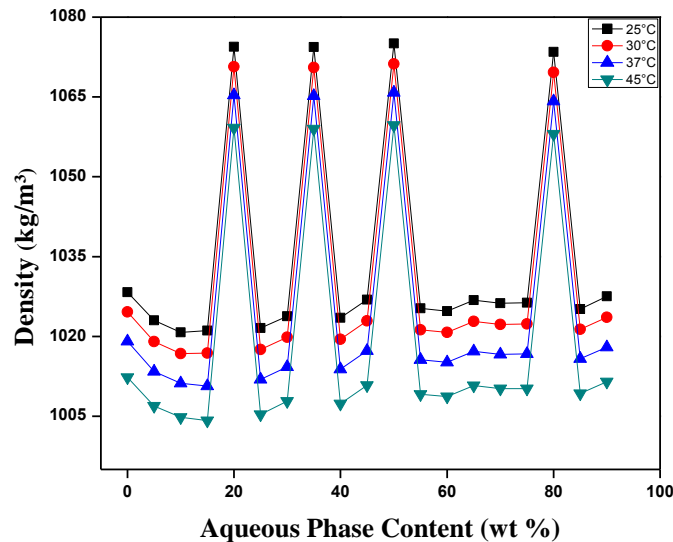


Fig 5:80 Variation of the density (ρ) of the system # 13 W+PG/TMAZ80+Sucrose myristate (M1695) /CCT +Ethanol as function of aqueous content along the dilution line N65 at different temperatures. The phase diagrams are presented in figures (5:33),(5:38),(5:43) at different at different temperatures (25,37,and 45°C)respectively .

Density results in static percolation model of data; since it is well noticed that density of the system decreases as the temperature increases. Density decreases until 15% w/o is formed , between 15% up to 80% undergoes big fluctuation through bicontinuous water rich medium to oil rich medium until 80 % aqueous content after which o/w system is formed. Results showed steady fashion between density and temperature.

System # 14 MT75CE W+PG/TMAZ80+Sucrose myristate (M1695) /CCT +Ethanol

The density was measured for the system W+PG/TMAZ80+ M1695/CCT+Ethanol where with aqueous solution made of (2/1)ratio , surfactants TMAZ80/ Sucrose myristate (M1695) in the ratio of (3/4) and equal unity of CCT oil with ethanol along the dilution line N65. Figures (5:81) and Table (5:38) displays the influence of aqueous content and temperature on the density (ρ).

Table 5:38 The density (ρ) for the system #14 W+PG/ TMAZ80+Sucrose myristate (M1695) /CCT +Ethanol at different aqueous contents and different temperatures.

W+PG (2/1) wt%	Density(kg/m ³)				
	T(°C) →	25	30	37	45
0		1060.102	1056.179	1050.764	1004.566
5		1008.57	1004.555	998.939	992.502
10		1023.482	1019.482	1013.841	1007.197
15		1010.605	1006.608	1000.962	994.486
20		1023.883	1019.881	1014.251	1007.683
25		1011.953	1007.912	1002.242	995.737
30		1012.835	1008.792	1003.11	996.605
35		1013.494	1009.466	1003.786	997.253
40		1056.631	1052.724	1047.276	1041.034
45		1024.666	1020.671	1015.011	1008.507
50		1015.805	1010.76	1006.071	999.539
55		1017.063	1013.001	1007.265	1000.549
60		1016.474	1012.445	1006.74	1000.178
65		1025.155	1021.127	1015.454	1008.911
70		1056.306	1052.439	1046.994	1040.74
75		1016.378	1012.091	1005.899	998.163
80		1057.216	1053.338	1047.881	1041.602
85		1019.312	1015.32	1009.585	1003.033
90		1020.133	1016.152	1010.508	1003.991

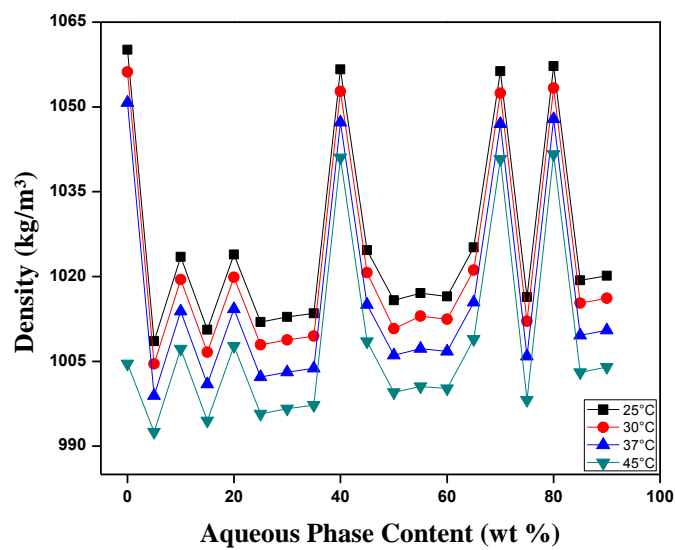


Fig 5:81 Variation of the density (ρ) of the system # 14 W+PG/TMAZ80+Sucrose myristate (M1695) /CCT +Ethanol as function of aqueous content along the dilution line N65 at different temperatures. The phase diagrams are presented in figures (5:34),(5:39),(5:44) at different temperatures (25,37,and 45°C)respectively .

Density results in static percolation model of data; since it is well noticed that density of the system decreases as the temperature increases. Density decreases until 5% w/o is formed , between 35% up to 75% undergoes big fluctuation through bicontinuous water rich medium to oil rich medium until 80 % aqueous content after which o/w system is formed. Results showed steady fashion between density and temperature.

System # 15 MT100CE W+PG/TMAZ80/CCT +Ethanol

The density was measured for the system W+PG/TMAZ80 /CCT+ Ethanol where with aqueous solution made of (2/1)ratio , surfactant TMAZ80 in the ratio of (100%) and equal unity of CCT oil with ethanol along the dilution line N65. Figures (5:82)and Table (5:39) displays the influence of aqueous content and temperature on the density (ρ).

Table 5:39 The density (ρ) for the system #15 W+PG/ TMAZ80/CCT +Ethanol at different aqueous contents and different temperatures.

W+PG (2/1) wt%	Density(kg/m ³)				
	T(°C) →	25	30	37	45
0		995.434	991.401	985.733	973.786
5		1040.912	1036.944	1031.373	1024.919
10		998.271	994.305	988.721	982.17
15		1040.89	1036.925	1031.395	1025.084
20		1020.284	1016.247	1010.586	1004.074
25		1000.399	996.326	990.594	984.023
30		1039.683	1035.729	1030.178	1023.852
35		1005.105	1001.033	995.292	988.702
40		1005.977	1001.883	996.138	989.548
45		1005.803	1001.701	995.945	989.381
50		1006.825	1002.733	996.969	990.349
55		1041.966	1037.995	1032.41	1026.005
60		1025.728	1021.684	1015.991	1009.453
65		1005.39	1001.297	995.526	988.886
70		1005.64	1001.931	996.148	989.501
75		1006.889	1002.771	996.97	990.301
80		1007.34	1003.263	997.48	990.842
85		1007.923	1003.825	998.057	991.422
90		1010.017	1005.931	1000.166	993.527

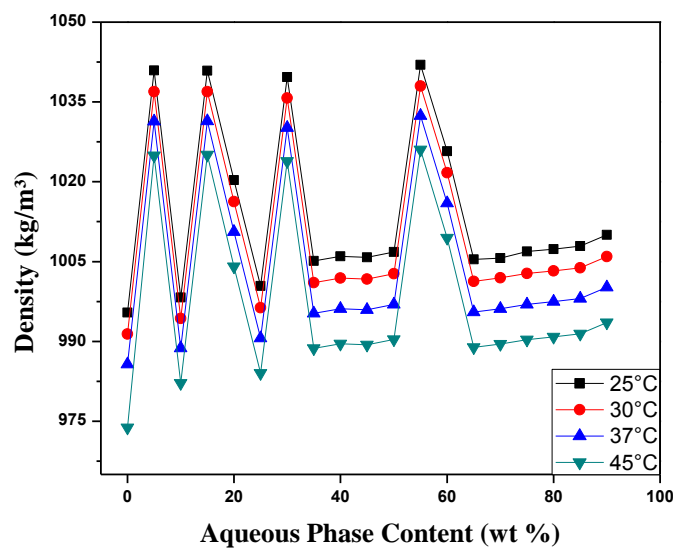


Fig 5:82 Variation of the density (ρ) of the system # 15 W+PG/TMAZ80 /CCT +Ethanol as function of aqueous content along the dilution line N65 at different temperatures. The phase diagrams are presented in figures (5:35),(5:40),(5:45) at different temperatures (25,37, and 45°C)respectively .

Density results in static percolation model of data; since it is well noticed that density of the system decreases as the temperature increases. Density increases until 5% w/o is formed , between 10% up to 70% undergoes big fluctuation through bicontinuous water rich medium to oil rich medium until 70 % aqueous content after which o/w system is formed. Results showed steady fashion between density and temperature.

Microemulsion densities usually decreases with the increases in the aqueous volume content at constant temperatures.

Most of the systems studied with the three different oils decreases in density up to about 15% aqueous content forming the water in oil microemulsion, passes through the bicontinuous stage between 20-65% aqueous content ending in the form of oil in water microemulsions after 70% aqueous content.

5.3.2.2 Ultrasonic Velocity Measurements

5.3.2.2.1 Determining the ultrasonic velocity for the systems using LIM oil

System # 1 MTOLE W+PG/ Sucrose myristate (M1695) /LIM +Ethanol

The ultrasonic velocity was measured for the system W+PG/ M1695/LIM+Ethanol where with aqueous solution made of (2/1)ratio , surfactant Sucrose myristate (M1695) (100%) and equal unity of LIM oil with ethanol along the dilution line N65. Figures (5:83) and Table (5:40) displays the influence of aqueous content and temperature on the velocity (V). Some of the samples couldn't be measured because they were too viscous in the system data were as follows.

Table 5:40 The ultrasonic velocity (V) for the system #1 W+PG/ Sucrose myristate (M1695) /LIM +Ethanol at different aqueous contents and different temperatures.

W+PG (2/1) wt%	USV (m/s)				
	T(°C) →	25	30	37	45
70		1439.11	1422.91	1400.63	1375.51
75		1430.99	1414.91	1393.24	1368.1
80		1431.64	1415.26	1392.99	1367.81
85		1437.26	1421.29	1399.35	1374.79
90		1437.64	1420.87	1398.4	1373.56

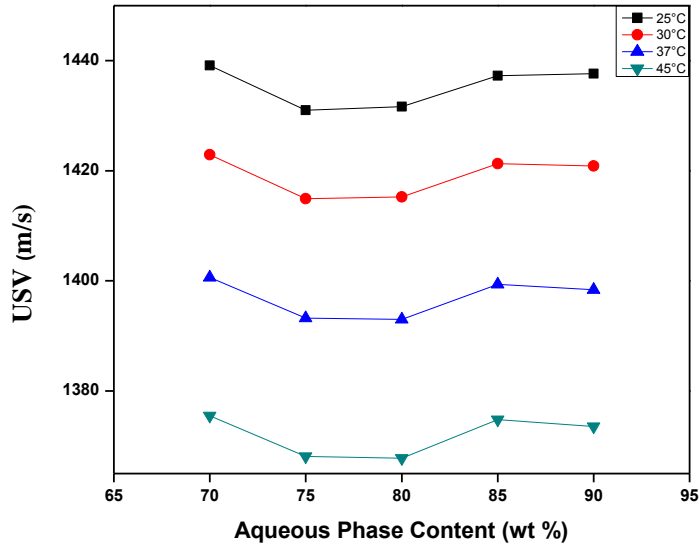


Fig 5:83 Variation of the ultrasonic velocity of the system # 1 W+PG/ Sucrose myristate (M1695) /LIM +Ethanol as function of aqueous content along the dilution line N65 at different temperatures. The phase diagrams are presented in figures (5:1),(5:6),(5:11) at different temperatures (25,37,and 45°C)respectively .

Ultrasonic velocity decreases with increase in temperature at constant aqueous content, in steady fashion.

Ultrasonic velocity of the system seems to decrease at constant temperature up to 70% forming w/o microemulsions ,passing through bicontinuous inversion between 70%and 85% after which o/w microemulsion is formed.

System # 2 MT25LE W+PG/ TMAZ80+Sucrose myristate (M1695) /LIM +Ethanol

The ultrasonic velocity was measured for the system W+PG/ TMAZ80+M1695/LIM +Ethanol where with aqueous solution made of (2/1) ratio , surfactants TMAZ80/ Sucrose myristate (M1695)in the ratio of (1/4) and equal unity of LIM oil with ethanol along the dilution line N65. Figures (5:84)and Table (5:41)displays the influence of aqueous content and temperature on the velocity (V). Some of the samples couldn't be measured because they were too viscous in the system data were as follows.

Table 5:41 The ultrasonic velocity (V) for the system #2 W+PG/ TMAZ80+Sucrose myristate (M1695) /LIM +Ethanol at different aqueous contents and different temperatures.

W+PG (2/1) wt%	USV (m/s)				
	T(°C) →	25	30	37	45
65		1390.85	1519.45	1496.23	1468.71
70		1536.58	1519.22	1496.68	1473.4
75		1533.59	1514.42	1490.05	1463.72
80		1544.69	1527.4	1505.3	1481.78
85		1549.2	1530.93	1506.37	1479.14
90		1542.56	1526.09	1503.86	1489.32

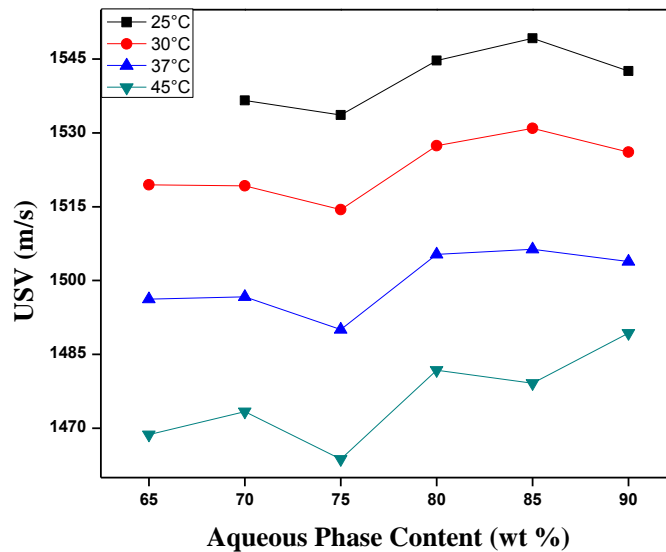


Fig 5:84 Variation of the ultrasonic velocity of the system # 2 W+PG/ TMAZ80+Sucrose myristate (M1695) /LIM +Ethanol as function of aqueous content along the dilution line N65 at different temperatures. The phase diagrams are presented in figures (5:2),(5:7),(5:12) at different temperatures (25,37,and 45°C)respectively.

Ultrasonic velocity decreases with increase in temperature at constant aqueous content, in steady fashion.

Ultrasonic velocity of the system seems to decrease at constant temperature up to 70% forming w/o microemulsions, passing through bicontinuous inversion between 70% and 80% after which o/w microemulsion is formed.

System # 3 MT50LE W+PG/ TMAZ80+Sucrose myristate (M1695) /LIM +Ethanol

The ultrasonic velocity was measured for the system W+PG/ TMAZ80+M1695/LIM+Ethanol where with aqueous solution made of (2/1) ratio, surfactants TMAZ80/ Sucrose myristate (M1695) in the ratio of (1/1) and equal unity of LIM oil with ethanol along the dilution line N65. Figures (5:85) and Table (5:42) displays the influence of aqueous content and temperature on the velocity (V). Some of the samples couldn't be measured because they were too viscous in the system data were as follows.

Table 5.42 The ultrasonic velocity (V) for the system #3 W+PG/ TMAZ80+Sucrose myristate (M1695) /LIM +Ethanol at different aqueous contents and different temperatures.

W+PG (2/1) wt%	USV (m/s)				
	T(°C) →	25	30	37	45
30		1524.58	1505.89	1481.84	1456.7
35		1525.16	1505.59	1480.09	1452.65
40		1530.52	1510.33	1484.27	1455.96
45		1538.32	1520.37	1495.2	1467.94
50		1530.68	1512.85	1489.26	1464.29
55		1535.58	1517.42	1493.03	1466.45
65		1538.21	1521.04	1498.49	1474.13
70		1545.61	1527.36	1502.83	1476.8
75		1541.94	1525	1502.21	1477.79
80		1548	1530.75	1507.88	1482.65
85		1552.69	1536.23	1513.68	1489.06
90		1550.28	1533.83	1511.39	1486.69

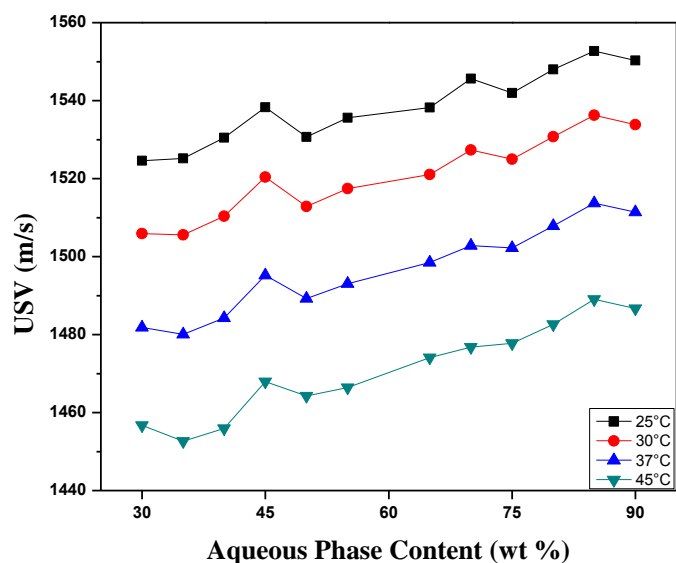


Fig 5:85 Variation of the ultrasonic velocity of the system # 3 W+PG/ TMAZ80+Sucrose myristate (M1695) /LIM +Ethanol as function of aqueous content along the dilution line N65 at different temperatures. The phase diagrams are presented in figures (5:3),(5:8),(5:13) at different temperatures (25,37,and 45°C)respectively.

Ultrasonic velocity decreases with increase in temperature at constant aqueous content, in steady fashion.

Ultrasonic velocity of the system increases at constant temperature from 15% up to 30% passing through bicontinuous inversion up to 65% where o/w microemulsion is formed.

System # 4 MT75LE W+PG/ TMAZ80+Sucrose myristate (M1695) /LIM +Ethanol

The ultrasonic velocity was measured for the system W+PG/ TMAZ80+M1695/LIM+Ethanol where with aqueous solution made of (2/1)ratio , surfactants TMAZ80/ Sucrose myristate (M1695)in the ratio of (3/4) and equal unity of LIM oil with ethanol along the dilution line N65. Figures (5:86) and Table (5:43) displays the influence of aqueous content and temperature on the velocity (V).

Table 5.43 The ultrasonic velocity (V) for the system #4 W+PG/ TMAZ80+Sucrose myristate (M1695) /LIM +Ethanol at different aqueous contents and different temperatures.

W+PG (2/1) wt%	USV (m/s)				
	T(°C) →	25	30	37	45
0		1514.79	1497.26	1473.76	1448.86
5		1508.48	1490.39	1466.66	1440.69
10		1515.31	1497.98	1474.51	1448.63
15		1512.09	1493.44	1469.58	1443.55
20		1510.14	1493.27	1469.9	1443.89
25		1517.86	1500.72	1477.45	1451.99
30		1518.5	1501.36	1478.24	1452.3
35		1522.93	1505.91	1482.57	1456.72
40		1529.6	1512.79	1489.34	1463.56
45		1531.14	1514.65	1491.07	1465.27
50		1530.78	1513.9	1490.87	1465.64
55		1535.52	1519.16	1495.84	1470.28
60		1539.33	1522.58	1499.68	1474.27
65		1544.58	1528.11	1505.73	1479.79
70		1550.37	1533.76	1510.92	1485.34
75		1546.27	1530.05	1506.79	1481.25
80		1556.35	1539.83	1517.07	1491.62
85		1555.14	1538.56	1515.83	1490.77
90		1558.1	1541.78	1519.17	1493.61

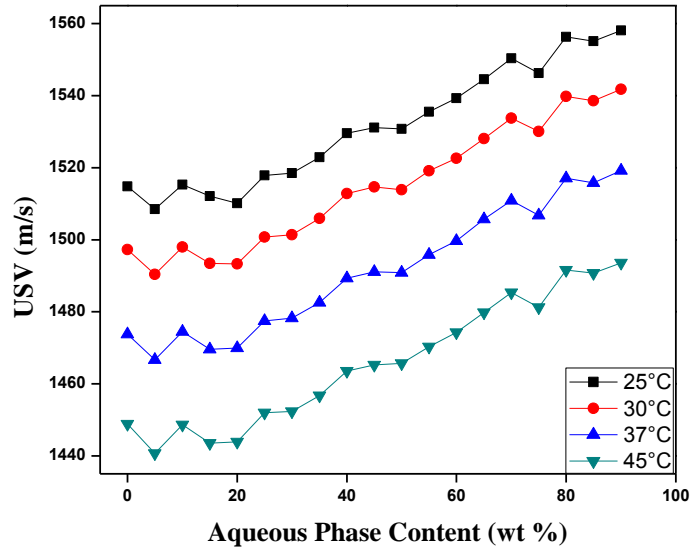


Fig 5:86 Variation of the ultrasonic velocity of the system # 4 W+PG/ TMAZ80+Sucrose myristate (M1695) /LIM +Ethanol as function of aqueous content along the dilution line N65 at different temperatures. The phase diagrams are presented in figures (5:4),(5:9),(5:14) at different temperatures (25,37,and 45°C)respectively.

Ultrasonic velocity decreases with increase in temperature at constant aqueous content, in steady fashion.

Ultrasonic velocity of the system seems to decrease at constant temperature up to 25% forming w/o microemulsions ,passing through bicontinuous inversion between 25 %and 70% after which o/w microemulsion is formed.

System # 5 MT100LE W+PG/ TMAZ80+Sucrose myristate (M1695) /LIM +Ethanol

The ultrasonic velocity was measured for the system W+PG/ TMAZ80+M1695/LIM+Ethanol where with aqueous solution made of (2/1)ratio , surfactants TMAZ80 in the ratio of (100%) and equal unity of LIM oil with ethanol along the dilution line N65. Figures (5:87)and Table (5:44) displays the influence of aqueous content and temperature on the velocity (V).

Table 5.44 The ultrasonic velocity (V) for the system #5 W+PG/ TMAZ80 /LIM +Ethanol at different aqueous contents and different temperatures.

W+PG (2/1) wt%	USV (m/s)				
	T(°C) →	25	30	37	45
0		1396.41	1380.5	1357.47	1331.25
5		1402.78	1385.86	1362.45	1336.11
10		1405.47	1389	1365.75	1339.39
15		1407.09	1390.17	1366.77	1340.41
20		1438.5	1422.31	1399.31	1373.3
25		1411.62	1394.75	1371.38	1345.06
30		1421.78	1405.66	1382.62	1356.45
35		1418.17	1401.31	1377.97	1351.91
40		1428.92	1412.3	1389.07	1362.83
45		1425.59	1408.73	1385.42	1359.36
50		1415.15	1398.58	1375.31	1348.92
55		1430.89	1414.06	1390.81	1364.95
60		1456.69	1440.29	1417.51	1391.7
65		1435.96	1419.19	1395.99	1370.04
70		1468.83	1452.83	1430.28	1404.71
75		1467.16	1450.85	1428.29	1402.95
80		1440.64	1424.34	1401.33	1375.26
85		1477.48	1461.32	1437.42	1412.58
90		1447.92	1431.32	1408.31	1382.54

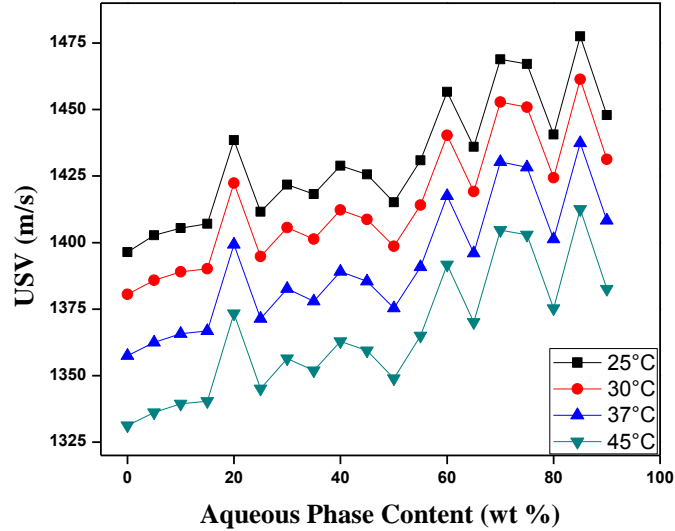


Fig 5:87 Variation of the ultrasonic velocity of the system # 5 W+PG/ TMAZ80+Sucrose myristate (M1695) /LIM +Ethanol as function of aqueous content along the dilution line N65 at different temperatures. The phase diagrams are presented in figures (5:5),(5:10),(5:15) at different temperatures (25,37,and 45°C)respectively.

Ultrasonic velocity decreases with increase in temperature at constant aqueous content, in steady fashion.

Ultrasonic velocity of the system seems to increases in relatively low increment at constant temperature up to 15% forming w/o microemulsions ,from 15% up to 25% passing through bicontinuous water rich medium inversion to water rich medium occur between 60 %and 75% beyond 80% aqueous content o/w microemulsion is formed.

5.3.2.2.2 Determining the ultrasonic velocity for the systems using IPM oil

System # 6 MTOIE W+PG/ Sucrose myristate (M1695) /IPM +Ethanol

The ultrasonic velocity was measured for the system W+PG/ M1695/IPM+Ethanol where with aqueous solution made of (2/1)ratio , surfactant Sucrose myristate (M1695) (100%) and equal unity of IPM oil with ethanol along the dilution line N65. Figures (5:88) and Table (5:45) displays the influence of aqueous content and temperature on the velocity (V). Some of the samples couldn't be measured because they were too viscous in the system data were as follows.

Table 5.45 The ultrasonic velocity (V) for the system #6 W+PG/ Sucrose myristate (M1695) /IPM +Ethanol at different aqueous contents and different temperatures

W+PG (2/1) wt%	USV (m/s)				
	T(°C) →	25	30	37	45
20		1404.14	1385.68	1361.07	1333.87
35		1424.89	1407.53	1383.85	1356.28
55		1424.02	1406.52	1384.19	1359.79
60		1418.6	1402.24	1349.82	1354.93
65		1423.27	1406.96	1384.63	1359.57
75		1428.87	1412.74	1390.67	1365.94
80		1430.11	1414.09	1392.52	1367.94
85		1444.49	1428.41	1406.3	1380.75
90		1438.68	1422.54	1400.74	1376.11

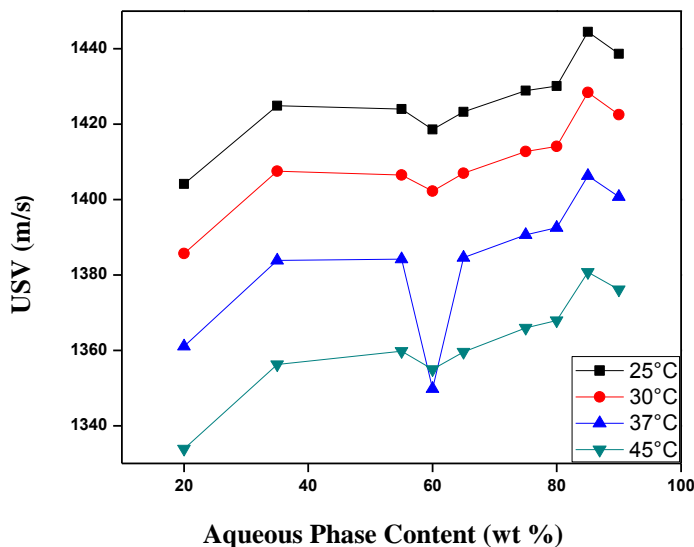


Fig 5:88 Variation of the ultrasonic velocity of the system # 6 W+PG/ Sucrose myristate (M1695) /IPM +Ethanol as function of aqueous content along the dilution line N65 at different temperatures. The phase diagrams are presented in figures (5:16),(5:21),(5:26) at different temperatures (25,37,and 45°C)respectively.

Ultrasonic velocity decreases with increase in temperature at constant aqueous content, in steady fashion.

Ultrasonic velocity of the system seems to increases at constant temperature up to 35% forming w/o microemulsions ,from 35% up to 55% passing through bicontinuous water rich medium from 55%up to 75% inversion to water rich medium occur beyond 80% aqueous content o/w microemulsion is formed.

System # 7 MT25IE W+PG/TMAZ80+ Sucrose myristate (M1695) /IPM +Ethanol

The ultrasonic velocity was measured for the system W+PG/TMAZ80+ M1695/IPM+Ethanol where with aqueous solution made of (2/1)ratio , surfactants TMAZ80/ Sucrose myristate (M1695) in the ratio (1/4) and equal unity of IPM oil with ethanol along the dilution line N65.

Figures (5:89) and Table (5:46) displays the influence of aqueous content and temperature on the velocity (V)

Table 5:46 The ultrasonic velocity (V) for the system #7 W+PG/ TMAZ80+Sucrose myristate (M1695) /IPM +Ethanol at different aqueous contents and different temperatures.

W+PG (2/1) wt%	USV (m/s)				
	T(°C) →	25	30	37	45
0		1400.88	1381.92	1357.38	1330.5
5		1455.32	1431.56	1401.78	1371.6
10		1403.99	1386.4	1362.54	1336.48
15		1403.05	1385.19	1361.49	1335.1
20		1407.34	1390.01	1366.55	1340.85
25		1412.82	1395.3	1371.51	1345.63
30		1406.08	1389.06	1365.77	1340.96
35		1418.18	1401.02	1377.98	1353.16
40		1410.76	1394.26	1372.65	1347.85
45		1424.12	1406.8	1383.45	1357.69
50		1422.15	1405.61	1382.82	1357.61
55		1434.46	1418.84	1396.55	1371.23
60		1430.35	1413.81	1391.44	1366.45
65		1430.95	1416.85	1394.64	1369.55
70		1440.61	1424.38	1401.93	1376.49
75		1440.65	1424.79	1403.1	1378.7
80		1443.24	1427.22	1405.16	1380.48
85		1453.61	1437.7	1415.75	1390.74
90		1400.88	1381.92	1357.38	1330.5

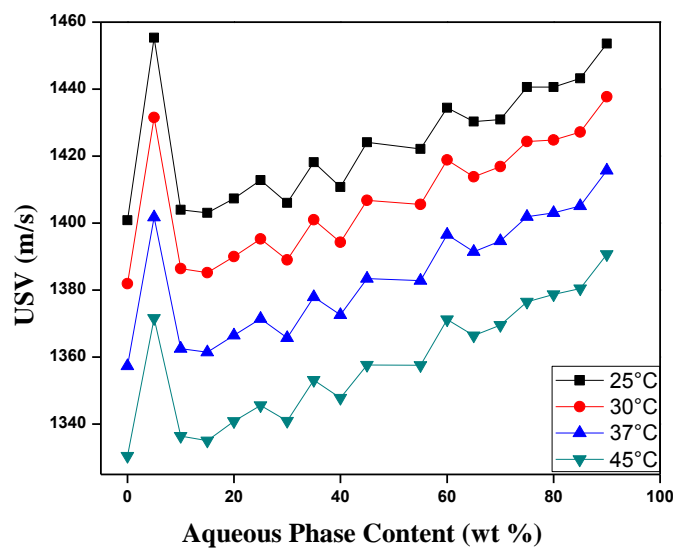


Fig 5:89 Variation of the ultrasonic velocity of the system # 7 W+PG/ TMAZ80+Sucrose myristate (M1695) /IPM +Ethanol as function of aqueous content along the dilution line N65 at different temperatures. The phase diagrams are presented in figures (5:17),(5:22),(5:27) at different temperatures (25,37,and 45°C)respectively.

Ultrasonic velocity decreases with increase in temperature at constant aqueous content, in steady fashion.

Ultrasonic velocity of the system seems to increases at constant temperature up to 5% forming w/o microemulsions ,from 10% up to 60% passing through bicontinuous oil rich medium inverted to water rich medium , beyond 60% aqueous content o/w microemulsion is formed.

System # 8 MT50IE W+PG/TMAZ80+ Sucrose myristate (M1695) /IPM +Ethanol

The ultrasonic velocity was measured for the system W+PG/TMAZ80+ M1695/IPM+Ethanol where with aqueous solution made of (2/1)ratio , surfactants TMAZ80/ Sucrose myristate (M1695) in the ratio (1/1) and equal unity of IPM oil with ethanol along the dilution line N65.

Figures (5:90) and Table (5:47) displays the influence of aqueous content and temperature on the velocity (V).

Table 5.47 The ultrasonic velocity (V) for the system #8 W+PG/ TMAZ80+Sucrose myristate (M1695) /IPM +Ethanol at different aqueous contents and different temperatures.

W+PG (2/1) wt%	USV (m/s)				
	T(°C) →	25	30	37	45
0		1407.73	1390.69	1367.29	1341.41
5		1401.37	1385.45	1362.57	1336.84
10		1408.74	1391.62	1368.29	1342.2
15		1425.29	1408.05	1384.56	1358.69
20		1414.74	1397.77	1374.61	1348.63
25		1431.41	1414.64	1391.1	1365.16
30		1425.3	1408.42	1385.25	1359.71
35		1416.8	1400.23	1377.44	1351.95
40		1417.05	1402.27	1380.66	1354.94
45		1418.35	1401.96	1379.03	1353.62
50		1449.07	1431.45	1407.55	1381.97
55		1427.33	1410.86	1388.87	1364.01
60		1432.01	1415.66	1393.04	1368.02
65		1428.51	1412.55	1390.62	1365.58
70		1443.73	1427.26	1404.89	1379.7
75		1440.72	1424.57	1402.19	1377.21
80		1441.74	1425.73	1403.49	1378.29
85		1444.83	1428.8	1406.52	1381.72
90		1450.73	1434.73	1413.01	1388.39

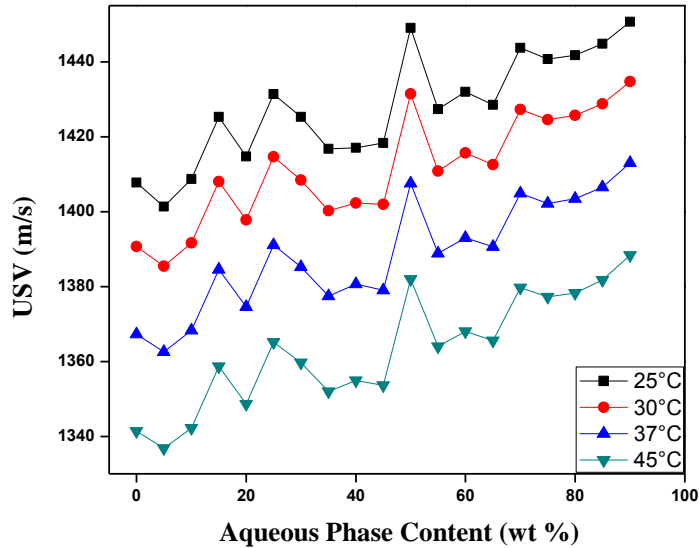


Fig 5:90 Variation of the ultrasonic velocity of the system # 8 W+PG/ TMAZ80+Sucrose myristate (M1695) /IPM +Ethanol as function of aqueous content along the dilution line N65 at different temperatures. The phase diagrams are presented in figures (5:18),(5:23),(5:28) at different temperatures (25,37,and 45°C)respectively.

Ultrasonic velocity decreases with increase in temperature at constant aqueous content, in steady fashion.

Ultrasonic velocity of the system seems to increases at constant temperature up to 15% forming w/o microemulsions ,from 20% up to 65% passing through bicontinuous oil rich medium inverted to water rich medium , beyond 70% aqueous content o/w microemulsion is formed.

System # 9 MT75IE W+PG/TMAZ80+ Sucrose myristate (M1695) /IPM +Ethanol

The ultrasonic velocity was measured for the system W+PG/TMAZ80+ M1695/IPM+Ethanol where with aqueous solution made of (2/1)ratio , surfactants TMAZ80/ Sucrose myristate (M1695) in the ratio (3/4) and equal unity of IPM oil with ethanol along the dilution line N65.

Figures (5:91) and Table (5:48) displays the influence of aqueous content and temperature on the velocity (V).

Table 5.48 The ultrasonic velocity (V) for the system #9 W+PG/ TMAZ80+Sucrose myristate (M1695) /IPM +Ethanol at different aqueous contents and different temperatures.

W+PG (2/1) wt%	USV (m/s)				
	T(°C) →	25	30	37	45
0		1408.88	1392.05	1369.08	1343.18
5		1419.58	1402.81	1379.7	1354.13
10		1408.8	1392.92	1370.39	1344.58
15		1429.27	1412.48	1389.35	1363.71
20		1422.25	1405.59	1382.61	1356.8
25		1413.83	1399.04	1376.32	1350.49
30		1414.48	1397.93	1374.99	1349.49
35		1414.04	1403.09	1380.67	1355.03
40		1426.65	1410.11	1387.21	1361.82
45		1426.36	1410.48	1388.12	1362.49
50		1428.03	1411.58	1388.82	1363.51
55		1430.33	1415.19	1393.17	1364.56
60		1435.52	1419.15	1396.49	1371.22
65		1432.59	1416.74	1394.34	1368.79
70		1446.64	1430.32	1407.65	1382.33
75		1443.79	1428.21	1406.79	1381.81
80		1449.84	1433.63	1411.27	1385.93
85		1449.73	1433.66	1411.27	1386.27
90		1451.66	1436.16	1414.71	1389.73

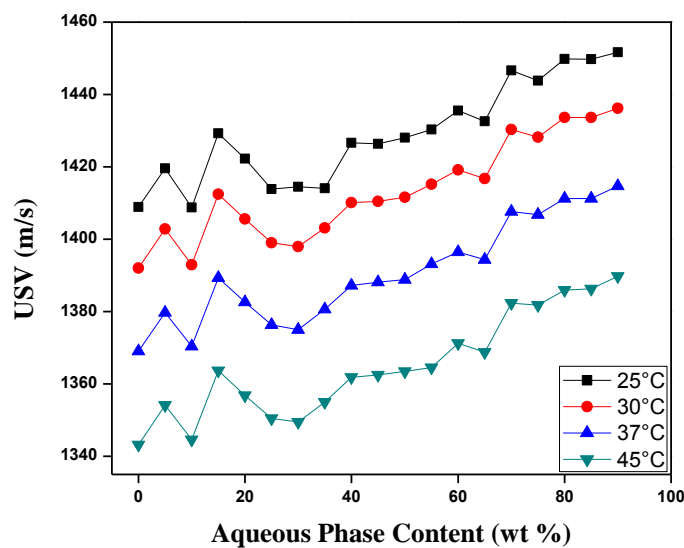


Fig 5:91 Variation of the ultrasonic velocity of the system # 9 W+PG/ TMAZ80+Sucrose myristate (M1695) /IPM +Ethanol as function of aqueous content along the dilution line N65 at different temperatures. The phase diagrams are presented in figures (5:19),(5:24),(5:29) at different temperatures (25,37,and 45°C)respectively.

Ultrasonic velocity decreases with increase in temperature at constant aqueous content, in steady fashion.

Ultrasonic velocity of the system seems to fluctuate at constant temperature up to 25% forming w/o microemulsions ,from 25% up to 70% passing through bicontinuous oil rich medium inverted to water rich medium , beyond 70% aqueous content o/w microemulsion is formed

System # 10 MT100IE W+PG/TMAZ80/IPM +Ethanol

The ultrasonic velocity was measured for the system W+PG/TMAZ80 /IPM+Ethanol where with aqueous solution made of (2/1)ratio , surfactant TMAZ80 (100%) and equal unity of IPM oil with ethanol along the dilution line N65. Figures (5:92) and Table (5:49) displays the influence of aqueous content and temperature on the velocity (V).

Table 5.49 The ultrasonic velocity (V) for the system #10 W+PG/ TMAZ80 /IPM +Ethanol at different aqueous contents and different temperatures.

W+PG (2/1) wt%	USV (m/s)				
	T(°C) →	25	30	37	45
0		1441.95	1425.33	1402.47	1377.08
5		1445.03	1428.88	1405.84	1380.19
10		1405	1388.42	1365.48	1339.62
15		1447.29	1431.07	1408.33	1383.56
20		1423.48	1406.87	1383.84	1358.25
25		1416.14	1400.49	1377.73	1351.79
30		1446.66	1430.14	1407.28	1381.96
35		1421.97	1405.37	1382.42	1356.44
40		1424.16	1407.61	1384.64	1358.9
45		1429.29	1412.81	1389.9	1364.03
50		1433.24	1416.69	1394.27	1368.19
55		1432.58	1416.14	1393.35	1367.51
60		1435.14	1418.68	1395.77	1370.13
65		1438.87	1422.41	1399.6	1373.8
70		1444.8	1428.22	1405.34	1379.97
75		1446.61	1430.31	1407.74	1382.26
80		1449.98	1433.54	1411.05	1386.75
85		1452.82	1436.85	1414.48	1389.03
90		1448.1	1431.55	1408.75	1383.58

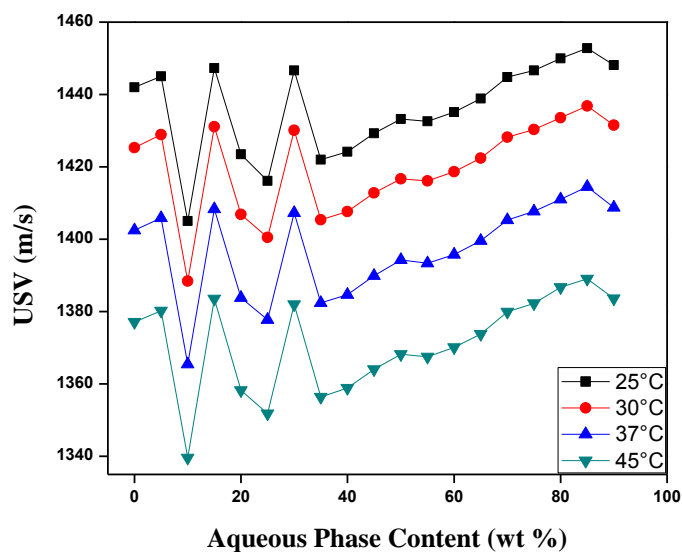


Fig 5:92 Variation of the ultrasonic velocity of the system # 10 W+PG/ TMAZ80/IPM +Ethanol as function of aqueous content along the dilution line N65 at different temperatures. The phase diagrams are presented in figures (5:20),(5:25),(5:30) at different temperatures (25,37,and 45°C)respectively.

Ultrasonic velocity decreases with increase in temperature at constant aqueous content, in steady fashion.

Ultrasonic velocity of the system decreases at constant temperature up to 10% forming w/o microemulsions ,from 15% up to 35% passing through bicontinuous oil rich medium inverted to water rich medium , beyond 40% aqueous content o/w microemulsion is formed

5.3.2.2.2 Determining the ultrasonic velocity for the systems using CCT oil

System # 11 MT0CE W+PG/ Sucrose myristate (M1695) /CCT +Ethanol

The ultrasonic velocity was measured for the system W+PG/ M1695/CCT+Ethanol where with aqueous solution made of (2/1)ratio , surfactant Sucrose myristate (M1695) (100%) and equal unity of CCT oil with ethanol along the dilution line N65. Figure (5:93) and Table (5:50) displays the influence of aqueous content and temperature on the velocity (V). Some of the samples couldn't be measured because they were too viscous in the system data were as follows.

Table 5:50 The ultrasonic velocity (V) for the system #11 W+PG/ Sucrose myristate (M1695) /CCT +Ethanol at different aqueous contents and different temperatures.

W+PG (2/1) wt%	USV (m/s)				
	T(°C) →	25	30	37	45
0		1403.23	1384.45	1359.43	1332.26
5		1403.14	1384.97	1360.74	1334.56
20		1410.18	1393.09	1369.96	1344.29
30		1414.45	1397.94	1375.56	1351.25
35		1419.78	1403.16	1383.13	1355
45		1424.8	1408.17	1386.24	1361.68
55		1426.02	1410	1388.05	1363.88
60		1429.94	1413.18	1391.16	1366.56
65		1436.51	1420.98	1399.75	1376.65
70		1437.32	1422.07	1400.42	1376
75		1441.61	1426.04	1404.75	1381.33
80		1446.31	1430.8	1409.35	1385.5
85		1451.1	1435.8	1414.48	1390.34
90		1459.66	1444.31	1423.1	1399.09

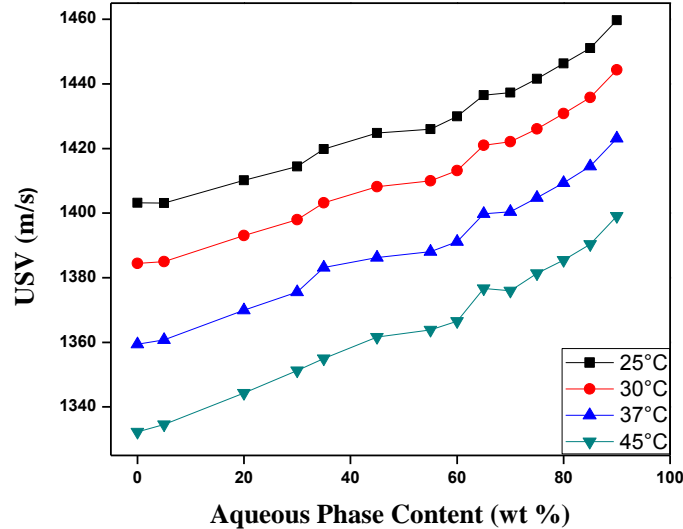


Fig 5:93 Variation of the ultrasonic velocity of the system # 11 W+PG/ Sucrose myristate (M1695) /CCT +Ethanol as function of aqueous content along the dilution line N65 at different temperatures. The phase diagrams are presented in figures (5:31),(5:36),(5:41) at different temperatures (25,37,and 45°C)respectively.

Ultrasonic velocity decreases with increase in temperature at constant aqueous content, in steady fashion.

Ultrasonic velocity of the system increase at constant temperature up to 30% forming w/o microemulsions ,from 35% up to 65% passing through bicontinuous oil rich medium inverted to water rich medium , beyond 70% aqueous content o/w microemulsion is formed

System # 12 MT25CE W+PG/ TMAZ80+Sucrose myristate (M1695) /CCT +Ethanol

The ultrasonic velocity was measured for the system W+PG/ TMAZ80+M1695/CCT+Ethanol where with aqueous solution made of (2/1)ratio , surfactants TMAZ80/ Sucrose myristate (M1695)in the ratio of (1/4) and equal unity of CCT oil with ethanol along the dilution line N65. Figures (5:94) and Table (5:51) displays the influence of aqueous content and temperature on the velocity (V).

Table 5.51 The ultrasonic velocity (V) for the system #12 W+PG/ TMAZ80+Sucrose myristate (M1695) /CCT +Ethanol at different aqueous contents and different temperatures.

W+PG (2/1) wt%	USV (m/s)				
	T(°C) →	25	30	37	45
0		1429.74	1411.7	1387.41	1360.85
5		1413.65	1396.51	1373.1	1347.32
10		1413.27	1396.15	1373.05	1347.27
15		1416.34	1399.13	1376.24	1350.66
20		1419.14	1402.2	1379.34	1353.79
30		1426.14	1409.71	1387.1	1361.98
35		1347.2	1475.45	1450.23	1423.04
40		1433.98	1417.14	1394.74	1369.58
45		1489.28	1468.82	1443.24	1416.31
50		1440.76	1424.67	1402.51	1378.46
55		1444.88	1428.34	1406.27	1381.34
60		1448.71	1433.08	1411.17	1386.56
65		1451.75	1435.84	1413.91	1389.75
70		1457.81	1441.68	1419.79	1395.09
75		1467.66	1448.53	1426.14	1401.45
80		1469.77	1454.58	1433.07	1408.54
85		1493.78	1473.35	1447.24	1420.18
90		1496.67	1475.98	1450.02	1422.7

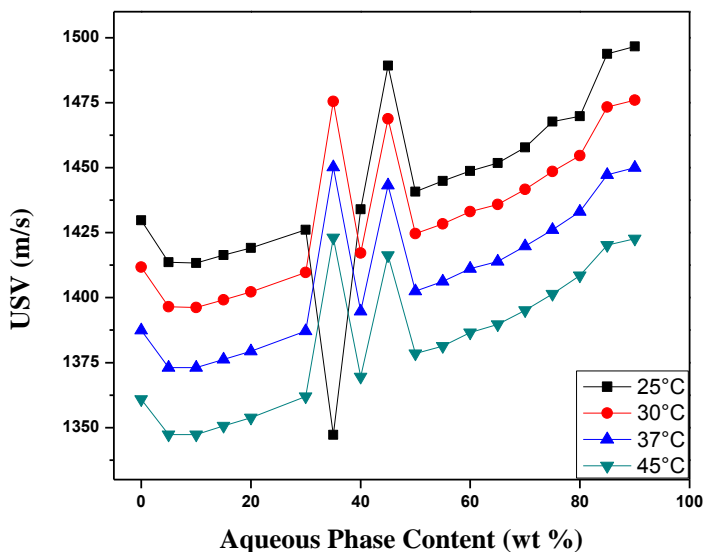


Fig 5:94 Variation of the ultrasonic velocity of the system # 12 W+PG/TMAZ80+ Sucrose myristate (M1695) /CCT +Ethanol as function of aqueous content along the dilution line N65 at different temperatures. The phase diagrams are presented in figures (5:32),(5:37),(5:42) at different temperatures (25,37,and 45°C)respectively.

Ultrasonic velocity decreases with increase in temperature at constant aqueous content, in steady fashion.

Ultrasonic velocity of the system increase at constant temperature in relatively low increment up to 35 % forming w/o microemulsions ,from 35% up to 50% passing through bicontinuous oil rich medium inverted to water rich medium , beyond 50% aqueous content o/w microemulsion is formed

System # 13 MT50CE W+PG/ TMAZ80+Sucrose myristate (M1695) /CCT +Ethanol

The ultrasonic velocity was measured for the system W+PG/ TMAZ80+M1695/CCT+Ethanol where with aqueous solution made of (2/1)ratio , surfactants TMAZ80/ Sucrose myristate (M1695)in the ratio of (1/1) and equal unity of CCT oil with ethanol along the dilution line N65.

Figures (5:95) and Table (5:52) displays the influence of aqueous content and temperature on the velocity (V).

Table 5:52 The ultrasonic velocity (V) for the system #13 W+PG/ TMAZ80+Sucrose myristate (M1695) /CCT +Ethanol at different aqueous contents and different temperatures.

W+PG (2/1) wt%	USV (m/s)				
	T(°C) →	25	30	37	45
0		1427.6	1414.33	1392.47	1367.63
5		1423.17	1406.68	1383.95	1358.79
10		1421.53	1405.92	1383.85	1359.24
15		1425.97	1409.75	1387.31	1362.01
20		1489.51	1471.71	1446.61	1419.7
25		1432.52	1416.17	1393.59	1368.48
30		1449.98	1433.71	1411.52	1386.43
35		1490.78	1472.19	1447.92	1421.58
40		1443.65	1427.43	1404.89	1379.82
45		1451.26	1434.99	1412.61	1387.33
50		1496	1478.19	1454.38	1428.59
55		1456.16	1439.87	1417.64	1392.54
60		1458.68	1442.24	1420.09	1395.02
65		1466.76	1449.99	1427.22	1401.95
70		1468.47	1452.37	1430.33	1405.28
75		1472.09	1456.1	1433.93	1409.12
80		1499.68	1482.66	1459.83	1434.52
85		1481	1465.02	1443.07	1418.14
90		1484.33	1468.51	1446.53	1422.02

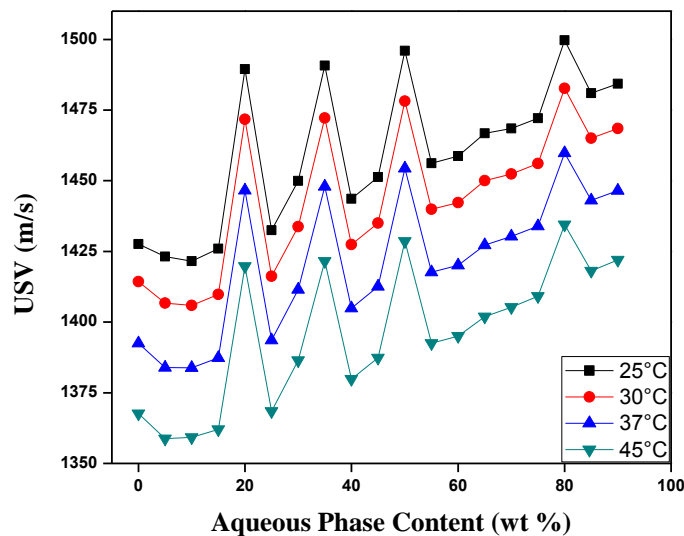


Fig 5:95 Variation of the ultrasonic velocity of the system # 13 W+PG/TMAZ80+ Sucrose myristate (M1695) /CCT +Ethanol as function of aqueous content along the dilution line N65 at different temperatures. The phase diagrams are presented in figures (5:33),(5:38),(5:43) at different temperatures (25,37,and 45°C)respectively.

Ultrasonic velocity decreases with increase in temperature at constant aqueous content, in steady fashion.

Ultrasonic velocity of the system decrease at constant temperature in relatively low decrement up to 15 % forming w/o microemulsions ,from 20% up to 55% passing through bicontinuous oil rich medium inverted to water rich medium , beyond 55% aqueous content o/w microemulsion is formed

System # 14 MT75CE W+PG/ TMAZ80+Sucrose myristate (M1695) /CCT +Ethanol

The ultrasonic velocity was measured for the system W+PG/ TMAZ80+M1695/CCT+Ethanol where with aqueous solution made of (2/1)ratio , surfactants TMAZ80/ Sucrose myristate (M1695)in the ratio of (3/4) and equal unity of CCT oil with ethanol along the dilution line N65. Figures (5:96) and Table (5:53) displays the influence of aqueous content and temperature on the velocity (V).

Table 5:53 The ultrasonic velocity (V) for the system #14 W+PG/ TMAZ80+Sucrose myristate (M1695) /CCT +Ethanol at different aqueous contents and different temperatures.

W+PG (2/1) wt%	USV (m/s)				
	T(°C) →	25	30	37	45
0		1489.42	1472.26	1449.01	1424
5		1426.38	1410.09	1387.83	1362.55
10		1449.93	1433.53	1410.79	1385.62
15		1435.58	1419.3	1396.92	1371.64
20		1454.78	1438.41	1415.77	1390.69
25		1442.97	1426.71	1404.18	1378.74
30		1447.77	1431.49	1408.89	1383.77
35		1451.68	1435.68	1413.56	1388.35
40		1494.96	1478.31	1455.52	1430.45
45		1469.74	1453.01	1430.46	1405.04
50		1465.65	1449.06	1426.73	1401.39
55		1469.22	1453.02	1430.47	1405.21
60		1471.52	1456.56	1434.52	1409.27
65		1479.44	1463.19	1440.6	1415.44
70		1498.32	1481.92	1459.46	1434.24
75		1485.48	1469.36	1446.96	1421.93
80		1511.38	1494.74	1472.09	1446.71
85		1491.87	1476.02	1453.56	1428.54
90		1498.36	1483.08	1461.59	1436.54

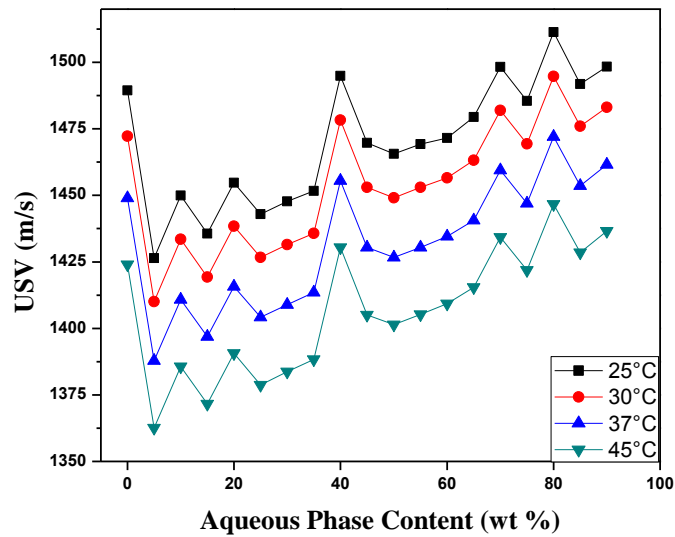


Fig 5:96 Variation of the ultrasonic velocity of the system # 14 W+PG/TMAZ80+ Sucrose myristate (M1695) /CCT +Ethanol as function of aqueous content along the dilution line N65 at different temperatures. The phase diagrams are presented in figures (5:34),(5:39),(5:44) at different temperatures (25,37,and 45°C)respectively.

Ultrasonic velocity decreases with increase in temperature at constant aqueous content, in steady fashion.

Ultrasonic velocity of the system decrease at constant temperature up to 5 % forming w/o microemulsions ,from 10% up to 75% passing through bicontinuous oil rich medium inverted to water rich medium , beyond75% aqueous content o/w microemulsion is formed

System # 15 MT100CE W+PG/ TMAZ80/CCT +Ethanol

The ultrasonic velocity was measured for the system W+PG/ TMAZ80 /CCT+Ethanol where with aqueous solution made of (2/1)ratio , surfactants TMAZ80 in the ratio of (100%) and equal unity of CCT oil with ethanol along the dilution line N65. Figures (5:97) and Table (5:54) displays the influence of aqueous content and temperature on the velocity (V).

Table (5:54) The ultrasonic velocity (V) for the system #15 W+PG/ TMAZ80/CCT +Ethanol at different aqueous contents and different temperatures.

W+PG (2/1) wt%	USV (m/s)				
	T(°C) →	25	30	37	45
0		1426.37	1410.07	1387.42	1362.02
5		1489.71	1473.11	1450.24	1424.57
10		1441.02	1426.49	1404.36	1378.85
15		1489.48	1472.79	1450.09	1424.61
20		1471.33	1454.86	1431.95	1406.21
25		1448.76	1432.36	1409.73	1384.09
30		1490.28	1473.74	1450.96	1425.73
35		1461.38	1444.94	1422.51	1396.86
40		1465.74	1449.11	1426.34	1400.62
45		1468.66	1452.37	1429.97	1404.44
50		1474.85	1461.13	1439.46	1414.25
55		1508.63	1492.15	1469.34	1443.9
60		1500.99	1484.52	1461.84	1436.2
65		1482.25	1465.28	1442.89	1417.3
70		1485.86	1469.41	1446.77	1421.11
75		1489.37	1473.12	1450.53	1425.38
80		1495.13	1479.71	1458.36	1433.44
85		1498.32	1482.19	1459.73	1434.54
90		1504.15	1488.51	1466.26	1441.01

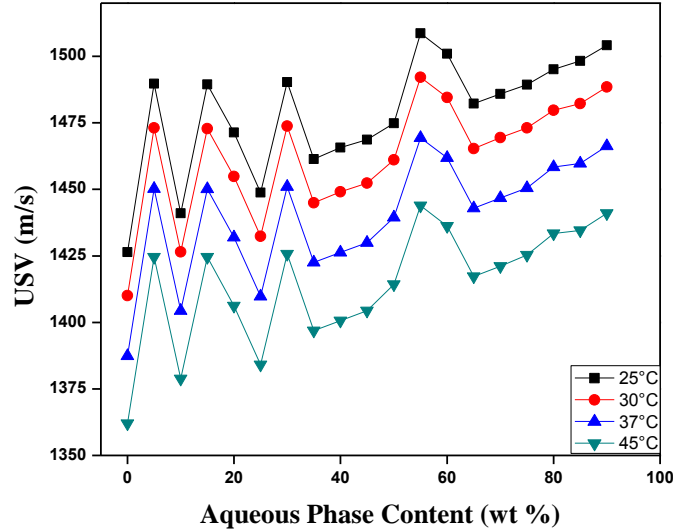


Fig 5:97 Variation of the ultrasonic velocity of the system # 15 W+PG/TMAZ80/CCT +Ethanol as function of aqueous content along the dilution line N65 at different temperatures. The phase diagrams are presented in figures (5:35),(5:40),(5:45) at different temperatures (25,37,and 45°C)respectively.

Ultrasonic velocity decreases with increase in temperature at constant aqueous content, in steady fashion.

Ultrasonic velocity of the system fluctuate at constant temperature up to 35 % forming w/o microemulsions ,from 40% up to 65% passing through bicontinuous oil rich medium inverted to water rich medium , beyond 65% aqueous content o/w microemulsion is formed.

Microemulsion densities usually decreases with the increases in the aqueous volume content at constant temperatures ,while ultrasonic velocities increase .

Most of the systems studied with the three different oils increases in ultrasonic velocity up to about 15% aqueous content forming the water in oil microemulsion, passes through the bicontinuous stage between 20-65% aqueous content ending in the form of oil in water microemulsions after 70% aqueous content.

5.4 Antimicrobial activity

Microbial activity was measured for the fifteen different systems in table 4:1 emulsion formed from mixed and single surfactants TMAZ80 + Sucrose myristate (M1695) in different ratios (0,25,50,75,100), and the three different oils mixed with ethanol (99,9%) in (1/1) ratio, titrated with an aqueous solution made of water and propylene glycol in (2/1) ratio. Titration with the aqueous solution was made with 5% increment as mentioned in sample preparation in 4.2.4.1.

These samples were tested against two different bacteria as Gram positive *Staphylococcus aureus* and Gram negative *Escherichia coli*.

All materials used in this study as in table 4:1 were tested against each of the two strains *Staphylococcus aureus* and *Escherichia coli* individually and tested for inhibition, results were as shown in table (5:55). Data in table was an average diameter for the triplicate repeated tests.

Table 5:55 Effect of each component of the formed systems against *Staphylococcus aureus* and *Escherichia coli*.

Material	Diameter of inhibition zone(mm)	
	<i>Staphylococcus aureus</i>	<i>Escherichia coli</i>
LIM	38	32
IPM	0	0
CCT	0	0
TMAZ80	0	0
M1695	14	10
Ethanol 99,9%	0	0
PG	0	0



Fig 5:98 Diameter of inhibition zone (mm) for individual contents on *Staphylococcus aureus*

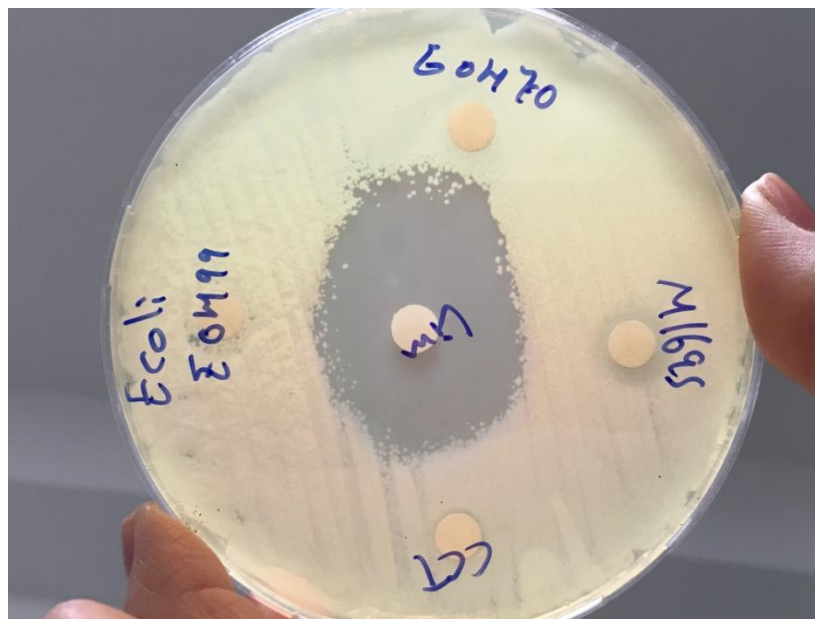


Fig 5:99 Diameter of inhibition zone (mm) for individual contents on *Escherichia coli*.

5.4.1 Gram positive bacteria *Staphylococcus aureus*

5.4.1.1 Investigating the effect of LIM oil systems on the Gram positive bacteria

System # 1 MT0LE W+PG/ Sucrose myristate (M1695) /LIM +Ethanol

Effect of the system is tested as inhibition of the bacterial growth zone, measured in (mm) ,work was done in triplicate and average of the collected data was considered as shown in table (5:56)

Table 5:56 Inhibition of the microbial activity of the *Staphylococcus aureus* caused by system #1 W+PG/ Sucrose myristate (M1695) /LIM +Ethanol

# of samples	W+PG (2/1) wt% Aqueous additions	Diameter of inhibition zone (mm)
1	0	13
2	5	13
3	10	13
4	15	12.5
5	20	13
6	25	13
7	30	13
8	35	14
9	40	15
10	45	13.5
11	50	14.5
12	55	13
13	60	11.5
14	65	13
15	70	13.5
16	75	12.5
17	80	13.5
18	85	11.5
19	90	12.5

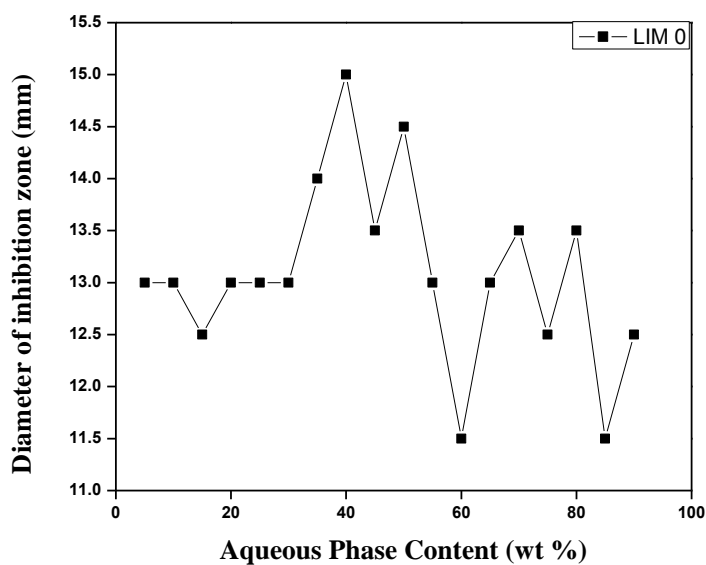


Fig 5:100 Inhibition of the microbial growth of the *Staphylococcus aureus* caused by system #1 W+PG/ Sucrose myristate (M1695) /LIM +Ethanol as function of aqueous content along the dilution line N65. The phase diagrams are presented in figures (5:1),(5:6),(5:11) at different temperatures (25,37,and 45°C)respectively .

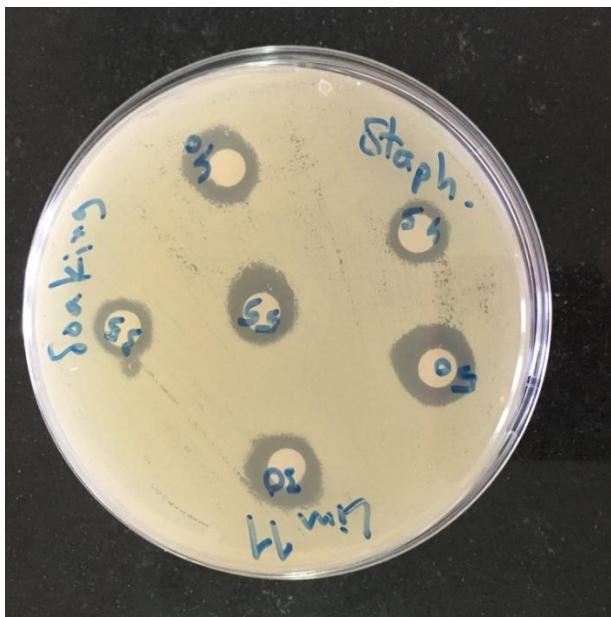


Fig 5:101 Diameter of inhibition zone (mm) for system #1 W+PG/Sucrose myristate M(1695)/LIM+EOH on *Staphylococcus aureus*

System # 2 MT25LE W+PG/ TMAZ80+Sucrose myristate (M1695) /LIM +Ethanol

Effect of the system is tested as inhibition of the bacterial growth zone, measured in (mm) ,work was done in triplicate and average of the collected data was considered as shown in table (5:57)

Table 5:57 Inhibition of the microbial activity of the *Staphylococcus aureus* caused by system #2 W+PG/ TMAZ80+Sucrose myristate (M1695) /LIM +Ethanol

# of samples	W+PG (2/1) wt% Aqueous additions	Diameter of inhibition zone (mm)
1	0	17
2	5	16
3	10	14.5
4	15	16.5
5	20	13
6	25	16
7	30	15
8	35	14.5
9	40	13.5
10	45	14.5
11	50	12
12	55	12.5
13	60	17
14	65	18.5
15	70	13.5
16	75	23
17	80	17
18	85	16.5
19	90	21.5

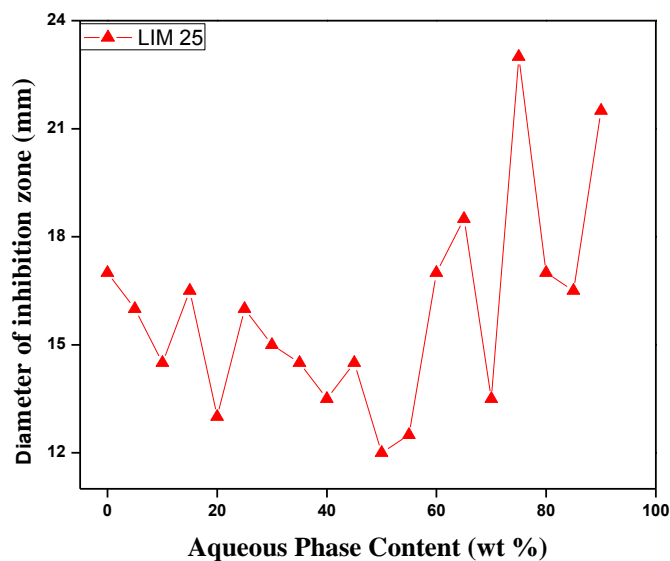


Fig 5:102 Inhibition of the microbial growth of the *Staphylococcus aureus* caused by system #2 W+PG/ TMAZ80+Sucrose myristate (M1695) /LIM +Ethanol as function of aqueous content along the dilution line N65. The phase diagrams are presented in figures (5:2),(5:7),(5:12) at different temperatures (25,37,and 45°C)respectively .



Fig 5:103 Diameter of inhibition zone (mm) for system #2 W+PG/TMAZ+ Sucrose myristate M(1695)/LIM+EOH on *Staphylococcus aureus*

System # 3 MT50LE W+PG/ TMAZ80+Sucrose myristate (M1695) /LIM +Ethanol

Effect of the system is tested as inhibition of the bacterial growth zone, measured in (mm) ,work was done in triplicate and average of the collected data was considered as shown in table (5:580

Table 5:58 Inhibition of the microbial activity of the *Staphylococcus aureus* caused by system #3 W+PG/ TMAZ80+Sucrose myristate (M1695) /LIM +Ethanol

# of samples	W+PG (2/1) wt% Aqueous additions	Diameter of inhibition zone (mm)
1	0	16.5
2	5	16
3	10	15.5
4	15	13.5
5	20	14.5
6	25	13
7	30	11.5
8	35	12
9	40	12.5
10	45	11.5
11	50	12.5
12	55	12
13	60	11.5
14	65	13
15	70	13.5
16	75	10.5
17	80	10
18	85	11
19	90	12

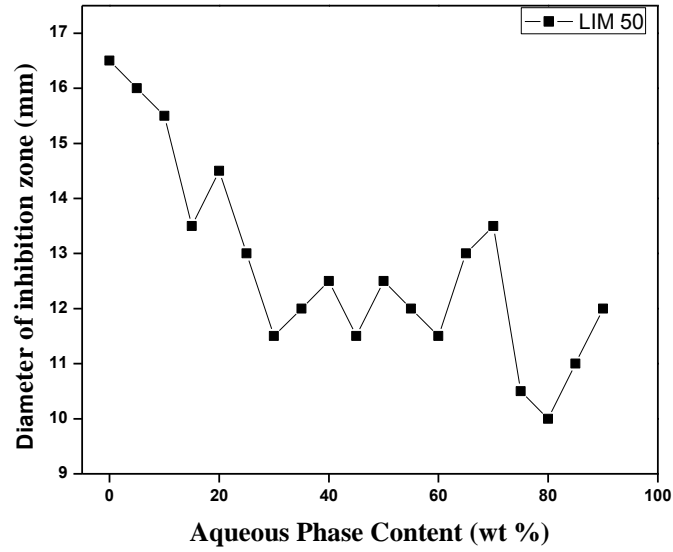


Fig 5:104 Inhibition of the microbial growth of the *Staphylococcus aureus* caused by system #3 W+PG/ TMAZ80+Sucrose myristate (M1695) /LIM +Ethanol as function of aqueous content along the dilution line N65. The phase diagrams are presented in figures (5:3),(5:8),(5:13) at different temperatures (25,37,and 45°C)respectively .

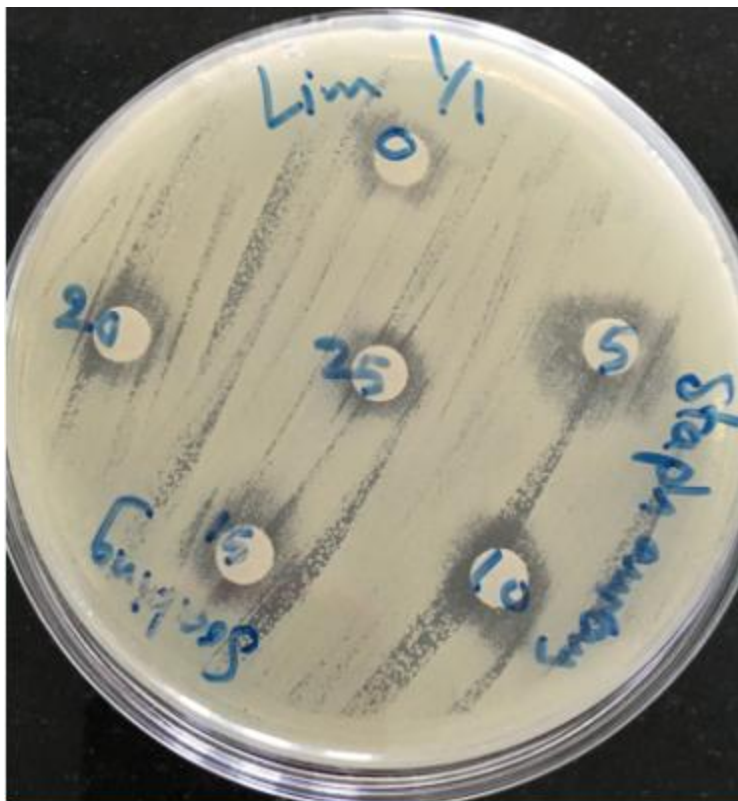


Fig 5:105 Diameter of inhibition zone (mm) for system #3 W+PG/TMAZ+Sucrose myristate M(1695)/LIM+EOH on *Staphylococcus aureus*

System #4 MT75LE and **system #5MT100LE** had No inhibition effect on *Staphylococcus aureus* because of the increase percent of the TMAZ80

Table (5:59) Shows the effect of *Staphylococcus aureus* growth inhibition measured as diameter of the clear zone caused as a function of surfactant using LIM oil.

Table 5:59 Diameter of inhibition zone (mm) as a function of surfactant concentration in LIM oil

# of samples	W+PG (2/1) wt% Aqueous additions	Diameter of inhibition zone (mm)		
		MT0LE	MT25LE	MT50LE
1	0	13	17	16.5
2	5	13	16	16
3	10	13	14.5	15.5
4	15	12.5	16.5	13.5
5	20	13	13	14.5
6	25	13	16	13
7	30	13	15	11.5
8	35	14	14.5	12
9	40	15	13.5	12.5
10	45	13.5	14.5	11.5
11	50	14.5	12	12.5
12	55	13	12.5	12
13	60	11.5	17	11.5
14	65	13	18.5	13
15	70	13.5	13.5	13.5
16	75	12.5	23	10.5
17	80	13.5	17	10
18	85	11.5	16.5	11
19	90	12.5	21.5	12

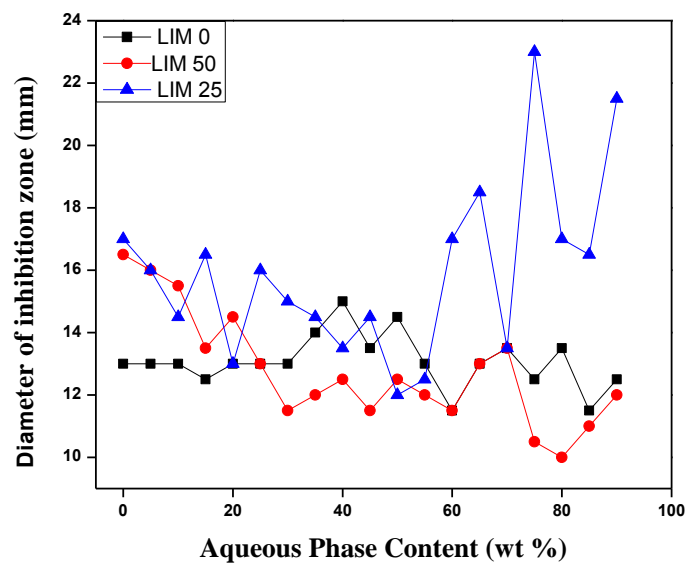


Fig 5: 106 Comparison of the microbial inhibition of the *Staphylococcus aureus* growth as a function of surfactant concentration using LIM oil .W+PG/ TMAZ80+Sucrose myristate (M1695) /LIM +Ethanol

5.4.1.2 Investigating the effect of IPM oil systems on the Gram positive bacteria:

System #6 MTOIE W+PG/ Sucrose myristate (M1695) /IPM+Ethanol

Effect of the system is tested as inhibition of the bacterial growth zone, measured in (mm) ,work was done in triplicate and average of the collected data was considered as shown in table (5:60)

Table 5:60 Inhibition of the microbial activity of the *Staphylococcus aureus* caused by system #6 W+PG/ Sucrose myristate (M1695) /IPM +Ethanol

# of samples	W+PG (2/1) wt% Aqueous additions	Diameter of inhibition zone (mm)
1	0	12
2	5	14.5
3	10	13
4	15	14
5	20	16
6	25	10.5
7	30	12.5
8	35	14
9	40	12
10	45	13
11	50	12.5
12	55	12
13	60	12
14	65	12.5
15	70	12
16	75	12.5
17	80	13
18	85	13.5
19	90	12

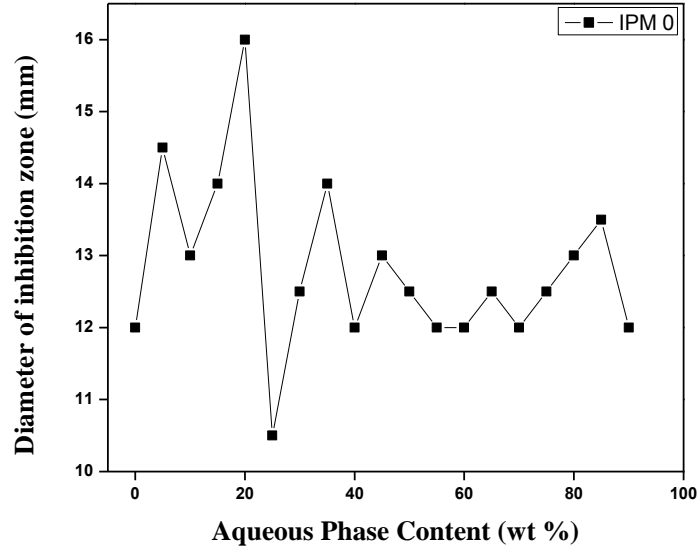


Fig 5:107 Inhibition of the microbial growth of the *Staphylococcus aureus* caused by system #6 W+PG/ Sucrose myristate (M1695) /IPM +Ethanol as function of aqueous content along the dilution line N65. The phase diagrams are presented in figures (5:16),(5:21),(5:26) at different temperatures (25,37,and 45°C)respectively .



Fig 5:108 Diameter of inhibition zone (mm) for system #6 W+PG/Sucrose myristate M(1695)/IPM+EOH on *Staphylococcus aureus*

System # 7 MT25IE W+PG/TMAZ80+Sucrose myristate (M1695) /IPM+Ethanol

Effect of the system is tested as inhibition of the bacterial growth zone, measured in (mm) ,work was done in triplicate and average of the collected data was considered as shown in table (5:61)

Table 5:61 Inhibition of the microbial activity of the *Staphylococcus aureus* caused by system #7 W+PG/ TMAZ80+Sucrose myristate (M1695) /IPM +Ethanol

# of samples	W+PG (2/1) wt% Aqueous additions	Diameter of inhibition zone (mm)
1	0	10
2	5	9.5
3	10	10
4	15	10
5	20	9.5
6	25	9
7	30	9
8	35	9.5
9	40	11
10	45	12
11	50	11
12	55	12.5
13	60	11.5
14	65	11
15	70	12
16	75	13.5
17	80	12
18	85	11.5
19	90	11.5

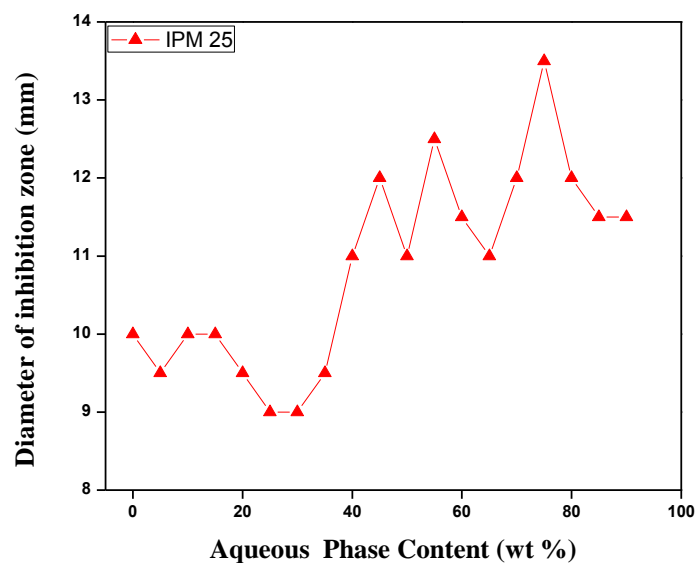


Fig 5:109 Inhibition of the microbial growth of the *Staphylococcus aureus* caused by system #7 W+PG/ TMAZ80+Sucrose myristate (M1695) /IPM +Ethanol as function of aqueous content along the dilution line N65. The phase diagrams are presented in figures (5:17),(5:22),(5:27) at different temperatures (25,37,and 45°C)respectively .

System # 8 MT50IE W+PG/TMAZ80+Sucrose myristate (M1695) /IPM+Ethanol

Effect of the system is tested as inhibition of the bacterial growth zone, measured in (mm) ,work was done in triplicate and average of the collected data was considered as shown in table (5:62)

Table 5:62 Inhibition of the microbial activity of the *Staphylococcus aureus* caused by system #8 W+PG/ TMAZ80+Sucrose myristate (M1695) /IPM +Ethanol

# of samples	W+PG (2/1) wt% Aqueous additions	Diameter of inhibition zone (mm)
1	0	10.5
2	5	11
3	10	11
4	15	9.5
5	20	9.5
6	25	9.5
7	30	9
8	35	9.5
9	40	10.5
10	45	9
11	50	9.5
12	55	9
13	60	8.5
14	65	7.5
15	70	10.5
16	75	8.5
17	80	8
18	85	10
19	90	9.5

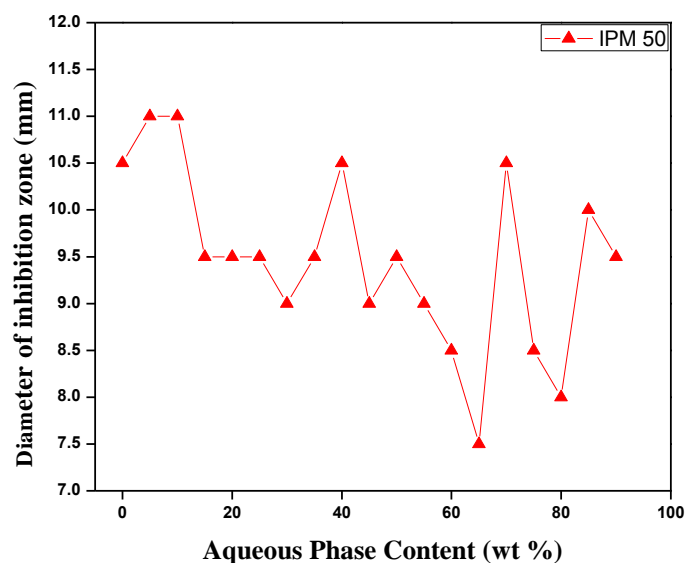


Fig 5:110 Inhibition of the microbial growth of the *Staphylococcus aureus* caused by system #8 W+PG/ TMAZ80+Sucrose myristate (M1695) /IPM +Ethanol as function of aqueous content along the dilution line N65. The phase diagrams are presented in figures (5:18),(5:23),(5:28) at different temperatures (25,37,and 45°C)respectively .



Fig 5:111 Diameter of inhibition zone (mm) for system #8 W+PG/ TMAZ80+ Sucrose myristate M (1695)/ IPM+EOH on *Staphylococcus aureus*

System #9 MT75IE and **system #10 MT100IE** had No inhibition effect on *Staphylococcus aureus* because of the increase percent of the TMAZ80

Table (5:63) Shows the effect of *Staphylococcus aureus* growth inhibition measured as diameter of the clear zone caused as a function of surfactant using IPM oil.

Table5:63 Diameter of inhibition zone(mm) as a function of surfactant concentration in IPM oil

# of samples	W+PG (2/1) wt% Aqueous additions	Diameter of inhibition zone (mm)		
		MTOIE	MT25IE	MT50IE
1	0	12	10	10.5
2	5	14.5	9.5	11
3	10	13	10	11
4	15	14	10	9.5
5	20	16	9.5	9.5
6	25	10.5	9	9.5
7	30	12.5	9	9
8	35	14	9.5	9.5
9	40	12	11	10.5
10	45	13	12	9
11	50	12.5	11	9.5
12	55	12	12.5	9
13	60	12	11.5	8.5
14	65	12.5	11	7.5
15	70	12	12	10.5
16	75	12.5	13.5	8.5
17	80	13	12	8
18	85	13.5	11.5	10
19	90	12	11.5	9.5

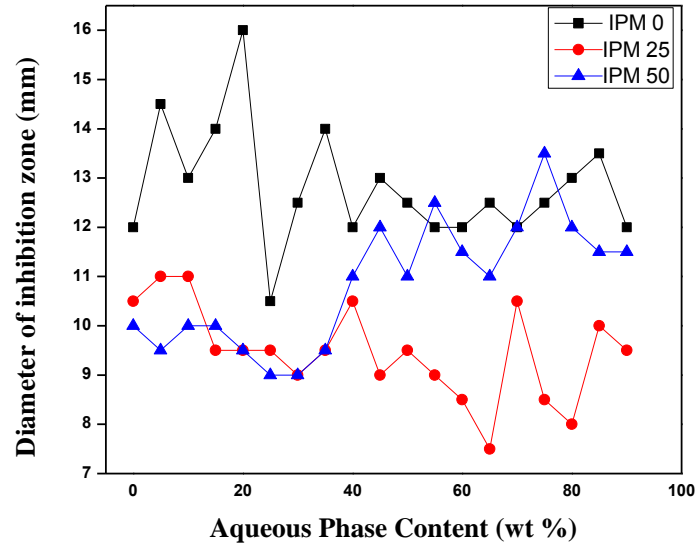


Fig 5:112 Comparison of the microbial inhibition of the *Staphylococcus aureus* growth as a function of surfactant concentration using IPM oil .W+PG/ TMAZ80+Sucrose myristate (M1695) /IPM +Ethanol.

5.4.1.3 Investigating the effect of CCT oil systems on the Gram positive bacteria:

System #11 MT0CE W+PG/ Sucrose myristate (M1695) /CCT +Ethanol

Effect of the system is tested as inhibition of the bacterial growth zone, measured in (mm) ,work was done in triplicate and average of the collected data was considered as shown in table (5:64)

Table 5:64 Inhibition of the microbial activity of the *Staphylococcus aureus* caused by system #11 W+PG/ Sucrose myristate (M1695) /CCT +Ethanol

# of samples	W+PG (2/1) wt% Aqueous additions	Diameter of inhibition zone (mm)
1	0	15.5
2	5	14.5
3	10	12.5
4	15	14.5
5	20	15
6	25	17.5
7	30	14.5
8	35	14.5
9	40	15.5
10	45	13.5
11	50	16
12	55	12.5
13	60	15.5
14	65	13.5
15	70	12.5
16	75	13.5
17	80	12.5
18	85	13
19	90	14.5

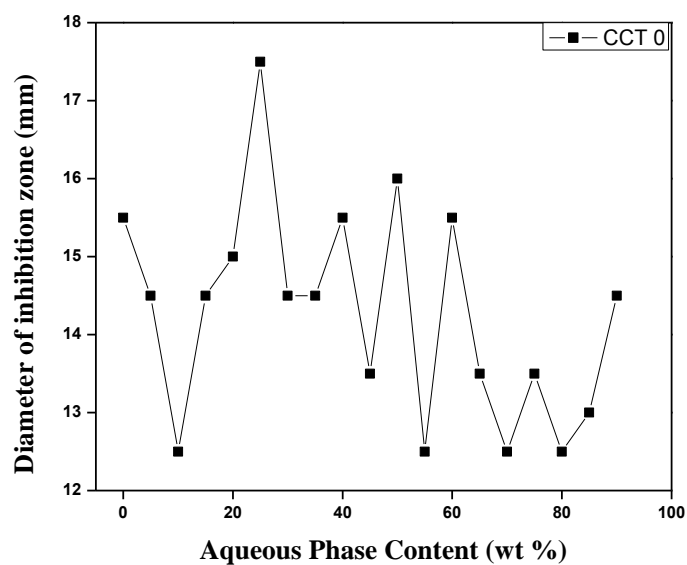


Fig 5:113 Inhibition of the microbial growth of the *Staphylococcus aureus* caused by system #11 W+PG/ Sucrose myristate (M1695) /CCT +Ethanol as function of aqueous content along the dilution line N65. The phase diagrams are presented in figures (5:31),(5:36),(5:41) at different temperatures (25,37,and 45°C)respectively .



Fig :114 Diameter of inhibition zone (mm) for system #11 W+PG/Sucrose myristate M(1695)/CCT+EOH on *Staphylococcus aureus*

System #12 MT25CE W+PG/ TMAZ80+Sucrose myristate (M1695) /CCT +Ethanol

Effect of the system is tested as inhibition of the bacterial growth zone, measured in (mm) ,work was done in triplicate and average of the collected data was considered as shown in table (5:65)

Table 5:65 Inhibition of the microbial activity of the *Staphylococcus aureus* caused by system #12 W+PG/ TMAZ80+Sucrose myristate (M1695) /CCT +Ethanol

# of samples	W+PG (2/1) wt% Aqueous additions	Diameter of inhibition zone (mm)
1	0	12
2	5	12.5
3	10	12.5
4	15	13
5	20	14
6	25	14.5
7	30	12
8	35	12
9	40	12.5
10	45	12.5
11	50	12.5
12	55	12
13	60	7.5
14	65	8
15	70	9
16	75	10
17	80	10
18	85	9.5
19	90	11.5

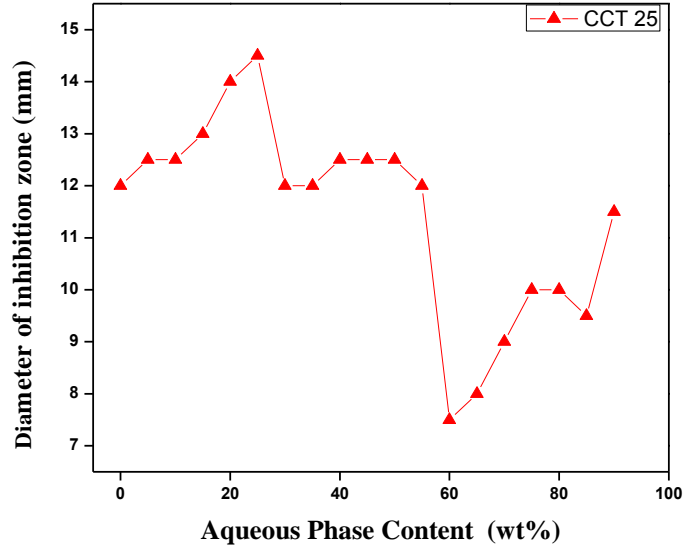


Fig 5:115 Inhibition of the microbial growth of the *Staphylococcus aureus* caused by system #12 W+PG/ TMAZ80+Sucrose myristate (M1695) /CCT +Ethanol as function of aqueous content along the dilution line N65. The phase diagrams are presented in figures (5:32),(5:37),(5:42) at different temperatures (25,37,and 45°C) respectively .



Fig: 5:116 Diameter of inhibition zone (mm) for system #12 W+PG/TMAZ80+Sucrose myristate M(1695)/CCT+EOH on *Staphylococcus aureus*

System #13 MT50CE ,system #14 MT75CE and system MT100CE had No inhibition effect on *Staphylococcus aureus* because of the increase percent of the TMAZ80

Table 5:66 Shows the effect of *Staphylococcus aureus* growth inhibition measured as diameter of the clear zone caused as a function of surfactant using CCT oil.

Table 5:66 Diameter of inhibition zone (mm) as a function of surfactant concentration in CCT oil

# of samples	W+PG (2/1) wt% Aqueous additions	Diameter of inhibition zone (mm)	
		MT0CE	MT25CE
1	0	15.5	12
2	5	14.5	12.5
3	10	12.5	12.5
4	15	14.5	13
5	20	15	14
6	25	17.5	14.5
7	30	14.5	12
8	35	14.5	12
9	40	15.5	12.5
10	45	13.5	12.5
11	50	16	12.5
12	55	12.5	12
13	60	15.5	7.5
14	65	13.5	8
15	70	12.5	9
16	75	13.5	10
17	80	12.5	10
18	85	13	9.5
19	90	14.5	11.5

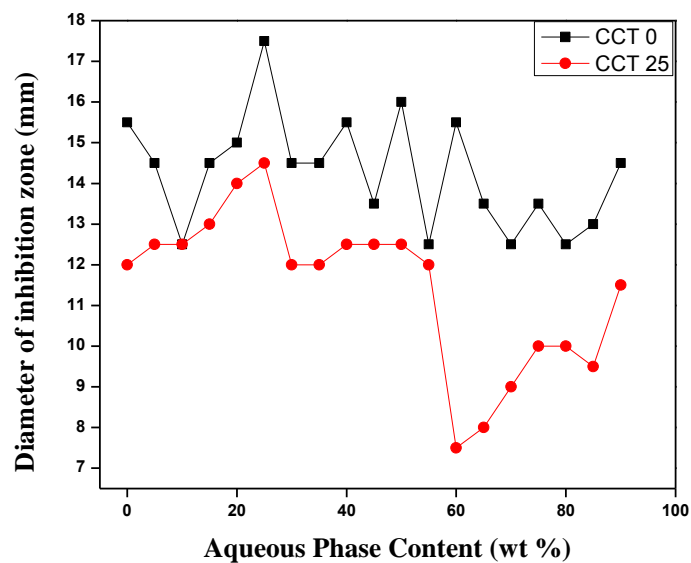


Fig 5:117 Comparison of the microbial inhibition of the *Staphylococcus aureus* growth as a function of surfactant concentration using CCT oil .W+PG/ TMAZ80+Sucrose myristate (M1695) /CCT +Ethanol.

5.4.2 Gram negative bacteria *Escherichia coli*

5.4.2.1 Investigating the effect of LIM oil systems on the Gram negative bacteria:

System # 1 MT0LE W+PG/ Sucrose myristate (M1695) /LIM +Ethanol

Effect of the system is tested as inhibition of the bacterial growth zone, measured in (mm) ,work was done in triplicate and average of the collected data was considered as shown in table (5:67)

Table 5:67 Inhibition of the microbial activity of the *Escherichia coli* caused by system #1 W+PG/ Sucrose myristate (M1695) /LIM +Ethanol

# of samples	W+PG (2/1) wt% Aqueous additions	Diameter of inhibition zone (mm)
1	0	13
2	5	18.5
3	10	12
4	15	14
5	20	14
6	25	13
7	30	12
8	35	13
9	40	11.5
10	45	12
11	50	12.5
12	55	11.5
13	60	13
14	65	11.5
15	70	12.5
16	75	12.5
17	80	13
18	85	11.5
19	90	11

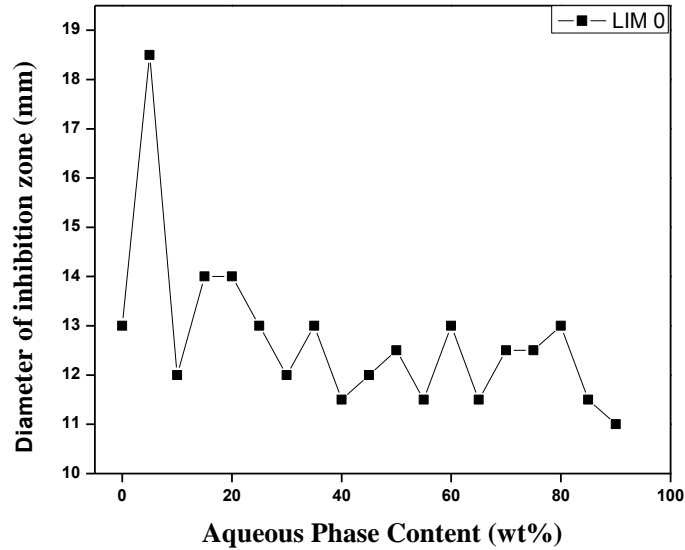


Fig 5:118 Inhibition of the microbial growth of the *Escherichia coli* caused by system #1 W+PG/ Sucrose myristate (M1695) /LIM +Ethanol as function of aqueous content along the dilution line N65. The phase diagrams are presented in figures (5:1),(5:6),(5:11) at different temperatures (25,37,and 45°C)respectively .



Fig 5:119 Diameter of inhibition zone (mm) for system #1 W+PG/ Sucrose myristate M (1695) / LIM + EOH on *Escherichia coli*

System # 2 MT25LE W+PG/TMAZ80+ Sucrose myristate (M1695) /LIM +Ethanol

Effect of the system is tested as inhibition of the bacterial growth zone, measured in (mm) ,work was done in triplicate and average of the collected data was considered as shown in table (5:68)

Table 5:68 Inhibition of the microbial activity of the *Escherichia coli* caused by system #2 W+PG/ TMAZ80+Sucrose myristate (M1695) /LIM +Ethanol

# of samples	W+PG (2/1) wt% Aqueous additions	Diameter of inhibition zone (mm)
1	0	14.5
2	5	14.5
3	10	16
4	15	15.5
5	20	16
6	25	16.5
7	30	14
8	35	15
9	40	14
10	45	17.5
11	50	15
12	55	14
13	60	15.5
14	65	15.5
15	70	13
16	75	15
17	80	15.5
18	85	16.5
19	90	17

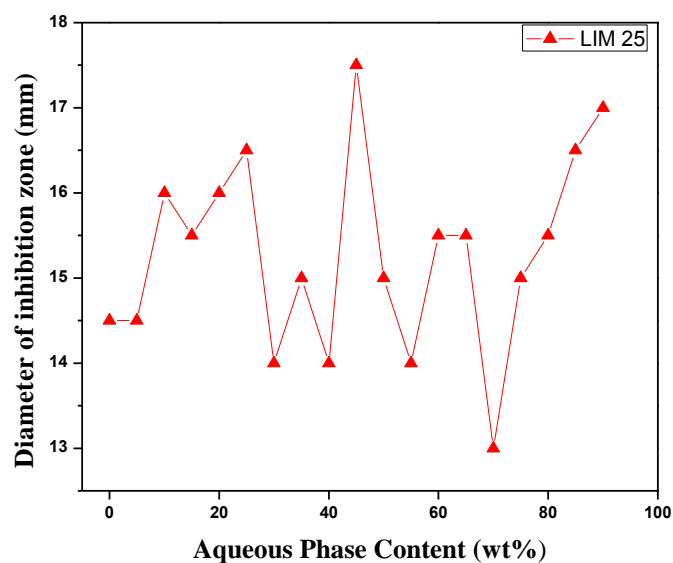


Fig 5:120 Inhibition of the microbial growth of the *Escherichia coli* caused by system #2 W+PG/TMAZ80+ Sucrose myristate (M1695) /LIM +Ethanol as function of aqueous content along the dilution line N65. The phase diagrams are presented in figures (5:2),(5:7),(5:12) at different temperatures (25,37,and 45°C)respectively .



Fig 5:121 Diameter of inhibition zone (mm) for system #2 W+PG/ TMAZ80+Sucrose myristate M (1695) / LIM + EOH on *Escherichia coli*

System # 3 MT50LE W+PG/TMAZ80+ Sucrose myristate (M1695) /LIM +Ethanol

Effect of the system is tested as inhibition of the bacterial growth zone, measured in (mm) ,work was done in triplicate and average of the collected data was considered as shown in table (5:69)

Table 5:69 Inhibition of the microbial activity of the *Escherichia coli* caused by system #3 W+PG/ TMAZ80+Sucrose myristate (M1695) /LIM +Ethanol

# of samples	W+PG (2/1) wt% Aqueous additions	Diameter of inhibition zone (mm)
1	0	12.5
2	5	11
3	10	10.5
4	15	13.5
5	20	11.5
6	25	14
7	30	10.5
8	35	11
9	40	12
10	45	12.5
11	50	11.5
12	55	11.5
13	60	13
14	65	12.5
15	70	12.5
16	75	12.5
17	80	12.5
18	85	12.5
19	90	12.5

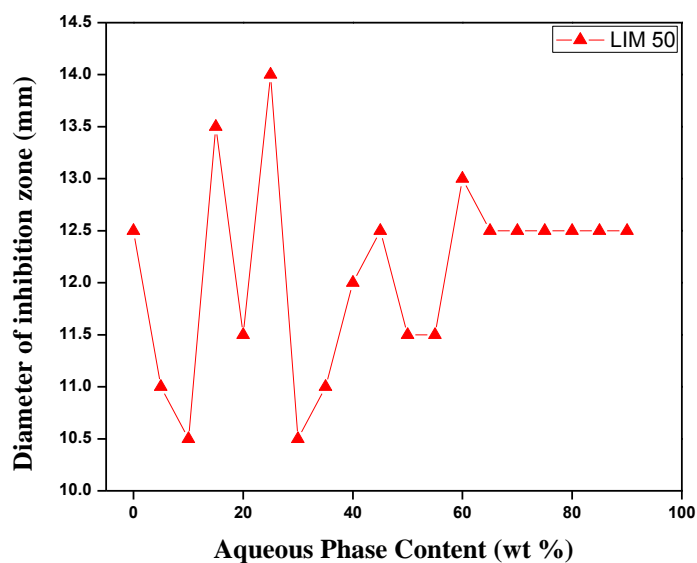


Fig 5:122 Inhibition of the microbial growth of the *Escherichia coli* caused by system #3 W+PG/TMAZ80+ Sucrose myristate (M1695) /LIM +Ethanol as function of aqueous content along the dilution line N65. The phase diagrams are presented in figures (5:3),(5:8),(5:13) at different temperatures (25,37,and 45°C)respectively .



Fig 5: 123 Diameter of inhibition zone (mm) for system #3 W+PG/TMAZ80+Sucrose myristate M(1695)/LIM+EOH on *Escherichia coli*

System #4 MT75LE and **system #5 MT100LE** had No inhibition effect on *Escherichia coli* because of the increase percent of the TMAZ80

Table (5:70) Shows the effect of *Escherichia coli* growth inhibition measured as diameter of the clear zone caused as a function of surfactant using LIM oil.

Table 5:70 Diameter of inhibition zone (mm) as a function of surfactant concentration in LIM oil

# of samples	W+PG (2/1) wt% Aqueous additions	Diameter of inhibition zone (mm)		
		MT0LE	MT25LE	MT50LE
1	0	13	14.5	12.5
2	5	18.5	14.5	11
3	10	12	16	10.5
4	15	14	15.5	13.5
5	20	14	16	11.5
6	25	13	16.5	14
7	30	12	14	10.5
8	35	13	15	11
9	40	11.5	14	12
10	45	12	17.5	12.5
11	50	12.5	15	11.5
12	55	11.5	14	11.5
13	60	13	15.5	13
14	65	11.5	15.5	12.5
15	70	12.5	13	12.5
16	75	12.5	15	12.5
17	80	13	15.5	12.5
18	85	11.5	16.5	12.5
19	90	13	14.5	12.5

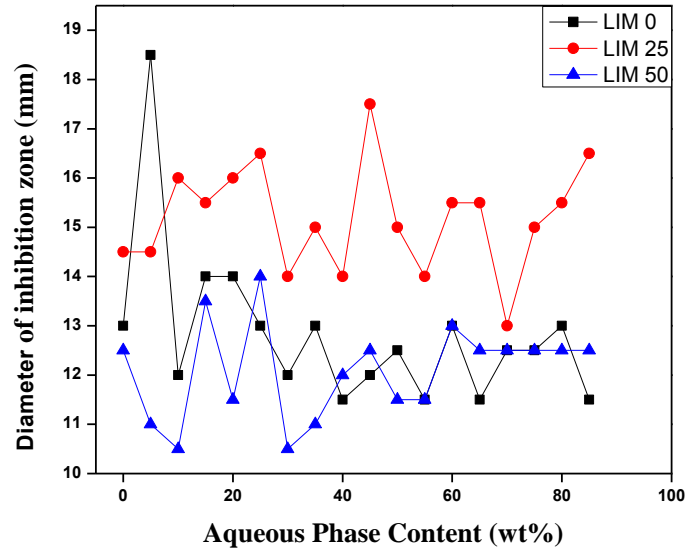


Fig 5:124 Comparison of the microbial inhibition of the *Escherichia coli* growth as a function of surfactant concentration using LIM oil .W+PG/ TMAZ80+Sucrose myristate (M1695) /LIM +Ethanol.

5.4.2.2 Investigating the effect of IPM oil systems on the Gram negative bacteria:

System # 6 MT0IE W+PG/ Sucrose myristate (M1695) /IPM +Ethanol

Effect of the system is tested as inhibition of the bacterial growth zone, measured in (mm) ,work was done in triplicate and average of the collected data was considered as shown in table (5:7 1)

Table 5:71 Inhibition of the microbial activity of the *Escherichia coli* caused by system #6 W+PG/ Sucrose myristate (M1695) /IPM +Ethanol

# of samples	W+PG (2/1) wt% Aqueous additions	Diameter of inhibition zone (mm)
1	0	10
2	5	7.5
3	10	11
4	15	10.5
5	20	14
6	25	13.5
7	30	13.5
8	35	14.5
9	40	16
10	45	15
11	50	15
12	55	16.5
13	60	15
14	65	15
15	70	15
16	75	15
17	80	15
18	85	15
19	90	15

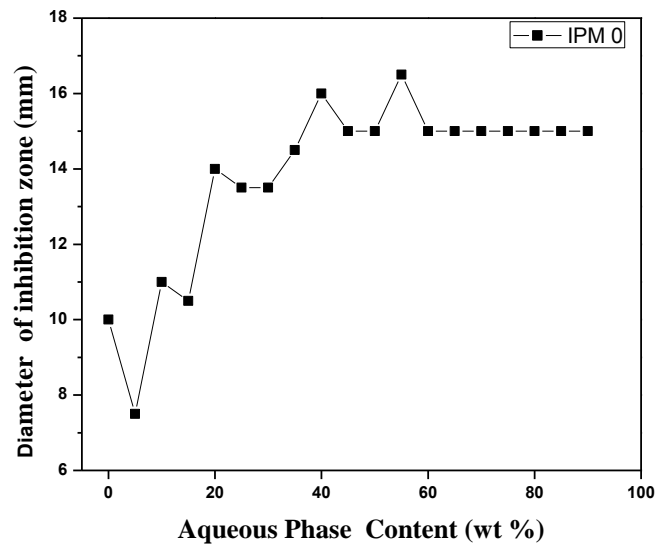


Fig 5:125 Inhibition of the microbial growth of the *Escherichia coli* caused by system #6 W+PG/ Sucrose myristate (M1695) /IPM +Ethanol as function of aqueous content along the dilution line N65. The phase diagrams are presented in figures (5:16),(5:21),(5:26) at different temperatures (25,37,and 45°C)respectively

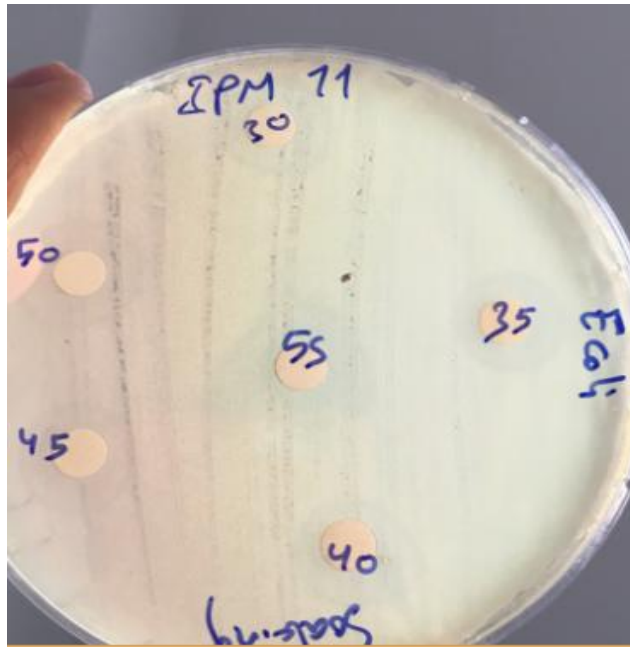


Fig 5:126 Diameter of inhibition zone (mm) for system #6 W+PG/ Sucrose myristate M (1695) / IPM +EOH on *Escherichia coli*

System # 7 MT25IE W+PG/TMAZ80+ Sucrose myristate (M1695) /IPM +Ethanol

Effect of the system is tested as inhibition of the bacterial growth zone, measured in (mm) ,work was done in triplicate and average of the collected data was considered as shown in table (5:72)

Table 5:72 Inhibition of the microbial activity of the *Escherichia coli* caused by system #7 W+PG/TMAZ80+ Sucrose myristate (M1695) /IPM +Ethanol

# of samples	W+PG (2/1) wt% Aqueous additions	Diameter of inhibition zone (mm)
1	0	7
2	5	13
3	10	14
4	15	12.5
5	20	12.5
6	25	13.5
7	30	12
8	35	13.5
9	40	11.5
10	45	12.5
11	50	14
12	55	14
13	60	7.5
14	65	12.5
15	70	12.5
16	75	11.5
17	80	12.5
18	85	12.5
19	90	11

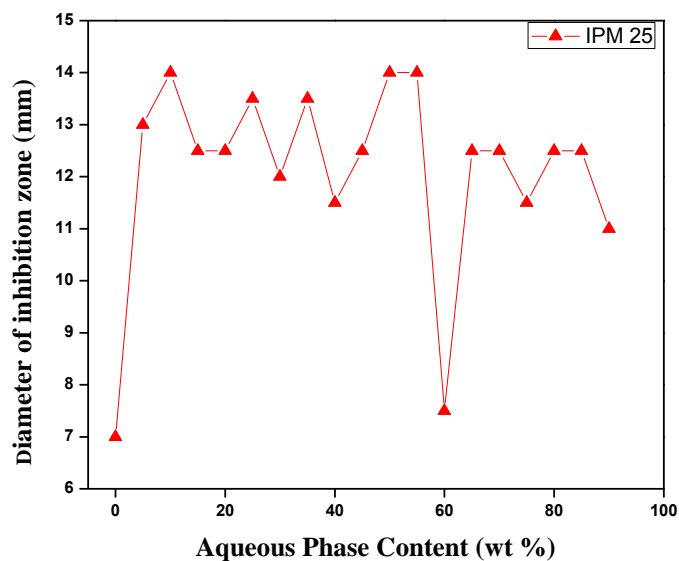


Fig 5:127 Inhibition of the microbial growth of the *Escherichia coli* caused by system #7 W+PG/TMAZ80+ Sucrose myristate (M1695) /IPM +Ethanol as function of aqueous content along the dilution line N65. The phase diagrams are presented in figures (5:17),(5:22),(5:27) at different temperatures (25,37,and 45°C)respectively .



Fig 5:128 Diameter of inhibition zone (mm) for system #7 W+PG/TMAZ80+Sucrose myristate M(1695)/IPM+EOH on *Escherichia coli*

System # 8 MT50IE W+PG/TMAZ80+ Sucrose myristate (M1695) /IPM +Ethanol

Effect of the system is tested as inhibition of the bacterial growth zone, measured in (mm) ,work was done in triplicate and average of the collected data was considered as shown in table (5:73)

Table 5:73 Inhibition of the microbial activity of the *Escherichia coli* caused by system #8 W+PG/TMAZ80+ Sucrose myristate (M1695) /IPM +Ethanol

# of samples	W+PG (2/1) wt% Aqueous additions	Diameter of inhibition zone (mm)
1	0	10
2	5	10
3	10	9.5
4	15	8
5	20	10
6	25	9.5
7	30	9.5
8	35	9
9	40	10
10	45	9
11	50	10.5
12	55	10
13	60	9.5
14	65	9
15	70	10
16	75	9
17	80	8
18	85	8.5
19	90	9

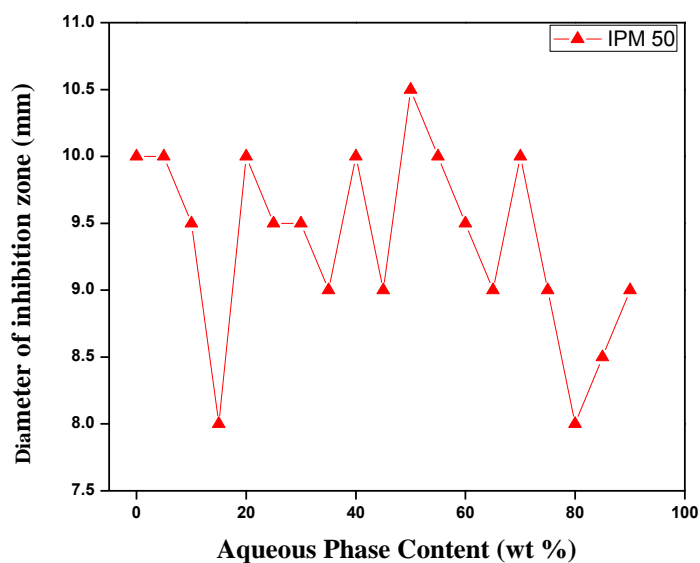


Fig 5:129 Inhibition of the microbial growth of the *Escherichia coli* caused by system #8 W+PG/TMAZ80+ Sucrose myristate (M1695) /IPM +Ethanol as function of aqueous content along the dilution line N65. The phase diagrams are presented in figures (5:18),(5:23),(5:28) at different temperatures (25,37,and 45°C)respectively .



Fig 5:130 Diameter of inhibition zone (mm) for system #8 W+PG/TMAZ80+Sucrose myristate M(1695)/IPM+EOH on *Escherichia coli*

System #9 MT75IE and **system #10 MT100IE** had No inhibition effect on *Escherichia coli* because of the increase percent of the TMAZ80

Table (5:74) Shows the effect of *Escherichia coli* growth inhibition measured as diameter of the clear zone caused as a function of surfactant using IPM oil.

Table 5:74 Diameter of inhibition zone (mm) as a function of surfactant concentration in IPM oil

# of samples	W+PG (2/1) wt% Aqueous additions	Diameter of inhibition zone (mm)		
		MT0IE	MT25IE	MT50IE
1	0	10	7	10
2	5	7.5	13	10
3	10	11	14	9.5
4	15	10.5	12.5	8
5	20	14	12.5	10
6	25	13.5	13.5	9.5
7	30	13.5	12	9.5
8	35	14.5	13.5	9
9	40	16	11.5	10
10	45	15	12.5	9
11	50	15	14	10.5
12	55	16.5	14	10
13	60	15	7.5	9.5
14	65	15	12.5	9
15	70	15	12.5	10
16	75	15	11.5	9
17	80	15	12.5	8
18	85	15	12.5	8.5
19	90	15	11	9

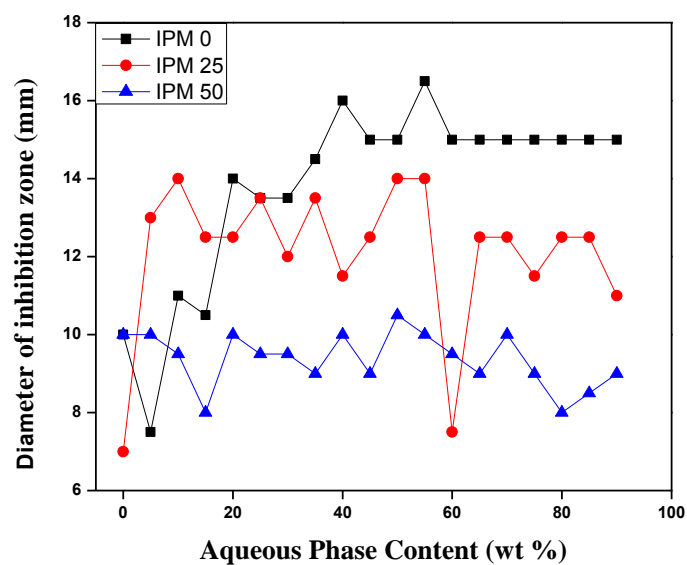


Fig 5:131 Comparison of the microbial inhibition of the *Escherichia coli* growth as a function of surfactant concentration using IPM oil .W+PG/ TMAZ80+Sucrose myristate (M1695) /IPM +Ethanol.

5.4.2.3 Investigating the effect of CCT oil systems on the Gram negative bacteria:

System # 11 MT0CE W+PG/ Sucrose myristate (M1695) /CCT +Ethanol

Effect of the system is tested as inhibition of the bacterial growth zone, measured in (mm) ,work was done in triplicate and average of the collected data was considered as shown in table (5:75)

Table 5:75 Inhibition of the microbial activity of the *Escherichia coli* caused by system #11 W+PG/ Sucrose myristate (M1695) /CCT +Ethanol

# of samples	W+PG (2/1) wt% Aqueous additions	Diameter of inhibition zone (mm)
1	0	10
2	5	11.5
3	10	11
4	15	11
5	20	10.5
6	25	14.5
7	30	12.5
8	35	12.5
9	40	13.5
10	45	11.5
11	50	13
12	55	11
13	60	12
14	65	11.5
15	70	11.5
16	75	12.5
17	80	12.5
18	85	12.5
19	90	10.5

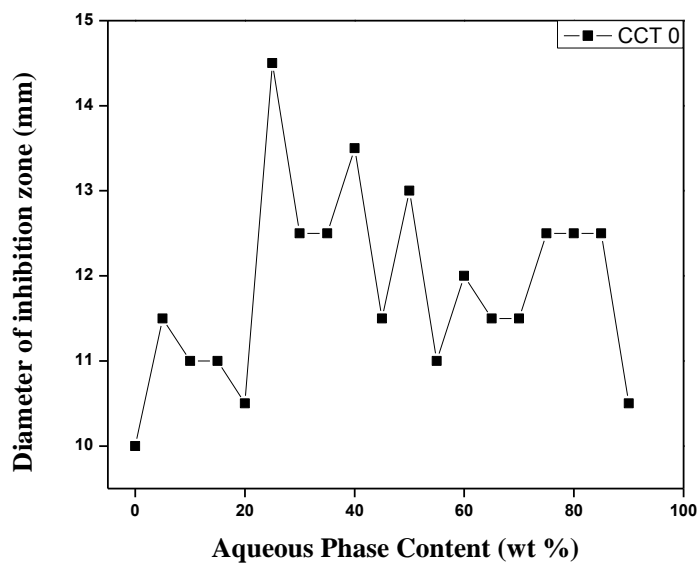


Fig 5:132 Inhibition of the microbial growth of the *Escherichia coli* caused by system #11 W+PG/ Sucrose myristate (M1695) /CCT +Ethanol as function of aqueous content along the dilution line N65. The phase diagrams are presented in figures (5:31),(5:36),(5:41) at different temperatures (25,37,and 45°C)respectively .

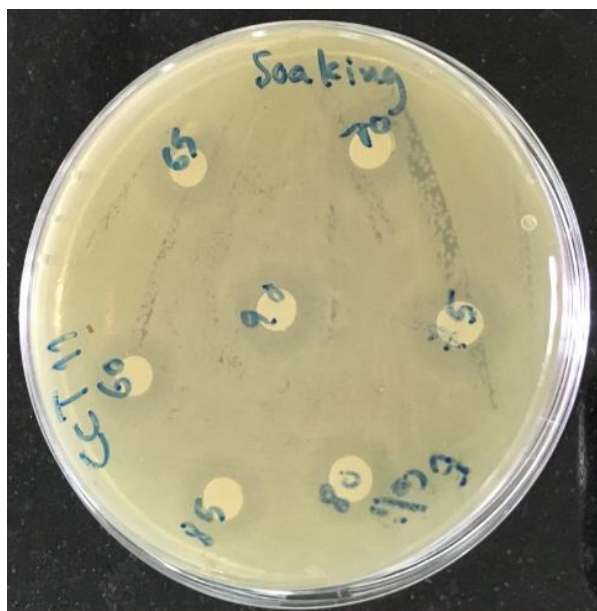


Fig 5:133 Diameter of inhibition zone (mm) for system #11 W+PG/ Sucrose myristate M (1695) /CCT+EOH on *Escherichia coli*

System # 13 MT50CE W+PG/ TMAZ80+Sucrose myristate (M1695) /CCT +Ethanol

Effect of the system is tested as inhibition of the bacterial growth zone, measured in (mm) ,work was done in triplicate and average of the collected data was considered as shown in table (5:76)

Table 5:76 Inhibition of the microbial activity of the *Escherichia coli* caused by system #13 W+PG/TMAZ80+ Sucrose myristate (M1695) /CCT +Ethanol

# of samples	W+PG (2/1) wt% Aqueous additions	Diameter of inhibition zone (mm)
1	0	13.5
2	5	11.5
3	10	13
4	15	12.5
5	20	12
6	25	12.5
7	30	11
8	35	11
9	40	11.5
10	45	13
11	50	11.5
12	55	11.5
13	60	11
14	65	11
15	70	12
16	75	12.5
17	80	10.5
18	85	12.5
19	90	11.5

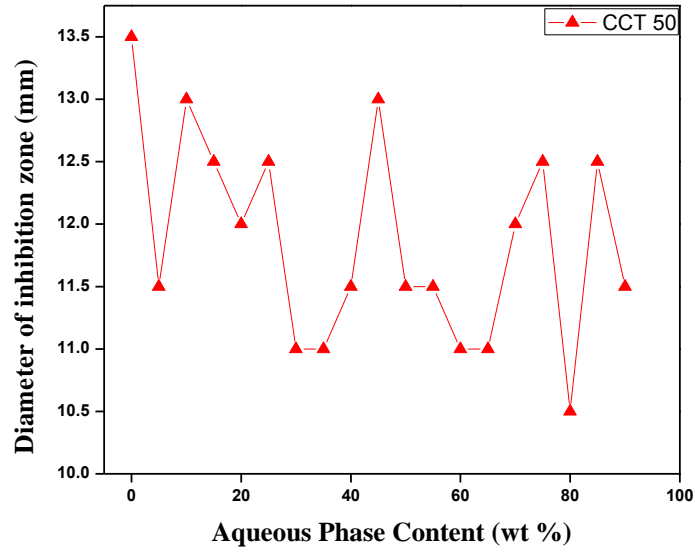


Fig 5:134 Inhibition of the microbial growth of the *Escherichia coli* caused by system #13 W+PG/TMAZ80+ Sucrose myristate (M1695) /CCT +Ethanol as function of aqueous content along the dilution line N65. The phase diagrams are presented in figures (5:33),(5:38),(5:43) at different temperatures (25,37,and 45°C)respectively .



Fig 5:135 Diameter of inhibition zone (mm) for system #13 W+PG/ TMAZ 80+ Sucrose myristate M (1695) /CCT+EOH on *Escherichia coli*

System # 15 MT100CE W+PG/ TMAZ80/CCT +Ethanol

Effect of the system is tested as inhibition of the bacterial growth zone, measured in (mm) ,work was done in triplicate and average of the collected data was considered as shown in table (5:77)

Table 5:77 Inhibition of the microbial activity of the *Escherichia coli* caused by system #15 W+PG/TMAZ80/CCT +Ethanol

# of samples	W+PG (2/1) wt% Aqueous additions	Diameter of inhibition zone (mm)
1	0	9
2	5	11
3	10	11
4	15	11.5
5	20	11.5
6	25	13
7	30	12
8	35	14.5
9	40	12
10	45	11.5
11	50	11
12	55	11.5
13	60	11.5
14	65	10.5
15	70	10.5
16	75	9
17	80	9
18	85	10
19	90	12

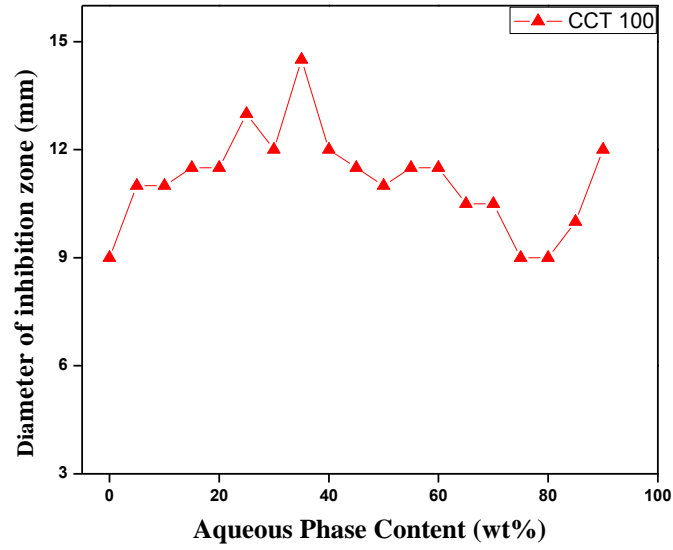


Fig 5:136 Inhibition of the microbial growth of the *Escherichia coli* caused by system #15 W+PG/TMAZ80/CCT +Ethanol as function of aqueous content along the dilution line N65. The phase diagrams are presented in figures (5:35),(5:40),(5:45) at different temperatures (25,37,and 45°C)respectively .

System #12 MT25CE and **system #14 MT75CE** had No inhibition effect on *Escherichia coli* because of the increase percent of the TMAZ80

Table (5:78)Shows the effect of *Escherichia coli* growth inhibition measured as diameter of the clear zone caused as a function of surfactant using CCT oil.

Table 5:78 Diameter of inhibition zone (mm) as a function of surfactant concentration in CCT oil

# of samples	W+PG (2/1) wt% Aqueous additions	Diameter of inhibition zone (mm)		
		MT0CE	MT50CE	MT100CE
1	0	10	13.5	9
2	5	11.5	11.5	11
3	10	11	13	11
4	15	11	12.5	11.5
5	20	10.5	12	11.5
6	25	14.5	12.5	13
7	30	12.5	11	12
8	35	12.5	11	14.5
9	40	13.5	11.5	12
10	45	11.5	13	11.5
11	50	13	11.5	11
12	55	11	11.5	11.5
13	60	12	11	11.5
14	65	11.5	11	10.5
15	70	11.5	12	10.5
16	75	12.5	12.5	9
17	80	12.5	10.5	9
18	85	12.5	12.5	10
19	90	10.5	11.5	12

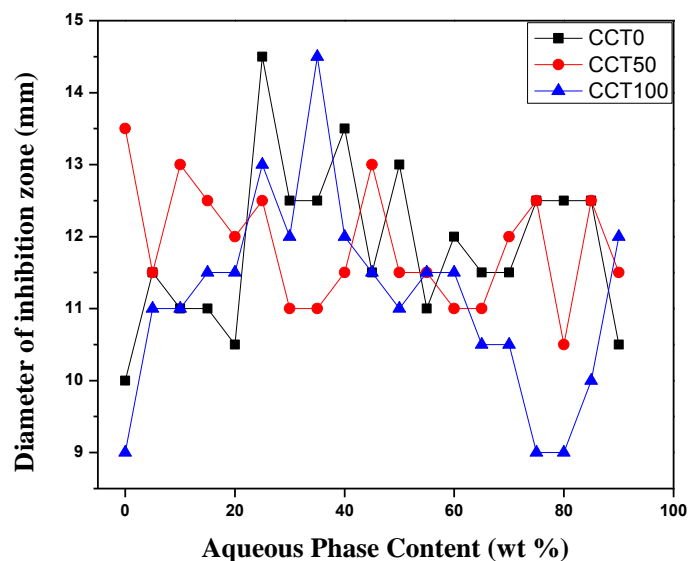


Fig 5:137 Comparison of the microbial inhibition of the *Escherichia coli* growth as a function of surfactant concentration using CCT oil .W+PG/ TMAZ80+Sucrose myristate (M1695) /CCT +Ethanol.

When comparing the inhibition effect of the systems using equal unity of the mixed surfactants against the two tested type of bacteria . Results as in table 5: 79 below showed that the diameters of inhibition zone (mm) against *Staphylocoous aureus* were larger than against *Escherichia coli* in both LIM and IPM oils. CCT oil at equal mixed unity of surfactants had no inhibition effect against both of them.

Table 5:79 Comparison in diameter of inhibition zone against *Staphylocoous aureus* and *Escherichia coli* using W+PG/ TMAZ80+Sucrose myristate (M1695) /oil +Ethanol with equal unity of surfactants

W+PG(2/1) wt %	Diameter of inhibition zone(mm)					
	Bacteria→	<i>Staphylocoous aureus</i>		<i>Escherichia coli</i>		
	OIL →	LIM	IPM	LIM	IPM	CCT
0		16.5	10.5	12.5	10	13.5
5		16	11	11	10	11.5
10		15.5	11	10.5	9.5	13
15		13.5	9.5	13.5	8	12.5
20		14.5	9.5	11.5	10	12
25		13	9.5	14	9.5	12.5
30		11.5	9	10.5	9.5	11
35		12	9.5	11	9	11
40		12.5	10.5	12	10	11.5
45		11.5	9	12.5	9	13
50		12.5	9.5	11.5	10.5	11.5
55		12	9	11.5	10	11.5
60		11.5	8.5	13	9.5	11
65		13	7.5	12.5	9	11
70		13.5	10.5	12.5	10	12
75		10.5	8.5	12.5	9	12.5
80		10	8	12.5	8	10.5
85		11	10	12.5	8.5	12.5
90		12	9.5	12.5	9	11.5

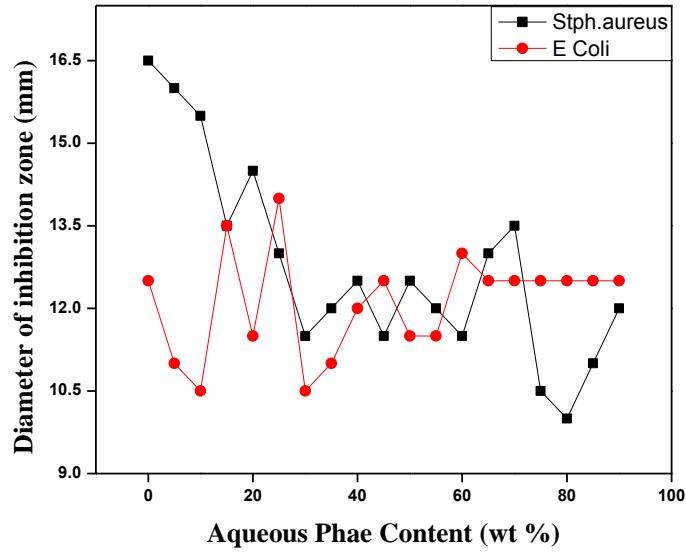


Fig 5:138 Comparison of the microbial inhibition of the *Staphylococcus aureus* and *Escherichia coli* growth using W+PG/ TMAZ80+Sucrose myristate (M1695) /LIM +Ethanol with equal unity of surfactant

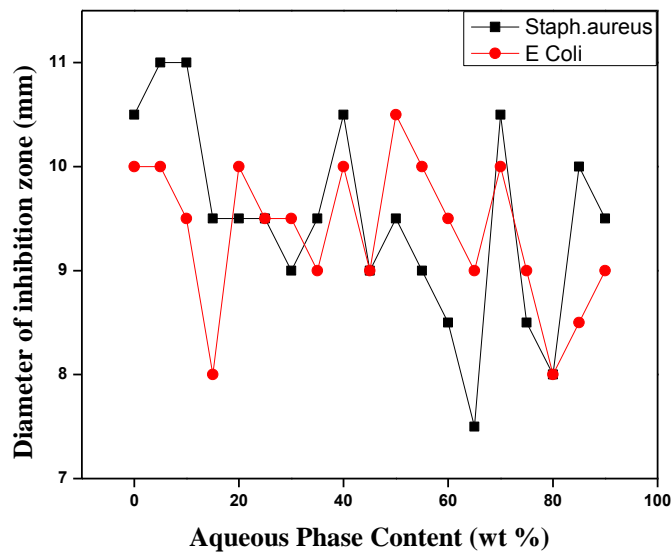


Fig 5:139 Comparison of the microbial inhibition of the *Staphylococcus aureus* and *Escherichia coli* growth using W+PG/ TMAZ80+Sucrose myristate (M1695) /IPM +Ethanol with equal unity of surfactants.

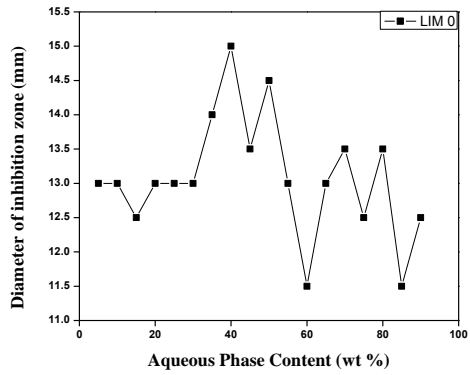
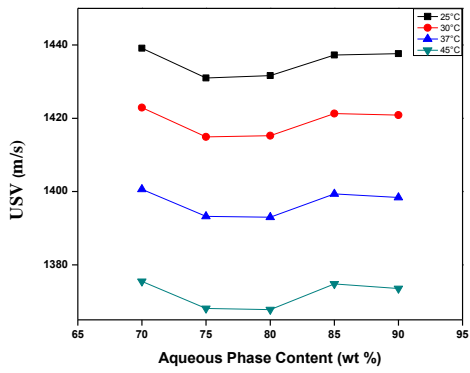
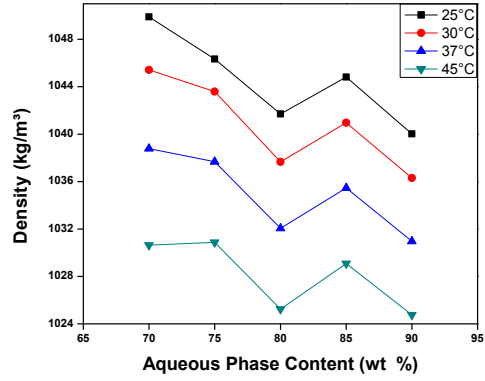
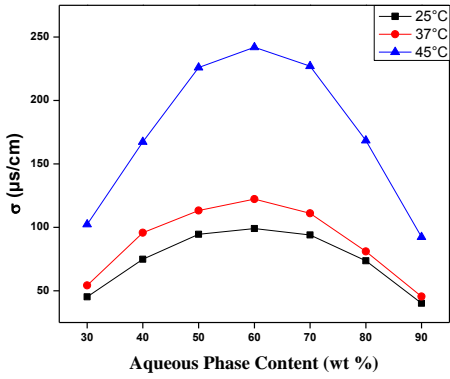
According to the results in table (5:55) LIM oil and sucrose myristate (M1695) are considered as positive controls against the two tested bacteria. Inhibition effect was detected against Gram positive bacteria *Staphylococcus aureus* more than Gram negative one *Escherichia coli* ; in *Staphylococcus aureus* diameters of inhibition zone were larger and were as total destruction while in *Escherichia coli* ;diameters of inhibition zone were less and there were reduction in population not total destruction.; this is due to the difference in structural component of the cell membrane . *Staphylococcus aureus* ;Gram positive bacteria has no lipid layer and has thick layer of peptidoglycan ,while *Escherichia coli* Gram negative, has lipid layer as outer layer of membrane and has very thin layer of peptidoglycan .The lipid layer of the Gram negative bacteria serves as a barrier which prevent the microemulsion from penetrating inside the microbial membrane ,and in Gram positive bacteria penetration is more easier since there is no lipid layer ,peptidoglycan which is a polymer of sugar and amino acid ,it allows particles of 2nm to pass easily through its layers thus enables the microemulsion to penetrate more easily and cause gross disturbance and disfunction of the membrane structure thus rupture of the cell membrane of the bacteria.

Most of the inhibition effect is shown in the bicontinuous phase .Rate of inhibition decreases with increase of ethoxylated surfactant ratio (decrease in sucrose myristate)

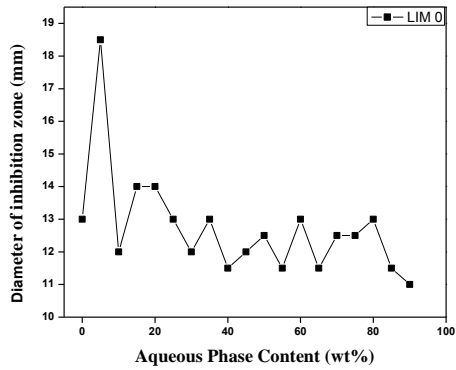
Highest inhibition were detected against *Staphylococcus aureus* in systems containing high content of sucrose myristate M(1695) and LIM oil due to the synergistic effect.

When over viewing the systems that had inhibition effect on the tested bacteria with the characterizations which were made for these systems ,figures are all illustrated as follows. Comparing the electrical conductivity ,density and the ultrasonic velocity for all the systems ,gave that almost all of the systems had the bicontinuous phase between(25-70) % aqueous, maximum inhibition of the tested bacteria occurred in the same phase.

Fig 5:140 System # 1 W+PG/ M1695/ LIM /EOH (M1695)100 %

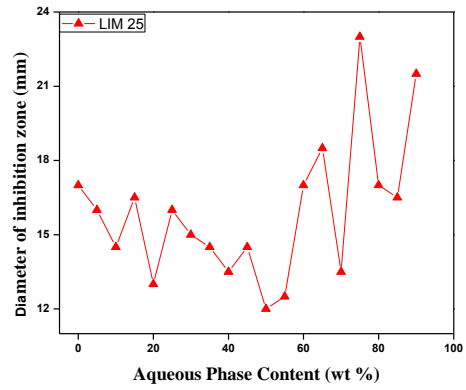
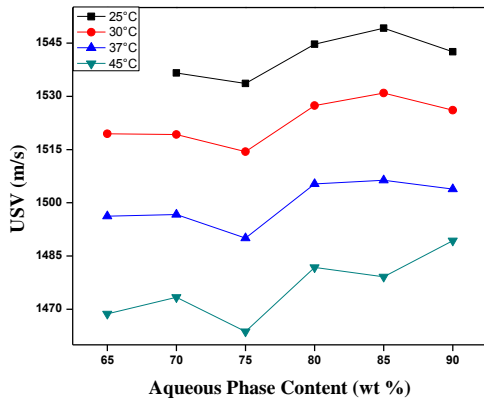
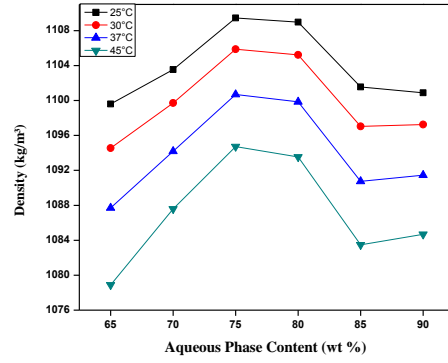
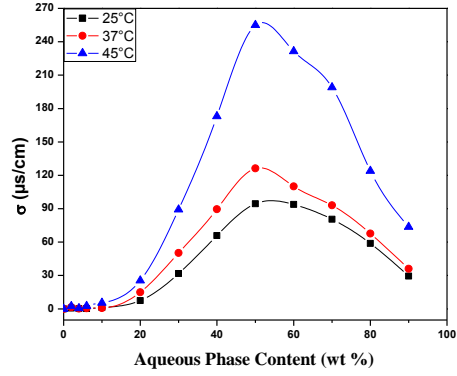


Staphylococcus aureus

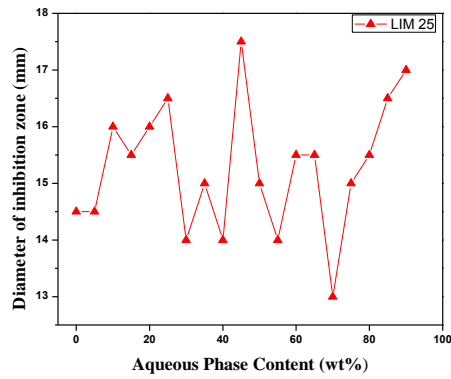


Escherichia coli

Fig 5:141 system #2 W+PG/TMAZ80/M1695/ LIM /EOH S(1/4)

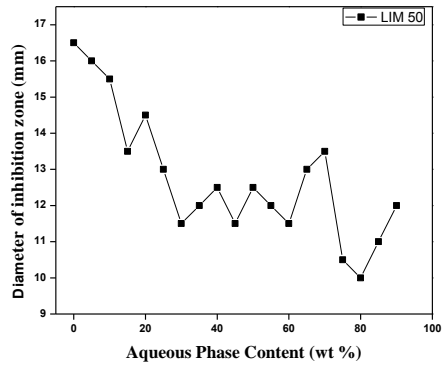
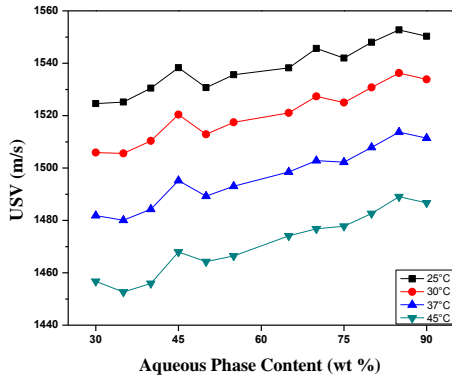
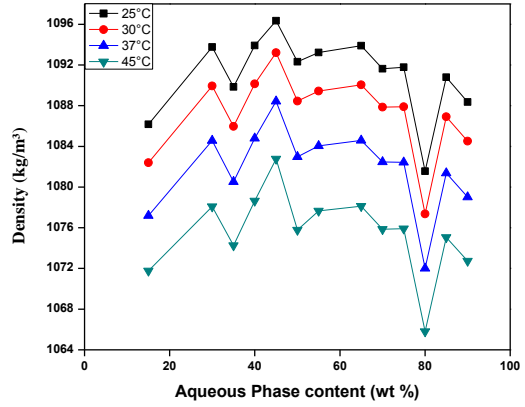
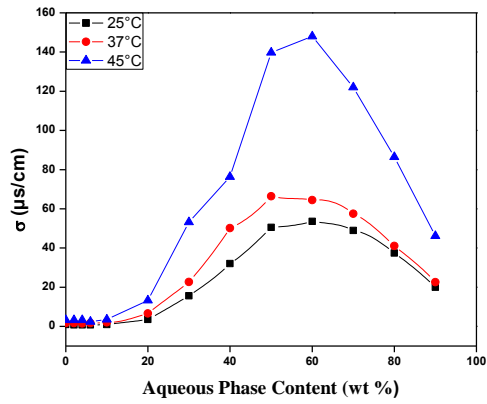


Staphylococcus aureus

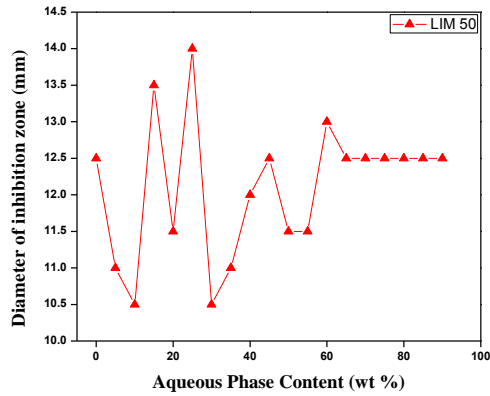


Escherichia coli

Fig 5:142 System #3 W+PG/TMAZ80/M1695/ LIM /EOH S(1/1)

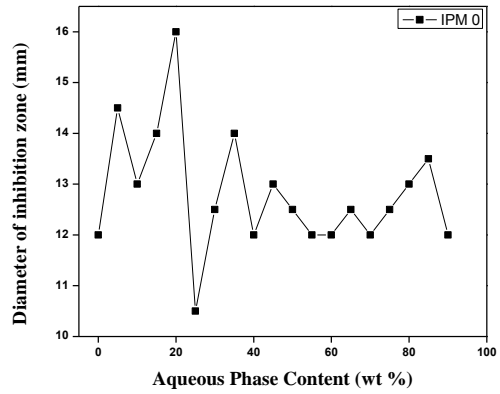
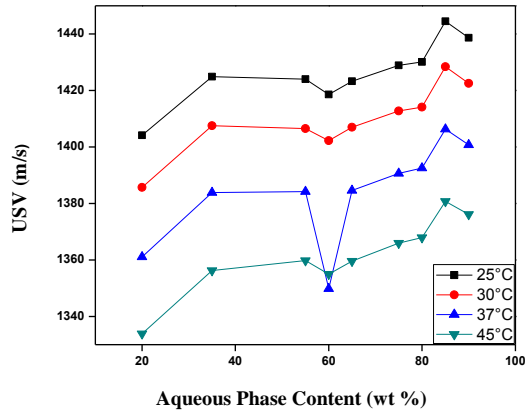
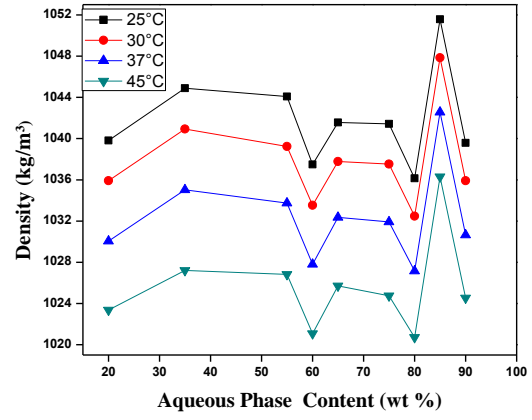
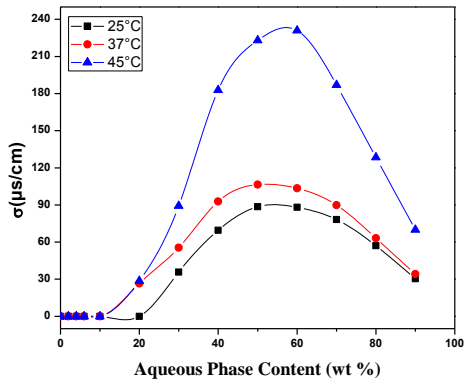


Staphylococcus aureus

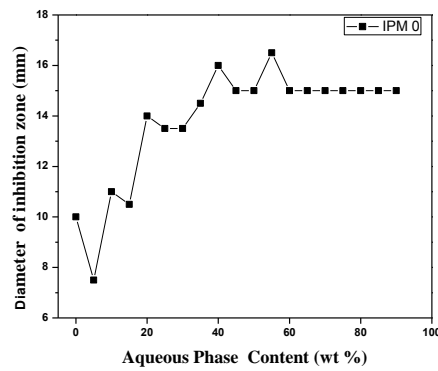


Escherichia coli

Fig 5:143 System # 6 W+PG/ M1695/ IPM /EOH (M1695 100%)

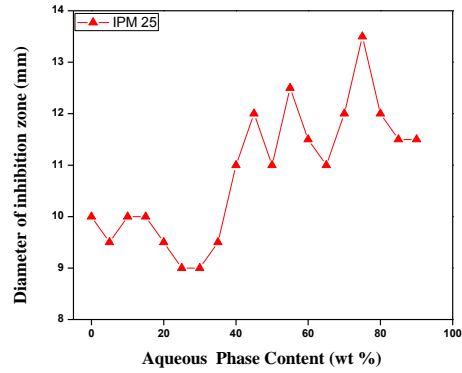
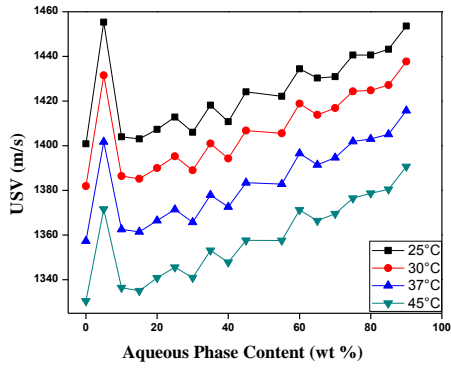
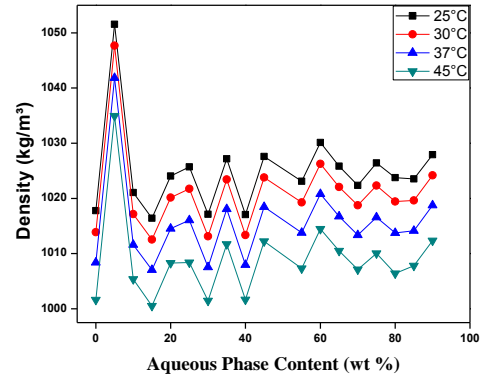
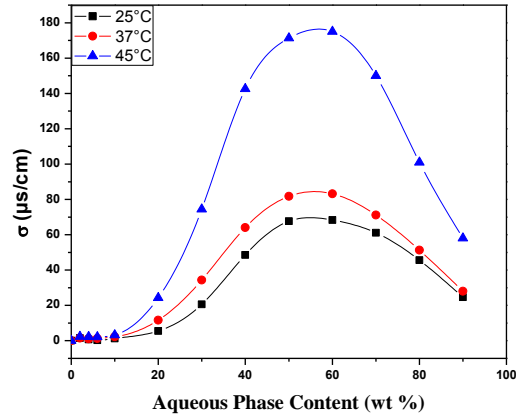


Staphylococcus aureus

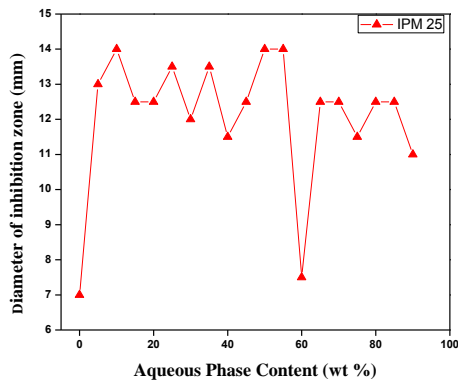


Escherichia coli

Fig 5:144 System #7 W+PG/TMAZ80/M1695/ IPM /EOH S(1/4)

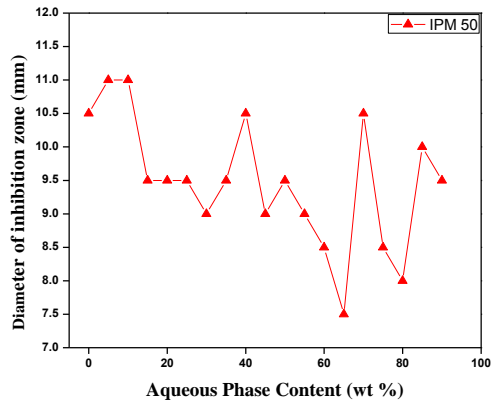
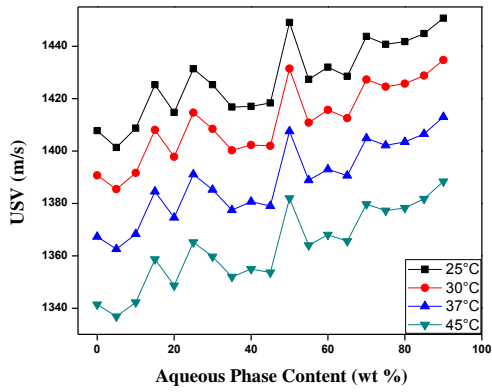
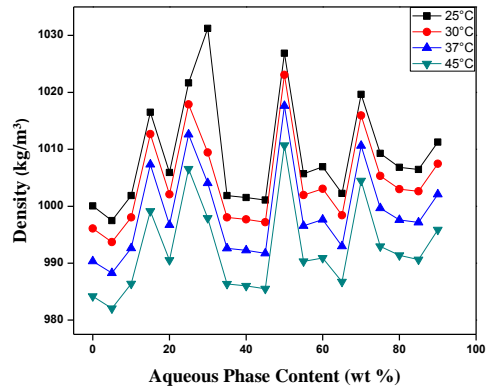
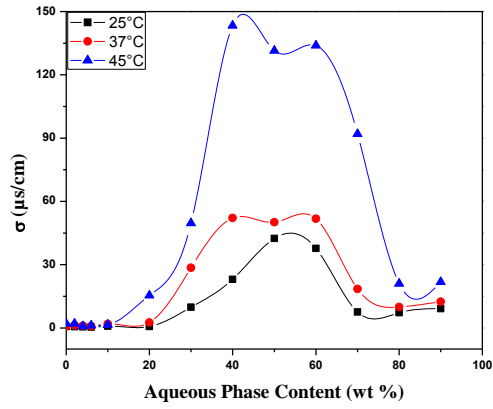


Staphylococcus aureus

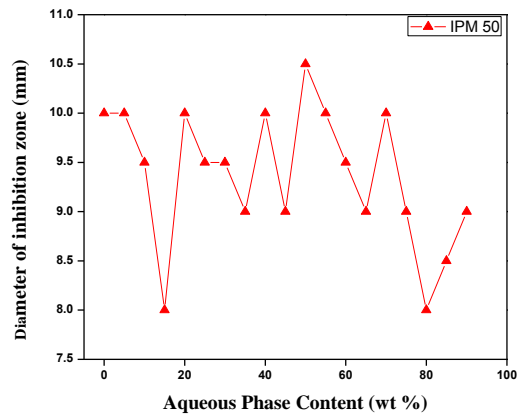


Escherichia coli

Fig 5:145 System #8 W+PG/TMAZ80/M1695/ IPM /EOH S (1/1)

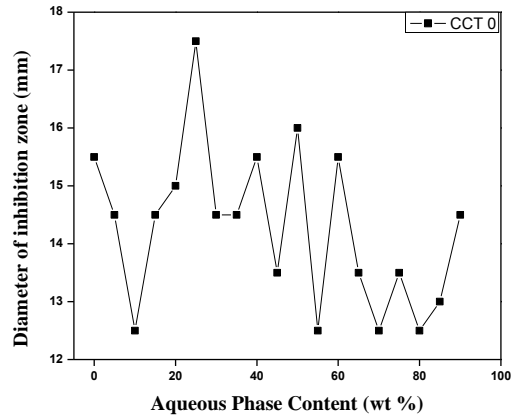
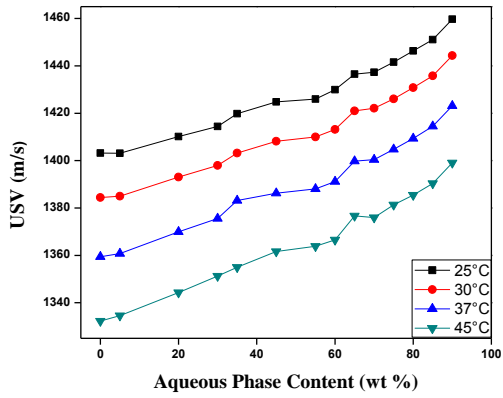
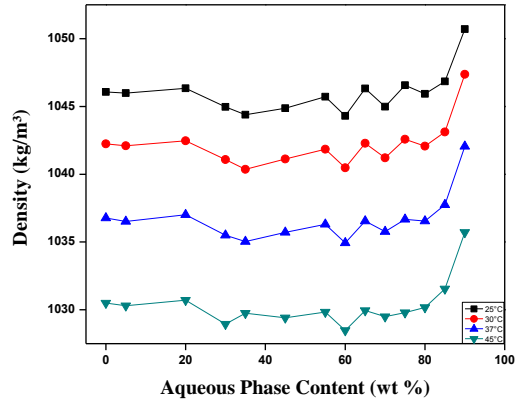
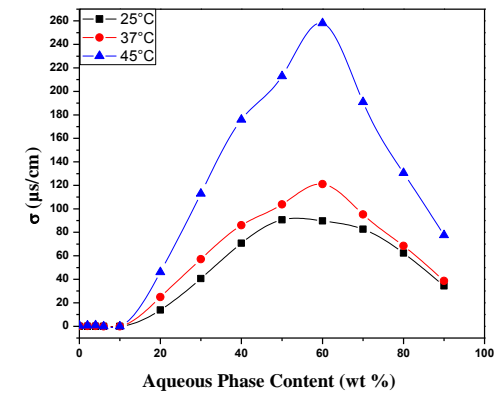


Staphylococcus aureus

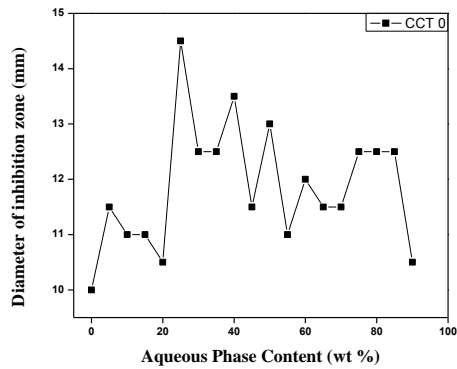


Escherichia coli

Fig 5:146 System #11 W+PG/M1695/ CCT /EOH (M1695 100%)

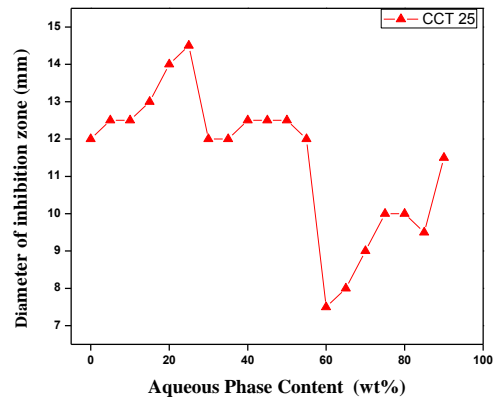
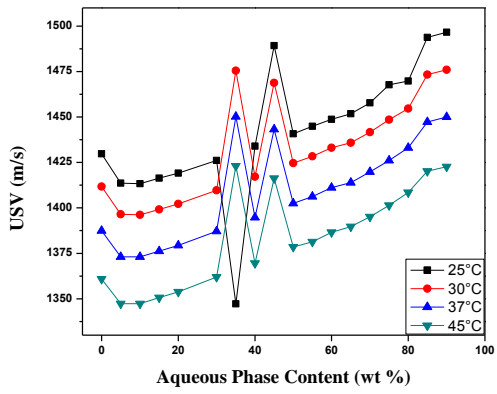
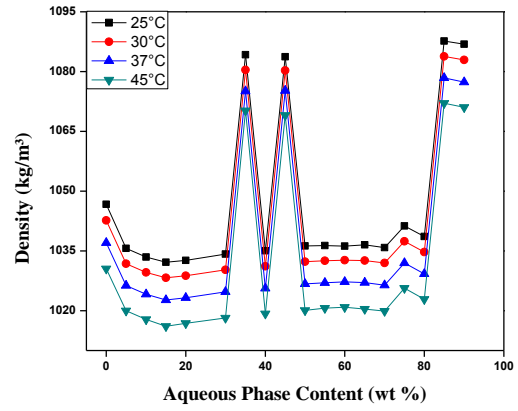
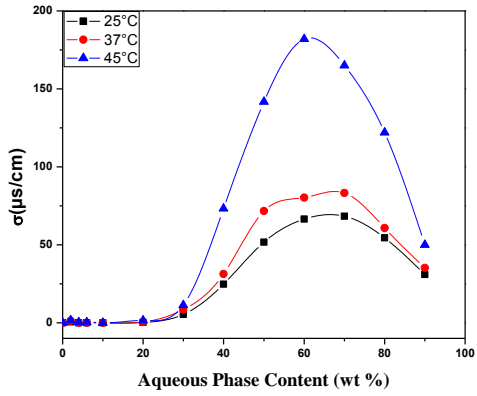


Staphylococcus aureus



Escherichia coli

Fig 5:147 System # 12 W+PG/TMAZ80/M1695/ CCT /EOH S (1/4)



Staphylococcus aureus

As for *Escherichia coli* inhibition occurred in systems # 13+15

Fig 5:148 System #13 W+PG/TMAZ80+ Sucrose myristate (M1695) /CCT +Ethanol S (1/1)

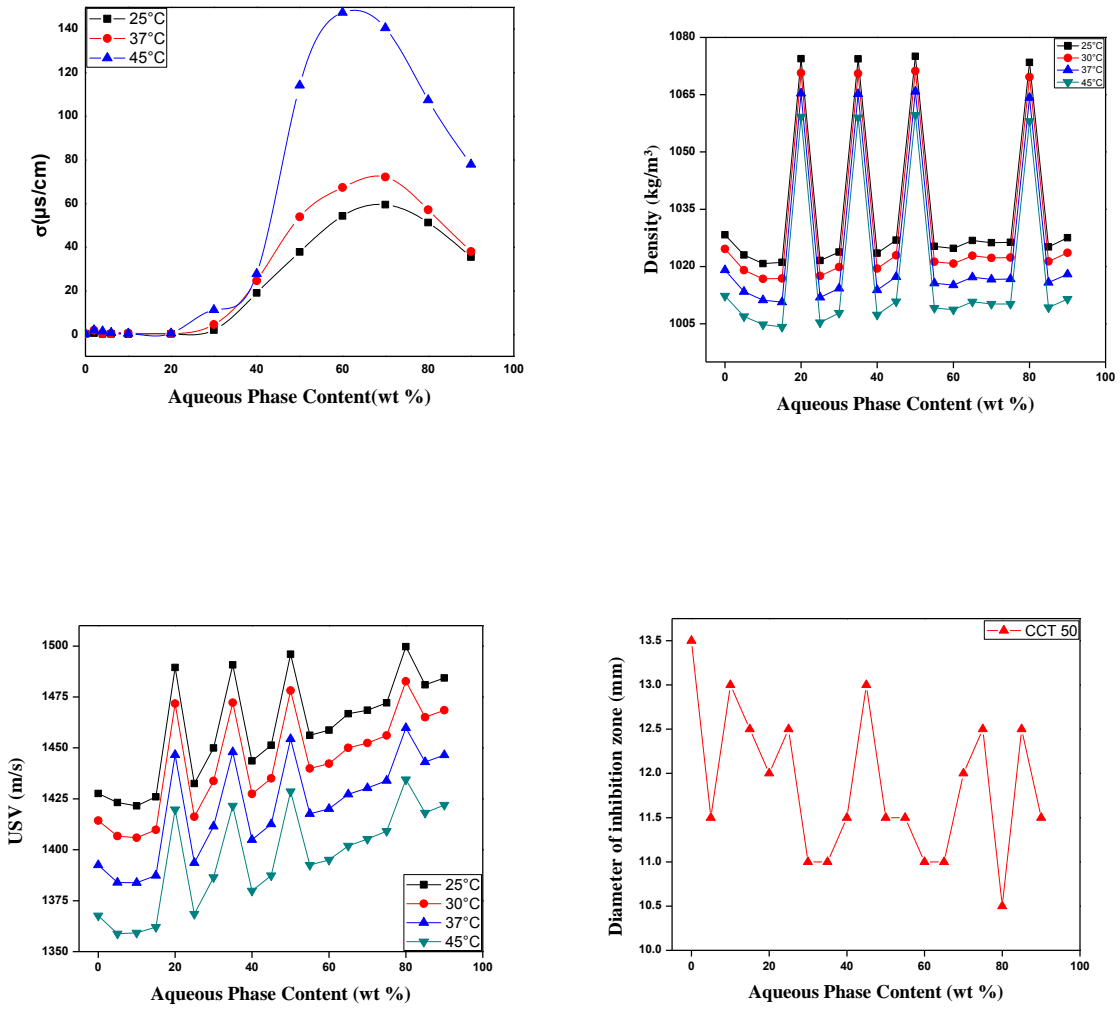
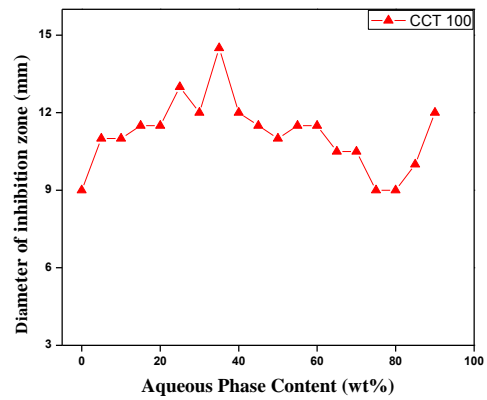
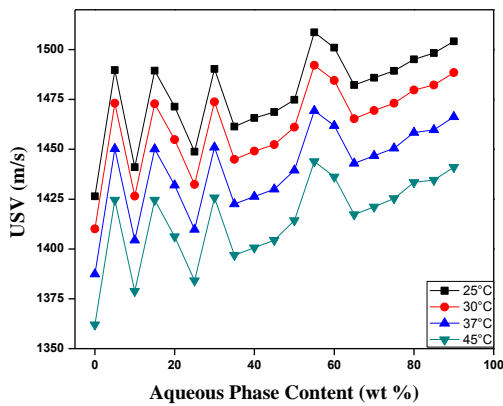
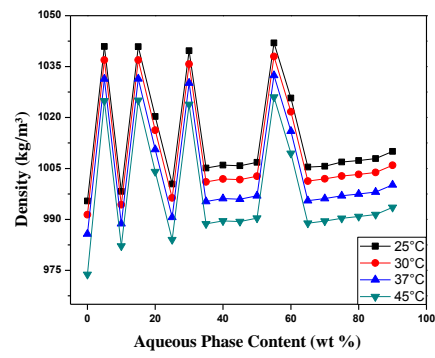
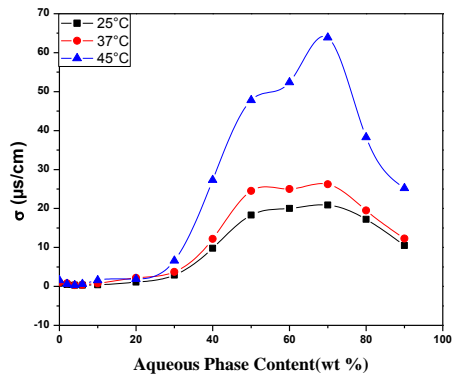


Fig 5:149 System #15 W+PG/TMAZ80/CCT +Ethanol (TMAZ80) 100%



Chapter Six

Conclusion

Mixed non ionic surfactants gave good results in constructing thermodynamically stable microemulsions. Sucrose myristate M(1695) and poly sorbate 80 TMAZ80 which both form temperature insensitive microemulsions were used . Mixing both of the surfactants in equal unity gave the maximum total monophasic region area $A_T(\%)$ in the three different oil types used. Systems with the cyclic limonene oil (LIM) gave the highest monophasic region area $A_T(\%)$ among all .Highest water solubility combined with minimum surfactant ratio needed to lower the interfacial tension between the two immiscible water and oil, while systems with capric caprylic triglyceride oil gave the lowest total monophasic region area $A_T(\%)$ due to the bulky fork shape of the triglyceride which makes it hard to penetrate in the palisade layer.

Characterization of the constructed microemulsion where tested using electrical conductivity ,density and ultrasonic velocity ,the different stages in the formation water in oil to bicontinuous phase ,ending in the formation of the reversed micellar under titration with aqueous water and propylene glycol solution were detected.

Results showed that the bicontinuous stage ranges from (15-20)% aqueous addition up to (65-70)% after which the formation of the oil in water droplets are formed.

Investigating the microbial activity against the systems formed showed that systems consisting of sucrose myristate M(1695) combined with limonene oil LIM had synergistic effect against Gram positive bacteria as well as Gram negative one.

Most of the systems tested had great impact on *Staphylococcus aureus* bacteria comparing with *Escherichia coli*, since it(*Staphylococcus aureus*) has no lipid layer while having thick layer of peptidoglycan which allows droplet size as small as 2nm to penetrate inside it makes it, thus making great impact in destruction of the bacterial cell ,while in the Gram negative bacteria having an outer lipid layer acts as a barrier for the microemulsion to penetrate inside the peptidoglycan layer.

Chapter Seven

References

- 1) Richard M. Pashley ,Marilyn E. et al : Applied Colloid and Surface Chemistry", 1 st Ed., John Wiley & SonsLtd, England.
- 2) Goodwin, Jim W.: Goodwin: "Colloids and Interfaces With Surfactants and Polymers An Introduction ".1 st Ed., John Wiley & Sons Ltd, England.
- 3) Eastoe, J.: Surfactant Chemistry. http://www.chm.bris.ac.uk/eastoe/Surf_Chem/3%2-Microemulsions.pdf
- 4) www.chm.bris.ac.uk/eastoe/Surf_Chem/3%20Microemulsions.pdf
- 5) Fanun M: Conductivity, viscosity, NMR and diclofenac solubilization capacity studies of mixed nonionic surfactants microemulsions, Journal of Molecular Liquids 135-5–13, 2007
- 6) Griffin, W. C: Classification of surface agents by HLB. Journal of Society of Cosmetics Chemists 1: 311- 326 , 1949
- 7) Prince, L.M: Microemulsions: Theory and Practice, New York, Academic Press, 1977.
- 8) Aboofazeli R, Lawrence M J: Investigations into the formation and characterization of phospholipid microemulsions. Pseudo-ternary phase diagrams of systems containing water-lecithin isopropyl myristate and alcohol: influence of purity of lecithin. Int. J.Pharm. 1-6:51-61,1994
- 9) Kumar. P, Mittal. K.C : Handbook of Microemulsions Science and Technology, Marcell Dekker, New York, 1999.
- 10) Fanun. M, :Microemulsions with Nonionic Surfactants and Mint Oil, Colloid Science Journal, 3: 9-14 ,2010.
- 11) Fanun.M and Salah Al-Diyn: Temperature Effect on the Phase Behavior of the Systems Water/Sucrose Laurate/Ethoxylated- mono-di-glyceride/Oil, Journal of Dispersion Science and Technology, 27:1119–1127, 2006_a
- 12) Fanun M, Salah Al-Diyn: Electrical conductivity and self diffusion-NMR studies of the system:Water/sucrose laurate/ethoxylated mono-di-glyceride /isopropylmyristate .Colloids and Surfaces A: Physicochem. Eng. Aspects, 277:83–89 ,2006_b

- 13) Friberg E: A non-aqueous microemulsion. *Colloid and polymer science*. 262: 3, 252–253, 1984
- 14) Al-Adham I, Khalil E, Al-Hmoud N.D et al: Microemulsions are membrane-active, antimicrobial, self-preserving systems. *Journal of Applied Microbiology*; 89:32-39. 2000
- 15) Garti N, Clement V, Fanun M, et al: Some characteristics of sugar ester nonionic microemulsions in view of possible food applications. *Journal of Agricultural and Food Chemistry*,48:9 ,3945-56 ,2000
- 16) Thevenin M.A ,Grossiord J.L , Poelman M.C : Sucrose esters/co- surfactant microemulsion systems for transdermal delivery: assessment of bicontinuous structures. *International Journal of Pharmaceutics* 137: 177-186, 1996
- 17) Fanun M : Surfactant Chain Length Effect on the Structural Parameters of Nonionic Microemulsions, *Journal of Dispersion Science and Technology*, 29:289–296, 2008
- 18) Garti N , Aserin A , Fanun M. : Non-ionic sucrose esters microemulsions for food applications. Part 1. Water solubilization, A: Physicochemical and Engineering Aspects 164: 27–38, 2000
- 19) Bansal V.K . Shah D.O and Oconnel J.P : Influence of Alkyl Chain Length Compatibility on Microemulsion Structure and Solubilization, *Journal of Colloid and Interface Science*, 75: 2, 1980
- 20) Fanun M: Conductive Flow Parameters of Mixed Nonionic Surfactants Microemulsions. *Journal of Dispersion Science and Technology*, 29:1426-1434,2008
- 21) Al-Adham I, Al-Hmoud ND, Khalil E et al: Collier Microemulsions are highly effective anti-biofilm agents. *Letters in Applied Microbiology*,36: 97–100, 2003
- 22) Hui Zhang.Fengqin Feng.Xiaowei Fu et al: Antimicrobial effect of food-grade GML microemulsions against *Staphylococcus aureus*. *European Food Research and Technology journal* 226:281-286,2007
- 23) Anjali CH, Madhusmita Dash, N Chandrasekaran, Amitava Mukherjee: Anti-Bacterial Activity of Sunflower oil Microemulsion . *International Journal of Pharmacy and Pharmaceutical Research* ,2, 1, 2010
- 24) Al-Adham I, Al-Nawajeh A.S.M , Khalil E et al: The Antimicrobial Activity of Oil-in-Water Microemulsions is predicted by their position within the Microemulsion

- Stability Zone. The International Arabic Journal of Antimicrobial Agents, 2 ,2:2 ,2012
- 25) Soumik Bardhan Kaushik Kundu,Sajal Das et al: Formation, thermodynamic properties, microstructures and antimicrobial activity of mixed cationic/non-ionic surfactant microemulsions with isopropyl myristate as oil. Journal of Colloid and Interface Science 430 :129–139 ,2014.
 - 26) Lou Xin: Antimicrobial structure-efficacy relationship of sugar fatty acid esters, Journal of Chemical and Pharmaceutical Research, 6,5:944-946, 2014
 - 27) Fanun M: , Microemulsion properties and applications, CRC press ,2009
 - 28) Shao S.Y.,Chhabra V, Patist A et al: Chain length compatibility effects in mixed surfactant systems for technological applications. Advances in Colloid and Interface Science 74:1-29 ,1998
 - 29) Fanun M: Microemulsions Formation on Water/Nonionic Surfactant/Peppermint Oil Mixtures, Journal of Dispersion Science and Technology. 30:399–405, 2009
 - 30) Stanislaw Pogorzelski: Surface tensometry studies on formulations of surfactants with preservatives as a tool for antimicrobial drug protection characterization . Journal of Biophysical Chemistry. 3,4 : 324-333 2012
 - 31) Garti N, Clement V, Leser M, et al: Sucrose ester microemulsion .Journal of molecular lipid.80 , 253-296 , 1999
 - 32) Leung R, SHAH D.O :Solubilization and Phase equilibria of Water in Oil Microemulsion. Journal of colloid and interface science . 120, 2,1987
 - 33) Kunieda H , Kadir H, Aramaki K,et al : Phase Behavior of Mixed Polyethoxylene-type Non ionic Surfactants in Water. Journal of molecular lipids. 90:157-166,2001
 - 34) Bidyut K. Paul Rajib K. Mitra: Water solubilization capacity of mixed reverse micelles: Effect of surfactant component, the nature of the oil, and electrolyte concentration. Journal of Colloid and Interface Science 288 :261–279, 2005
 - 35) Haiying, Liyi , Yang, et al: Antimicrobial Mechanism Analysis of an Oil in Water Microemulsion by DNA Microarray-Mediated Transcriptional Profiling of *Escherichia Coli*, Journal of Food Safty,34,2:176-183,2014

- 36) Fanun M,2015: Sucrose Myristate Micellar Systems:Formulation, Characterization and Cefuroxime Axetil Solubilization. Al Quds university,Palestine
- 37) Shakarnah A,2012: Biocompatible Microemulsion: Formulation, Characterization and Indomethacin Solubilization. Al Quds university,Palestine
- 38) Xiaowei Fu ,Fengqin Feng, Bin Huang :Physicochemical characterization and evaluation of a microemulsion system for antimicrobial activity of glycerol monolaurate. International Journal of Pharmaceutics 321 : 171–175,2006
- 39) Hui Zhang, Yinan Cui, Songming Zhu,et al: Characterization and antimicrobial activity of a pharmaceutical microemulsion. International Journal of Pharmaceutics. 395 :154–160,2010
- 40) Fanun M, Ayad Z,Mudalal S ,et al: Characterization of Water/Sucrose Laurate/n-Propanol/Allylbenzene Microemulsions. Journal of surfactants and detergents 15:505-512,2012
- 41) Solans C,kunieda H:Industrial Application of Microemulsions.CRC ,New York ,1997
- 42) Connie R,Donald C : Text book of Diagnostic Microbiology.5th eddition,2014

نظم مزيج من المستحلبات الدقيقة اللايونية وتشخيصها وفحص نشاطها كمضاد للنمو الميكروبي

اعداد الطالبة: لبنى عبد المعني كاظم ابو خلف

اشراف: د. منذر فنون

الملخص:

تقوم هذه الدراسة على خلط مكونات لا تختلط ببعضها البعض مثل الزيت والماء لتكوين مركبات تسمى مستحلبات دقيقة (Microemulsions) وذلك باضافة مادة لخفض التوتر السطحي بين الزيت والماء تسمى مستحلب (Surfactants) .

تم تكوين مستحلبات دقيقة باستخدام مواد سكرية وتم تشخيصها وتطبيقها كمضادات للنمو الميكروبي . تناولت هذه الرسالة عدة أنظمة تختلف فيما بينها في التركيب ونسبة المواد المضافة حيث تم خلط نوعان من خواص التوتر السطحي من النوع اللايوني وهما سكروز ميريسيتيت المعروف ب (M1695) ومركب سكري متعدد السوربيت 80 المعروف ب (TMAZ80) وتم بالبحث دراسة تأثير زيادة نسبة النوع الثاني بنسبة 25% كل خطوة من (0-100)% .

الوسط المائي المستخدم عبارة عن محلول مكون من الماء والبروبيلين جليكول , مكون بنسبة ثابتة وهي كمية الماء ضعف كمية البروبيلين جليكول . اما بالنسبة لانواع الزيوت المستخدمة فقد كانت ثلاث انواع مختلفة , زيت الحمضيات (LIM) وهو من الزيوت العطرية الحلقية . زيت الايزوبرويل ميريسيتيت (IPM) وهو من الزيوت الخطية واخيرا الكابريك كابرث ثلاثي الجلسيرايد (CCT) وهو من الزيوت الثلاثية الجلسيرايد .

تمت دراسة المستحلبات الناتجة (محلول مائي وبروبيلين جلكول \ مزيج من المستحلبات اللايونية او مستحلب منفرد الوسط الزيتي: نوع زيت واحد مضاف اليه الكحول بنسبة متساوية) على ثلاث درجات حرارة (25,37,45⁰س) .

في كل المراحل تم دراسة المساحة وحيدة الحالة (Monophasic region %) في رسومات الحالات الخاصة (Phase diagram) حيث تبين ان المساحة وحيدة الحالة كانت في حالات مزج المستحلبات بنسب متساوية اكبر من غيرها من النسب وعند مقارنتها حسب نوع الزيت المستخدم تبين ان الزيت الحلقي اعطى اكبر مساحة وحيدة الحالة وذلك بسبب الشكل الحلقي والحجم الجزيئي الاقل من غيره من الزيوت .

وعند التشخيص الفيزيائي للمستحلبات المختلفة المتكونة بفحص التوصيل الكهربائي والكثافة وسرعة الجزيئات لكل منها - خلال المراحل الكاملة لاضافة الوسط المائي بالتدرج - تم تحديد المناطق التي يتم فيها مراحل تكوين المستحلب .

من اهم اهداف هذه الرسالة هو فحص قدرة المستحلب المكون العمل كمضاد للميكروبات , وقد تم تعريض نوعين من البكتيريا حسب التصنيفات العامة لانواع البكتيريا - Gram positive/ *Staphylococcus aureus* والنوع الثاني Gram negative / *Escherichia coli* ووجد ان المستحلبات المكونة من الزيوت الحلقية بالتزامن مع خافض التوتر السطحي سكروز ميريسيتت لها القدرة الاكبر لمنع النمو الميكروبي, وكذلك تبين ان القضاء على الميكروبات عند زيادة نسبة المركب السكري متعدد السوربيت وانخفاض نسبة سكروز ميريسيتت تقل. وايضا وجد ان المستحلبات المكونة لها القدرة على قتل جميع الميكروبات من نوع *Staphylococcus aureus* ولكنها لا تعطي نفس التأثير على *Escherichia coli* بل تعمل على تقليل العدد الميكروبي وليس المنع الكامل.

Appendix A

Collected data of the electrical conductivity for the fifteen systems grouped as type of oil, data that couldn't be measured on the device indicated as (-).

Data of the electrical conductivity for the systems with LIM oil

Appendix A1 Electrical conductivity for system #1 W+PG/sucrose myristate (M1695)/LIM +Ethanol at 10 to 50°C in increasing steps of 5°C temperatures along with the titrations.

Temperatures (°C)										
W+PG (2/1) wt%	10	15	20	25	30	35	37	40	45	50
30	-	-	-	45.2	48.1	52.2	54.3	64.4	102.3	108.2
40	52.2	55.6	62.9	74.8	77.6	88.8	95.7	137.4	167.4	192
50	67.4	70.6	79.2	94.6	97.8	111.1	113.3	120.4	226	246
60	73.6	76.3	83.5	99	111.4	118	122.3	179.5	242	250
70	75.8	78.6	86.6	94	101	108	111	118	227	235
80	59.6	64.6	67.6	73.7	77.4	79	81	38.2	168.5	175
90	35	37.2	38.8	40.2	42.5	44.4	45.5	47.5	92.3	89.3

Appendix A2 Electrical conductivity for system #2 W+PG/TMAZ80+sucrose myristate (M1695)/LIM+ Ethanol (1/4) at 10 to 50°C in increasing steps of 5°C temperatures along with the titrations.

Temperatures (°C)										
W+PG (2/1) wt%	10	15	20	25	30	35	37	40	45	50
0	-	-	-	-	-	-	-	-	-	-
2	0.3	0.3	1.2	0.7	0.8	1	1.4	1.4	2.4	2.4
4	-	0.3	0.3	0.3	0.3	0.3	0.3	0.3	0.6	2.2
6	-	-	-	0.3	0.5	0.5	0.5	-	2.5	-
10	-	-	-	1.2	1.2	0.7	0.7	-	5.4	-
20	-	-	-	7.5	10.8	12.1	15	15	25.5	27.6
30	-	15.6	25.6	31.8	38.5	47.3	50.3	79.8	89.2	115.9
40	43.5	46.5	57.8	65.9	74.2	84.3	89.6	100	173	217
50	62.5	76.7	84.8	94.4	104.5	123	126.2	240	255	270
60	71.3	78.1	86.4	93.85	98.8	107.3	110	183	231.5	253
70	69	69.7	73.3	80.6	85.6	93.1	93	98	199	210
80	49.1	51.2	55.6	58.8	62.2	62.7	67.7	68.2	124	137.1
90	27	28.6	29	29.4	33.8	35.7	36	36.9	73.6	71.7

Appendix **A3** Electrical conductivity for system #3 W+PG/TMAZ80+sucrose myristate (M1695)/LIM+ Ethanol (1/1) at 10 to 50°C in increasing steps of 5°C temperatures along with the titrations

W+PG (2/1) wt%	Temperatures (°C)									
	10	15	20	25	30	35	37	40	45	50
0	0.8	0.8	0.8	1	1.3	1.7	1.7	1.7	3.3	3.1
2	0.4	0.5	0.5	0.8	1.3	1.3	1.7	1.7	3.3	3.1
4	0.4	0.4	0.6	0.8	1.3	1.5	1.5	1.7	3.3	3.2
6	0.3	0.3	0.4	0.8	1.1	1.2	1.7	1.8	2.4	2.4
10	0.4	0.4	0.6	1	1.7	2.1	2.1	2.1	3.6	3.6
20	1.4	1.4	3.3	3.6	5	6.6	6.6	7.6	13.3	14.9
30	6.4	7.3	11.8	15.6	17.5	20.7	22.7	26	53.2	56.9
40	21.1	21.8	29.8	32.1	39.2	42.2	50.2	53.4	76.3	113.4
50	32.8	33.2	38.2	50.5	53.7	59.6	66.4	69.6	139.8	156
60	35.3	38.2	43.9	53.6	58.8	62	64.5	72	148	158
70	37.5	42.3	44.5	49	53.8	57.6	57.5	61	122	123.7
80	30.1	32.2	33.7	37.4	39.7	40	41.1	44.2	86.5	86.4
90	16.5	18.1	19.1	20	21.3	22	22.6	23.5	46.2	45.7

Appendix **A4** Electrical conductivity for system #4 W+PG/TMAZ80+sucrose myristate (M1695)/LIM+ Ethanol (3/4) at 10 to 50°C in increasing steps of 5°C temperatures along with the titrations.

W+PG (2/1) wt%	Temperatures (°C)									
	10	15	20	25	30	35	37	40	45	50
2	1	0.9	2.6	2	3	3.1	3.7	2.7	5	6
4	0.6	0.8	1.4	1.4	0.2	0.3	0.4	0.4	0.4	1
6	0.3	0.3	0.3	0.3	0.4	0.6	0.6	0.6	0.7	1.1
10	0.3	0.3	0.4	0.7	1	1.6	2	1.4	1.5	0.7
20	0.3	0.3	1.1	1.5	1.8	5.6	5.7	6.7	1.4	3.3
30	1.5	2	5	5.9	7.4	9.4	10.4	22.9	52	91.9
40	5	7.6	10.2	15.5	18.3	20.4	31.2	56.6	101.8	123.9
50	16.6	17.4	20.5	33.3	41	68.4	82.2	96.4	207	217
60	22.3	19.2	28.3	41.4	59.3	60.9	64.35	81.35	177	217
70	16.6	23.2	24.9	27.9	37.2	41	46.6	59.3	151	172
80	19.2	21.8	21.3	23.7	26.9	27.3	29.3	32.7	79.4	98.8
90	15.7	17.2	18.6	19	20.3	21	21.1	20.7	47.2	50

Appendix A5 Electrical conductivity for system #5 W+PG/TMAZ80/LIM+ Ethanol at 10 to 50°C in increasing steps of 5°C temperatures along with the titrations.

W+PG (2/1) wt%	Temperatures (°C)									
	10	15	20	25	30	35	37	40	45	50
2	1.5	2	3.7	3.5	4.2	3.4	4.3	3.2	5.6	4.5
4	-	1.5	1.5	1.1	1.1	1.6	1.5	1.2	2.2	2
6	0.3	0.3	0.4	0.7	0.8	0.6	0.7	0.8	2.2	1.5
10	0.3	0.3	0.3	1	1	1	1.1	1.2	2.2	2.2
20	0.9	1.2	2	2	2.2	3.8	4.5	4.8	8.8	10.2
30	2.7	4.2	4.7	8.8	9.3	12.7	14.2	15.3	20.1	28.7
40	1.95	2.3	4.3	5.1	7.1	11.3	12.2	33.3	64.8	74.4
50	2.7	3.3	4.5	6.2	7.2	12.3	14.8	44.4	117.6	126.4
60	6.8	7.65	8.5	10.3	11.2	12.4	13.1	50.6	120.6	145.5
70	8.9	10	10.3	12.7	11.8	13.6	13.6	14.5	27	41
80	9.5	9.7	6.9	10.1	11.2	12.2	12.3	10	18.4	18.6
90	11.4	12.1	12.6	13	14.1	14.6	14.8	15.8	24.3	33.4

Appendix B

Data of the electrical conductivity for the systems with IPM oil

Appendix B1 Electrical conductivity for system #6 W+PG/sucrose myristate (M1695)/IPM +Ethanol at 10 to 50°C in increasing steps of 5°C temperatures along with the titrations.

W+PG (2/1) wt%	Temperatures (°C)									
	10	15	20	25	30	35	37	40	45	50
20	-	-	-	-	18.1	21.4	26.5	28.7	28.6	31.3
30	-	-	-	35.7	39.9	47.5	55.4	65.1	89.3	94.5
40	26.4	51.8	64.6	69.5	78.9	86.75	92.8	141.6	182.8	192.4
50	58.8	72	76.8	88.5	94.5	104.5	106.5	111.7	223	238
60	60.4	72.8	77.4	88.1	95.2	98.8	103.5	107.5	231	212
70	38.1	61	74	78.15	82.3	85	89.8	92	187	195
80	47.2	49.6	53.4	57	60	62.3	63.2	65.5	128.5	125.2
90	25.7	27.6	29	30.3	32.7	33.7	34.1	35.1	70	59.7

Appendix **B2** Electrical conductivity for system #7 W+PG/TMAZ80+sucrose myristate (M1695)/IPM +Ethanol (1/4) at 10 to 50⁰C in increasing steps of 5⁰Ctemperatures along with the titrations.

W+PG (2/1) wt%	Temperatures (°C)									
	10	15	20	25	30	35	37	40	45	50
2	0.3	0.3	1.8	1.5	1.4	1.2	1.5	1.2	2.3	2.4
4	-	-	0.9	0.7	0.5	0.9	1	1.3	2.2	2.2
6	-	-	0	0.3	0.7	0.7	1.3	1.3	2.1	2.1
10	-	-	0	1.3	1.7	2.2	2.2	2.2	3.2	3.2
20	-	-	4.7	5.5	7.6	11	11.6	11.6	24.3	25.2
30	-	-	16.6	20.6	23.3	25.7	34.4	36.2	74.4	84.6
40	31	33.4	39.5	48.5	52.6	58	64.1	110.1	142.6	153.9
50	45.2	47.3	54.6	67.7	75.1	77.4	81.7	83.9	171.3	179
60	47.2	57.3	58.3	68.3	77.5	79.3	83.2	86.2	175	192
70	40.5	52.7	56.6	61.1	67	67.9	71.2	73	150	154
80	38	40.4	43.1	45.6	48.2	50.7	51.3	53	101	106
90	20.3	22	23.8	24.6	26.5	27.5	28	28.8	58	54

Appendix **B3** Electrical conductivity for system #8 W+PG/TMAZ80+sucrose myristate (M1695)/IPM +Ethanol (1/1) at 10 to 50⁰C in increasing steps of 5⁰Ctemperatures along with the titrations.

W+PG (2/1) wt%	Temperatures (°C)									
	10	15	20	25	30	35	37	40	45	50
0	0.5	0.5	0.5	0.7	0.9	1	0.9	1.1	2.1	2.1
2	0.4	0.4	0.4	0.6	0.8	1.4	1.2	1	2.1	2.1
4	0.3	0.3	0.3	0.5	0.6	0.6	1	1.2	0.8	1.7
6	0.2	0.2	0.2	0.4	0.6	0.5	0.8	0.9	1.2	1.3
10	0.2	0.2	0.2	0.8	1.2	1.2	1.9	1.9	1.5	2.2
20	0	0	0.3	0.7	1.2	2.8	2.6	3.3	15.4	19.4
30	0	2	5	9.8	13.3	16.3	28.5	38.8	49.7	69.5
40	11.3	13.8	19.2	23	31.9	43.9	52.1	64.2	143.4	171
50	17.6	19.2	23.6	42.4	47	47.6	50.1	68.4	131.5	190
60	20.4	23	28.6	37.7	45.8	48.7	51.8	70.6	133.9	161.2
70	5.7	8.1	9.5	7.55	13.4	16.4	18.5	27.7	92	124
80	6.8	7.7	8.6	7.2	8.4	9.3	9.9	11.6	21	37.7
90	5.5	6.7	7.3	9.1	11.4	12.3	12.5	13.8	21.8	24

Appendix **B4** Electrical conductivity for system #9 W+PG/TMAZ80+sucrose myristate (M1695)/IPM +Ethanol (3/4) at 10 to 50⁰C in increasing steps of 5⁰Ctemperatures along with the titrations.

W+PG (2/1) wt%	Temperatures (°C)									
	10	15	20	25	30	35	37	40	45	50
2	0.5	0.5	1.5	2	2.5	1.9	2.2	2	4.3	4.2
4	0.6	0.6	0.4	0.5	1.2	0.7	1	1	1.1	1.3
6	0.2	0.2	0.2	0.3	0.5	0.3	0.3	0.6	1.2	1.2
10	0.3	0.3	0.4	0.4	0.6	0.6	1.1	0.8	0.8	0.7
20	0.5	0.6	1.1	1.5	1.8	2.3	2.7	1	2.4	2.5
30	1	1.8	2.9	4.2	5.3	7.3	8	9	18.3	20.9
40	11.3	12.6	13.8	15.2	20	21.9	25	27.3	55.6	62.4
50	23.3	25.5	28.6	36.1	37.2	43.3	45.5	51.5	95.2	105.8
60	29.3	32.3	37.2	43.3	45.5	50.7	52.7	57.2	104.6	110
70	35.8	37.1	42.5	44.9	47.3	47.8	52.7	56	107.6	118.6
80	31.8	34.4	35.7	38.3	40	41.5	42.2	44.6	82.6	82.9
90	22.1	23.2	24.4	25.2	26.5	27	27.6	28.6	56.6	50.2

Appendix **B5** Electrical conductivity for system #10 W+PG/TMAZ80/IPM +Ethanol at 10 to 50⁰C in increasing steps of 5⁰Ctemperatures along with the titrations.

W+PG (2/1) wt%	Temperatures (°C)									
	10	15	20	25	30	35	37	40	45	50
2	0.6	0.8	1.7	2	2.3	2	2.3	1.7	0.4	0.4
4	0.3	0.3	0.3	0.3	0.3	0.3	0.3	0.3	0.3	0.3
6	0.3	0.3	0.2	0.3	0.3	0.5	0.5	0.5	0.6	0.4
10	0.3	0.3	0.4	0.5	0.7	1	1.2	0.8	0.5	0.6
20	0.3	0.3	0.3	1.1	1.1	1.5	1.4	2.2	4	4.3
30	1.3	1.8	3.5	6	6.6	7.3	8.7	10	13.2	15.7
40	9.9	10.3	11.3	15.1	17.2	19	23.1	27.5	49.5	51.3
50	16.6	18.4	21.2	27.3	30.8	31.7	33.3	38.3	68.5	83.3
60	25.6	23.4	27.7	33.5	37.1	37.7	40.4	39	79.5	88.2
70	31.6	34.8	33.9	36.7	39	39.5	42.7	45	89	92
80	32.4	34.1	36	37.7	38.8	39.1	39.7	42	94	80.2
90	28.4	29.5	20.1	30.8	31.5	32	32.5	33	66.2	58

Appendix C

Data of the electrical conductivity for the systems with CCT oil

Appendix C1 Electrical conductivity for system #11 W+PG/sucrose myristate (M1695)/CCT +Ethanol at 10 to 50⁰C in increasing steps of 5⁰Ctemperatures along with the titrations.

W+PG (2/1) wt%	Temperatures (°C)									
	10	15	20	25	30	35	37	40	45	50
0	-	-	-	-	0.2	0.2	0.2	0.2	0.5	0.6
2	-	-	-	-	0.3	0.3	0.3	0.3	0.7	0.9
4	-	-	-	-	0.3	0.3	0.3	0.4	0.8	0.8
20	-	-	13.9	13.8	16.9	20	24.8	27.3	46.1	59.7
30	-	-	34.6	40.6	44.1	51.1	57.2	61.4	113	129.5
40	40	55.4	64.8	70.7	79.2	81.2	86.1	92	176	202
50	55.6	65.8	75.9	90.6	102	103.9	103.8	116	213	216
60	62.1	77.5	84.3	89.7	96.5	118	121	132	258	229
70	59.7	71.9	75	82.7	87.8	90.9	95.2	97.1	191	188
80	51.1	54.9	57.8	62.3	65.5	66.5	68.5	71.6	130.5	137.9
90	29.1	30.8	31.9	34.4	36.7	38.4	38.7	39.8	77.6	76.6

Appendix C2 Electrical conductivity for system #12 W+PG/TMAZ80+sucrose myristate (M1695)/CCT+Ethanol (1/4) at 10 to 50⁰C in increasing steps of 5⁰Ctemperatures along with the titrations.

W+PG (2/1) wt%	Temperatures (°C)									
	10	15	20	25	30	35	37	40	45	50
2	-	-	0.3	0.5	1.2	0.8	1.2	0.8	1.6	15
20	-	-	-	0.2	0.2	0.4	0.4	0.8	1.5	2.7
30	-	1.2	2.1	5.4	6	6.3	8.5	10.4	11.3	13.1
40	7.5	16.4	21	24.8	26.1	28.4	31.3	37.7	73.3	87.7
50	31.7	24.4	40.3	51.7	60.4	59.5	71.7	92.35	141.7	156
60	43.1	51.1	57.3	66.5	73.7	77	80.3	108.15	182	173
70	52	56.8	62	68.3	75.8	80.2	83.3	82.4	165	173
80	44.6	48.6	50.2	54.5	57.4	58.8	60.8	64.4	122	126
90	26	27.3	29.4	30.9	33.1	34.6	35.2	36.5	50	69

Appendix C3 Electrical conductivity for system #13 W+PG/TMAZ80+sucrose myristate (M1695)/CCT+Ethanol (1/1) at 10 to 50°C in increasing steps of 5°C temperatures along with the titrations.

W+PG (2/1) wt%	Temperatures (°C)									
	10	15	20	25	30	35	37	40	45	50
0	0.3	0.3	0.3	0.3	0.3	0.3	0.3	0.3	0.3	0.3
2	0.3	0.3	0.7	0.7	2.2	1.2	2	1.2	2.1	2.2
4	0.3	0.3	0.3	0.3	0.3	0.4	0.4	0.5	1.5	2.2
6	0.2	0.2	0.3	0.3	0.4	0.4	0.5	0.4	0.8	0.6
10	0.2	0.2	0.3	0.2	0.4	0.5	0.7	0.4	0.5	0.8
20	0.3	0.3	0.3	0.3	0.4	0.4	0.4	0.4	0.6	1.3
30	0.6	0.6	0.8	2.1	2.9	3.6	4.6	5.3	11.3	12.3
40	5.9	7.6	16.4	19.1	22	22.8	24.7	26.5	27.8	29.1
50	23.3	26.5	29.3	37.9	47.7	49.2	54	67.45	114.3	117.4
60	34.1	42.4	46.7	54.4	62	62.8	67.4	102.7	147.6	158
70	46.1	48.3	49	59.6	63	66.7	72.2	73.7	140.6	146.3
80	41.5	45.9	49	51.3	54.2	56	57.2	59.7	107.5	118.3
90	31.3	33.7	34.1	35.5	36.6	37.6	38.1	49.6	78	74.8

Appendix C4 Electrical conductivity for system #14 W+PG/TMAZ80+sucrose myristate (M1695)/CCT+Ethanol (3/4) at 10 to 50°C in increasing steps of 5°C temperatures along with the titrations.

W+PG (2/1) wt%	Temperatures (°C)									
	10	15	20	25	30	35	37	40	45	50
0	0.7	0.9	1	1.2	1.3	1.4	1.4	1.4	2.8	2.8
2	0.5	0.5	0.8	0.8	1.3	1.7	1.4	1.4	2.8	2.8
4	0.5	0.5	0.6	0.8	1.2	1.7	1.7	1.2	2.9	2.8
6	0.3	0.3	0.3	0.8	1.1	0.6	1.1	0.8	2.2	1.4
10	0.3	0.3	0.6	0.8	1.2	1.1	1.3	1.3	2.4	2.2
20	1	1.6	2.1	2.4	2.4	2.6	2.6	5.4	11.5	11.5
30	4.1	5.2	8.6	13.6	16.4	17.8	22.5	24.5	50.4	53.2
40	13	26.5	31	35.8	46.2	48.3	51.5	54.9	90.7	117.7
50	26.6	38	56.3	72.2	77.1	78.1	83.8	87.3	164.4	173
60	36	49.6	63.7	78.9	86.2	87.9	89	97.2	181	203
70	50	58.3	67.9	73.5	89.2	91.3	93.5	95.5	192	210
80	37.5	43.6	49.8	58.8	67.5	71.6	72.2	79	135.2	149
90	25.1	26.9	34.3	34.9	46.2	50.8	51.7	53	106	100

Appendix C5 Electrical conductivity for system #15 W+PG/TMAZ80/CCT+ Ethanol at 10 to 50°C in increasing steps of 5°C temperatures along with the titrations.

		Temperatures (°C)								
W+PG (2/1) wt%	10	15	20	25	30	35	37	40	45	50
0	0.6	0.6	0.8	0.8	0.8	1	1	0.8	1.6	1.1
2	0.4	0.4	0.5	0.5	0.9	0.9	0.8	0.8	0.6	0.6
4	0.3	0.3	0.3	0.3	0.4	0.3	0.3	0.3	0.3	0.6
6	0.2	0.2	0.2	0.3	0.3	0.3	0.4	0.3	0.6	0.4
10	0.3	0.3	0.3	0.4	0.7	0.7	0.8	0.8	1.6	1.6
20	0.9	0.9	1	1.1	1.1	1.1	2.2	2.5	1.9	2.9
30	0.6	0.6	1.2	2.9	3.2	3.6	3.7	5.7	6.6	8.3
40	4.7	6.3	7.8	9.8	11.6	12	12.2	20.3	27.3	33.5
50	9.7	10.7	13.5	18.3	22.2	23.5	24.5	22.8	47.8	53.7
60	12.3	14.2	17.2	20	23.6	24.2	25	29.7	52.4	56
70	15	16.8	18.7	20.9	22.8	24.7	26.2	26.7	63.9	66.7
80	13.7	14.6	15.8	17.2	18.1	19	19.5	20.6	38.3	41.4
90	8.5	9.5	10	10.5	11.3	12.1	12.3	12.6	25.2	25

Appendix D

Density in (kg/m³) of each constituent in this study at different temperatures:

		Density(kg/m ³)			
T (°C)		25	30	37	45
Sample					
Water		996.945	995.541	993.219	990.099
CCT		944.677	940.852	935.519	929.449
LIM		840.471	836.554	831.055	824.742
IPM		849.53	845.766	840.499	834.486
PG		1033.475	1029.746	1024.473	1018.358
TM80		1073.888	1069.947	1064.422	1058.116
EOH 99.9%		786.425	782.111	776.007	768.929

Appendix E

Ultrasonic velocity in (m/s) of each constituent in this study at different temperatures:

		USV (m/s)			
Sample \ T (°C)	25	30	37	45	
Water	1497.3	1509.55	1523.91	1536.68	
CCT	1370.85	1354.15	1331.07	1305.15	
LIM	1322.12	1302.94	1275.82	1245.06	
IPM	1321.37	1303.49	1278.69	1250.78	
PG	1521.1	1507.02	1487.33	1464.76	
TM80	1540.26	1523.69	1500.75	1476.19	
EOH 99.9%	1144.63	1128.03	1104.47	1077.21	